

Strengthening of concrete structures by the use of mineral-based composites

System and design models for flexure and shear



Thomas Blanksvärd



DOCTORAL THESIS

**Strengthening of concrete
structures by the use of mineral-
based composites**

System and design models for flexure and shear

Thomas Blanksvärd

Luleå University of Technology
Department of Civil, Mining and Environmental Engineering
Division of Structural Engineering
SE - 971 87 Luleå
Sweden
www.ltu.se/shb

“The roots of education are bitter, but the fruit is sweet”
// Ἀριστοτέλης

Strengthening of concrete structures using mineral-based composites

THOMAS BLANKSVÄRD

Avdelningen för byggkonstruktion

Institutionen för Samhällsbyggnad

Luleå Tekniska Universitet

Akademisk avhandling

som med vederbörligt tillstånd av Tekniska fakultetsnämnden vid Luleå tekniska universitet för avläggande av teknologie doktorsexamen, kommer att offentligt försvaras i

universitetssal F1031, fredagen den 24 april 2009, klockan 10.00

Fakultetsopponent: Professor Thanasis C. Triantafillou, Department of Civil Engineering, University of Patras, Patras Greece

Betygsnämnd: Professor Henrik Stang, Department of Civil Engineering, Technical University of Denmark, Lyngby Denmark.

Professor Timo Aho, Department of Construction Technology, Oulu University, Oulu, Finland.

Professor emeritus Ralejs Tepfers, Avdelningen för konstruktionsteknik, Chalmers tekniska högskola, Göteborg Sverige.

Docent Kjell Eriksson, Avdelningen för hållfasthetslära, Luleå tekniska universitet, Luleå Sverige.

Tekn. Dr. Anders Wiberg, Anläggningsunderhåll, Grontmij, Stockholm Sverige.

Tryck: Universitetstryckeriet, Luleå

ISBN: 978-91-86233-23-5

ISSN 1402-1544

Luleå 2009

www.ltu.se

Front page: The illustration shows concrete members strengthened in shear and bending. The member strengthened in shear is in the front since more time was spent on exploring the aspects of shear strengthening using mineral-based composites (MBC). The filmstrip at the bottom shows applications of the MBC system starting from the inside of a silo to strengthening of balconies.

Preface

Every expedition has to have a purpose and a defined finishing line. My exploration journey as a PhD student started in September 2004. The official purpose with this mission was to investigate the suitability of using mineral-based composites for strengthening of existing concrete structures. During the last four and a half years I have learned that the unofficial purpose with this expedition was to explore my own suitability as a researcher and how to strengthen myself as an individual. The outcome of all expeditions is highly dependent on the surrounding environment, people and finances. I would therefore like to extend my personal gratitude to the following:

For the financial support I am grateful to the Swedish Road Administration, the Development Fund of the Swedish Construction Industry (SBUF), Skanska Sverige AB, the European Integrated Project “Sustainable Bridges” and Sto Scandinavia AB. Elsa and Sven Thysell’s foundation, Maj and Hidling Brosénius Foundation, Wallenberg Foundation and Ångpanneföreningen are appreciated for scholarships enabling me to travel outside Sweden to present my research and make new friends.

Prof. Björn Täljsten, I have travelled the world under your wings and gathered knowledge not possible elsewhere. Thanks for being both a friend and firm supervisor, I hope to work with you in the future. Dr Anders Carolin, the deputy supervisor, for all on and off topic conversations and being a great mentor.

The laboratory investigations would not have been possible without the helpful members in the lab, Mr. Håkan Johansson, Civ Eng, Georg Danielsson, Mr. Lars Åström, Mr. Thomas Forsberg and Dr. Claes Fahleson

The staff at the division of Structural Engineering with its head Prof. Mats Emborg, for bringing me diversity in conversations and festivities. I would also like to send a special thought to my colleagues and friends in the research group “Innovative Materials and Structures” Gabbe, Mackan and Bennitz for all the help and support.

I mentioned that my expedition started in 2004, this was not entirely true. I have followed my father in the laboratory ever since I learned to walk. During my early missions in the division of Structural Engineering I met Prof. Lennart Elfgren who has given me insightful comments during my entire visit at the university. So thank you Dad for giving me confidence, showing me that the university was not a scary place and for all the useful and endless discussions regarding civil engineering

I would also like to extend my gratitude to my mom, brother and sister for always being there, believing in me and defining me as a person.

When the academic environment became too dull, I took refuge in my band SlideShow. Thank you Poe Deprey, Foxy Black and Nicky Dollars for living the rock n roll life style with me.

Saved for last, the most important dynamic factor in my life is my wife. With your everlasting energy you bring colour and shape to the otherwise grey and square subsistence. Thank you for being you and always understanding that sometimes it requires 18h days to finish a PhD. If I need help with notations or to do NSMR strengthening, you are always first in line.

- Multiply it by infinity, take it to the depths of forever and you will still only have a glimpse of how much I love you.

This concludes my seemingly 30 year long expedition in the jungle called Luleå University of Technology. Now, it is off in to the horizon and beyond.

Thomas Blanksvärd
April 2009

Summary

A great number of society's resources are invested in existing concrete structures, such as bridges, tunnels, different kind of buildings etc. All of these structures have both an expected function and an expected life span. However, both the function and the life span can be influenced by external factors, e.g. degradation and altered load situations. Further influencing aspects could be mistakes in design or during the construction phase. Repairing and/or strengthening these structures could maintain or increase the function as well as the life span.

To strengthen concrete structures by using adhesively bonded fibres or fibre reinforced polymers (FRP) has been shown to be an excellent way of improving the load bearing capacity. The most common adhesive used for this type of strengthening is epoxies. Unfortunately, there are some drawbacks with the use of epoxy adhesives such as diffusion tightness, poor thermal compatibility with concrete and requirements for a safe working environment which might lead to allergic reactions if proper protective clothing is not used. A further limiting factor is the requirement on the surrounding temperature at application. A commonly recommended minimum temperature at the time for application is 10°C, which makes the preparations regarding application during colder seasons much more complicated. However, some of these drawbacks could be reduced by substituting the epoxy adhesive for a mineral-based bonding agent with similar material properties as concrete.

The strengthening system and also the topic of this thesis is termed "mineral-based composites" (MBC). The MBC consists in this context of grids of carbon FRP with high tensile strength that are bonded to an existing concrete surface by the use of a cement based bonding agent.

The scientific approach in this thesis includes analytical methods to describe load bearing capacity for the strengthened concrete structure in both flexure and shear. The analytical approaches are then verified against experimental results. Above the theoretical and experimental performance of the MBC system a review of state of the art research has been made in order to collate and map existing mineral-based strengthening systems other than the MBC system.

To develop and verify the theoretical models and to compare the performance of the MBC system to other possible designs of mineral-based strengthening systems, six papers are appended in the thesis.

- The first paper describes the performance of the MBC system when used in flexural strengthening. The experimental program in this paper consists of a concrete slab strengthened with both the MBC system and epoxy based system. In addition, a parametric study was made on small scale beam specimens to evaluate the performance of using different cement-based bonding agents.
- The second paper describes the performance of the MBC system when used as shear strengthening. This study consists of experimental results of 23 reinforced concrete beams with different concrete qualities, internal shear reinforcement ratios together with different variations of the CFRP grid design and mineral-based bonding agents. In addition, a comparison is also made to traditional epoxy-based strengthening. This paper also has an analytical approach to estimate the shear resistance.
- The third paper describes existing mineral-based strengthening systems and how these perform in comparison to the proposed MBC strengthening system in shear and flexure.
- The fourth paper maps different possibilities to design and combine various materials in order to obtain a mineral-based strengthening system. This paper also consists of experimental research on the tensile behaviour of the MBC system when using high performance fibre reinforced cementitious bonding agents (engineered cementitious composites - ECC). In addition, these results and discussions are also coupled to the observations made in flexural and shear strengthening.
- The fifth paper gives suggestions on how to estimate the shear bearing capacity of MBC strengthened concrete beams. The suggested shear design approaches are mainly based on traditional shear design models based on truss analogy, but one design presented is based on the compression field theory.
- The sixth and last paper describes the strain development in a shear strengthened concrete beam both with and without the MBC system.

All of the results from the investigations made in this thesis indicate that the MBC system contributes to increasing the load bearing capacity for strengthened concrete structures considerably. It is also shown that the MBC system can give competitive strengthening effects compared to existing epoxy bonded strengthening systems. From the experimental investigations on the shear strengthened beams it is shown that the strains in the shear span are lowered compared to a non strengthened specimen. This reduction of strains is also shown in the transition zone between the development of macro cracks from micro cracks. The suggested analytical approach in order to estimate the load bearing capacity of strengthened concrete structures in both flexure and shear indicates that realistic estimations can be made. The flexural design is straightforward while the shear design is more intricate. It is however concluded that a simple and safe design could be made based on the “additional” approach using a 45° truss.

Sammanfattning (Swedish)

En betydande del av samhällets tillgångar är investerade i vår existerande infrastruktur som t ex järnvägsbroar, vägbroar, tunnlar, dammar, fastigheter etc. En majoritet av dessa konstruktioner är byggda av armerad betong. Samtliga av dessa betongkonstruktioner har både en förväntad funktion och en förväntad livslängd. Men både funktionen och livslängden kan komma att ändras på grund av yttre påverkande faktorer som till exempel nedbrytning och förändrade belastningsförhållanden. Ytterligare kan vara tidiga misstag i projekteringsfasen eller under själva uppförandet. Genom reparation och/eller förstärkning kan både funktion och livslängd hos dessa konstruktioner ofta återställas eller till och med uppgraderas.

Förstärkning av betongkonstruktioner genom att limma fast kolfiberväv eller kolfiberkompositer har visat sig vara en bra och tillförlitlig metod för att öka bärförmågan hos befintliga konstruktioner. Det lim som till största delen används vid denna typ av förstärkning är epoxilim. Dessvärre har epoxilim vissa nackdelar, så som diffusionstäthet, dålig termisk kompatibilitet med betong och krav på skyddad arbetsmiljö. Ytterligare en begränsande faktor är kravet på en lägsta omgivande temperatur, vanligtvis 10°C, vid limning. Vissa av dessa nackdelar kan reduceras genom att byta ut epoxilimet mot en mineralbaserad vidhäftningsprodukt med egenskaper liknande betongens.

Förstärkningssystemet som omfattas av denna avhandling har benämningen ”mineralbaserade kompositer” (MBC) och omfattar kolfibernet med hög draghållfasthet som fästs på en befintlig betongkonstruktion med ett cementbaserat bruk.

Det vetenskapliga förfarandet i denna avhandling omfattar analytiska metoder för att beskriva bärförmågan för den förstärkta betongkonstruktionen i både böjning och tvärkraft. De analytiska metoderna är sedan verifierade mot laboratorieförsök. Utöver de teoretiska och experimentella resultaten för MBC systemet så ingår även en aktuell granskning och kartläggning av existerande mineralbaserade förstärkningssystem och därmed möjliga materialkombinationer och utformningar, dvs. andra än MBC systemet.

Avhandlingen består av en litteraturstudie och sex bifogade artiklar.

- Den första artikeln beskriver hur MBC system uppför sig vid förstärkning i böjning. I denna artikel ingår provning av en större betongplatta som förstärkts med MBC systemet och epoxibaserade system samt en parametersstudie på småskaliga provkroppar med MBC systemet och olika cementbaserade bruk.

- Den andra artikeln beskriver hur förstärkningssystemet presterar vid förstärkning i tvärkraft. Denna studie omfattar experimentella resultat på 23 balkar med olika betongkvaliteter, armeringsmängd samt olika variationer av MBC systemet och jämförelse mot traditionell epoxibaserad förstärkning. Dessutom innehåller denna artikel en analytisk uppskattning av tvärkraftskapaciteten.
- Den tredje artikeln beskriver olika existerande förstärkningssystem och hur dessa presterar i jämförelse med MBC systemet i böjning och tvärkraft.
- Den fjärde artikeln kartlägger olika möjligheter till att kombinera material i mineralbaserade förstärkningssystem för att optimera dessa system. Dessutom ingår även experimentella försök med ett högpresterande fiberförstärkt cementbruk (ECC). Denna artikel omfattar även resultat och diskussion om MBC systemets beteende i enaxligt drag, brottenergiupptagande förmåga samt hur dessa observationer kopplas till iakttagelser i böj- och tvärkraftsförstärkning.
- Den femte artikeln behandlar en rekommendation till dimensionering för tvärkraft av MBC system baserat på traditionella dimensioneringsmetoder med fackverksteori samt en ny tillämpning baserat på tryckfältsteori.
- Det sjätte bidraget beskriver hur töjningsutvecklingen sker i tvärkraft för betongbalkar med och utan MBC systemet.

Resultaten från dessa undersökningar indikerar på att MBC systemet bidrar till att öka bärförmågan hos förstärkta betongelement och att denna ökning kan i vissa avseenden jämföras med epoxibaserad förstärkning. Det är även visat att MBC systemet, i tvärkraftsförstärkning, bidrar till att minska töjningar i det armerade betongtvärsnittet i övergångszonen mellan tillväxten av mikrosprickor till makrosprickor samt att töjningarna reduceras även under öppningen av makrosprickor. Analytiska metoder för att uppskatta bärförmåga för förstärkning i böjning och tvärkraft är redovisade och dessa indikerar på att realistiska uppskattningar är möjliga. Dimensionering av bärförmågan i böjning är relativt enkel medan dimensionering i tvärkraft är lite mer komplicerad. En av slutsatserna gällande tvärkraftsdimensioneringen är att det är möjligt på ett enkelt sätt använda befintliga dimensionerings anvisningar grundade i "additions" principen och 45° fackverksteori för att uppnå en säker uppskattning av bärförmågan i tvärkraft.

Notations and symbols

Upper case letters

| | | |
|-------------|---|-------------------|
| A | Dimensionless parameter | [-] |
| A_c | Area of concrete cross section | [m ²] |
| A_f | Fibre area | [m ²] |
| A_{fx} | Area of fibres in longitudinal CFRP tows | [m ²] |
| A_{fz} | Area of fibres in transverse CFRP tows | [m ²] |
| A'_s | Compressive steel reinforcement | [m ²] |
| A_s | Tensile steel reinforcement | [m ²] |
| A_{sl} | Longitudinal tensile steel reinforcement area (beams) | [m ²] |
| A_{sx} | Area of longitudinal steel reinforcement | [m ²] |
| A_{sz} | Area of transverse steel reinforcement | [m ²] |
| B | Dimensionless parameter | [-] |
| C | Constant | [-] |
| C_1 | Constant | [N/m] |
| C_2 | Constant | [N] |
| C_3 | Constant | [Nm] |
| C_4 | Constant | [N] |
| C_5 | Constant | [Nm] |
| C_6 | Constant | [N] |
| C_7 | Constant | [Nm] |
| C_8 | Constant | [N] |
| C_9 | Constant | [Nm] |
| $C_{R,d,c}$ | Coefficient for concrete | [-] |
| E_c | Modulus of elasticity for concrete | [Pa] |
| E_f | Modulus of elasticity for fibres | [Pa] |
| E_{fx} | Modulus of elasticity for longitudinal fibres | [Pa] |
| E_{fz} | Modulus of elasticity for transverse fibres | [Pa] |
| E_{MBA} | Modulus of elasticity for the mineral-based binder | [Pa] |
| E_s | Modulus of elasticity for steel | [Pa] |
| F_1 | Constant | [-] |
| F_2 | Constant | [-] |
| F_c | Compressive force in concrete | [N] |

| | | |
|--------------|--|-------------------|
| F_f | Tensile force in fibre | [N] |
| F_s | Force in tensile reinforcement | [N] |
| F'_s | Force in compressive reinforcement | [N] |
| F_1 | Constant | [-] |
| F_2 | Constant | [-] |
| F_D | Diagonal force | [N] |
| F_L | Longitudinal force | [N] |
| F_V | Vertical force | [N] |
| I_1 | Moment of inertia for stage I | [m ⁴] |
| I_2 | Moment of inertia for stage II | [m ⁴] |
| I_c | Moment of inertia for a concrete beam | [m ⁴] |
| I_s | Moment of inertia for steel reinforcement | [m ⁴] |
| K | Factor for shear reinforcement | [-] |
| M | Moment | [Nm] |
| M_{cr} | Cracking moment | [Nm] |
| N_D | Diagonal force | [N] |
| N_{tot} | Total normal force | [N] |
| N_v | Tensile force due to shear | [N] |
| P | Force | [N] |
| T | Tensile force | [N] |
| T_y | Tensile force in reinforcement when yielding | [N] |
| V | Shear force | [N] |
| V_c | Shear force in Concrete | [N] |
| V_d | Design shear resistance | [N] |
| V_f | Shear resistance contribution of fibres | [N] |
| V_i | Shear resistance resultant of variable depth | [N] |
| V_{MBA} | Shear resistance contribution of miner-based binder | [N] |
| V_n | Nominal shear strength | [N] |
| V_s | Shear resistance contribution of steel reinforcement | [N] |
| $V_{Rd,c}$ | Design shear resistance of concrete | [N] |
| $V_{Rd,max}$ | Maximum design shear resistance of concrete | [N] |
| $V_{Rd,s}$ | Design shear resistance of steel reinforcement | [N] |
| V_u | Ultimate shear resistance | [N] |

Lower case letters

| | | |
|--------|---|-----|
| a_g | Aggregate size | [m] |
| b'_w | Effective width of strengthened cross section | [m] |
| b_w | Width of cross section | [m] |
| c_x | Maximum distance for longitudinal reinforcement | [m] |
| c_z | Maximum distance for transverse reinforcement | [m] |

| | | |
|-------------------|--|------|
| d | Effective depth | [m] |
| d_s | Distance to tensile reinforcement | [m] |
| d'_s | Distance to compressive reinforcement | [m] |
| d_{bx} | Diameter of longitudinal reinforcement | [m] |
| d_{bz} | Diameter of transverse reinforcement | [m] |
| f_{2max} | Maximum principal compressive stress | [Pa] |
| f_c | Cylinder compressive strength | [Pa] |
| f_{cc} | Concrete compressive stress | [Pa] |
| f_{cd} | Design value for concrete compressive strength | [Pa] |
| f_{ck} | Characteristic value for concrete compressive strength | [Pa] |
| f_{cr} | Compressive strength for concrete at cracking | [Pa] |
| f_{ct} | Concrete tensile strength | [Pa] |
| $f_{c,l}$ | Tensile stress in lower part of a beam | [Pa] |
| $f_{c,u}$ | Compressive stress in upper part of a beam | [Pa] |
| $f_{f,ef}$ | Effective stress in fibres | [Pa] |
| $f_{\bar{f}x}$ | Stress in longitudinal CFRP | [Pa] |
| $f_{\bar{f}x,ef}$ | Effective stress in longitudinal CFRP tows | [Pa] |
| $f_{\bar{f}xcr}$ | Stress in longitudinal CFRP at a crack | [Pa] |
| $f_{\bar{f}z}$ | Stress in transverse CFRP | [Pa] |
| $f_{\bar{f}z,ef}$ | Effective stress in transverse CFRP tows | [Pa] |
| $f_{\bar{f}zcr}$ | Stress in transverse CFRP at a crack | [Pa] |
| f_m | Tensile stress due to moment | [Pa] |
| $f_{MBA,t}$ | Tensile stress in mineral-based binder | [Pa] |
| f_s | Stress in steel | [Pa] |
| f_{sx} | Longitudinal stress in steel | [Pa] |
| f_{sxcr} | Longitudinal stress in steel at a crack | [Pa] |
| f_{sy} | Yield stress in steel | [Pa] |
| f_{syz} | Yield stress in transverse steel reinforcement | [Pa] |
| f_{sz} | Transverse stress in steel | [Pa] |
| f_{szcr} | Transverse stress in steel at a crack | [Pa] |
| f_t | Tensile stress | [Pa] |
| $f_{t,max}$ | Maximum tensile stress | [Pa] |
| f_x | Longitudinal stress | [Pa] |
| f_y | Yield stress | [Pa] |
| f'_y | Yield stress in compressive reinforcement | [Pa] |
| f_{yd} | Design value for yield stress | [Pa] |
| f_{yk} | Characteristic value for yield stress | [Pa] |
| f_{yl} | Yield strength of tensile reinforcement | [Pa] |
| f_{yx} | Yield strength of longitudinal reinforcement | [Pa] |
| f_{yz} | Yield strength of transverse reinforcement | [Pa] |
| f_z | Transverse stress | [Pa] |
| h | Depth (height of element) | [m] |
| h_{ef} | Effective depth (Effective height) | [m] |
| j | Factor for reducing the effective depth | [-] |
| k | Size factor | [-] |

| | | |
|-----------------|--|------|
| k_c | Constant | [-] |
| k_f | Factor considering reinforcement bond | [-] |
| s | Stirrup distance | [m] |
| s_{fz} | Distance between transverse CFRP tows | [m] |
| s_{fx} | Distance between longitudinal CFRP tows | [m] |
| s_{mx} | Longitudinal crack spacing | [m] |
| s_{mz} | Transverse crack spacing | [m] |
| s_x | Distance between longitudinal reinforcement | [m] |
| s_{xe} | Effective longitudinal crack spacing | [m] |
| s_θ | Distance between diagonal cracks | [m] |
| t_{MBC} | Thickness of MBC strengthening | [m] |
| t_{MBA} | Thickness of miner-based binder | [m] |
| u | Displacement | [m] |
| ν | Shear stress | [Pa] |
| ν_1 | Dimensionless factor | [-] |
| ν_2 | Dimensionless factor | [-] |
| ν_3 | Dimensionless factor | [-] |
| $\nu_{average}$ | Average shear stress | [Pa] |
| ν_c | Shear stress in concrete | [Pa] |
| ν_{ci} | Shear stress at crack | [Pa] |
| ν_f | Shear stress resistance due to fibres | [Pa] |
| ν_{max} | Maximum shear stress | [Pa] |
| ν_{min} | Minimum shear stress | [Pa] |
| ν_s | Shear stress resistance due to steel reinforcement | [Pa] |
| ν_u | Ultimate shear stress | [Pa] |
| w | Crack width | [m] |
| x | Distance to neutral axis | [m] |
| x_0 | Distance for applied load | [m] |
| y_0 | Depth of compressive area | [m] |
| z_0 | Centre of gravity | [m] |
| z_i | Distance from top of the cross section to the point of gravity | [m] |
| $z_{gg,c}$ | Centre of gravity for gross concrete cross section | [m] |

Greek letters

| | | |
|-----------------|---|-----|
| α_1 | Factor accounting for the bond characteristics of reinforcement | [-] |
| α_2 | Factor accounting for the sustained or repeated loading | [-] |
| α_s | Ratio between the modulus of elasticity for steel and concrete | [-] |
| β | Crack angle (upper bound solution) | [°] |
| Δ | Deflection | [m] |
| Δ_{cr} | Deflection for cracked cross section | [m] |
| ε | Strain | [-] |
| ε_1 | Principal tensile strain | [-] |
| ε_2 | Principal compressive strain | [-] |

| | | |
|---------------------------|---|-----|
| ε'_c | Strain in compressive reinforcement | [-] |
| ε_{c2} | Strain at maximum concrete compressive strength (parabolic behaviour) | [-] |
| ε_{c3} | Strain at maximum concrete compressive strength (bi-linear behaviour) | [-] |
| ε_{c0} | Initial compressive strain | [-] |
| ε_c | Concrete compressive strain | [-] |
| $\varepsilon_{c,u}$ | Concrete strain in upper part of a beam | [-] |
| ε_{cu} | Ultimate concrete compressive strain | [-] |
| ε_{cu2} | Ultimate compressive strain (parabolic behaviour) | [-] |
| ε_{cu3} | Ultimate compressive strain (bi-linear behaviour) | [-] |
| ε_{cr} | Tensile cracking strain for concrete | [-] |
| ε_f | Strain in fibre | [-] |
| ε_{fux} | Ultimate strain in longitudinal CFRP tows | [-] |
| $\varepsilon_{fx,ef}$ | Ultimate strain in longitudinal CFRP tows | [-] |
| ε_{fuz} | Ultimate strain in transverse CFRP tows | [-] |
| $\varepsilon_{fz,ef}$ | Effective strain in transverse CFRP tows | [-] |
| ε_l | Strain in lower part of a beam | [-] |
| ε_s | Strain in tensile reinforcement | [-] |
| ε'_s | Strain in compressive reinforcement | [-] |
| ε_{s0} | Strain in tensile reinforcement due to initial loading | [-] |
| ε_{t0} | Initial tensile strain | [-] |
| ε_x | Longitudinal strain | [-] |
| ε_y | Yield strain | [-] |
| ε_z | Transverse strain | [-] |
| $\dot{\varepsilon}^{(p)}$ | Plastic strain rate | [-] |
| Φ | Reinforcement degree | [-] |
| Φ_z | Transverse reinforcement degree | [-] |
| Φ_x | Longitudinal reinforcement degree | [-] |
| γ | Partial coefficient | [-] |
| γ_c | Partial coefficient for concrete | [-] |
| γ_n | Partial coefficient for the safety class at ultimate limit state | [-] |
| γ_{xz} | Shear strain | [-] |
| η | Reduction factor for vertical CFRP tows | [-] |
| η_{MBA} | Ratio for moduli of mineral-based binder and concrete | [-] |
| ι | Factor considering environmental aspects | [-] |
| λ | Reduction factor considering the concrete compression zone | [-] |
| θ | Direction of the plane of principal stress/strain | [°] |
| θ_{cr} | Inclination of crack | [°] |
| ρ_{bal} | Ratio for balanced cross section | [-] |

| | | |
|---------------|---|------|
| ρ_{f1} | Comparative parameter for yielding of the compressive reinforcement | [-] |
| ρ_{f2} | Comparative parameter for non yielding compressive reinforcement | [-] |
| ρ_{fb} | Ratio for balanced cross section | [-] |
| ρ_{fn} | Ratio for normally reinforced cross section | [-] |
| ρ_{fo} | Ratio for over reinforced cross section | [-] |
| ρ_{fx} | Ratio for longitudinal CFRP tows | [-] |
| ρ_{fz} | Ratio for transverse CFRP tows | [-] |
| ρ_l | Ratio for tensile reinforcement | [-] |
| ρ_{max} | Ratio for maximum reinforced cross section | [-] |
| ρ'_s | Ratio for compressive steel reinforcement | [-] |
| ρ_s | Ratio for tensile steel reinforcement | [-] |
| ρ_x | Longitudinal steel reinforcement ratio | [-] |
| ρ_z | Transverse steel reinforcement ratio | [-] |
| σ_2 | Principal compressive stress (limit analysis) | [Pa] |
| σ_c | Concrete compressive stress (limit analysis) | [Pa] |
| σ_{sz} | Stress in transverse steel reinforcement (limit analysis) | [Pa] |
| σ_x | Longitudinal stress (limit analysis) | [Pa] |
| σ_z | Transverse stress | [Pa] |
| σ^* | State of stress at or within the yield surface | [Pa] |
| τ | Shear stress (limit analysis) | [Pa] |
| τ_{xz} | Shear stress in the xz-plane (limit analysis) | [Pa] |
| ξ | Factor considering the size effect in shear (BBK design) | [-] |
| ψ | Ratio of maximum shear reinforcement contribution | [-] |
| ζ | Reduction factor for concrete compressive strength | [-] |

Table of content

| | | |
|----------|--|-----------|
| 1 | <u>INTRODUCTION</u> | 1 |
| 1.1 | BACKGROUND | 1 |
| 1.1.1 | NEED FOR REHABILITATION | 1 |
| 1.1.2 | CONCRETE STRENGTHENING | 2 |
| 1.1.3 | MINERAL-BASED STRENGTHENING SYSTEMS | 3 |
| 1.2 | HYPOTHESIS AND RESEARCH QUESTIONS | 4 |
| 1.3 | OBJECTIVE | 4 |
| 1.4 | LIMITATIONS | 4 |
| 1.5 | SCIENTIFIC APPROACH AND METHODS | 5 |
| 1.6 | THESIS GUIDE | 7 |
| 1.7 | ADDITIONAL PUBLICATIONS | 9 |
| 2 | <u>MINERAL-BASED STRENGTHENING</u> | 11 |
| 2.1 | DEFINITION OF MINERAL-BASED STRENGTHENING SYSTEM | 11 |
| 2.2 | CONSTITUENTS | 12 |
| 2.2.1 | BINDERS | 12 |
| 2.2.2 | FIBRE COMPOSITES | 17 |
| 2.3 | COMBINATIONS – EXISTING SYSTEMS | 21 |
| 2.4 | INTERACTION BETWEEN CONSTITUENTS | 23 |
| 2.4.1 | TRANSITION ZONE BETWEEN BINDER AND FIBRE COMPOSITE | 23 |
| 2.4.2 | CRACK CONTROL | 24 |
| 2.4.3 | SHRINKAGE | 26 |
| 3 | <u>FLEXURE AND SHEAR DESIGN FOR CONCRETE STRUCTURES</u> | 31 |
| 3.1 | INTRODUCTION | 31 |
| 3.2 | FLEXURAL CAPACITY | 31 |
| 3.2.1 | FLEXURAL RESPONSE OF REINFORCED CONCRETE STRUCTURES | 31 |
| 3.3 | SHEAR CAPACITY | 38 |
| 3.3.1 | INTRODUCTION | 38 |
| 3.3.2 | TRUSS ANALOGY | 42 |

| | | |
|------------|---|-----------|
| 3.3.3 | SEMI-EMPIRICAL “ADDITION” APPROACH | 44 |
| 3.3.4 | COMPRESSION FIELD APPROACHES | 51 |
| 3.3.5 | LIMIT ANALYSIS APPROACH | 69 |
| 3.4 | SHEAR DESIGN MODELS | 86 |
| 3.4.1 | FIXED ANGLE - TRUSS ANALOGY | 86 |
| 3.4.2 | LIMIT ANALYSIS AND VARIABLE ANGLE – TRUSS ANALOGY | 88 |
| 3.4.3 | EVALUATION OF DESIGN MODELS | 91 |

4 FLEXURE AND SHEAR DESIGN FOR MBC STRENGTHENING 97

| | | |
|------------|--|------------|
| 4.1 | INTRODUCTION | 97 |
| 4.2 | FLEXURAL DESIGN | 97 |
| 4.2.1 | POSSIBLE FAILURE MODES | 97 |
| 4.2.2 | STRESSES AND STRAINS FOR DIFFERENT FAILURE MODES | 98 |
| 4.2.3 | STRAIN RELATIONSHIPS FOR THE CROSS SECTION | 102 |
| 4.2.4 | FAILURE MODE CRITERION | 108 |
| 4.2.5 | SIMPLIFIED DESIGN – CONCRETE MEMBERS WITH NO COMPRESSIVE REINFORCEMENT | 109 |
| 4.2.6 | ESTIMATION OF FLEXURAL CAPACITY OF ONE-WAY SLABS | 111 |
| 4.3 | SHEAR DESIGN | 115 |
| 4.3.1 | INTRODUCTION | 115 |
| 4.3.2 | “ADDITION” APPROACH BASED ON 45° TRUSS ANALOGY | 117 |
| 4.3.3 | VARIABLE ANGLE TRUSS APPROACH | 118 |
| 4.3.4 | MODIFIED COMPRESSION FIELD THEORY | 119 |
| 4.3.5 | ADDITIONAL REMARKS | 125 |
| 4.3.6 | ESTIMATION OF SHEAR CAPACITY FOR REINFORCED CONCRETE BEAMS | 127 |

5 DISCUSSION AND CONCLUSIONS 133

| | | |
|------------|---------------------------------------|------------|
| 5.1 | DISCUSSION | 133 |
| 5.2 | CONCLUSION | 135 |
| 5.3 | SUGGESTIONS ON FUTURE RESEARCH | 136 |

REFERENCES 139

| |
|-------------------------------|
| APPENDIX A – PAPER I |
| APPENDIX B – PAPER II |
| APPENDIX C – PAPER III |
| APPENDIX D – PAPER IV |
| APPENDIX E – PAPER V |
| APPENDIX F – PAPER VI |

1 Introduction

1.1 Background

1.1.1 Need for rehabilitation

Concrete is a composite material made from sand, gravel and cement. The cement is a blend of various minerals and when mixed with water a chemical reaction is created that binds the sand and gravel into a stiff solid mass. Concrete as defined above has been used for many thousands of years. The oldest known surviving concrete is to be found in the former Yugoslavia and was thought to have been laid in 5,600 BC using red lime as the cement. The Romans further developed the concrete with the use of light weight aggregates and bronze reinforcement as in the roof of the Pantheon in Rome. However, the thermal incompatibility between bronze and concrete became evident with concrete spalling as a negative aspect to durability. After the Romans, little or no progress happened until the industrial revolution when Joseph Aspdin and others started to burn cement clinker.

In the 1850s a patent by William Wilkinson of Newcastle, U.K. was proposed for using steel rods in concrete, Joyce and Brown (1966). By joining a material with excellent compressive behaviour (concrete) and a material with great tensile properties (steel), the steel reinforced concrete was born. This time having similar thermal expansion and being under the right circumstances the steel was protected from both physical and chemical attack by the concrete.

However, the statement above is the ideal scenario. Many of the existing reinforced concrete structures in the world are subjected to environments that do not positively affect the durability. There are a number of different aspects contributing to the degradation of reinforced concrete structures. Three main types are identified here, *physical* (water and moisture transport, freezing, shrinkage, fatigue, abrasion, early age cracking etc.), *mechanical* (excessive loading, vibration, explosion, settlements, impact etc.) and *chemical* (depassivation of steel, chloride intrusion, corrosion, salt crystallization etc.). In addition to these concrete deficiencies can be originated in the design phase (poor detailing, calculation errors etc.) and construction phase (poor workmanship, mistakes, material insufficiencies etc.). In addition, since the society changes over time so also does the demand on structural sustainability. The demand on a bridge 60 years ago will not be the same as on a bridge today with increasing loads and traffic volumes.

In the most optimum and simplified way, any investments should follow the “law-of-fives”, see Figure 1.1

The law of fives: “One Euro spent in Phase A equals to five Euros in Phase B equals twenty five Euros in Phase C equals to one-hundred-and-twenty-five Euros in Phase D. This implies that a little extra attention to “good engineering practice” during Phase A will reduce the cost under operation of the structure”, Fib Bulletin 3 (1999).

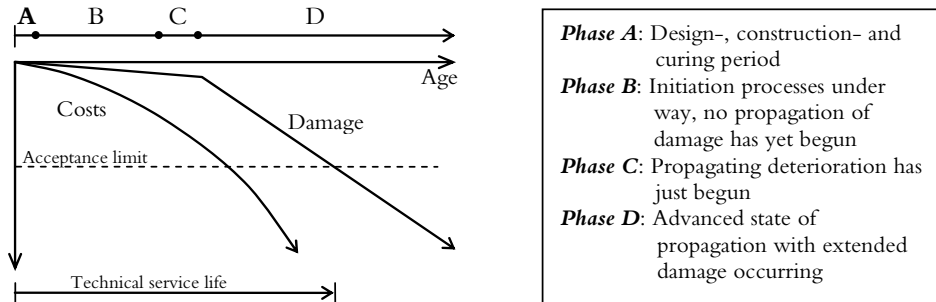


Figure 1.1. Service life of a concrete structure. Fib Bulletin 3 (1999)

Thus, if suitable measures are made in due time, money and resources can be saved. One of the suitable measures can be repair or strengthening of a structure instead of replacing it. In the European funded research project, Sustainable Bridges, a cost proposal was illustrated, Sustainable Bridges (2004). The cost for replacing a 100 m² bridge in Great Britain is approximately 1.4 M€. The cost for repair of a typical bridge is approximately 3 k€/m². This means that the savings for each bridge that can be repaired instead of replaced is 1.1 M€. A preliminary inventory indicates that there exists about 500 000 bridges in need of repair or strengthening in Western Europe.

1.1.2 Concrete strengthening

Traditional methods of repairing and strengthening concrete structures can be widening the cross section, using external pre-stressing or steel plate bonding etc. Alternatively, a non corrosive material, such as fibre reinforced polymers (FRP) can be bonded to the surface of the structure. FRP materials possess three mechanical properties of interest; high tensile strength, high modulus of elasticity and linear elastic stress-strain behaviour. One of the critical parameters in strengthening existing structures is the choice of bonding material between the FRP and concrete surface, Rizkalla et al. (2003).

Strengthening systems with the use of continuous carbon fibres in an epoxy matrix bonded to concrete structures has proven to be a successful methodology since the late 1980s, Meier, (1987), Triantafillou and Plevris (1992), Tepfers (1998), Fukuyama and Sugano (2000) and Nordin (2003). However, these methods present some important disadvantages such as the use of organic resins (especially epoxies) which create a hazardous working environment for the manual worker and have low permeability, diffusion tightness, poor thermal compatibility with concrete and sensitivity to moisture at application. In addition, most of the epoxies are also sensitive to low temperatures at

application and after being installed cannot normally withstand temperatures above 70 °C.

Strengthening civil structures with the use of a bonding material that is more compatible with the concrete is of great interest. Using mineral-based bonding agents such as fine grained mortars in combination with high strength fibres or FRPs is one way of creating a more environmentally friendly and sustainable strengthening system. In this thesis these strengthening systems are referred to as mineral-based strengthening systems.

1.1.3 Mineral-based strengthening systems

The mineral-based composites can be divided into two main components, namely *binder* and *fibre composite*. There exists a vast complexity when it comes to the binders. It has to have excellent properties, not only, to bond with the base concrete but also have good workability and be cost efficient. In addition, the binder/bonding agent has to be able to transfer stresses to the fibre composite in an efficient manner. The fibre composite has to have excellent tensile properties and be designed to be compatible with the binder/bonding agent.

There exist numerous variations on how to design both the binder/bonding agent and the fibre composites. Fine grained mortars are often used as binders/bonding agents. For bridging cracks and to provide a better stress distribution in the binder/bonding agent chopped or milled fibres can be used, this is further elaborated in chapter 2 and appended Paper III and Paper IV. The fibre composite can be tailor-made with different geometries and different mechanical properties. Common designs of fibre composites are unidirectional rods and sheets or two dimensional textiles or grids. When combining different binders/bonding agents and different fibre composites a mineral-based strengthening system is obtained. So far there exist a few mineral-based strengthening systems around the world. Examples of these are textile reinforced concrete (TRC), textile reinforced mortars (TRM), fibre reinforced composites (FRC) and the mineral-based composites (MBC), Rilem report 36 (2006), Triantafillou and Papanicolau (2006), Wu and Teng (2002) and Blanksvärd (2007). The TRC is developed in Aachen and Dresden, Germany, and TRM is developed in Patras, Greece, common for these systems is that they use a textile as the fibre composite. The FRC is developed in Detroit, USA, and uses continuous fibre composites. The MBC was first developed in Luleå, Sweden, and is the topic of this thesis.

The MBC system involves using a grid of fibre composite and the assembly of the strengthening system is fairly uncomplicated. The surface of the base concrete in need of strengthening is first prepared by removing the cement laitance with a surface roughening method, e.g. sand blasting or water jetting. The strengthening system is applied in four consecutive steps. Firstly, a surface primer is applied on the roughened base concrete surface to reduce moisture transport from the polymer modified mortar to the fairly dry base concrete. Secondly, one layer of a cementitious bonding agent is applied on the primed base concrete surface. Thirdly, the FRP is applied on the first mortar layer (in the present thesis a CFRP grid is used). Finally, a second layer of

mortar is applied on top of the first layer and the FRP. A more elaborate description is shown in Paper III and Blanksvärd (2007).

1.2 Hypothesis and research questions

In the initiation of this PhD program one important hypothesis was stated:

- Using mineral-based bonding agents in combination with carbon fibre reinforced polymers will create a competitive repair and strengthening system for concrete structures.

The work in this thesis has aimed to answer the following research questions:

- Can MBC systems be used for concrete repair and strengthening?
- Can MBC systems obtain a comparable strengthening effect as for externally epoxy bonded CFRP systems?
- Is it possible to estimate the ultimate load carrying capacity for MBC strengthened concrete members, in flexure and shear, by using existing design or slightly modified design models?

Additionally, what modifications of the MBC system need to be done to create a practical and usable strengthening system?

1.3 Objective

The first objective within the research project was to verify that the MBC system could be applied and bonded to a concrete surface. Secondly, the strengthening effect was investigated and thirdly, analytical models were further modified.

1.4 Limitations

Since it is not possible to cover all aspects concerning the behaviour of the MBC system subjected to flexure and shear loading, there are some overall limiting factors. Only a two dimensional and epoxy-impregnated orthogonal grid was used together with fine grade mortars. In addition to this, only commercially available mortars were used. Only rectangular geometry of specimens was considered in the analytical approach. In the analytical approach there is no consideration to anchorage or other bond failures. Further, the influence on bond regarding drying shrinkage is not within the scope of this thesis but is commented on in both chapter 2 and in the suggestions for future research.

In the shear design some further limitations were adopted. Design was based on continuity regions with evenly distributed stresses. No consideration is taken to the discontinuity regions, see Figure 1.2. No axial loads such as pre-stressing are considered and the shear reinforcement in the concrete elements are primarily to be considered as orthogonal to the longitudinal axis. The shear design only contemplates traditional beams with a constant cross section and does not deal with walls, deep beams etc.

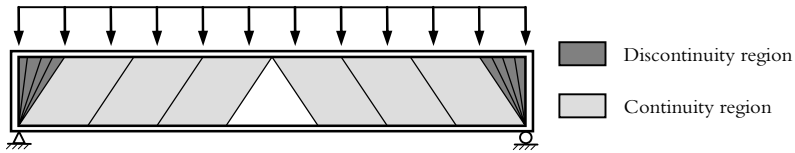


Figure 1.2. Continuity regions and discontinuity regions for shear.

1.5 Scientific approach and methods

The traditional way of doing a PhD thesis at Luleå University of Technology, division of Structural Engineering, can be divided into the following steps. First, the hypothesis of the research is stated. Then the researcher embarks on the first stage gathering knowledge, normally by doing a vast literature study within the field of research. After gathering the state of the art knowledge, research questions are stated and investigations are made based in both theory and experiments to give answers to the stated questions. Half-way into the PhD, normally after two and a half years, the researcher is offered the possibility to write a “Licentiate thesis”, which in layman terms is the equivalent of a half doctoral thesis. After writing the Licentiate thesis the researcher can chose two primary paths, one leading to working in the industry and the other towards finishing the PhD. If the researcher chooses to continue with the PhD studies, a doctoral thesis is produced but in more theoretical depth compared with the previous Licentiate thesis. This has been the order in which the present thesis was produced.

All of the work within the thesis is based on an extended summary supported by peer reviewed journal and conference papers. The methods for obtaining answers to the research questions lie within surveying existing mineral-based strengthening systems i.e. finding suitable materials and composing a strengthening system, theoretically investigating the performance of the chosen system and finally planning and performing experimental tests to produce physical evidence or indications.

This thesis comprises six papers spanning from material and composite behaviour to flexural and shear strengthening using the MBC system and also discussing the behaviour of different mineral-based strengthening systems. In *Paper I*, the flexural behaviour of the MBC system compared to epoxy bonded sheets was discussed based on larger reinforced concrete specimens subjected to four-point bending together with a small scale pilot study testing the influence of different mineral-based bonding agents. This was the first paper written on the topic of MBC strengthening and it gave some significant input that concrete beams could be strengthened for increased flexure resistance. After the findings in the field of flexural strengthening, a natural way of proceeding was to continue within the field of shear strengthening due to the biaxial geometry of the CFRP grid. Pilot test series on shear strengthened beams with a rectangular cross section was conducted using mineral-based bonding agents with different mechanical properties together with using grids with different geometries and carbon fibre content. These pilot studies showed that the MBC system has potential to

reach similar ultimate shear loads as for epoxy bonded CFRP sheets. After the pilot studies the best suited materials were chosen in more a comprehensive experimental study in four-point bending investigating the influence of steel shear reinforcement. These beams were designed using the Swedish design code BBK (2004). The ultimate loads based on this design indicated that the beams should have failed in shear. However, at the ultimate load it was revealed that the failure mode was not in shear but yielding of the tensile reinforcement and thus crushing of the concrete in the compression zone. The specimens were monitored using both strain gauges and photometric measurements; see e.g. SB-MON (2007) and Aho et al. (2007). It was possible to see how the MBC system behaved during increased shear loading. These results from shear strengthening are summarized in *Paper II* and the behaviour of the MBC strengthened beams during the initiation of shear cracks in *Paper VI*.

Following the recommended design for shear resistance indicates that there is conservatism in the shear design models. Therefore, the background to designing reinforced concrete in shear had to be investigated thoroughly in order to obtain a more comprehensive design model for MBC systems when used for shear strengthening. This is presented in *Paper V* for the MBC system and in *chapter 3* a more elaborated background on shear design of concrete beams is given. *Chapter 4* summarizes the suggestions on how to design reinforced concrete beams strengthened with the MBC system for both flexure and shear. However, there are other ways of designing mineral-based strengthening systems. *Paper III* compares different mineral-based strengthening systems mainly using different types of fibre composites. In this paper it can be seen that the MBC system performs quite well in comparison to other strengthening systems.

During the development of the MBC system at Luleå University of Technology another PhD project at Technical University of Denmark was initiated. In that PhD project the aim was set to investigate the tensile behaviour of both fibre composite and binder and how the MBC system acts as bonded to a concrete surface. Furthermore, that PhD project also investigated the possibility of using engineered cementitious composites (ECC) as a binder/bonding agent for its excellent crack bridging abilities. Both the work done within this PhD project and the one at Technical University of Denmark progressed side by side with mutual discussion and planning. The results from this collaboration are summarised in *Paper IV* together with a mapping of possible constituents that can be used in a mineral-based strengthening system. In *chapter 2* this mapping is further and more comprehensively elaborated together with a full description of the MBC system. An overview of how the different papers interconnect with each other going from a flexural point of view in *Paper I* to *Paper III*, switching to shear behaviour in *Paper III* and progressing to *Paper II*, *Paper V* and *Paper VI*, are shown in Figure 1.3. *Paper IV* is the paper that describes the material behaviour, along with the behaviour of the MBC component bonded to a concrete surface and also gives concepts for how to implement the systems for industrial use. All output in the form of discussion, conclusion, answers to research questions and suggestions for future research are presented in *chapter 5*.

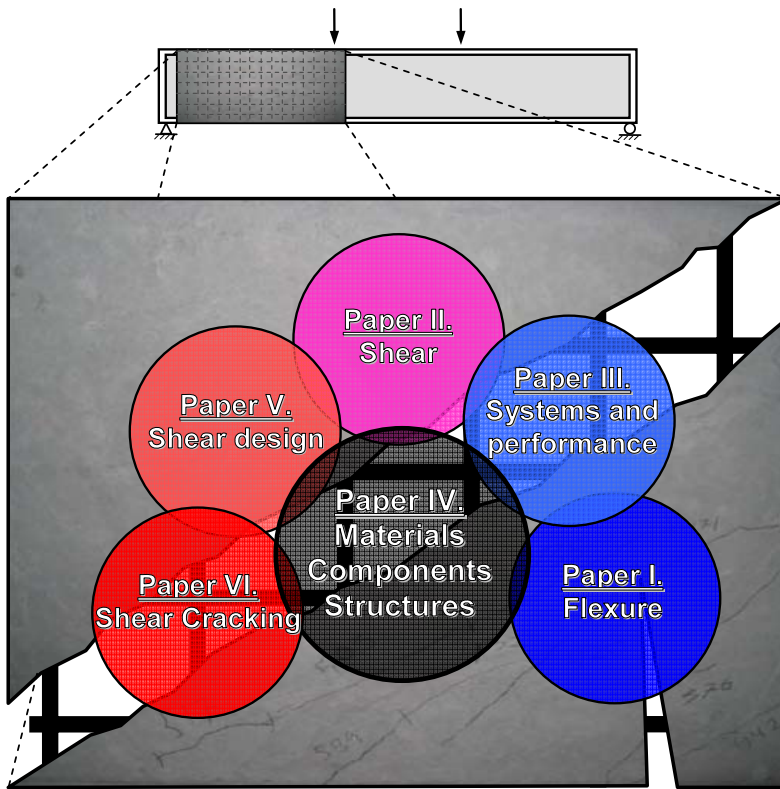


Figure 1.3. Connections of papers in the thesis, illustrated for a beam with flexure and shear cracks.

1.6 Thesis guide

This chapter describes briefly the structure of the thesis in order for the reader to obtain a clear overview of the content and ease the reading of this thesis.

- Chapter 2 gives an introduction to the materials, components and possibilities of designing a mineral-based strengthening system for concrete structures.
- Chapter 3 presents the fundamental concepts of designing concrete for shear.
- Chapter 4 describes the suggested designs for calculating the load carrying capacity of reinforced concrete structures strengthened with the MBC system developed at Luleå University of Technology. These design proposals concern both flexural and shear strengthening.

- Chapter 5 is the last chapter and here both discussion and conclusions derived from the content in this thesis are given along with suggestions for future research.
- Appendix A is the Paper I, titled “Mineral-based bonding of carbon FRP to strengthen concrete structures”. Published in the *Journal of Composites for Construction* (2007). Authors are Björn Täljsten and Thomas Blanksvärd. My contribution to this paper consists of evaluating, performing and planning parts of the experimental tests and co-writing the text and figures.
- Appendix B is the Paper II, titled “Shear strengthening of concrete structures with the use of mineral based composites (MBC)”. Published in the *Journal of Composites for Construction* (2008). Authors are Thomas Blanksvärd, Björn Täljsten and Anders Carolin. My contribution to this paper consists of planning the test series in collaboration with the co-authors, performing the experimental tests evaluating and writing major parts of the paper.
- Appendix C is the Paper III, titled “Strengthening of concrete structures with cement based bonded composites”. Published in the *Journal of Nordic Concrete Research* (2008). Authors are Thomas Blanksvärd and Björn Täljsten. My contribution to this paper consists of performing a literature study, evaluating the results and writing major parts of the paper.
- Appendix D is the Paper IV, titled “From material level to structural use of MBC – an overview”. Submitted to the *Journal of Materials and Structures* (2009). Authors are Katalin Orosz, Thomas Blanksvärd, Björn Täljsten and Gregor Fischer. My contribution to this paper is being a small part of the planning of the dogbone and wedge splitting tests, performing material tests and shear tests, planning, evaluating and writing the paper with the first author.
- Appendix E is the Paper V, titled “Shear design for concrete strengthened with mineral based composites”. Submitted to *ACI Structural Journal* (2009). Authors are Thomas Blanksvärd, Björn Täljsten and Lennart Elfgren. My contribution to this paper is planning and writing the paper with the supervision of the co-authors.
- Appendix F is the Paper VI, titled “Shear crack propagation in MBC strengthened concrete beams”. Published in the proceedings of the 4th *International Conference on FRP Composites in Civil Engineering* (2008). Authors are Thomas Blanksvärd, Anders Carolin and Björn Täljsten. My contribution in this paper was planning and writing the paper with the supervision of the co-authors. This paper gives me a special joy since I was decorated with the Mirco Roš silver medal from the research institute EMPA in Zürich, Switzerland. With the motivation “Excellent paper” – Urs Meier head of EMPA and one of the pioneers in strengthening concrete with FRPs.

1.7 Additional publications

During my PhD study I have also managed to make additional publications which are not included in this thesis. The following is a list of all publications divided into thesis, journal papers, conference papers, reports and popular science.

Licentiate thesis

Blanksvärd, T. (2007) *Strengthening of concrete structures by the use of mineral based composites*. Licentiate thesis 2007:15, Luleå University of Technology, department of civil and environmental engineering, ISBN: 91-85685-07-3, pp. 300.

Journal papers

Johnsson, H., Blanksvärd, T., and Carolin, A. (2006). *Glulam members strengthened by carbon fibre reinforcement*. *Materials and Structures*, 40(1), pp. 47-56.

Conference papers

Täljsten, B., and Johansson, T. (2005) *Mineral Based Bonding of CFRP to Strengthen Concrete Structures*. Proceedings of the Nordic Concrete Research Meeting, Sandefjord, Norway, 13-16 June, pp. 343-345.

Täljsten, B., and Johansson, T. (2005) *Mineral Based Bonding of CFRP to strengthen Concrete Structures*. in proceedings of ICCRRR 2005 – International Conference on Concrete Repair, Rehabilitation and Retrofitting, Cape Town, South Africa, 21-23 November.

Johansson, T., and Täljsten, B. (2005). *End Peeling of Mineral Based CFRP Strengthened Concrete Structures- A Parametric Study*. in proceedings of BBFS – International Symposium on Bond Behaviour of FRP in Structures, Hong Kong, China, 7-9 December, pp. 205-212.

Blanksvärd, T., Carolin, A., Täljsten, B., and Rosell, E. (2006) *Mineral based bonding of CFRP to strengthen concrete structures*. Proceedings of the Third International Conference on Bridge Maintenance, Safety and Management, Porto, Portugal, 16-19 July, CD-publication and extended abstracts.

Blanksvärd, T., and Täljsten, B. (2008) *CFRP and mineral based bonding agents to strengthen concrete structures*. Proceeding of the 20th Symposium on Nordic Concrete Research and Development, Bålsta, Sweden, 8-11 June 2008, pp. 189-190.

Täljsten B., Blanksvärd, T., and Carolin, A., (2007), "*Mineral based bonding of CFRP to strengthen concrete structures*", International Conference in Wroclaw, Poland, October 2007, ISBN 978-83-7125-161-0, pp. 331-339

Täljsten B., Orosz K., and Blanksvärd, T. (2006), "*Strengthening of Concrete Beams in Shear with Mineral Based Composites, Laboratory tests and theory*". Third International Conference on FRP Composites in Civil Engineering. Miami, Florida, USA, 13-15 December 2006, pp 609-612.

-Best Paper award on Conference.

Reports

Johansson, T. (2005) *Strengthening of concrete structures by Mineral Based Composites*. Research report 2005:10, Luleå University of Technology, Division of Structural Engineering, Department of Civil and Environmental Engineering.

Johansson, T. (2005) *Förstärkning av fönsterram: en förstudie av trätvärsnitt förstärkta med kolfiberkompositstavar*. Technical report 2005:14, Luleå University of Technology, Division of Structural Engineering, Department of Civil and Environmental Engineering. [in Swedish]

Blanksvärd, T. (2006). *Mechanical properties of different geometries of CFRP grid: tensile evaluation of material properties*. Research report 2006:06, Luleå University of Technology, Division of Structural Engineering, Department of Civil and Environmental Engineering.

Popular science

Blanksvärd, T. (2007) *Förstärkning av betong med mineralbaserade kompositer*. Väg- och vattenbyggaren, 5, November, pp. 70-75. [in Swedish]

2 Mineral-based Strengthening

2.1 Definition of mineral-based strengthening system

The definition, in this thesis, of a mineral-based strengthening system is “a high strength and light weight fibre material bonded to a concrete surface using fine grade mineral-based binder”. This chapter is an extension of the mapping of typical constituents in mineral-based strengthening systems mentioned in both Paper III and Paper IV. Similar mapping of typical constituents in mineral-based strengthening systems can be found in Blanksvärd (2007) and Johansson (2005).

Figure 2.1 shows the key parameters for mineral-based strengthening systems. First there must be a concrete structure in need of repair or strengthening. Then a mineral-based strengthening system should be chosen. There exist a number of combinations for how to configure a mineral-based strengthening system, mainly based on the chosen constituents. A mineral-based strengthening system can be subdivided in to two categories depending on the use of *binder* and *fibre composite*. Logically, the binder is used to bond the fibre composite to the structure and the function of the fibre composite is basically to resist and redistribute stresses in the strengthened structure. The mechanical and workability properties of the binder depend on the minerals used as binder, what kind of additives that are implemented and the mixture of constituents, this is elaborated further in chapter 2.2.1. In addition, there exist many combinations of the choice of fibre composites. Depending on the application and required properties of the mineral-based strengthening system, different fibre materials can be used. These properties depend on the use of fibre, if the fibres are impregnated with a polymer matrix and also the geometry of the fibre composite. Different configurations of the fibre composites are elaborated in section 2.2.2.

The behaviour of the mineral-based strengthening system is highly dependent on the interaction between the chosen binder and fibre composite, often referred to as bond in the transition zone between these two constituents. Another source of interaction is then the bond between the concrete structure and the mineral-based binder. The latter is not within the scope of this thesis, but nevertheless a short description of problems that can occur due to drying shrinkage is shown in section 2.4.3. The different sorts of interactions are shortly described in section 2.4.

A short description of different combinations existing in mineral-based strengthening systems is given in section 2.3.

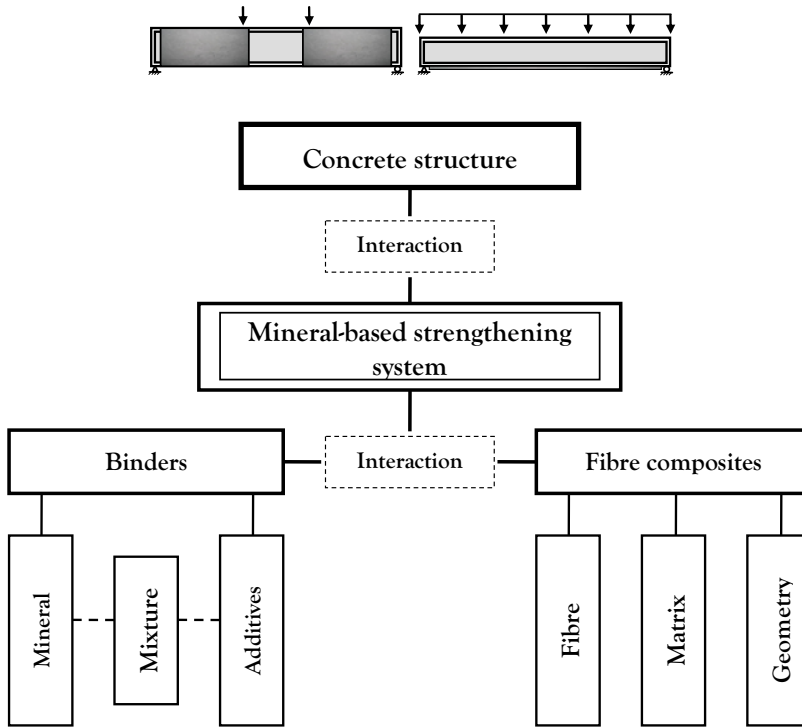


Figure 2.1. Mapping of constituents in mineral-based strengthening systems.

2.2 Constituents

As mentioned above, the behaviour of the mineral-based strengthening system is highly dependent on the chosen constituents. This chapter will describe the most common constituents for both binders and fibre composites and their differences. By tailoring proper minerals together with additives will give a high performance binder, discussed in the end of chapter 2.2.1, Engineered Cementitious Composites (ECC). The most common designs of fibre composites are described in section 2.2.2.

2.2.1 Binders

There exist many combinations of how to design the binders used in a mineral-based strengthening system. Although the design of different binders is not within the scope of this thesis it is important to show that there exist opportunities to tailor-make the binders in mineral-based strengthening systems. The design of the binders depends on what type of properties that are desired and the chosen type of fibre composite. Desired properties can be workability, bond, tensile strength, compressive strength, flexural strength, shear strength, crack bridging ability etc.

Minerals

This section will state some of the suitable minerals that are compatible with concrete. Examples of these minerals can be ordinary Portland cement, fly ash, silica fume etc. The most common approach is to combine/mix these minerals and to add some fine grade aggregates <2 mm. To further enhance the properties additives can be added in form of polymers, fibres and super plasticizers. The final product is defined by the mixing proportions of the constituents. Different additives and the influence of mixing proportions are discussed below.

Additives

Addition of different polymers enhances the properties of ordinary Portland cement. However, there are also a number of chemical admixtures, such as water reducing agents, ashes, aluminosilicate, superplasticizers, etc., that further improve the quality of the mineral-based binder. Other ways to improve the performance can be by adding reinforcing fibres. All of the above mentioned improvements can enhance strength, shorten setting time, decrease autogenous shrinkage, control alkali aggregate reaction, reduce the risk of chloride induced corrosion of embedded steel, improve the durability, etc. (Li and Ding, 2003).

Polymers

The most common application of polymers is made by replacing a part or all of the cement hydrate binder of conventional mortar or concrete with polymers. The polymeric compound modifies or improves the properties of cement mortar and concrete, such as strength, deformability, adhesion, water resistance and durability. The polymer-based admixtures are often referred to as polymer modified mortars (PMM) and polymer modified concrete (PMC). Compared with ordinary cement mortar and concrete, the properties of polymer modified mortar and polymer modified concrete depend greatly on the polymer content or polymer-cement ratio rather than the water-cement ratio (Ohama, 1998).

The classification of polymer-based admixtures can be divided into four main types: Polymer latex or polymer dispersion, redispersible polymer powder, water-soluble polymer and liquid polymer. This is, however, not dealt with in this thesis and can be further studied in Wagner (1965), Schweite et al. (1969), Wagner and Grenely (1978), Beeldens et al. (2003) and Ohama (1998).

Superplasticizers

An additional type of low molecular-weight water-based polymer is the superplasticizers, which are primarily surface active agents that allow a large reduction of the water content without loss of workability. Thus, to increase the fluidity of fresh mineral-based binders (e.g. mortars) for pumping, increasing the strength and prolong the durability of hardened binder, a small quantity of superplasticizers are often added into the mixture. Some superplasticizers can lose entrained air and control the setting

time or hardening process without other side effects, (Hewlett, 1988). However, the single application of some superplasticizers can develop complications in the form of excessive bleeding, segregation and early loss of workability. Using them in combination with latex polymers could minimize these complications.

Note, there is often a compatibility problem between superplasticizers and the polymer modified mortar or concrete. The choice of polymers and superplasticizers to be added to the Portland cement is therefore of great significance (Ray and Gupta, 1994, 1995).

Chopped or milled fibres

In order to obtain high performance binders for utilization in special applications, such as shotcreting, strengthening or mining. The incorporation of fibres in mineral-based binders can be either

- Chopped or milled short fibres
- Continuous fibres

Continuous fibres are more expensive and not easily mixed into the cement matrix. Chopped or milled fibres have less mechanical efficiency compared to continuous fibres. Different types of fibres can be used, such as steel, glass, carbon, polypropylene and natural fibres (Groth, 2000; Cuyppers et al., 2006; Garcés et al., 2005 and Agopyan et al., 2005). Drying shrinkage can be reduced by adding fibres in mineral-based binders. However, incorporating fibres in the binder will generally reduce the compressive strength, thus increasing the permeability (Gutiérrez et al., 2005). These insufficiencies can be bridged through the use of supplementary materials that will lead to a densification of the binder matrix, e.g. substituting cement for fly ash or silica fume. In the case of polypropylene reinforcing fibres, a suitable proportion of 2.0% is recommended; with an addition of 0.5% melamine formaldehyde dispersion, (Garcia Santos et al., 2005), where the melamine formaldehyde is a polymer dispersion additive. As stated above, adding silica fume will improve the mechanical properties, such as compressive strength and flexural strength for cement based matrices, especially for the use of steel and glass fibres. Incorporating silica fume will generally improve the water absorption properties due to a reduction of permeable voids, (Gutiérrez et al., 2005). Durability problems can occur if the porosity of the concrete or mortar is increased. The increase in porosity will increase the chloride penetration, which is a disadvantage if steel is incorporated in the mineral-based binder. When incorporating carbon fibres into the mortar a content of 0.5% of cement weight will give an optimum increase in flexural strength, (Garcés et al., 2005).

In the case of continuous fibres the load bearing capacity and crack loads are highly dependent on the design of the fibre bundles and the fibre material itself. A study on mechanical properties for glass and carbon yarn reinforced mortar was performed by Langlois et al. (2007). Their study showed the effectiveness of the yarns, where the most significant difference was between the glass yarn and carbon yarn, with glass fibre yarn having the best effectiveness. The study also indicated that the glass yarn samples had better penetration and bond to the mortar matrix. Still, the carbon yarn

incorporated specimens had better strength over time when compared to the glass yarn reinforced mortars.

Mixtures

Water to cement ratio

Schulze (1999) investigated the influences of water to cement ratio and cement content on the properties of polymer modified mortar. The study shows that the compressive strength decreases with increasing water cement ratio, and that the cement content is of minor influence. A higher cement content and higher water cement ratio induce increased shrinkage and water absorption. The flexural strength is nearly independent of the water to cement ratio and cement content in unmodified mortars at water to cement ratios of 0.4-0.6. This contradicts some previously published work, e.g. Wendehorst (1992), but confirms other data, e.g. Beton (1990). The flexural strength in polymer modified mortars is increased in comparison to the unmodified mortars. There is only a small increase of the flexural strength with a decreasing water to cement ratio at a constant cement level in the formula. However, there is a distinctive increase in flexural strength with decreasing water to cement ratio when the mortar is stored in water.

Polymer to cement ratios

The polymer to cement ratio, P/C, is defined as the weight ratio of the amount of total solids in the polymers to the amount of cement in the modified mortar or concrete mixture Ohama, (1995).

Compared with ordinary cement mortar and concrete, the properties of polymer modified mortar and concrete depend more on the polymer content or polymer to cement ratio than the water to cement ratio. Three-point bending tests show that the maximum load is fairly constant for mortars with a P/C ratio 7.5 wt.% or lower. Flexural strength increases with a further addition of polymers, where the P/C ratio is between 10 to 15 wt.%. A P/C ratio higher than 15 wt.% decreases the mechanical strength Pascal et al. (2004) and Van Gemert et al. (2005). The improvement of the tensile and flexural strength for polymer modified mortars with latex rubber is explained by the formation of continuous polymer networks within the mortar at P/C ratios higher than 10 wt.%, Justnes and Oye (1990). Similarly, the retardation of cement hydration is compensated by the presence of the polymer film, which influences the flexural strength, Van Gemert et al. (2005).

Engineered cementitious composites (ECC)

Optimisation of minerals, additives and mixtures can render a mineral-based binder with superior tensile properties compared to ordinary quasi brittle polymer modified mortars. An example of this optimisation is the engineered cementitious composites (ECC) developed by Victor Li and associates. Another acronym for ECC mentioned in literature is high performance fibre reinforced cementitious composites (HPFRCC),

Shi and Mo (2008), where HPFRCC is the common name for cementitious composites with strain hardening properties. This section will briefly discuss the ECC as a mineral-based binder. Fibre bridging and strain hardening abilities of the ECC (and HPFRCC materials in general) is further discussed in section 2.4.2.

ECC is a mortar-based composite that is reinforced with short random fibres, such as polyethylene (PE) or polyvinyl alcohol (PVA). The use of PVA fibres has better tensile crack bridging properties while the use of PE fibres shows a better compressive behaviour, Fischer and Li (2007). ECC is a micromechanically designed material in contrast to general HPFRCC. ECC uses a micromechanical model to tailor-make the required properties. By using this micromechanical tool, the fibre amount used in the ECC is typically 2% by volume. Thus, ECC is designed to resist large tensile and shear forces but at the same time has compatible properties, such as compressive strength and thermal expansion, to ordinary concrete based on Portland cement Li (2002). The excellent tensile properties of ECC come from a tensile strain hardening behaviour originating in the formation and development of micro cracks. Instead of having one or a few widening cracks as for traditional mortars, the micro cracks in ECC remain fairly constant at increasing strain. This behaviour is governed by the crack bridging effect of the fibres, so by increasing the deformation will just render new crack formations.

A typical tensile behaviour of ECC is shown in Figure 2.2. After the formation of the first crack the composite undergoes plastic yielding and pseudo strain hardening up to the strain level at which a macroscopic crack is formed. This tensile strain level is usually 150-350 times that of normal concrete, Fisher and Li (2007) and Lepech and Li (2008). Using this material with these tensile and shear properties as the binder in a mineral-based strengthening system would be optimal.

Note, and this is the author's opinion after working with the ECC, it is not clear that the workability with the ECC is the most optimal for the hand lay up technique of the MBC system described in Paper III. However, a material design methodology and batching sequence for large scale commercial batching of ECC processing is stated in Lepech and Li (2008). There are also experimental results showing that the ECC can be used as wet-mix shotcreting Kim et al. (2004).

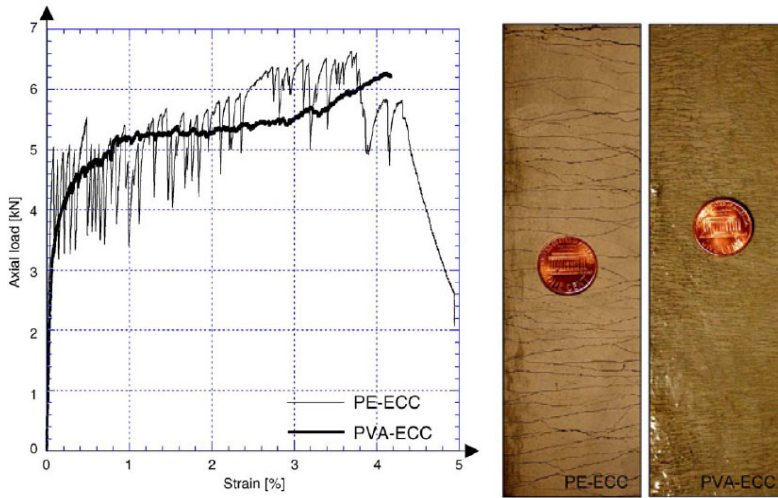


Figure 2.2. Tensile stress-strain behaviour and tensile cracking of ECC with PE and PVA fibres, Fischer and Li (2007).

2.2.2 Fibre composites

Fibre reinforced composite materials can mainly be divided into two categories; short fibre reinforced materials and continuous fibre reinforced materials. The short fibre reinforced materials are typically employed in applications of compression moulding and sheet moulding. These applications are not within the scope of this thesis and are hereafter not mentioned any further. The other type of fibre materials is the continuous fibre materials which are frequently used in structural applications. The continuous fibre materials can be produced as unidirectional sheets, weaves or different geometries. Further, the fibres can also be pre-impregnated with a given matrix (resin) and in those cases are commonly named fibre reinforced polymers (FRP). The main function of the matrix is to transfer forces between fibres, and to a lesser degree protect the fibres from environmental impact. The behaviour and mechanical properties of the fibre composite strongly depends on the types of fibres being used, if the fibres are pre-impregnated or on the chosen geometry. The next section will give some examples of different fibres and possible matrices and their mechanical properties and also typical geometries of the fibre composites used in mineral-based strengthening systems. It is important to state that most fibre composites are generally orthotropic in their nature.

Fibres

The most commonly used fibres in civil structural applications are glass-, carbon- and aramid fibres. The mechanical properties and cost of these fibres varies, with carbon fibre having the best potential regarding strength and stiffness while glass fibres are less costly and have a greater potential of elongation. Common for these fibres is that they

have higher failure strength than steel and are linearly elastic until failure, see Figure 2.3. A short description of each fibre type is given below.

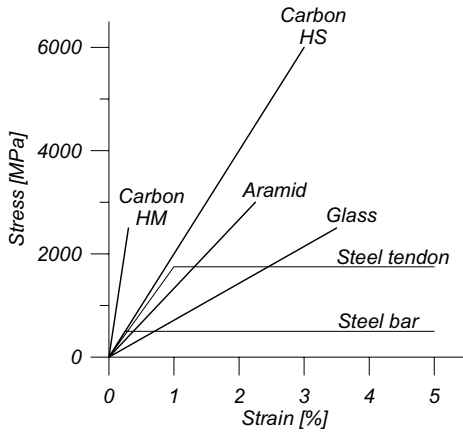


Figure 2.3. Properties of different fibres and typical reinforcing steel. HS stands for High Strength and HM for High elastic Modulus, Carolin (2003).

Carbon fibre

Carbon fibres were developed in Great Britain in the search for a stiff, strong and lightweight material. Carbon fibre, which is an inorganic fibre, is manufactured in bundles of about $1\text{--}5 \cdot 10^4$ individual fibres with a diameter of 5–15 μm . Two main production processes are needed to manufacture carbon fibre, with the raw material differentiating the two processes. The best and most costly carbon fibres are manufactured from polyacrylonitrile (PAN). These are also the most current fibres for load carrying purposes with a high modulus of elasticity of 200–800 GPa and ultimate elongation 0.3–2.5%, where the stiffer fibre has the lower elongation. Carbon fibres do not absorb water, are resistant to many chemical solutions, do not corrode and withstand fatigue very well. Carbon fibre is electrically conductive and might result in galvanic corrosion if in direct contact with steel.

Glass fibre

Glass fibre is an inorganic fibre manufactured using melted glass compressed through an opening with a diameter of 1–3 mm and then extended to give the fibre a thickness of 3–20 μm . The glass fibres can have a modulus of elasticity in the range of 70–85 GPa and an ultimate elongation of 2–5% depending on the quality. Glass fibres are sensitive to moisture and alkaline environments, but are protected with the correct choice of matrix (alkali resistant AR).

Aramid fibre

Aramid fibres are mostly known from the brand name Kevlar. Aramid is used in articles such as bulletproof garments, sails or products where high energy absorption is needed.

The aramid fibre is an organic fibre manufactured from a solution with aromatic polyamide. The diameter of the fibres is 10–15 μm and the modulus of elasticity ranges from 70–200 GPa, with an ultimate elongation of 1.5–5% depending on the quality. Aramid fibres are sensitive to high temperatures, moisture and ultra violet radiation, and are therefore not suitable for all applications in construction industries.

Matrix

As mentioned above, the purpose of the matrix material is to bind the fibres and transmit and distribute shear forces between the fibres, giving them environmental protection. It is important for the matrix used in concrete to withstand and protect the fibres from the alkaline environment in the concrete. Fibre composites used in the structural applications probably contain a matrix of thermosetting resins, which can be vinylester, epoxy or occasionally polyester. The properties of these matrix materials are shown in Table 2.1. The more favourable matrix is considered to be epoxy. Epoxies have good strength, bond, creep properties and a very good chemical resistance. When the fibres are impregnated into a matrix the mechanical properties of the combined composite are defined by both the properties of the matrix and the fibres.

Table 2.1. Properties for different matrix materials, based on *Betongrapport nr 9 (2002)*

| Material | Density [kg/m^3] | Tensile strength [MPa] | Tensile modulus [GPa] | Failure strain [%] |
|------------|--------------------------------|---------------------------|--------------------------|-----------------------|
| Polyester | 1000-1450 | 20-100 | 2,1-4,1 | 1,0-6,5 |
| Epoxy | 1100-1300 | 55-130 | 2,5-4,1 | 1,5-9,0 |
| Vinylester | 1120 | 80-90 | 3,2 | 4-5 |

Geometry

The possibilities of designing a fibre composite to be used in a mineral-based strengthening system are mainly defined or limited by our imagination. However, up to now there exist some commonly used designs on utilised fibre composites. This section of the thesis will merely show typical designs of fibre composites. The next section shows existing mineral-based strengthening systems using different designs on the fibre composites.

The fibres can be placed in different directions in the composite and thus form a large amount of geometries with different mechanical properties. If the fibres are placed in one direction the fibre composite becomes unidirectional. The fibres can also be aligned in many directions, thus creating a bi or multi directional fibre composite.


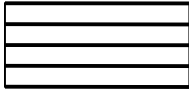
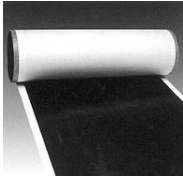

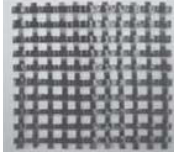



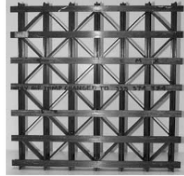
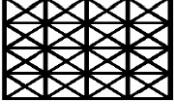

Table 2.2 shows different geometries for fibre composite strengthening materials, which can of course also be 3D geometries. Further, combinations of different fibre types in the same fibre composite can also be made Grace et al. (2002). This depends on the required behaviour of the fibre composite, eg. using a stiff fibre in one direction and a fibre with high strain capacity in the other.

Pultruded rods are typical unidirectional fibre composites, i.e. the fibre orientation follows the length direction of the composite. The surface of the rod can be covered with quartz sand to increase the bond strength between the rod and the mineral-based binder. Studies on sanded carbon fibre rods have been shown to work but with limited load bearing capacity compared to epoxy bonded rods Carolin et al. (2005).

Woven fabrics, such as textiles, sheets or weaves, are commonly made of orthogonal interlacing yarns called warp and fills. The warp and fill yarns pass over and under each other, resulting in every single yarn getting a crimped shape. The density of the fills and warps can be controlled independently of each direction during the manufacturing of the fabric. There are many possibilities with different designs of the woven fabrics, from a single yarn to advanced 3D designs Roye and Gries (2005). The penetrability of the mineral-based binder into the fabric is affected by the density of the warp and fill yarns, i.e. higher density leads to lesser penetrability, this is further discussed in section 2.4.1.

The main difference between a *grid* and a fabric is that the grid is not woven. Grids can also be called meshes or nets. To produce a grid the continuous fibres are braided or bundled into shape and then impregnated with a resin. Grids can be manufactured in a large variety of geometries, from dense meshes for reinforcing boards and panels to reinforcing nets for slabs. The advantages of grids are that they have higher mechanical properties than consolidated woven fabric and smoother, better surface aspects. They are also considered to be highly thermo-formable.

Table 2.2 Different geometries for fibre composites. Figures from Möller et al. (2005), Triantafillou and Papanicolaou (2006) and Han and Tsai (2003).

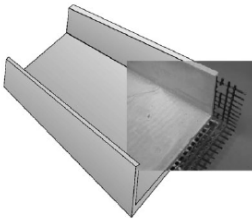
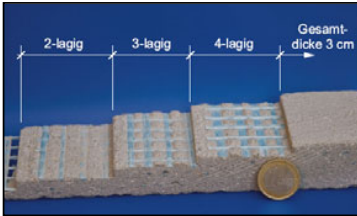
| | Mono-axial | Biaxial | Triaxial | Multi-axial |
|------------------------|--|--|---|---|
| 1 Dimensions |  <p>Pultruded rods</p> | - | - | - |
| 2 Dimensions |  <p>Sheet</p>  |  <p>Plane Weave/grid</p>   |  <p>Triaxial Weave/grid</p>   |  <p>Multi-axial Weave/grid</p>  |

2.3 Combinations – Existing systems

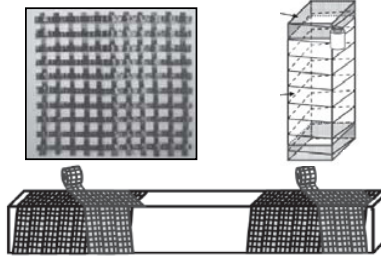
Combining different mineral-based binder with different types of fibre composites will render a mineral-based strengthening system. Textile reinforced concrete (TRC), developed in Germany is the most researched system. This system utilises mainly AR-glass fibres with a textile geometry. The TRC does not only concern concrete strengthening but can be applied to concrete structures with complex shapes such as arches and pre-stressed bridges, see Figure 2.4. There are many publications on the performance of this system and the reader is referred to a state of the art report in Rilem report 36 (2006). Another system similar to the TRC is the textile reinforced mortar (TRM) developed in Greece. This system uses a carbon fibre textile with a fine grade mortar and has shown excellent concrete strengthening properties Triantafillou et al. (2006) and Triantafillou and Papanicolaou (2006). Yet another system is the fibre reinforced cement (FRC), developed in the United States. This system is different from the TRC and TRM since it uses unidirectional carbon fibre sheets which are impregnated with a cement slurry, but it has also shown good ductility properties Wu and Teng (2002), Wu (2004) and Wu and Sun (2005). The last system to be

mentioned is the mineral-based composites (MBC) which is also the topic of this thesis. This system uses a carbon fibre grid together with fine grade mortars or ECC. These systems are not elaborated further in this chapter but are compared in Paper III and to some extent in Paper IV. All of the different systems are shown in Figure 2.4.

Textile reinforced concrete (TRC)



Textile reinforced mortar (TRM)



Fiber reinforced cement (FRC)



Mineral based composites (MBC)

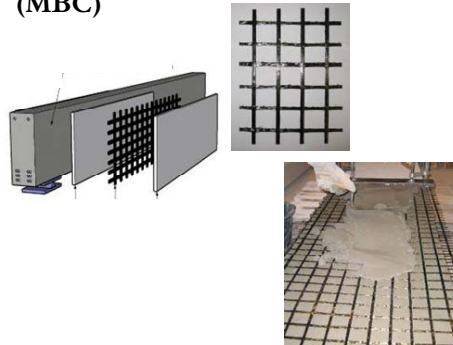


Figure 2.4. Different existing strengthening systems. Figures for TRC, Curbach and Jesse (2009), Shorn et al. (2004), Curbach et al. (2007) and also courtesy of A. Brueckner 2006-06-01. TRM, Triantafyllou and Papanicolau (2006) and Triantafyllou et al. (2006). FRC, courtesy of H.C. Wu.

2.4 Interaction between constituents

2.4.1 Transition zone between binder and fibre composite

A very important parameter when using a mineral-based binder is the bond between the latter and the fibre composite. This briefly discusses some issues that might arise in the intermediate transition. If a textile fabric is used the mineral-based binder can have problems in penetrating the fibre bundle. This penetration is highly dependent on the filament density in the bundle, e.g. amount of fibre filaments in a bundle. Further, if the stitches are dense and small then the filaments will be tightened and the mineral-based binder will not penetrate deeply into the bundle Peled et al. (2008). This typical bond behaviour of a textile fabric is illustrated in Figure 2.5. In order to activate the inner filaments the textile fabric can be impregnated with epoxy resin. This will lead to a significant increase in the ultimate tensile strength of a system with textiles embedded in a mineral-based binder Hegger et al. (2006).

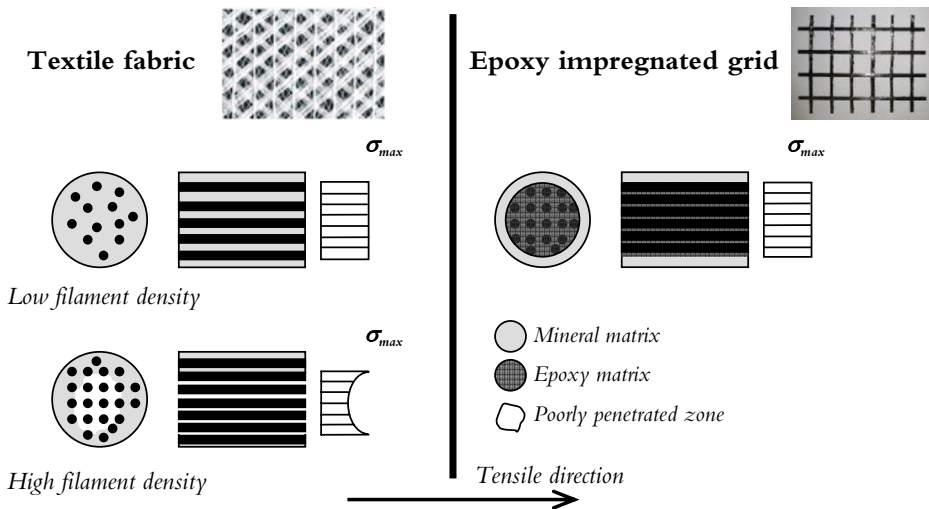


Figure 2.5. Tensile behaviour of textile fabrics and epoxy impregnated grid.

Furthermore, the crimped geometry of the individual yarn, or fibre, is expected to reduce the reinforcement efficiency compared to a straight yarn and may lead to stress concentration in the bonding material. However, in polymer modified mortars the crimped geometry of the individual yarn might be advantageous, since it may provide mechanical anchoring. The interlacing between the warps and the fills in the fabric may develop a frictional resistance at their contact points Peled et al. (1998).

In Raupach et al. (2006), the influence of polymer-modified mortars has been investigated in TRC. Added to the binder in high amounts, the polymers will form a secondary cohesive matrix, if the polymer is able to form a film the (interfacial) bond in a TRC will be improved. Both tensile strength and strains at failure were significantly

improved by polymer modification so that the embedded textile could be used more efficiently in a polymer-modified matrix.

2.4.2 Crack control

As mentioned above, in the transition zone between the fibre composite and the binder, bond is crucial for the performance of the strengthening system. If the binder contains short chopped PVA fibres, a chemical bond between the PVA fibres and the binder is built up. A mineral-based binder with short PVA fibres is the ECC mentioned earlier. Using fibre composites together with the deformation compatibility of the binder with PVA fibres results in fibre bridging, multiple cracking and strain hardening. These crack bridging effects of fibre composites in synergy with ECC are discussed in Paper IV. A short description of the mechanisms involving ECC is detailed below.

Fibre bridging and multiple cracking – crack control through strain hardening materials

Fibre bridging after first cracking of the mineral-based binder is quite well detectable in PVA-reinforced binders. For mineral-based strengthening systems, the mechanism is important because with adequately chosen binders, a mineral-based strengthening system can be altered/improved resulting in a more efficient strengthening material under tension or shear.

The deformation behaviour of composites containing cementitious binders (concrete, fibre reinforced concrete) and high performance fibre reinforced cement composites (HPFRCC) is typically distinguished according to their tensile stress-strain characteristics and post-cracking response, Stang and Li (2004). From Fischer and Li (2007), it is shown that brittle matrices, such as plain mortar and concrete, lose their tensile load-carrying capacity almost immediately after formation of the first crack as illustrated in Figure 2.6.

The addition of fibres in conventional fibre reinforced concrete (FRC) can increase the toughness of cementitious matrices significantly; however, their tensile strength and especially strain capacity and ductility beyond first cracking are not enhanced Li (1992). FRC is therefore considered to be a quasi-brittle material with tension softening behaviour, i.e. a decaying load and immediate localization of composite deformation at first cracking in the FRC matrix, see Figure 2.6. In contrast, strain hardening fibre reinforced cementitious composites such as HPFRCCs, Shi and Mo (2008), are defined by an ultimate strength higher than their first cracking strength and the formation of multiple cracking during the inelastic deformation process, see Figure 2.6. This means that after the onset of the first macro-crack, the tensile load still continues to increase, this is also known as strain hardening or plastic hardening.

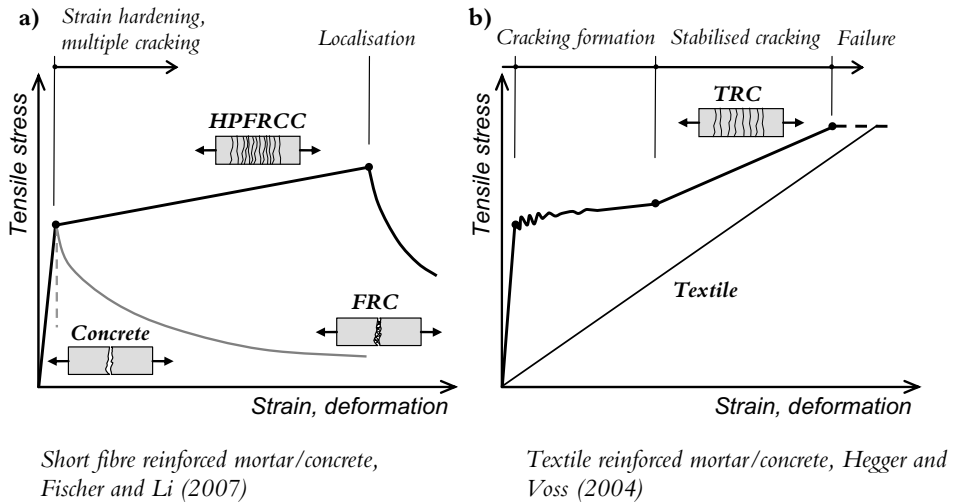


Figure 2.6. Tensile behaviour of a) strain hardening and tension softening materials and b) textile reinforced concrete.

ECC is often considered to be homogenous and isotropic in the uncracked state, due to the low fibre fraction, short fibre length and a random fibre distribution. Subjected to tension, it initially exhibits *multiple cracking* with associated overall *hardening*, which later changes to softening as fracture *localises*, see Figure 2.6 a Fischer and Li (2007). After the peak load, the crack continues to open and remaining fibres still generate some resistance against crack opening until these break or pull out, and this is known as the tension softening regime. This strain hardening and multiple crack formation ensures that a mineral-based strengthening system using these kind of binders will maintain its stability also after cracking.

Compared to ordinary FRCs the use of textiles instead of short fibres will result in higher load carrying capacity. Reinforcing a cementitious matrix with a textile will result in a TRC system as mentioned earlier. Figure 2.6 b) shows a typical tensile behaviour of a textile reinforced concrete, Hegger and Voss (2004). Similar to the FRC and HPFRCC (ECC) the tensile behaviour is in accordance to the stiffness of the concrete. When the tensile strength of the cementitious matrix is reached, a stage of crack formation will initiate. This multiple crack formation stage is dependent on the bond between textile and matrix. After the formation of a certain number of cracks, no more cracks will develop and the filaments in the textile are strained up to the strength of the filaments and failure occurs when the tensile strain of the reinforcement (textile) is achieved. For further information about the tensile behaviour of TRC the author suggest the reader to study the Rilem Report 36 (2006).

The tensile behaviour of the MBC system using a CFRP grid in association with quasi brittle mortars and ECC as matrix is discussed in Paper IV.

2.4.3 Shrinkage

The curing and environmental conditions are important factors that govern the service life strength as well as the performance of concrete structures and that of repaired or strengthened concrete structures with the use of an overlay, i.e. strengthening concrete structures with the use of mineral-based binders as described above. Although the problems arising due to shrinkage are not studied in this thesis, this chapter should be considered as a discussion of possible bond problems that can occur when applying mineral-based strengthening systems.

The curing conditions and especially shrinkage are significantly influenced by the surrounding environment, such as temperature, relative humidity, in-situ rainfall and wind velocity. Another influencing factor is the composition of the materials used for the structure. Casting an overlay and thus adjoining a fresh material onto an older structure can result in durability problems such as cracking and de-lamination along the transition zone between the two materials. These occurrences are mostly dependent on differential movements, i.e. volume changes, between the base concrete and the overlay caused by shrinkage, temperature variations or both, poor workmanship or external loads, Bolander and Berton (2004). Differential shrinkage is generally considered to have the most significant critical influence on the service life performance of composite members, Beushausen and Alexander (2005). Tensile stress relaxation or creep plays an important role in the stress development in overlays. This section will briefly discuss the shrinkage mechanisms with a suggestion on how to calculate peeling and shear stresses in an overlay.

Shrinkage mechanisms

When considering shrinkage in overlay composite systems, the movements from the newly cast overlay will be restrained or impeded by the older base concrete. If these restraint stresses attain the resistance strength of the overlay, cracks will be initiated and then propagate through the overlay. Figure 2.7 shows the critical effects of restrained shrinkage in the form of cracks and problems that can occur near the free edges. The latter refers to the shrinkage stress fields near the free edges that may initiate lifting or peeling forces, thus forcing the overlay to separate from the base concrete, an occurrence that is also known as edge-lifting or curling, see Figure 2.7. Shrinkage mechanisms will first be briefly addressed, followed by a short introduction on how to calculate stresses at the free edges due to shrinkage. Generally shrinkage is divided into three groups depending on the age of the member; plastic shrinkage, autogenous shrinkage and drying shrinkage.

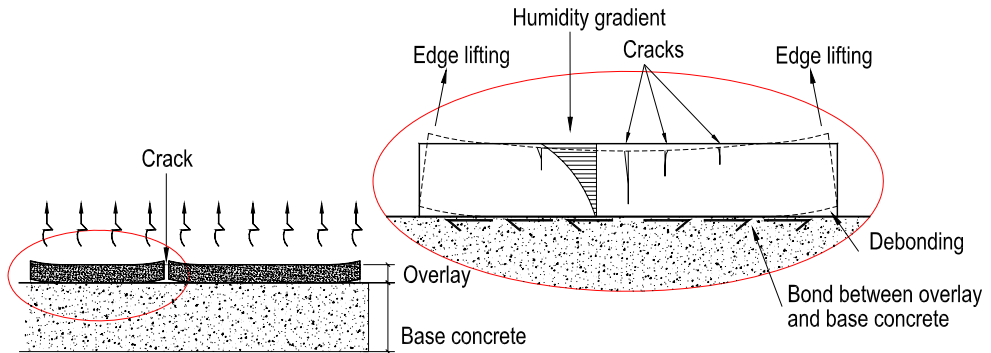


Figure 2.7. Critical effects of shrinkage for a bonded overlay inducing cracks and edge-lifting, modified from Carlswärd (2006).

Plastic shrinkage

Plastic shrinkage occurs within a few hours after casting and is highly dependant on the evaporation conditions and thus the evaporation rate, which in turn causes volume changes. As the plastic shrinkage increases, the new concrete hardens and leads to a considerable reduction in strain capacity. Cracks will occur when the shrinkage exceeds the strain capacity. The probability of cracking depends on the shrinkage rate and the strain capacity development. The easiest way to reduce plastic shrinkage is to retain the water evaporation by covering or adding water. Another way of controlling plastic shrinkage cracks is to reinforce the concrete or mortar with fibres. By using randomly distributed fibres of steel, polypropylene, nylon, etc., bridging forces that prevent or limit cracks can be obtained, Grzybowski and Shah (1990), Qi et al. (2003), Song et al. (2005) and Banthia and Gupta (2006). Plastic shrinkage can be reduced by controlling the admixture or adding superplasticizers and shrinkage reducing agents (SRA), Al-Amoudi et al. (2006) and Bentz et al. (2001). Note that the plastic shrinkage strain is increased with an increasing dosage of silica fume, Kockal and Turker (2007).

Autogenous shrinkage

A macroscopic volume change occurring with no moisture transfer to the surrounding environment is called autogenous shrinkage, referring to the chemical process of cement binding water in cement paste or concrete. Autogenous shrinkage in the hardened stage is related to self-desiccation as the cement tries to obtain extra water from the pore cavities. This process is highly dependent on the type of cement and temperature, Bentz et al. (2001). Autogenous shrinkage is usually a concern in high strength or high performance concrete (> 40 MPa), where there is a low water-to-cement (w/c) ratio, Holt (2001).

Drying shrinkage

Drying shrinkage is foremost a consequence of cement paste contraction when water leaves the pore system. The most important concrete or mortar mix components that affect the drying shrinkage are the amount of water per volume of concrete or mortar and the cement content, Al-Saleh and Al-Zaid (2006). The internal relative humidity (RH) in the pores is therefore of utmost significance. Shrinkage at high RH values will primarily be dependent on the evaporation of free water from the capillary pores in the cement gel, accounting for RH values from 45 to nearly 100%, Carlswärd (2006). If the RH values are lower, shrinkage will mostly depend on the removal of adsorbed water from the pore walls. Generally, it is the first time shrinkage that involves the most trouble for concrete structures; with varied saturation and drying, both swelling and shrinkage are smaller than the first time shrinkage. As mentioned before, consequences come in the form of cracks, de-lamination or edge-lifting/curling.

Shrinkage stresses that induce debonding

This section briefly describes the influence of shrinkage stresses that can induce critical debonding of an overlay cast on an older base concrete member. An assumption of the distribution of normal and shear stresses caused by shrinkage of an overlay in the transition zone between the overlay and an older concrete member is recorded in Figure 2.8. Critical areas, considering de-lamination and curling, when casting an overlay arise in the vicinity of the free edges as the normal stresses are transferred from the overlay to the base concrete. The normal stress in the overlay can be compared to normal stresses introduced by pre-stressed tendons. Pre-stressed tendons require a certain length to develop full pre-stress, as the normal stress in the overlay develops, with zero normal stress in the ends reaching a constant value at a certain distance from the edge, l_r . In the transfer zone where normal stresses are generated and developed to a constant value, shear stresses arise in the interface between the overlay and base concrete. If the tensile strength is reached and a crack appears in the overlay a similar situation will arise around the edges of the crack.

It is important to approximate the bond shear stresses and the edge-lifting force due to shrinkage, especially when mounting thin strengthening systems. A prediction method on how to calculate these relations for a simple supported composite beam is presented in Jonasson (1977, 1978) and further clarified by Carlswärd (2006). However, since no research regarding shrinkage induced debonding has been carried out in the present research this is not discussed further in the thesis.

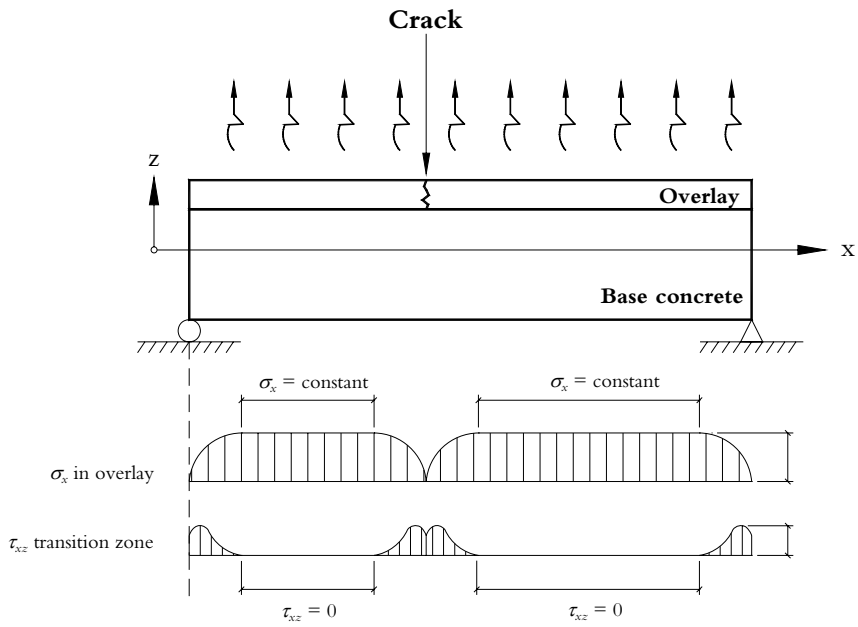


Figure 2.8. Proposed distribution for normal stress in the overlay and shear stresses in the transition zone, based on Carlswärd (2006).

3 Flexure and shear design for concrete structures

3.1 Introduction

This chapter will foremostly describe different design approaches for calculating the behaviour of reinforced concrete subjected to flexural and shear loading.

The first sections describe the flexural response on reinforced concrete using plane sectional analysis. The flexural response of reinforced concrete later on forms the basis for a design proposal for estimating the flexural resistance of MBC strengthened concrete members in chapter 4.

In subsequent sections a more detailed background on the most common various shear design approaches are discussed. These sections should be considered as a state-of-the-art review of shear design approaches. For the experienced reader, these sections will not provide any new research relevance but show the fundamental differences between the identified shear design approaches. Three primarily shear design approaches are identified and further elaborated. These approaches are the basis for the shear design proposal for shear strengthened beams using the MBC system given in Paper V and in chapter 4.

3.2 Flexural Capacity

This section will briefly discuss some of the aspects of designing concrete beams subjected to flexural loading. The plane section analysis in Paper V, using the modified compression field theory (see section 3.3.4) for beams subjected to combined shear and flexure, is based on the longitudinal equilibrium stated in this section. The main purpose of this section is to show one approach on how to calculate the longitudinal strain development for reinforced concrete beams.

3.2.1 Flexural response of reinforced concrete structures

Different stages of concrete during flexural loading

A flexural loaded steel reinforced concrete beam can be divided into three stages (I, II and III) up to failure. *Stage I* concerns non-cracked sections and the load is often relatively small. As the flexural load increases, the stresses and strains in cross section will increase and if the stresses exceed the tensile strength of the concrete then cracks will progress from the tensile portion of the cross section. With increasing load, these cracks will grow towards the neutral axis of the cross section. As the concrete cracks it is assumed that there will be no tensile contribution of the concrete and that all of the tensile stresses are taken by the tensile reinforcement. The concrete section has now

reached *stage II*. If the flexural load is further increased then the ultimate strength of the cross section will be reached and the section has reached *stage III*. This stage is characterised by the concrete compressive strength and/or the tensile strength of the reinforcement. The three stages are shown in Figure 3.1.

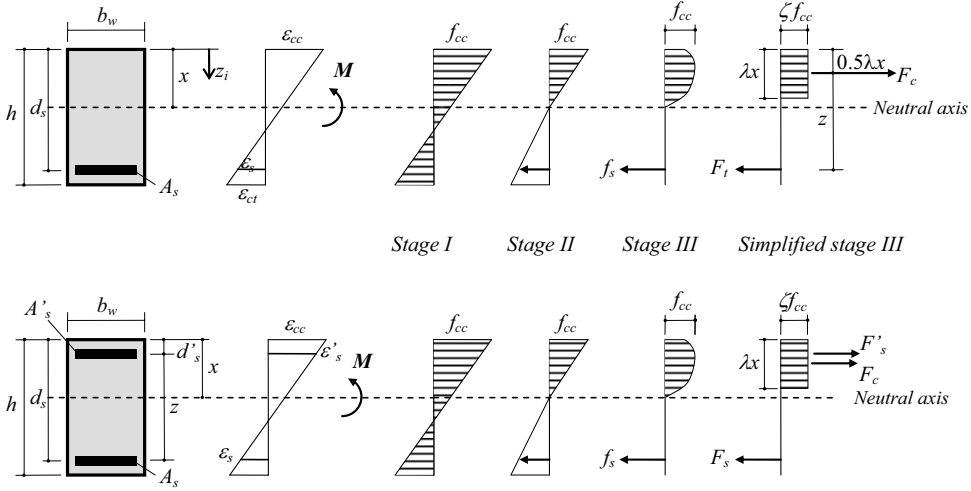


Figure 3.1. Different stages for reinforced concrete beams with rectangular cross sections, single and double reinforced.

The non-linear concrete compressive stress distribution in stage III, can be simplified to a linear distribution by reducing the compressive strength by a factor ζ and the effective depth by λ . These reduction factors are typically suggested to be $\zeta = 0.4$ and $\lambda = 0.8$ in BBK (2004) and in EC2-1 (2004) these factors are considered to be a function of the concrete compressive strength as

$$\lambda = 0.8 \text{ for } f_{ck} \leq 50 \text{ MPa}$$

$$\lambda = 0.8 - \frac{(f_{ck} - 50)}{400} \text{ for } 50 \leq f_{ck} \leq 90 \text{ MPa} \tag{3.1}$$

$$\zeta = 1.0 \text{ for } f_{ck} \leq 50 \text{ MPa}$$

$$\zeta = 1.0 - \frac{(f_{ck} - 50)}{200} \text{ for } 50 \leq f_{ck} \leq 90 \text{ MPa} \tag{3.2}$$

Non-cracked sections

The concrete beam can be assumed to be non-cracked if the tensile stress in the beam is below the concrete tensile strength. To calculate the stresses in the cross section the

moment of inertia needs to be known. Assuming full composite action between concrete and steel reinforcement, thus the strain in the reinforcement being equal to the strain in the concrete taken at the same level, will give the following relationship between concrete and steel reinforcement together with applying Hooke's law.

$$\frac{f_c}{E_c} = \frac{f_s}{E_s} \Rightarrow f_s = \frac{E_s}{E_c} f_c = \alpha_s f_c \quad (3.3)$$

Where f_c and f_s is the strength of concrete and steel respectively and E_c and E_s are the modulus of elasticity for concrete and steel respectively. The stresses in the cross section can be obtained by Navier's formula according to

$$f = \frac{M}{I_c + \alpha_s I_s} z_i = \frac{M}{I_1} z_i \quad (3.4)$$

Where I_c and I_s are the moment of inertia for the concrete and steel respectively and I_1 is the ideal moment of inertia for the composite cross section. z_i is the distance from the top of the cross section, see Figure 3.1.

The distance to the centre of gravity from the upper side of the cross section, z_0 , can be calculated according to the Steiner theorem for a double reinforced cross section, eq. (3.5). The ideal moment of inertia is obtained in a similar way in eq. (3.6) for rectangular cross sections.

$$z_0 = \frac{A_c z_{g,c} + (\alpha_s - 1) A_s d_s + (\alpha_s - 1) A'_s d'_s}{A_c + (\alpha_s - 1) A_s + (\alpha_s - 1) A'_s} \quad (3.5)$$

$$\begin{aligned} I_1 &= I_c + (\alpha_s - 1) I_s = \\ &= \frac{b_w h^3}{12} + b_w h \left(z_0 - \frac{h}{2} \right)^2 + (\alpha_s - 1) A_s (d_s - z_0)^2 + (\alpha_s - 1) A'_s (d'_s - z_0)^2 \end{aligned} \quad (3.6)$$

Where $z_{g,c}$ is the centre of gravity and A_c is the area of the gross cross section of concrete. After obtaining the ideal moment of inertia, the maximum stresses in the lower, $f_{c,l}$, and upper, $f_{c,u}$, part of the cross section as well as the stresses in the tensile steel reinforcement can be obtained by

$$f_{c,u} = \frac{M}{I_1} z_0 \quad (3.7)$$

$$f_{c,l} = \frac{M}{I_1} (h - z_0) \quad (3.8)$$

$$f_s = \alpha_s \frac{M}{I_1} (d_s - z_0) \quad (3.9)$$

It will now be possible to estimate whether the cross section is cracked or not. The tensile strength of concrete and the maximum calculated tensile stress in the lower part

of the cross section caused by a flexural load, M , is compared. If the tensile strength is lower than the calculated tensile stress then the cross section is considered cracked and the section is moved into *stage II*.

Cracked sections

In *stage II* the cross section is assumed to be cracked, thus the concrete tensile strength is reached in the tensile part of the beam and therefore no tensile contribution of the concrete is considered, see the horizontal equilibrium in Figure 3.2. The distance to the neutral axis can be calculated by considering this equilibrium. To simplify, the compression reinforcement that replaces the concrete area in the compression zone is enlarged by $\alpha_s - 1$. The tensile reinforcement is enlarged by α_s since no concrete is considered in the tensile zone. The distance, x , to the neutral axis is obtained by moment equilibrium around the neutral axis and solving the second order equation according to

$$bx \frac{x}{2} + (\alpha_s - 1)A'_s (x - d'_s) = \alpha_s A_s (d_s - x) \Rightarrow$$

$$x^2 + \frac{2}{b} [(\alpha_s - 1)A'_s + \alpha_s A_s] x - [(\alpha_s - 1)A'_s d'_s - \alpha_s A_s d_s] = 0 \quad (3.10)$$

The moment of inertia for the cracked section in *stage II* can then be obtained by eq. (3.11). After calculating the moment of inertia in stage II, the stresses in the cross section can be obtained in a similar way as in eq. (3.7) and (3.8). After calculating the maximum stress in the upper part of the cross section and the stress in the tensile reinforcement and assuming linear elastic behaviour will give the strains in the upper part of the cross section and in the tensile reinforcement, see eq. (3.12). Knowing the maximum strain, ε_{α} , and assuming that plane sections will remain plane will give the strain in the lower part of the cross section, ε_l .

$$I_2 = \frac{bx^3}{12} + bx \left(\frac{x}{2} \right)^2 + (\alpha_s - 1)A'_s (x - d'_s)^2 + \alpha_s A_s (d_s - x)^2 \quad (3.11)$$

$$\varepsilon_{\alpha} = \varepsilon_{\alpha} = \frac{f_{c,u}}{E_c} \quad (3.12)$$

$$\varepsilon_s = \frac{f_s}{E_s} \quad (3.13)$$

$$\varepsilon_l = \frac{\varepsilon_s (h - x)}{d_s - x} \quad (3.14)$$

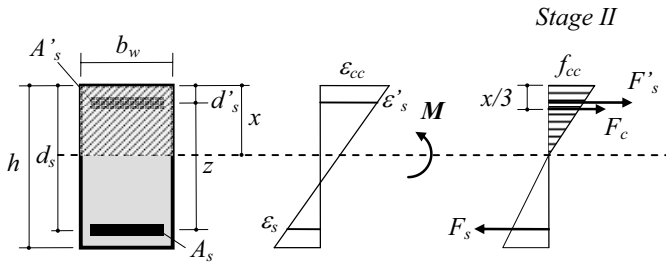
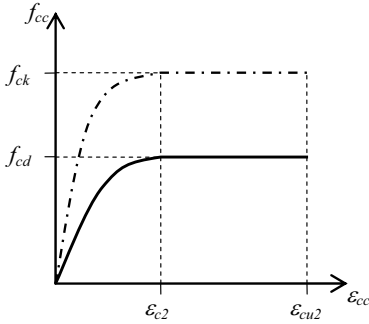


Figure 3.2. Stage II for a rectangular reinforced concrete cross section.

Alternatively, the compressive stress development can be adopted as in EC2-1 (2004), by assuming a parabola-rectangular or a bi-linear behaviour, see Figure 3.3. Knowing the compressive stress, then the compressive strain can be back calculated from the compressive stress-strain relationships given in EC2-1 (2004) as shown in Figure 3.3.

a) Parabola-rectangular

 For $0 \leq \varepsilon_{cc} < \varepsilon_{c2}$

$$f_{cc} = f_{cd} \left[1 - \left(1 - \frac{\varepsilon_{cc}}{\varepsilon_{c2}} \right)^n \right] \quad (3.15)$$

 For $\varepsilon_{c2} \leq \varepsilon_{cc} < \varepsilon_{cu2}$

$$f_{cc} = f_{cd} \quad (3.17)$$

 For $f_{ck} \geq 50$ MPa

$$n = 1.4 + 23.4 \left[\frac{90 - f_{ck}}{100} \right]^4 \quad (3.19)$$

 Otherwise $n = 2$

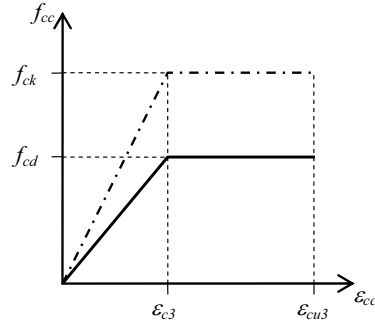
 For $f_{ck} \geq 50$ MPa

$$\varepsilon_{c2} = 2.0 + 0.085 (f_{ck} - 50)^{0.53} \quad (3.20)$$

 Otherwise $\varepsilon_{c2} = 2$

 For $f_{ck} \geq 50$ MPa

$$\varepsilon_{cu2} = 2.6 + 35 \left(\frac{90 - f_{ck}}{100} \right)^4 \quad (3.21)$$

 Otherwise $\varepsilon_{cu2} = 3.5$
b) Bi-linear

 For $f_{ck} \geq 50$ MPa

$$\varepsilon_{c3} = 1.75 + 0.55 \left[\frac{f_{ck} - 50}{40} \right] \quad (3.16)$$

 Otherwise $\varepsilon_{c3} = 1.75$

 For $f_{ck} \geq 50$ MPa

$$\varepsilon_{cu3} = 2.6 + 35 \left(\frac{90 - f_{ck}}{100} \right)^4 \quad (3.18)$$

 Otherwise $\varepsilon_{cu3} = 3.5$

Figure 3.3. Concrete stress-strain relationships for design and section analysis, based on EC2-1 (2004).

Cracked cross section criterion

One problematic aspect of using this approach is to know when the cross section is cracked or non-cracked. The principal factors affecting the initial or short-time deflections for reinforced concrete beams are modulus of elasticity, load distribution, support conditions, load level and degree of cracking along the beam, Branson (1977).

A typical behaviour of initial or short-time deflections vs. applied moment are shown in Figure 3.4 for the ratio between applied moment and deflection to cracking moment and cracking deflection. In this figure a typical experimental behaviour is also shown. The non-cracked section is calculated based on the ideal moment of inertia, I_i .

The discrepancy between predictions and experimental results could be explained by bond-slip behaviour between reinforcement and steel and the non linear behaviour of reinforced concrete. This is however not within the scope of this thesis and is therefore not discussed any further.

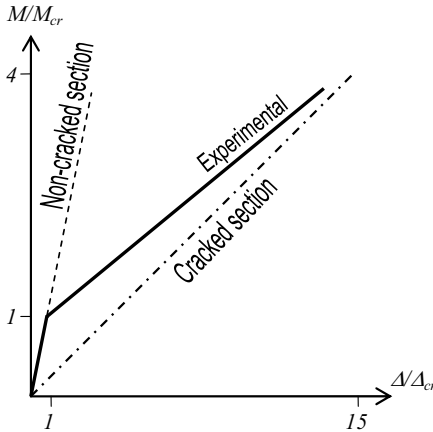


Figure 3.4. Typical moment-deflection for reinforced concrete members subjected to flexural loads, based on Branson (1977).

However, the flexural behaviour calculated in Paper V, is based on the cracking criteria given in BBK (2004). The tensile stress due to applied moment should not exceed the stress in eq. (3.22) for the cross section to be assumed as non-cracked.

$$f_m = \underbrace{\left(0.6 + \frac{0.4}{\sqrt[4]{h}}\right)}_k \frac{f_{ct}}{t} \quad (3.22)$$

where f_{ct} is the concrete tensile strength and t is a factor taking environmental aspects into consideration (for laboratory testing this factor is set to 1.0). h is the depth of the beam in meters. Note that the factor k should not be smaller than 1 or higher than 1.45.

3.3 Shear capacity

3.3.1 Introduction

Design methods for reinforced concrete beams subjected to flexural loading are based on physical models that are clearly verified on experimental results, Betonghandbok (1990) and Popov (1999). However, when considering a beam subjected to shear forces the conditions are reversed. Despite vast research efforts in the area over the last 100 years, no solitary and fully accepted physical model describing the influence of the shear force and its behaviour at shear failure has been adopted. There are different designs and explanations of how to calculate the shear distribution of concrete members all over the world. The reason for this is that shear failure is a complicated mechanism, dependent on many factors and that different approaches have been used in different countries. This will be discussed more thoroughly in the coming sections in this thesis.

A concrete beam subjected to both flexural and shear loading (bi-axial loading) will typically crack diagonally in two ways, web-shear cracking and flexure-shear cracking. Web-shear cracking is assumed to be forming in the web near the centroid (neutral axis) of the member that has not been cracked previously. The second type of diagonal cracking develops as an extension of previously existing flexural cracks, namely flexure-shear cracks. Both of these diagonal cracking types are shown in Figure 3.5. The development of the flexure-shear cracks is a rather complex problem.

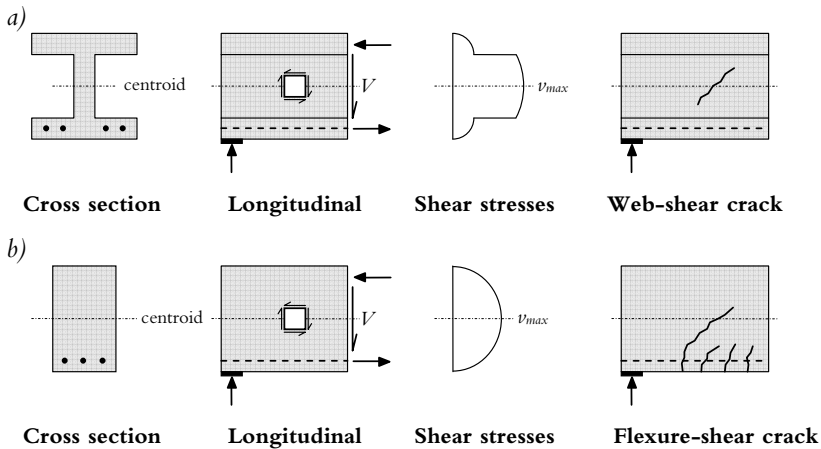


Figure 3.5. Types of diagonal cracking. a) Web-shear cracking and b) Flexure-shear cracking.

When a concrete member is subjected to shear deformations (bi-axial loading) the shear will be resisted by the compression zone, internal friction (aggregate interlocking) and dowel forces in the flexural reinforcing bars, Hedman and Losberg (1975). A schematic figure that shows the shear resistance components mentioned above is shown in Figure 3.6 below.

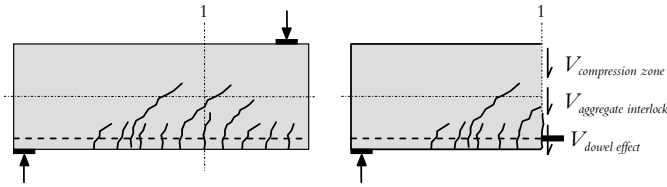


Figure 3.6. Experimentally determined components of shear resistance for cracked reinforced concrete.

The effects of both aggregate interlocking and the dowel effect are quite hard to assess. When considering bi-axially loaded members (including flexural load) one must study the composition of deformation state and failure condition. All of these within the failure zone where the extension corresponds to the ultimate spread of a diagonal shear crack.

It is preferable if the principal failure modes associated with shear failures are determined before elaborating the different approaches of how to calculate the shear resistance. The most commonly observed failure developments render three principal failure modes illustrated in figure 3.7.

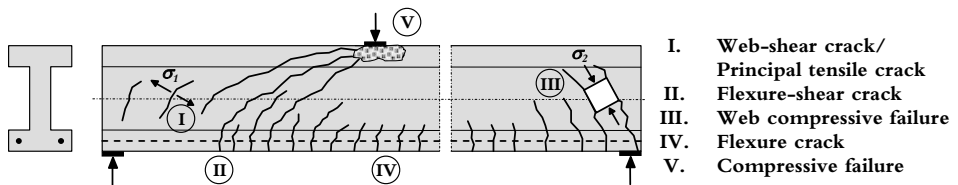


Figure 3.7. Typical cracks and failure modes for bi-axially loaded beam.

- I) *Web-shear failure* could be relevant within the areas of the member which is not influenced by flexural cracks. Typically, these failures are significant for the load bearing capacity for members with no shear reinforcement. The failure arises when the principal tensile stress reaches the tensile strength of concrete and then diagonal shear cracks occur. If the member has shear reinforcement, then load can be increased after the occurrence of web-shear cracks.
- II) *Flexure-shear failure* is contemporary in areas where flexure cracks have occurred. Here the cracks form as flexural cracks in the tensile zone of the member and thereafter propagate diagonally towards the compression zone of the member. The ultimate failure is often characterised by local crushing or splitting of the concrete in the compression zone. Reinforcement crossing the diagonal shear crack contributes to the shear resistance and then the shear resistance is characterised by the yield strength of the

reinforcement. The shear reinforcement and the longitudinal reinforcement can be regarded as tensile ties in a truss, see Figure 3.8. The diagonal area of concrete between the shear cracks performs as the diagonal compressive struts in a truss, see Figure 3.8. The dowel effect of the longitudinal tensile reinforcement crossing the flexure-shear cracks significantly improves the shear load resistance.

- III) *Web compressive failure* is an upper limit of the shear resistance. Here the diagonal concrete between the shear cracks (compressive struts in the truss) fail by compression. This is often valid for a cross section over-reinforced in shear, where the concrete compression strength is reached before the reinforcement yields. This upper limit is thus set, for a given concrete strength, because increasing the reinforcement in shear will not contribute to the shear resistance.

Web-shear failure is not dominant for members reinforced in shear, for such cases *flexure-shear failure* or *web compressive failure* are the dominant failure modes.

As mentioned in the failure modes II) *Flexure-shear failure* and III) *Web compressive failure*, the shear resistance can be analysed by a 45° truss analogy where the shear reinforcement performs as tensile ties. This truss analogy was foremost derived by Mörsch and is further described in section 3.3.2. However, the shear resistance estimation based on the Mörsch truss analogy is generally underestimated compared to experimental results. An improved agreement is obtained if the nominal total shear resistance of the concrete, V_u , member is understood as the sum of the shear resistance, V_c , at flexure-shear failure *without* shear reinforcement and the shear resistance, V_s , obtained by the truss analogy at the yield strength of the shear reinforcement.

$$V_u = V_c + V_s \quad (3.23)$$

The methodology described above is often referred to as the “additional principle” but is hereafter in this thesis named “*addition*” approach and is further described in section 3.3.3. However, instead of compensating the conservative Mörsch 45° truss analogy by adding a concrete contribution in the “*addition*” approach, the inclination of the diagonal concrete compressive strut could be assumed to be lower than 45°. These variable angle truss models, where the inclination of the diagonal compressive struts θ are set to an additional unknown, are further described in section 3.3.5.

During recent years new and more theoretically advanced models has been derived. These are based on more profound theoretical foundations. One of these methods is the compression field approach which takes the compression softening of the concrete, due to successive cracking, into consideration, this is described further in chapter 3.3.4. Other methods are based on the theory of limit analysis and concrete plasticity, Nielsen (1999). The hypothesis is based on the assumption that the web is fully plasticized in the ultimate limit state. Thus, the shear reinforcement yields at the same time as the concrete in the web are deformed in an ideal plastic manner due to the diagonal compressive forces. Further development using concrete plasticity for members

subjected to shear has also been made by the Cracked Membrane Model Kaufmann and Marti (1998). The limit analysis is further described in section 3.3.5.

A schematic overview and partitioning of the different fundamental shear design approaches is shown in Figure 3.8. These are divided into the classical approach of truss analogy, “addition” approach, compression field approach and limit analysis approach. Note that the variable angle truss model is subcategorised in the limit analysis approach although such approaches were used well before applying limit analysis and concrete plasticity Kupfer (1964). The reason for subcategorising it under limit analysis methods is because it was put on a sound physical basis through the lower bound theorem and limit analysis.

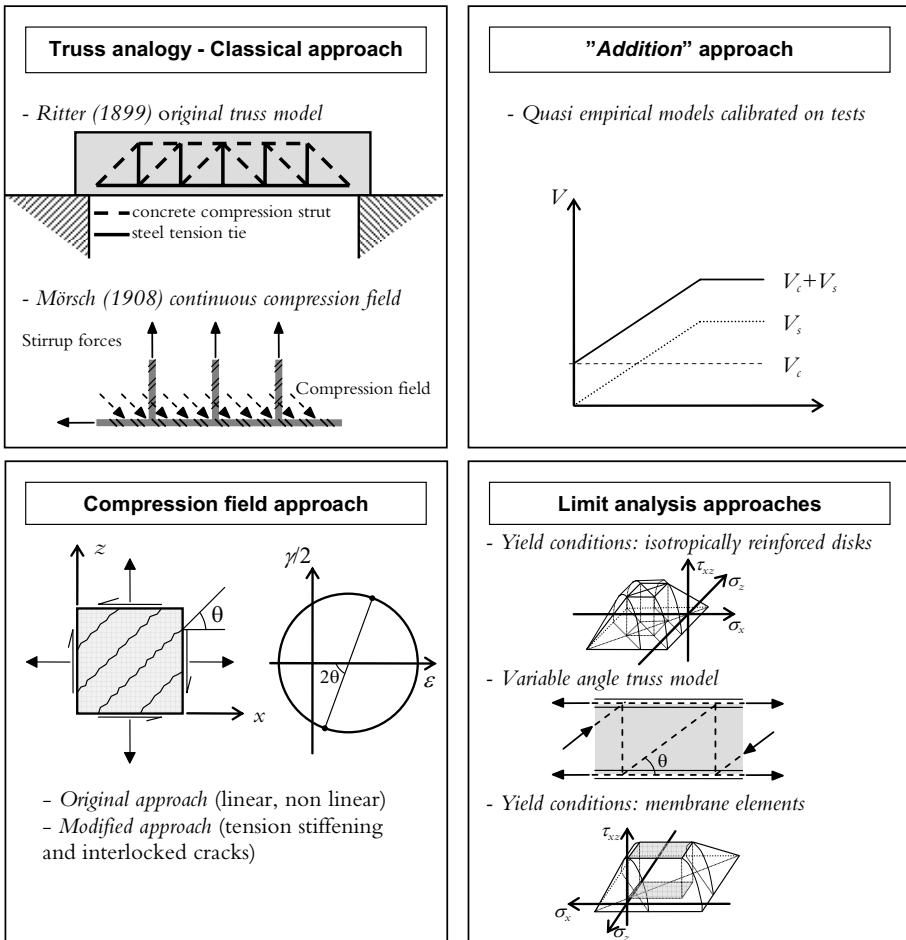


Figure 3.8. Different methods for designing reinforced concrete structures in shear.

3.3.2 Truss analogy

The flow of forces in a cracked reinforced concrete beam was explained by Ritter (1899) in terms of a truss analogy, see Figure 3.9. In that truss model the tensile reinforcement is assumed to be the tension chord and the flexural compression zone in the beam is assumed to be the top chord. The diagonal compression stresses in the concrete are assumed to be the diagonal compression strut and the vertical tension is assumed to be taken by the tensile ties (stirrups) in the truss model, see Figure 3.9.

Mörsch, Mörsch (1908) and Mörsch (1922), advanced the 45° truss model by showing that the diagonal compression struts do not have to go from the top of one stirrup to the bottom of the next stirrup, see Figure 3.9 a). However, instead of having discrete diagonal compression struts it could be assumed to be a continuous field of diagonal compression resisting the shear, see Figure 3.9 b). Both Ritter's and Mörsch truss models neglect the concrete tensile strength contribution and assume that the inclination of the diagonal compression struts remains 45° after cracking of the cross section.

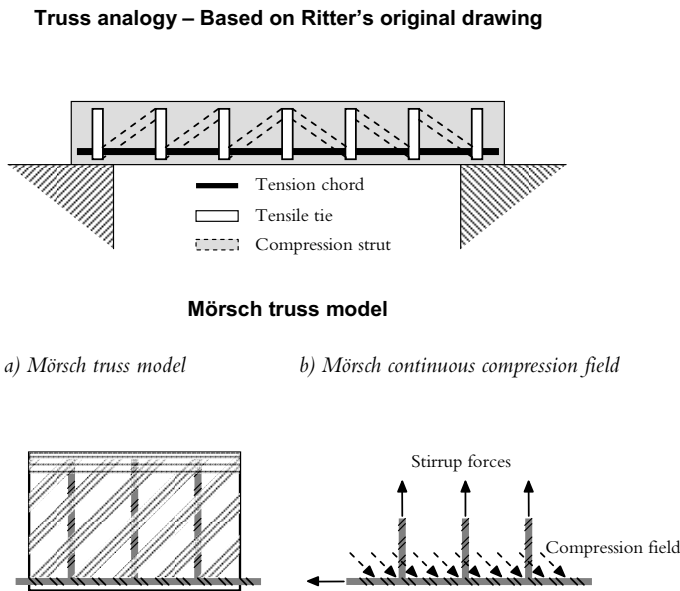


Figure 3.9. Truss models based on Ritter's (1899) truss analogy and Mörsch's (1908 and 1922) truss model.

Assumed geometry and equilibrium for the 45° Mörsch truss model is given in Figure 3.10. The shear stresses are assumed to be uniformly distributed over an effective shear area of the width, b_w , and the effective depth, z (internal lever arm), of the cross section in Figure 3.10 a).

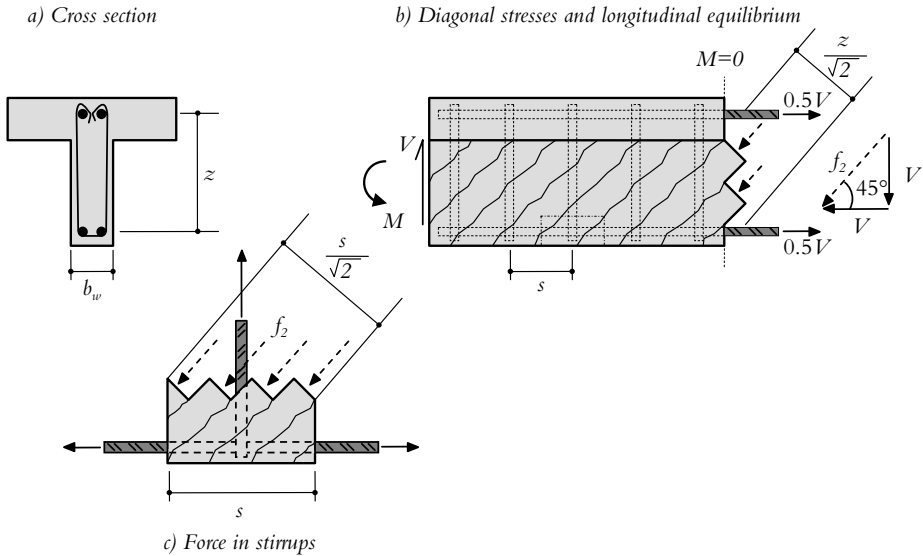


Figure 3.10. Geometry, forces, stresses and equilibrium for the 45° truss model.

Using the equilibrium shown in Figure 3.10 b) makes it possible to obtain the required diagonal principal compressive stresses. Since the total diagonal compressive force amounts to $f_2 b_w z / \sqrt{2}$ and the diagonal component of the applied shear force equals $\sqrt{2}V$, then the principal compressive stress can be expressed as

$$f_2 = \frac{2V}{b_w z} \quad (3.24)$$

In Figure 3.10 b), the horizontal component of the applied shear force equals V and to maintain equilibrium then the longitudinal reinforcement has to balance with a tensile force N_v . Thus the longitudinal reinforcement will have to take a tensile force equal to $N_v = V$.

The vertical component of the diagonal principal compressive forces is taken by the stirrups, $A_s f_{sz}$, shown in Figure 3.10 c). Taking the vertical component of the diagonal compressive forces as $f_2 b_w s/2$ gives the vertical tensile force in the stirrups according to

$$V_s = V = A_s f_{sz} \frac{z}{s} \quad (3.25)$$

It should however be pointed out that after experimental validation of the truss model, Mörsch found that his model was giving conservative estimations. For beams containing stirrups the inclination of the diagonal compressive stresses became flatter than the suggested 45°. He also stated that determining the actual inclination of the

diagonal compressive stresses was mathematically impossible, due to the additional unknown inclination θ . This predicament is further elaborated in section 3.3.5 for the variable angle truss model.

3.3.3 Semi-empirical “addition” approach

As mentioned in the previous section, comparing the estimation made by the Mörsh 45° truss model gives conservative values. Typical experimental shear behaviour (stirrup stresses) and the shear behaviour predicted by the 45° Mörsh truss model are shown in Figure 3.11. The conservatism in the 45° Mörsh truss model originates in the neglect of the tensile stresses in the concrete and the assumption of the 45° inclination of the compressive strut. Thus, the model predicts that a beam with no shear reinforcement would have zero shear resistance. This is clearly not the case because a concrete beam without shear reinforcement will fail after the formation of diagonal cracks. In the 1950s it was still recommended by researchers, Hognestad (1952), to use eq. (3.25) for design. Since by using the conservative 45° Mörsh truss model approach will result in members having some reserve shear resistance when failing in flexure.

Nevertheless, to overcome the discrepancy between experimental results and those predicted by the conservative Mörsh truss analogy a new contemplation was made. By formally estimating the members total shear resistance, V_u , as the sum of the shear resistance at flexure-shear failure with no shear reinforcement, V_c , and the shear resistance from the presumed truss model at yielding of the shear reinforcement, V_s . Thus adding up to the “addition” approach in eq. (3.23). It should however be pointed out that the “addition” approach does not intend to give a functional description of the failure. But should be considered as a systematic revision of experimental results and the foundation for shear resistance calculations for ultimate limit design.

Formulas and constants derived in the “ V_c+V_s ” approach are founded on statistical evaluations of a vast set of experimental data. The upper limit of the shear resistance of the concrete members without shear reinforcement, V_c , is often given by the web-shear failure. The upper limit for the total shear resistance, V_u (with active shear reinforcement) is given by the web compressive failure, Figure 3.7. The “ V_c+V_s ” approach is adopted, among others, in the North American shear design code ACI (2008) and Swedish BBK (2004), these design models will be described further in the upcoming sections.

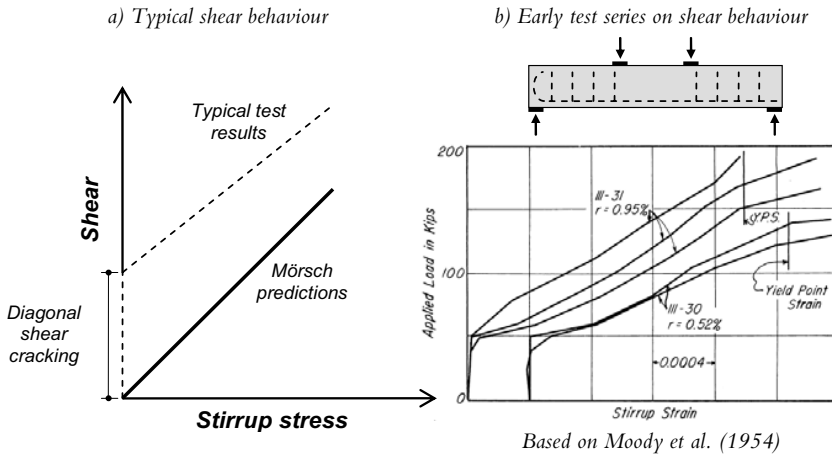


Figure 3.11. Typical shear reinforcement behaviour, tests and predictions.

North American shear design - ACI

The North American shear design proposal is based on the report ACI-ASCE (1962) with the following four concepts regarding shear:

- i. Diagonal tension is considered to be a bi-axial stress problem which has to consider both horizontal tensile stresses caused by flexure and shearing stresses.
- ii. Shear failure may occur by formation of a critical diagonal shear crack or by shear compressive failure in the compression zone at a higher load. The latter is only valid if redistribution of internal forces is accomplished.
- iii. Formation of the critical diagonal crack occurs at a certain load. This load must be considered in design as the ultimate load carrying capacity of the reinforced concrete member *with no* shear reinforcement.
- iv. The shear and flexural stress distribution over a cross section is considered to be unknown.

Regarding the last point (iv.), the actual distribution of the shear stresses over the cross section was not fully clarified at the time for writing the ACI-ASCE (1962) (this is still debated among researchers). The average shear stress was deemed to be advisable to use in the ACI shear design, even though it does not include the refinement/reduction of the internal lever arm (eq. $0.9d$). Therefore, the unit shear stress used in the following part is based on the average stress on the full effective cross section as:

$$v = \frac{V}{b_w d} \quad (3.26)$$

The derivation of the ACI shear design is based on the assumption that the critical diagonal crack (see previous iii.) is the governing failure for beams with no shear

reinforcement. In ACI-ASCE (1962), three variables are indicated to be of primary interest for the shear capacity, based on systematic studies on 440 beam shear tests with no shear reinforcement, namely, the percentage of longitudinal reinforcement, ρ_x , the dimensionless quantity of the moment to shear ratio M/Vd and the quality of the concrete expressed in concrete compressive strength, f'_c .

Both the localisation and inclination of the diagonal tension cracks indicate that they are caused by principal tensile stresses. The diagonal tension strength is based on the equation for principal stress in a point.

$$f_{t,max} = \frac{f_t}{2} + \sqrt{\left(\frac{f_t}{2}\right)^2 + v^2} \quad (3.27)$$

It is stated in, ACI-ASCE (1962), that this kind of approach was evaluated in the past but with unsuccessful results because of difficulties in expressing the tensile bending stress, f_t , and the shearing stress, v . A more successful method based on this approach is given in section 3.3.4 for the compression field theory.

The tensile stress, f_t , is assumed to be proportional to the tensile steel stress, f_s , computed by the cracked section theory.

$$f_t = const \cdot \frac{f_s}{n} = C \frac{M}{n\rho_x j d^2 b_w} \quad (3.28)$$

Where n is the modulus of elasticity ratio E_s/E_c . Neglecting the variation of the internal lever arm reduction factor, j , and introducing a new constant $F_1=C/j$ renders the expression of the tensile stress as

$$f_t = F_1 \frac{M}{n\rho_x d^2 b_w} \quad (3.29)$$

The magnitude of the shear stress in concrete is assumed to be proportional to the average shear stress on the cross section and shown as.

$$v = F_2 \frac{V}{b_w d} \quad (3.30)$$

By inserting eq. (3.29) and (3.30) in the principal stress eq. (3.27) and rearranging, gives the following relationship between the external shear, V , and the principal stress, $f_{t,max}$

$$\frac{V}{b_w d} = \frac{f_{t,max}}{\frac{F_1}{2} \frac{M}{nV\rho_x d} + \sqrt{\left(\frac{F_1}{2} \frac{M}{nV\rho_x d}\right)^2 + F_2^2}} \quad (3.31)$$

assuming that diagonal tension cracks occur when the diagonal tensile strength of concrete is exceeded by the principal tensile stress, $f'_t \leq f_{t,max}$, and that the factors F_1 and F_2 are constant. Inserting these assumptions in (3.31) and rearranging leads to:

$$\frac{V}{b_w d f'_t} = \frac{1}{C_1 \frac{E_c}{E_s \rho_x} \frac{M}{Vd} + \sqrt{\left(C_1 \frac{E_c}{E_s \rho_x} \frac{M}{Vd} \right)^2 + C_2}} \quad (3.32)$$

where C_1 and C_2 are dimensionless constants. Eq. (3.32) was first derived by Morrow and Viest (1957) in order to relate the nominal shear stress, eq. (3.26), to the three primary influencing variables:

- As the concrete strength, f'_t increases so does the nominal shear stress, ν
- The nominal shear stress, ν decreases as the M/Vd ratio increases
- Increasing longitudinal reinforcement ratio increases the nominal shear stress, ν

Eq. (3.32) can be subdivided into two major groups of variables, $V/b_w d f'_t$ and $(E_c/E_s \rho_x)(M/Vd)$. Further simplifications are then made on these two groups. The diagonal concrete tensile strength f'_t , and the modulus of elasticity E_c , are approximated as functions of $\sqrt{f'_c}$ and the modulus of elasticity E_s , for the steel reinforcement is assumed to be constant,. Using the three approximations in eq. (3.32) for the two groups of variables gives

$$A = \frac{V}{b_w d \sqrt{f'_c}} \quad (3.33)$$

$$B = \frac{\sqrt{f'_c} M}{\rho_x Vd} \quad (3.34)$$

The two parameters A and B logically represent the properties of the considered cross section thus permitting correlation of test data on diagonal tension strength on beams with no shear reinforcement in a two dimensional plot. A quantitative relationship between these two parameters was then derived based on data from 194 beams. Values for the parameter A and the inverse of parameter $(1/B)$ for all 194 beams are shown in Figure 3.12.

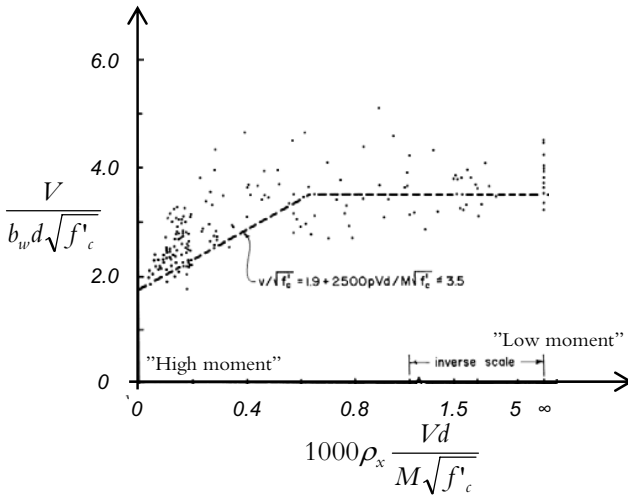


Figure 3.12. Derivation of shear design equation in ACI, units in psi, from ACI-ASCE (1962).

The parameter A calculated on the test data shows that the diagonal tension strength increases from a minimum of approximately 2 to a maximum of approximately 4. The parameter $1/B$ increases from 0 to approximately 0.8 based on the experimental data. The trend of these experimental data is then the foundation on the shear design in the ACI (2008). This trend is then expressed by two straight lines corresponding to eq. (3.35) for psi units and eq. (3.36) for MPa units.

$$\frac{V}{b_w d \sqrt{f'_c}} = 1.9 + 2500 \rho_x \frac{Vd}{M \sqrt{f'_c}} \leq 3.5 \quad [\text{units in psi}] \quad (3.35)$$

$$\frac{V}{b_w d \sqrt{f'_c}} = 0.16 + 17 \rho_x \frac{Vd}{M \sqrt{f'_c}} \leq 0.29 \quad [\text{units in MPa}] \quad (3.36)$$

As it is shown in the Figure 3.12 and in eq. (3.35) and (3.36) the nominal shear stress, v eq. (3.26), is predicted to decrease as the moment-to-shear ratio increases going from $0.29 \sqrt{f'_c}$ [MPa] for zero moment to $0.16 \sqrt{f'_c}$ [MPa] for very high moments. It should also be noted that there is a considerable scattering in the observed values for the assumed parameters A and B in Figure 3.12.

As a simplification ACI (2008) permits the shear resistance at flexure-shear cracking for a reinforced concrete beam to be

$$V_c = 2 \sqrt{f'_c} b_w d \quad [\text{units in psi}] \quad (3.37)$$

$$V_c = 0.17 \sqrt{f'_c} b_w d \quad [\text{units in MPa}] \quad (3.38)$$

thus, not taking into consideration the dowel effect by the longitudinal reinforcement and only considering the concrete strength. Eq. (3.35) or (3.36) may be used if a more detailed analysis is made, although they overestimate the influence of f'_c and underestimate the influence of ρ_x and Vd/M , ACI-ASCE (1962). It is also mentioned in ACI (2008) that the shear strength decreases as the overall depth of the beam increases, this type of “size effect” is handled by the “addition” approach in the Swedish BBK (2004) described below.

The steel contribution, V_s , is calculated based on the 45° Mörsh truss model, see eq. (3.25).

There exists an upper limit on how much inherent shear resistance a concrete member has. This limit is also based on experimental results according to ACI-ASCE (1962), see Figure 3.13. Here the design criteria is based on the “addition” approach where the ultimate shear strength is based on a linear relationship according to

$$v_u = \frac{V}{b_w d} = \underbrace{K\rho_z f_y}_{v_s} + v_c \tag{3.39}$$

Here v_c is based on eq. (3.35) and (3.36) divided by the effective cross sectional area. The upper limit of $K\rho_z f_y$ or v_u is found in tests (see Figure 3.13) where a safe limit in most cases corresponds to

$$v_u = 8\sqrt{f'_c} \text{ [units in psi]} \tag{3.40}$$

$$v_u = 0.67\sqrt{f'_c} \text{ [units in MPa]} \tag{3.41}$$

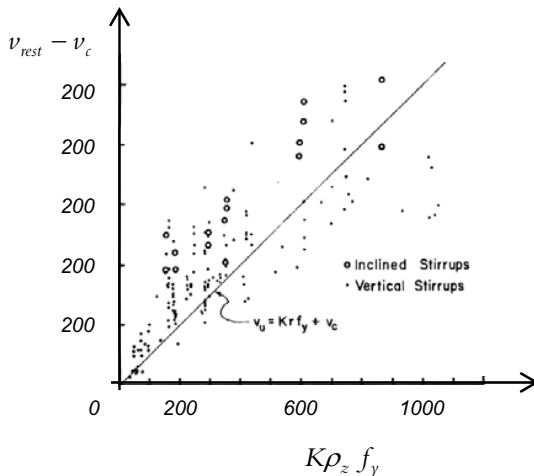


Figure 3.13. Shear strength of beams with web reinforcement, units in psi, based on ACI-ASCE (1962).

Swedish shear design - BBK

In the Swedish design code, BBK (2004), the shear resistance of concrete members is based on Hedman and Losberg (1975). Here, two cases were investigated; the influence of longitudinal reinforcement and the influence of shear reinforcement. In this way the principle of super positioning (“addition” approach) could be divided into a concrete contribution, V_c , and a steel contribution, V_s . The concrete contribution to the shear capacity was expressed in Hedman and Losberg (1975) as

$$V_c = (1.6 - d)b_w df_v \quad (3.42)$$

where b_w is the beam or slab width, d is the effective depth and f_v is the nominal shear stress given by

$$f_v = k_c \left(1 + 50 \frac{A_{sx}}{b_w d} \right) \sqrt{f'_c} \quad (3.43)$$

Where A_{sx} is the longitudinal reinforcement area and f'_c is the cylinder compressive strength. k_c is a constant with a mean value of 0.09 and a coefficient of variance (COV) of 15%. A linear regression on 249 shear reinforced beams was used to investigate the “addition” approach in Hedman and Losberg (1975) expressed as

$$\frac{V_u}{b_w d \sqrt{f'_c}} = k_c + \frac{A_{sz} f_{sz} \frac{0.85d}{s}}{b_w d \sqrt{f'_c}} \quad (3.44)$$

Where V_u is the total shear capacity, see also eq. (3.23), A_{sz} is the shear reinforcement area and f_{sz} is stress in the shear reinforcement (taken as the yield strength in ultimate limit state). The COV of eq. (3.44) compared to experimentally measured values was estimated to 18 % (Jeppsson, 2003).

In eq. (3.43) the nominal shear stress is proportional to the mean square root of the concrete cylinder compressive strength. Hedman and Losberg also suggested that $\sqrt{f'_c}$ could be replaced with 25 % of the tensile strength ($0.25f_{ct}$), BBK (2004) uses 30 % of the characteristic concrete tensile strength ($0.30f_{ct}$). In BBK (2004) eq. (3.42) is also modified for the size effect, depending in the effective depth of the beams. A reduced effective depth is favourable for the nominal shear stress Betonghandbok (1990). The steel contribution, V_s , for beams with vertical stirrups is calculated using the 45° Mörsch truss model according to eq. (3.25). A description of the shear design in BBK (2004) is described in section 3.4.1. The ratio for the experimental shear stress results normalised against the predictions plotted against the longitudinal reinforcement ratio is shown in Figure 3.14.

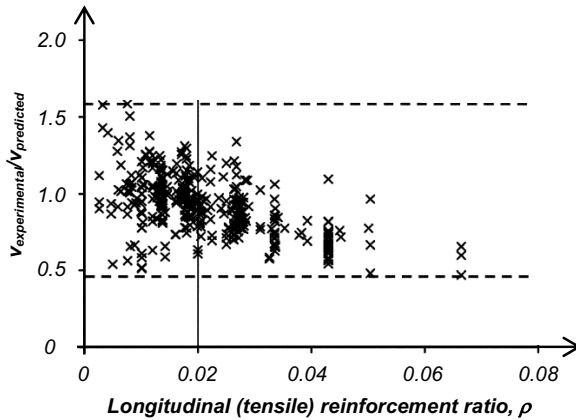


Figure 3.14. Experimental nominal shear stress normalised against prediction plotted to the longitudinal shear reinforcement ratio, based on Hedman and Losberg (1978).

The upper limit or the maximum shear resistance is given as the web compressive failure based on the classical truss model correlated to experimental results in Hedman and Losberg (1975):

$$V_u \leq 0.25b_w df_{cc} \quad (3.45)$$

3.3.4 Compression field approaches

Compression field approaches assumes fictitious rotating cracks that are stress free and parallel to the principal (diagonal) compressive direction. A uniform uniaxial compressive stress field is considered and thus local variations of the stresses in the concrete and reinforcement due to bond effect (e.g. tension stiffening) are neglected. Kupfer (1964) applied the Mörsh truss analogy to find the inclination of the diagonal cracks in the web of reinforced concrete girders. In this approach the concrete tensile strength was neglected assuming a linear elastic truss and the complementary strain energy of the truss with respect to the crack inclination was minimised in order to obtain the shear stresses. Further extensions on this basis can be found in Baumann (1972).

The previously mentioned compression field approaches assumed a linear elastic response and thus a linear compression field. Collins and Mitchell (1978) presented a non linear approach for shear based on the tension field theory derived by Wagner (1929) for thin walled metal girders.

Applying the Wagner tension field for reinforced concrete together with the assumption that the concrete will not take any tensile stresses after cracking and that the

shear is taken by a field of diagonal compressive stresses will give the following expression for the inclination of the diagonal compressive stresses, θ ,

$$\tan^2 \theta = \frac{\varepsilon_x - \varepsilon_2}{\varepsilon_z - \varepsilon_2} \tag{3.46}$$

Where ε_x is the longitudinal strain of the web, ε_z is the transverse strain of the web and ε_2 is the principal compressive strain. All tensile strains are positive and compressive strains are negative. The compatibility relationship for ε_x , ε_z and ε_2 expressed in eq. (3.46) is based on the Mohr's circle of strains. It is important to point out that the Collins and Mitchell approach to compression field theory is based on average stresses and strains. This means that the stresses and strains are measured over a length that includes several cracks, see Figure 3.15. Further, the most debatable assumption and the foundation of this compression field approach is that the principal stress and strain direction, θ , is equal to the crack inclination, θ_{cr} . This assumption is further discussed in Paper V. It is possible to obtain the principal tensile strain from Mohr's circle shown in Figure 3.15 along with the shear strain in the web as

$$\varepsilon_1 = \varepsilon_x + \varepsilon_z - \varepsilon_2 \tag{3.47}$$

$$\gamma_{xz} = 2(\varepsilon_x - \varepsilon_2) \cot \theta \tag{3.48}$$

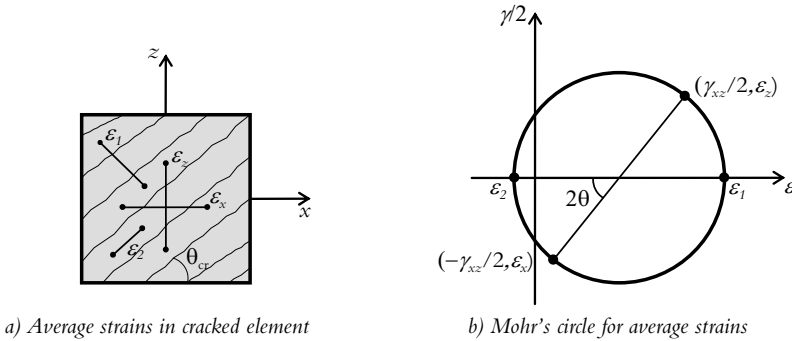


Figure 3.15. Compatibility conditions for a cracked web element, based on Collins and Mitchell (1991).

Consider a symmetrically reinforced concrete beam subjected to only shear, shown in Figure 3.16. For a given shear load there exist four unknowns: stress in longitudinal reinforcement f_x , stress in stirrups f_v , diagonal compressive stress f_2 and the inclination of the diagonal compressive stresses θ . To solve these unknowns there are three equilibrium equations and one compatibility equation, eq. (3.46). For carrying out a non-linear analysis, the constitutive relations (stress-strain relationships) for concrete and reinforcement can be used, see Figure 3.21. This allows a complete load and deformation analysis of a structural member.

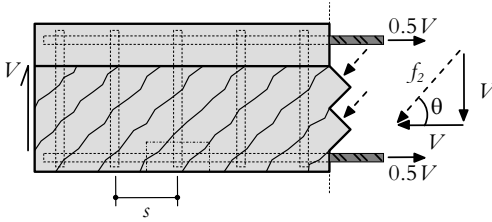


Figure 3.16. Reinforced concrete beam with symmetrical reinforcement subjected to shear.

However, response predictions based on compression field theory typically overestimate the deformations and give conservative load capacities since the concrete tensile strength is neglected. If web compressive failure is governing, the compression field theory still can give overestimated load capacities if incorrect constitutive relations for the compression softening are considered. There exist different approaches or modifications on how to deal with these shortcomings of the compression field theory. These modifications can be subdivided into two categories:

- Rotating inclination of cracks, accounting for the tension stiffening effect through empirical relationships between average stresses and strains between the cracks, Vecchio and Collins (1986) and Hsu (1988).
- Fixed interlocked cracks relating the constitutive laws between average shear stress to the average shear strain, Pang and Hsu (1996).

The so called rotating angle softened truss model (RA-STM), Hsu (1988), is basically similar to the modified compression field theory (MCFT), Vecchio and Collins (1986). The difference between RA-STM and MCFT lies within the limitations of the stresses in the reinforcement. The fixed angle softened truss model (FA-STM) is essentially similar to the RA-STM. In the FA-STM, the normal stresses acting on the crack surface is neglected and an empirical relationship between the shear stresses acting on the crack faces and the associated average shear strain due to crack slip is introduced. In the following section the MCFT will be described since it was the first model to consider tension stiffening effect and is also adopted in Canadian code, CSA (1994).

Modified compression field theory (MCFT)

Vecchio and Collins (1982) investigated the stress-strain relationship for diagonally cracked reinforced concrete elements in pure shear. It was found that the principal compressive stress, f_2 , was a function of not only the principal compressive strain, ϵ_2 , but also the coexisting principal tensile strain, ϵ_1 . The uniaxial compressive strength is often approximated by a parabola according to eq. (3.49). This parabola function is supposed to describe the typical strain softening behaviour of concrete in uniaxial compression shown in Figure 3.17 a) and b).

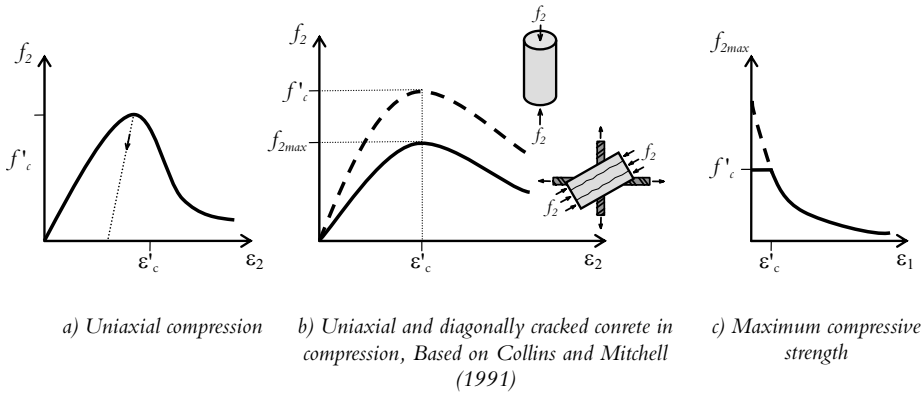


Figure 3.17. Reinforced concrete beam with symmetrical reinforcement subjected to shear.

$$\frac{f_2}{f'_c} = 2 \left(\frac{\varepsilon_2}{\varepsilon'_c} \right) - \left(\frac{\varepsilon_2}{\varepsilon'_c} \right)^2 \quad (3.49)$$

Where f'_c is the peak compressive strength and ε'_c is the strain at the peak compressive strength (normally given in the range of 0.002–0.0035 depending on the concrete quality). As stated above, the uniaxial compressive stress–strain relationship differs from the compressive behaviour in shear. In uniaxial compressive the concrete member is only subjected to small amounts of tensile strains due to the Poisson's effect. In a diagonally cracked web the concrete is subjected to substantial tensile strains and the compressive strain may also need to be transmitted through previously formed cracks. In order to deal with this discrepancy, Vecchio and Collin (1986) proposed the following empirical relationship for the maximum diagonal compressive strength in shear, f_{2max} , to the peak compressive strength, f'_c , see also the previous Figure 3.16 c.

$$\frac{f_{2max}}{f'_c} = \frac{1}{0.8 + 170\varepsilon_1} \leq 1.0 \quad (3.50)$$

The equilibrium conditions for MCFT are derived in Vecchio and Collins (1986) by using a symmetrically reinforced cross section subjected to pure shear. It is assumed that the shear load is taken by the diagonal compressive stresses, f_2 , together with the diagonal tensile stresses, f_1 , shown in Figure 3.18.

It is also assumed that the tensile stress variation between the cracks have hyperbolic shape with a maximum between the cracks and zero values at the cracks, see Figure 3.18 b). Since the equilibrium equations are obtained from integration of the stresses over the cross section, it is appropriate to use the average values for the tensile stresses. The diagonal compressive stress, f_2 , can be derived from Mohr's circle in Figure 3.18 c) as in eq. (3.51) (or alternatively using equilibrium in Figure 3.18 b).

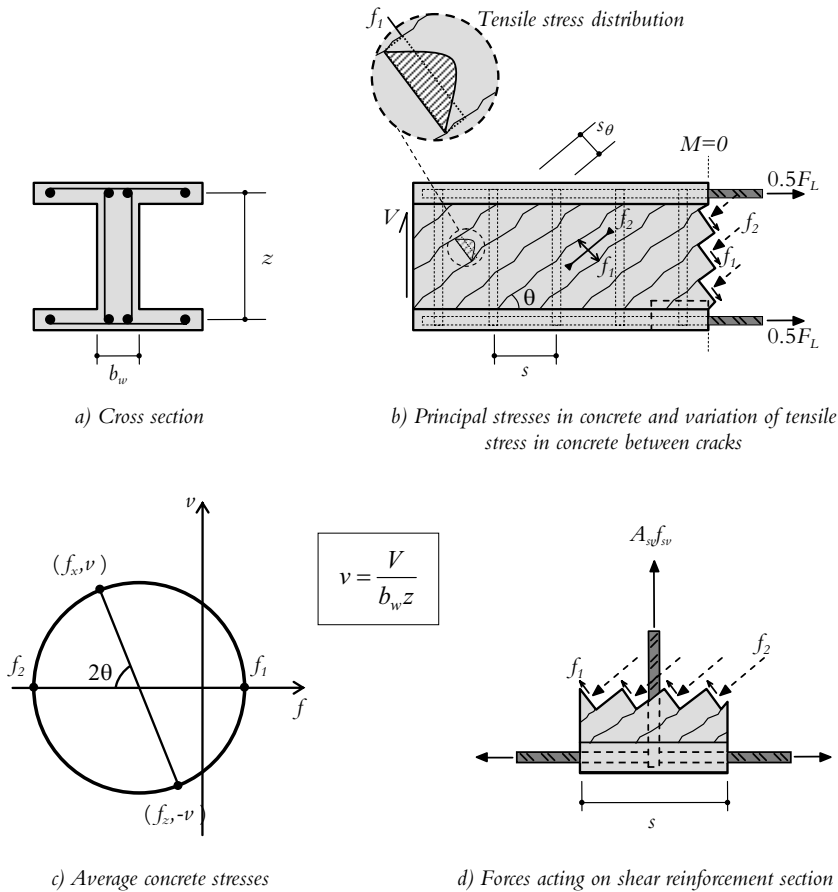


Figure 3.18. Modified compression field theory, conditions for equilibrium. Based on Collins and Mitchell (1991).

$$f_2 = (\tan \theta + \cot \theta)v - f_1 \quad (3.51)$$

Where the shear stress is assumed to be constant over the cross section as $v = V/b_w z$. The tensile contribution in MCFT changes the static system when compared to the Mörsh compression stress field in Figure 3.9 b), to the forces acting on the shear reinforcement section in Figure 3.18 d). In the later the diagonal compressive stresses are pushing the flanges apart while the diagonal tensile stresses are clamping them together. This means that the unbalanced vertical component must be taken by the tension in the shear reinforcement. Using Figure 3.18 d), the equilibrium can be expressed as

$$A_{sz}f_{sz} = (f_2 \sin^2 \theta - f_1 \cos^2 \theta) b_w s \quad (3.52)$$

Where f_{sz} is the average stress in the stirrups. Using the expression for the diagonal compressive stress in eq. (3.51) in the expression above will give the shear force as

$$V = \underbrace{\frac{A_{sz}f_{sz}}{s}}_{V_{steel}} z \cot \theta + \underbrace{f_1 b_w z \cot \theta}_{V_{concrete}} \quad (3.53)$$

The expression for the shear resistance given above consists of the sum of the shear reinforcement contribution due to tension in the stirrups and the concrete contribution due to the tensile stresses in the concrete. This has the same attributes as the ACI and BBK provisions as “addition” approach, see eq. (3.23).

Considering the longitudinal reactions, then the unbalanced longitudinal component of the diagonal concrete stresses must be taken by tensile stresses in the longitudinal reinforcement. Longitudinal equilibrium can be expressed according to Figure 3.18 b) as

$$A_{sx}f_{sx} = (f_2 \cos^2 \theta - f_1 \sin^2 \theta) b_w z \quad (3.54)$$

where A_{sx} is the longitudinal reinforcement area and f_{sx} is the average stress in the longitudinal reinforcement. Using the expression of the diagonal compressive in eq. (3.51) gives the force in the longitudinal reinforcement as

$$A_{sx}f_{sx} = V \cot \theta - f_1 b_w z \quad (3.55)$$

Load transfer between cracks

Considering a reinforced concrete element subjected to tensile loading, Vecchio and Collins (1986) recommended the first average stress-strain relationship based on empirical results, see Figure 3.19. The authors calibrated this relationship further based more experiments and the recommended stress-strain relationship is shown in eq. (3.56) and (3.57).

$$f_1 = E_c \varepsilon_1 \quad \text{if } \varepsilon_1 \leq \varepsilon_{cr} \quad (3.56)$$

$$f_1 = \frac{\alpha_1 \alpha_2 f_{cr}}{1 + \sqrt{500 \varepsilon_1}} E_c \varepsilon_1 \quad \text{if } \varepsilon_1 > \varepsilon_{cr} \quad (3.57)$$

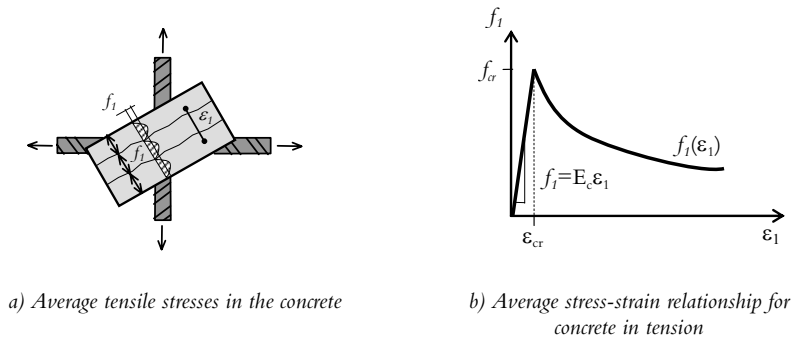


Figure 3.19. Modified compression field theory, conditions for equilibrium. Based on Collins and Mitchell (1991).

By assuming average stresses and strains over the cross section local variations will not be considered. Thus, the stresses in the crack will not be represented by the calculated average value in MCFT. At higher shear loads the yield limit of the shear reinforcement will be reached at a crack location.

Since the equilibrium equations so far do not consider these locally high stresses, a “crack check” needs to be established, Bentz (2000). This is done by looking at the stress state in between cracks and the stress state in the crack, see Figure 3.20.

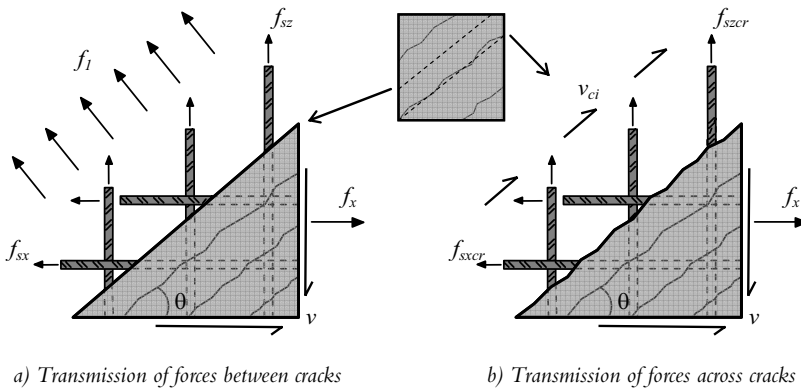


Figure 3.20. Transmission of stresses/forces a) between cracks and b) across cracks.

The stress state in between cracks includes the concrete contribution. However, the concrete contribution across the crack will be zero, $f_t = 0$. At higher shear forces, the concrete may still be able to transmit tension forces due to aggregate interlock. Therefore, a local shear stress, ν_{ci} , is introduced to the stress state across the crack, see Figure 3.20 b. Note, this assumption is not in accordance with principal stress state,

since in the principal stress plane there should be no shear stresses. The “crack check” is basically to assume that the two states of stresses in Figure 3.20 a) and b) have to be statically equivalent. Transverse force equilibrium, eq. (3.58), will give the following upper limit for the resisting principal stress, f_1 eq. (3.59), in the structure assuming that the transverse steel reinforcement will yield at the crack, $f_{szcr} = f_{sy}$.

$$A_{sz} f_{sz} \frac{z}{s} \cot \theta + f_1 b_w z \cot \theta = A_{sz} f_{sy} \frac{z}{s} \cot \theta + v_{ci} b_w z \quad (3.58)$$

$$f_1 = v_{ci} \tan \theta + \frac{A_{sz}}{s b_w} (f_{sy} - f_{sz}) \quad (3.59)$$

The upper limit of the ability to transmit shear stresses across the crack depends on the crack width and is based on the experimental results in Walraven (1981) and Vecchio and Collins (1986), eq. (3.60). The crack width is expressed in eq. (3.61) and is taken as the product of the principal tensile strain and the average crack diagonal spacing, see Figure 3.18 b) and Figure 3.21.

$$v_{ci} = \frac{0.18 \sqrt{f'_c}}{0.3 + \frac{24w}{a + 16}} \quad (3.60)$$

$$w = \varepsilon_1 s_\theta \quad (3.61)$$

where w is the crack width and a is the maximum aggregate size in mm. The diagonal spacing of the cracks is based on a logical expression depending on both the crack spacing from both longitudinal and transverse reinforcement, see eq. 10 in Figure 3.21. The longitudinal and transverse crack spacing can be calculated using the recommendation in CEB-FIP (1972). A summary of all equations used in the MCFT is shown in Figure 3.21.

Solution technique for MCFT

Since the MCFT is an iterative process requiring that the 15 equations in Figure 3.21 be solved in order to calculate the shear resistance, Collin and Mitchell (1991) gave a suitable solution technique for calculating the shear resistance given as

- Step 1 Choose a starting value of ε_1 at which to perform the calculations.
- Step 2 Estimate the diagonal inclination θ .

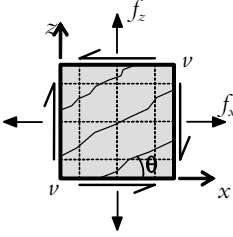
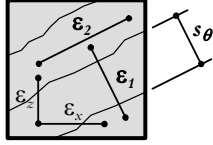
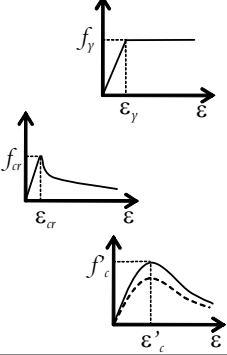
| | Stresses and strains | Cracks |
|--------------------|--|--|
| EQUILIBRIUM |  | <p><u>Average stresses</u></p> <ol style="list-style-type: none"> $f_x = \rho_x f_{sx} + f_1 - \nu \cot \theta$ $f_z = \rho_z f_{sz} + f_1 - \nu \tan \theta$ $\nu = (f_1 + f_2) / (\tan \theta + \cot \theta)$ <p><u>Stresses in crack</u></p> <ol style="list-style-type: none"> $f_{sxc} = \frac{(f_x + \nu \cot \theta + \nu_i \cot \theta)}{\rho_x}$ $f_{szc} = \frac{(f_z + \nu \tan \theta + \nu_i \tan \theta)}{\rho_z}$ |
| GEOMETRY |  | <p><u>Average strains</u></p> <ol style="list-style-type: none"> $\tan^2 \theta = (\epsilon_x + \epsilon_2) / (\epsilon_z + \epsilon_2)$ $\epsilon_1 = \epsilon_x + \epsilon_z + \epsilon_2$ $\gamma_{xz} = 2(\epsilon_x + \epsilon_2) \cot \theta$ <p><u>Crack widths</u></p> <ol style="list-style-type: none"> $w = s_\theta \epsilon_1$ $s_\theta = 1 / \left(\frac{\sin \theta}{s_{mx}} + \frac{\cos \theta}{s_{mz}} \right)$ |
| MATERIAL |  | <p><u>Stress – strain</u></p> <p>Steel:</p> <ol style="list-style-type: none"> $f_{sx} = E_s \epsilon_x \leq f_{yx}$ $f_{sz} = E_s \epsilon_z \leq f_{yz}$ <p>Concrete:</p> <ol style="list-style-type: none"> $f_1 = f_{cr} / (1 + \sqrt{500 \epsilon_1})$ $f_2 = \frac{f'_c}{0.8 + 170 \epsilon_1} \left[2 \frac{\epsilon_2}{\epsilon'_c} - \left(\frac{\epsilon_2}{\epsilon'_c} \right)^2 \right]$ <p><u>Shear stress on crack</u></p> <ol style="list-style-type: none"> $\nu_i \leq \frac{0.18 \sqrt{f'_c}}{0.3 + 24 w / (a_g + 16)}$ |

Figure 3.21. Summary of equilibrium, geometry (compatibility) and constitutive (material) relationships, for modified compression field theory, based on Bentz et al. (2006).

•Step 3 Calculate w from $w = \epsilon_1 s_m \theta$, where:

$$s_\theta = \frac{1}{\frac{\sin \theta}{s_{mx}} + \frac{\cos \theta}{s_{mz}}}$$

$$s_{mx} = 2 \left(c_x + \frac{s_x}{10} \right) + 0.25 k_1 \frac{d_{bx}}{\rho_x}$$

$$s_{mz} = 2 \left(c_z + \frac{s}{10} \right) + 0.25 k_1 \frac{d_{bz}}{\rho_z}$$

where $\rho_z = A_{sz}/(b_w s)$ and $\rho_x = (A_{sx})/(A_c)$ and k_t is 0.4 for deformed bars or 0.8 for plain bars or bonded strands. The original intention with the equation above, CEB-FIP (1972) was to calculate crack spacings on the surface of the member. For the use in MCFT and calculation of the shear stresses, v_d , on the crack surface in the shear region then the crack spacing in the shear area of the member is of interest. Collins and Mitchell modified the CEB-FIP equation to take account of the fact that crack spacings become larger as the distance from the reinforcement increases. Therefore in their suggested equation for calculating the crack spacing they suggest to use the maximum distance from the reinforcement (c_x and c_z) instead of the concrete cover distance. It should also be mentioned that their equation considers the strain gradient to be 0.25 and thus assumes uniform tensile straining. s_x is the distance in between the longitudinal reinforcement and s is the distance between the stirrups.

- Step 4 Estimate the shear strength, f_v .
- Step 5 Calculate f_1 and take the smallest value

$$\varepsilon_1 \leq \varepsilon_{\sigma} \text{ then } f_1 = E_c \varepsilon_1$$

$$\varepsilon_1 > \varepsilon_{\sigma} \text{ then } f_1 = \frac{\alpha_1 \alpha_2 f_{\sigma}}{1 + \sqrt{500 \varepsilon_1}}$$

where α_1 is a factor accounting for bond characteristics of reinforcement.

$\alpha_1 = 0.7$ for plain bars, wires or bonded strands, where α_2 is a factor accounting for sustained or repeated loading. $\alpha_1 = 0$ for non bonded reinforcement bars; $\alpha_2 = 1.0$ for short-term monotonic loading; $\alpha_2 = 0.7$ for sustained and/or repeated loading

Limitations of the principal tensile stress

To maintain equality of transmitted forces across cracks (at the crack and at the centre between cracks), see Figure 3.20. For these stresses must be statically equivalent. The two sets of stresses are required to produce the same vertical force.

$$A_{sz} f_{sz} \left(\frac{z}{s} \cot \theta \right) + f_1 b_w z \cot \theta = A_{sz} f_{sz} \left(\frac{z}{s} \cot \theta \right) + v_d b_w z$$

For this equality to remain then f_1 is limited to

$$f_1 = v_d \tan \theta + \frac{A_{sz}}{s b_w} (f_{sy} - f_{sz})$$

Where, the upper limit of the shear stresses due to aggregate interlock is

$$v_{ci} = \frac{0.18\sqrt{f'_c}}{0.3 + \frac{24w}{a + 16}} \quad (\text{MPa and mm})$$

Stresses in the transverse reinforcement up to the yield point

$$f_{sy} = E_s \varepsilon_y$$

- Step 6 Calculate the shear force, V , from

$$V = f_1 b_w z \cot \theta + \frac{A_{sz} f_{sz}}{s} z \cot \theta$$

- Step 7 Calculate f_2 from

$$f_2 = (\tan \theta + \cot \theta) v - f_1$$

Where, $v = \frac{V}{b_w z}$

- Step 8 Calculate the principal compressive stress, $f_{2,max}$, from

$$f_{2,max} = \frac{f'_c}{0.8 + 170\varepsilon_1}$$

Note that f_2 can also be formulated as $f_2 = f_{2,max} \left[2 \left(\frac{\varepsilon_2}{\varepsilon'_c} \right) - \left(\frac{\varepsilon_2}{\varepsilon'_c} \right)^2 \right]$

- Step9 Check that $f_2 \leq f_{2,max}$.

If $f_2 > f_{2,max}$, then the compression stress is higher than the concrete compression strength and therefore the solution is not possible. Return to step 1 and choose a smaller ε_1 .

- Step 10 Calculate the principal compressive strain by evolving step 8.

$$f_2 = f_{2,max} \left[2 \left(\frac{\varepsilon_2}{\varepsilon'_c} \right) - \left(\frac{\varepsilon_2}{\varepsilon'_c} \right)^2 \right] \Rightarrow$$

$$\varepsilon_2^2 - 2\varepsilon'_c \varepsilon_2 + \frac{f_2}{f_{2,max}} \varepsilon'_c{}^2 = 0$$

$$\varepsilon_2 = \varepsilon'_c \left(1 \pm \sqrt{1 - \frac{f_2}{f_{2,max}}} \right)$$

According to Collins and Mitchell (1991) the suitable way is to take the smaller value, thus.

$$\varepsilon_2 = \varepsilon'_c \left(1 - \sqrt{1 - \frac{f_2}{f_{2\max}}} \right)$$

- Step 11 Calculate the longitudinal and transverse strains ε_x and ε_t from

$$\tan^2 \theta = \frac{\varepsilon_x - \varepsilon_2}{\varepsilon_t - \varepsilon_2} \Rightarrow \text{and } \varepsilon_1 = \varepsilon_x - \varepsilon_t - \varepsilon_2 \Rightarrow$$

$$\varepsilon_x = \tan^2 \theta (\varepsilon_t - \varepsilon_2) + \varepsilon_2 \text{ and } \varepsilon_t = \varepsilon_x - \varepsilon_1 - \varepsilon_2$$

Thus leading to

$$\varepsilon_x = \frac{\varepsilon_1 \tan^2 \theta + \varepsilon_2}{1 + \tan^2 \theta}$$

$$\varepsilon_t = \frac{\varepsilon_1 + \varepsilon_2 \tan^2 \theta}{1 + \tan^2 \theta}$$

- Step 12 Calculate the stress in the stirrup

$$f_{sz} = E_s \varepsilon_t \leq f_{sy}$$

- Step 13 Ensure that the estimate of f_v in “step 4” is correct. If not, revise the estimate and return to “step 5”

Pure shear or combination of shear and moment

For a member subjected to a combination of shear and moment, the strains vary over the cross section of the beam (height/depth). It is possible to reduce the computational cost if the following simplifications are made

- Ignoring that the shear stresses redistributes at higher moments. This means that the shear stress is assumed to be given by
- $v = \frac{V}{b_w z}$ (constant shear stresses over the cross section)
- The bi-axial stresses and strains are considered at only one level of the web. The strains in the longitudinal direction at this location, ε_x , are used to calculate, θ , this inclination is then assumed to be constant over the depth of the web

Before this simplified procedure can be done a decision has to be made on where strains, ε_x , should be taken in the web. One conservative way is to take the highest value of, ε_x , but increasing, ε_x , will reduce the shear capacity. However, beams with web reinforcement have considerable capacity for redistribution of shear stresses (thus

being transferred from the most highly strained areas of the cross section to the less strained areas). Note, members containing no web reinforcement have inferior capacity of redistributing these shear stresses and for such members the highest longitudinal strain, ϵ_x , in the web should be used. In Collins and Mitchell (1991) it is shown that a still conservative value for, ϵ_x , could be taken at mid-depth/height ($z/2$) of the member. The solution technique is now separated from each other, by considering that the member is loaded in pure shear or by combined shear and moment.

| Pure shear | Combined shear and moment |
|---|--|
| <p>•Step 14</p> <p>Calculate the stresses in the longitudinal reinforcement</p> $f_{sx} = E_s \epsilon_x \leq f_{sy}$ <p>•Step 15</p> <p>Calculate the axial forces on the member</p> $N = A_{sx} f_{sx} - \frac{V}{\tan \theta} + f_1 b_w z - f_c (A_c - b_w z)$ <p>Where the axial compression stress, f_c, acts on the concrete areas outside the web.</p> <p>If ϵ_x is tensile then naturally the axial compression stress, $f_c = 0$. But for $\epsilon_x > 0$ then</p> $f_c = f'_c \left[2 \left(\frac{\epsilon_x}{\epsilon'_c} \right) - \left(\frac{\epsilon_x}{\epsilon'_c} \right)^2 \right]$ <p>•Step 16</p> <p>Control that the axial load equals the desired value (usually zero). If undesired value is obtained then make a new estimate of θ and return to “step 2”. Increasing θ will increase N.</p> | <p>•Step 14</p> <p>Find the strain distribution that corresponds to the desired moment. Then determine the corresponding axial load N_p. Using analysis of plane sections with the strain at the chosen level set to the ϵ_x value calculated in “step 11”.</p> <p>•Step 15</p> <p>Find the axial force of the member from the influence of the longitudinal compressive stresses in the concrete over the cross sectional area $b_w d$ caused by shear</p> $N = N_p - V \cot \theta$ <p>•Step 16</p> <p>Control that N equals the desired axial load on the member. If this is not the case then make a new estimate of θ and return to Step 3. Increasing θ will increase N.</p> |

•Step 17

To maintain equilibrium (between the stresses at the centre of diagonal cracks and the stresses acting on the crack), control that the longitudinal reinforcement can carry stresses across the crack according to

$$A_{sx}f_{sy} \geq A_{sx}f_{sx} + f_1b_wz + \left[f_1 - \frac{A_{sz}}{b_w s} (f_{sy} - f_{sz}) \right] b_w z \cot^2 \theta$$

If the longitudinal reinforcement will yield at a crack this may limit the magnitude of tensile stresses transmitted by the concrete. The equation above is based on equilibrium that the two sets of stresses (in concrete and at crack) produce the same horizontal force.

As shown above, using a full MCFT analysis for design requires that the 15 basic equations in Figure 3.21 have to be solved using the iterative process involving steps 16 to 17. This process is not suitable for practical design and a simplified approach is given in Bentz et al. (2006) and also implemented in the Canadian design code, CSA (2004). One of the main simplifying assumptions is that the shear strength of members with no stirrups is controlled by aggregate interlocking together with a conservative assumption that the failure occurs just before yielding of the transverse reinforcement. Further simplifications are also made by limiting the strains, such as for yielding of the stirrups ($\epsilon_z \geq 0.002$), crushing of concrete ($\epsilon_2 \approx 0.002$) and also limiting the longitudinal strain at failure (ϵ_x) to 0.002. The calculation procedure of the shear resistance according to the simplified MCFT involves a few steps more than the shear design given by, e.g. ACI (2008). As a first step, the longitudinal strain ϵ_x has to be assumed and then this assumption has to be checked for convergence by control of the longitudinal equilibrium (x-direction) and assuming that the longitudinal reinforcement is not yielding. Using this convergence control is quite straight forward for members subjected to pure shear, for members subjected to combinations of shear and bending moment the control becomes more intricate. The upper limit of the maximum shear stress is taken as $0.25f_c$ and the last check is to see if the longitudinal reinforcement can transmit the shear stress along the crack without exceeding its yield stress. In Bentz et al. (2006), the average ratio between experimental to predicted shear resistance for 102 concrete membrane elements was 1.11 with a COV of 13%. While doing a full analysis using the MCFT on the same set of specimens will predict an average of 1.01 with a COV of 12.2%.

The simplified MCFT is basically a linear relationship when considering the longitudinal strain, ε_x , and gives reasonable results for strains given in the limited area of up to strain levels of 0.002. Note, for the use of longitudinal reinforcement with linear elastic strain development such as FRPs (ultimate strains ranging from approximately 0.01-0.03), a second order approximation based on MCFT and simplified MCFT can be found in Hoult et al. (2008).

Simplified Modified compression field theory

The shear strength of a section is assumed to be a function of the two parameters β , factor for the tensile stresses in the cracked concrete, and θ , the inclination of the diagonal compressive stresses in the web of the section. In the simplified modified compression field theory, β and θ is developed as simplified equations determined from MCFT.

In the simplified MCFT the shear strength of an element is modelled in the flexural region of a beam and therefore it is assumed that the clamping stresses, f_z see Figure 3.20, will be negligible small ($f_z = 0$). These so called “clamping stresses” are high net vertical compressive stresses near the point loads and reactions (e.g. freely supported, four point bending tests) and they cause stirrup strains in these locations to be close to zero. Further assumed simplifications are regarding the strains in the element that leads to limitations of the maximum shear stresses acting on the element. The limitations on the strains are as follows (also stated in the section above):

- For the transverse reinforcement to reach the yield limit at failure then the strain, ε_z , needs to exceed approximately 0.002.
- For the concrete to be crushed then the strain, ε_2 , will have to reach approximately 0.002.

However if ε_z and ε_2 both are 0.002 at failure then eq. (3), (6), (7), (13), and (14) in Figure 3.21 from the MCFT predicts the maximum shear stress to be approximately $0.28f_c$. If the longitudinal stresses, ε_x , are small then the predicted shear stress at failure is predicted to approximately $0.32f_c$.

- If failure occurs before yielding of the transverse reinforcement the simplified MCFT conservatively assumes that the shear stresses will be $0.25f_c$.
- If failure occurs at a shear stress level below $0.25f_c$ then it is assumed that at failure, the stresses in transverse reinforcement in between cracks (f_{sz}) and stresses at cracks (f_{scr}) will equal the yield stress (f_y).

By summing the forces in the z-direction at the crack using eq. (5) in Figure 3.21 and assuming $f_z = 0$ and $f_{scr} = f_y$ then shear stress can be express as

$$v = v_d + \rho_z f_y \cot \theta \tag{3.62}$$

Eq. (2) in Figure 3.21 can also be rearranged, with $f_z = 0$.

$$v = \underbrace{f_1 \cot \theta}_{v_c} + \underbrace{\rho_z f_y \cot \theta}_{v_s} \quad (3.63)$$

Both of the proposed equations above can be expressed as

$$v = v_c + v_s = \beta \sqrt{f'_c} + \rho_z f_y \cot \theta \quad (3.64)$$

Comparing the two equations above and that the principal tensile stress according to eq. (13) in Figure 3.21 is

$$\beta = \frac{0.33 \cot \theta}{1 + \sqrt{500 \varepsilon_1}} \quad (3.65)$$

The value of β must satisfy the limit of the shear strength of concrete, v_c , according to eq. (15) in Figure 3.21.

$$\beta \leq \frac{0.18}{0.31 + \frac{24w}{(a_g + 16)}} \quad (3.66)$$

The crack width, w , is calculated by multiplying the principal strain, ε_1 , to the inclined crack spacing, s_θ . The latter is in turn dependent on the crack spacing in the x and z direction (s_{mx} and s_{mz}), see also eq. (10) in Figure 3.21. Note that a_g is the maximum aggregate size in the concrete. Since both the inclination, θ , and the principal tensile strain, ε_1 , are unknown an expression for the β value must be expressed.

In the simplified MCFT it is assumed that the β values depend on the longitudinal strain ε_x and the effective crack spacing parameter s_{xe} . In Bentz et al. (2006), they suggest that these two factors affect the shear strength β and crack inclination θ as “strain effect factor” and “size effect factor” and that these can be multiplied by each other.

$$\beta = f(\varepsilon_x, s_{xe}) = \text{“strain effect factor”} \cdot \text{“size effect factor”} \quad (3.67)$$

$$\theta = f(\varepsilon_x, s_{xe}) = \text{“strain effect factor”} \cdot \text{“size effect factor”} \quad (3.68)$$

It is however noted that these factors are not really independent, but for the simplified calculation of the MCFT this interdependence is ignored. The shear strength factor and crack inclination factor is calculated based on the MCFT dependence on the longitudinal strain and crack spacing parameters, see the next page.

As a simplification the crack spacing in the x and z direction (s_x and s_y) can be taken as the internal distance of the reinforcement taken in the orthogonal direction of each direction. Or as stated in ASCE-ACI 445 (1998), if the concrete member contains more shear reinforcement than the specified minimum shear reinforcement (e.g. $\rho_s f_y >$

$0.06\sqrt{f'_c}$) then the crack spacing is assumed to be well controlled and the effective crack spacing, s_{xe} , can be taken as 300 mm. For members containing only flexural reinforcement, the vertical crack spacing near the mid-depth of the member, s_x , is assumed to be equal to $0.9d$. In order to account for the aggregate interlocking the effect on the crack spacing the following expression was derived from eq. 15 in Figure 3.21 based on concrete members having no transverse reinforcement.

$$s_{xe} = \frac{35s_x}{a_g + 16} \geq 0.85s_x \quad (3.69)$$

For high strength concrete $f'_c > 70$ MPa, the cracks will go through the aggregate rather than around the aggregates. This will reduce the aggregate interlocking effects and to account for this the aggregate size, a_g , is set to zero.

“Strain effect factor”

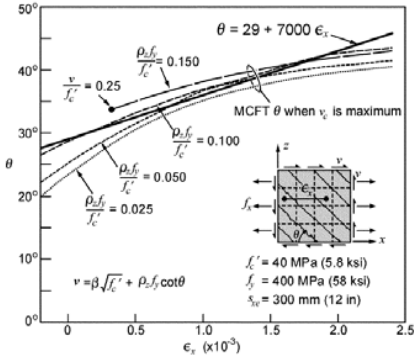


Figure 3.22. With transverse reinforcement, Bentz et al. (2006)

$$\theta = 29 + 7000\varepsilon_x \quad (3.70)$$

“Size effect factor”

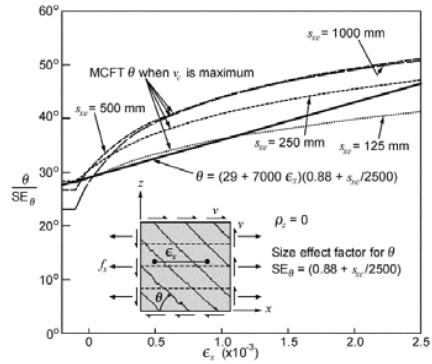


Figure 3.23. With no transverse reinforcement, Bentz et al. (2006)

$$SE_\theta = 0.88 + s_{xc}/2500 \quad (3.71)$$

$$\theta = (29 + 7000\varepsilon_x) \cdot (0.88 + s_{xc}/2500) \leq 75^\circ \quad (3.72)$$

It can be seen that the suggested equation gives conservative values for nearly all combinations of the ε_x and s_{xc} . It is also noted that underestimating q is conservative since it will produce higher strains in the longitudinal reinforcement.

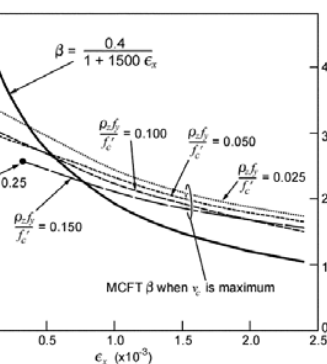


Figure 3.24. With transverse reinforcement, Bentz et al. (2006)

$$\beta = \frac{0.4}{1 + 1500\varepsilon_x} \quad (3.73)$$

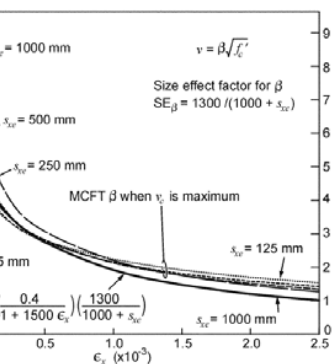


Figure 3.25. With no transverse reinforcement, Bentz et al. (2006)

$$SE_\beta = \frac{1300}{1000 + s_{xc}} \quad (3.74)$$

$$\beta = \frac{0.4}{1 + 1500\varepsilon_x} \cdot \frac{1300}{1000 + s_{xc}} \quad (3.75)$$

It can be seen that the suggested equation is giving conservative values for all values but not when the ε_x and s_{xc} are small

Now the expressions are made for, β , θ and s_{xe} and the only unknown in is the longitudinal strain, ε_x . The longitudinal strain at mid depth of the concrete member is conservatively taken as half of the tensile strain in the flexural tensile reinforcement caused by the bending moment and the shear. The longitudinal strain is then expressed as

$$\varepsilon_x = \nu \frac{1 + \frac{M}{Vz}}{2E_s \rho_l} = \frac{V + \frac{M}{z}}{2E_s A_s} \quad (3.76)$$

Where ν is the shear stress and is assumed to be constant over the cross section, thus $\nu = V/(b_w d)$ and ρ_l is the tensile reinforcement ratio taken as $\rho_l = A_s/(b_w d)$.

Solution technique for simplified MCFT

The solution procedure for calculating the shear resistance according to the simplified MCFT is done in six steps.

- Step 1 Estimate a value for the longitudinal strain, ε_x .
- Step 2 Calculate the effective crack spacing, s_{xe} .
- Step 3 Calculate the β and θ according to eq. (3.75) and (3.72).
- Step 4 Calculate the shear stress, ν according to eq. (3.64).
- Step 5 Calculate the shear force, V .
- Step 6 Calculate the longitudinal strain, ε_x , according to eq. (3.76). Compare this value to the estimates value in step 1. Return to step 1 until convergence is obtained.

This thesis will focus on the simplified MCFT and the MCFT for MBC strengthened concrete system, see chapter 4 and Paper V.

3.3.5 Limit analysis approach

The history of plasticity dates back to the 1860s, Tresca (1864). But it was not until the 1950s that it was put on a sound physical basis by researchers such as Daniel Drucker and William Prager. This section summarises the basic concepts of limit analysis based on concrete plasticity for perfectly plastic material behaviour. For simplicity a rigid-perfectly plastic material behaviour is assumed. By doing so, complicated formulations including elastic strains are avoided. This means that the stresses remain constant at failure and even for large deformations. It should be noted that an elastic-perfectly plastic material will have no elastic strain increments occurring in the ultimate limit state. This implies that the limit theorems found for rigid-perfectly plastic material behaviour are also valid for elastic-perfectly plastic materials, Kaufmann (1998). Typical load and deformation behaviour for rigid-perfectly plastic and elastic-perfectly plastic

materials are shown in Figure 3.26. A rigid-plastic material behaviour is not a realistic estimation but can be used when the plastic strains are much larger than the elastic strains.

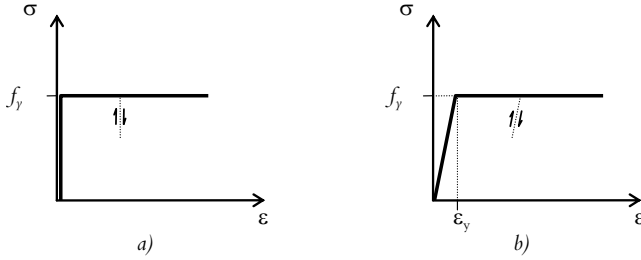


Figure 3.26. Load and deformation for a) Rigid-perfectly plastic material and b) Elastic-perfectly plastic material.

At failure, the plastic strains or preferably the plastic strain increments $d\boldsymbol{\epsilon}^{(p)}$ (also equivalent to plastic strain rates $\dot{\boldsymbol{\epsilon}}^{(p)}$) are of the most interest since a rigid-perfectly plastic material behaviour is assumed. In this case the strain rate is not a differential of the strains with respect to time but rather just a scalar, t . The product $\boldsymbol{\sigma} \cdot \dot{\boldsymbol{\epsilon}}^{(p)}$ should be considered as work or dissipation rather than power or rate of dissipation.

The yield surface is determined by the yield condition $f = f(\boldsymbol{\sigma}) = 0$ shown in Figure 3.27 as the perimeter of a non-plastic domain $f(\boldsymbol{\sigma}) < 0$. This means that the body remains rigid for all states of stress below the yield limit, $f(\boldsymbol{\sigma}) < 0$. For stress combinations at the yield surface plastic flow may occur, $f(\boldsymbol{\sigma}) = 0$. By assuming that the associated flow rule, eq. (3.77), is valid, thus, that the non-plastic domain is convex and that the plastic strain increments at failure are perpendicular to the yield surface, see Figure 3.27. Based on these assumptions, one obtains eq. (3.78).

$$\dot{\boldsymbol{\epsilon}}^{(p)} = \lambda \text{grad } f = \lambda \frac{\partial f}{\partial \boldsymbol{\sigma}} \tag{3.77}$$

$$(\boldsymbol{\sigma} - \boldsymbol{\sigma}^*) \dot{\boldsymbol{\epsilon}}^{(p)} \geq 0 \tag{3.78}$$

where, λ is an arbitrary non-negative factor, the actual stress state at the yield surface is denoted $\boldsymbol{\sigma}$ and corresponds to $\dot{\boldsymbol{\epsilon}}^{(p)}$, $\boldsymbol{\sigma}^*$ is a stress state at or within the yield surface. Figure 3.27 shows the state of stresses, yield surface and the plastic strain rate. By rearranging eq. (3.78), one obtains the maximum energy dissipation given by von Mises (1928).

$$dD(\dot{\boldsymbol{\epsilon}}^{(p)}) = \boldsymbol{\sigma} \dot{\boldsymbol{\epsilon}}^{(p)} \geq \boldsymbol{\sigma}^* \dot{\boldsymbol{\epsilon}}^{(p)} \tag{3.79}$$

The principle of maximum energy dissipation is that the (virtual) dissipation per unit volume done on a given strain rate, $\dot{\boldsymbol{\epsilon}}$, assumes a maximum for the associated state of stress, $\boldsymbol{\sigma}$. The actual dissipation dD per unit volume is uniquely determined by the strain rate vector, $\dot{\boldsymbol{\epsilon}}$, for any yield surface. In this section the maximum energy dissipation is shown based on the assumption of convexity of the yield surface and normality of the plastic strain rates. Another approach is by first assuming the principal of maximum dissipation and then the convexity of the yield surface and the associated flow rule will follow from that, this is shown in Nielsen (1999). For further extensions on how to go from a unit body, as shown in Figure 3.27, to entire bodies or systems the reader is referred to Prager (1955) or more comprehensively in Nielsen (1999). The theorems (or extreme principles) of limit analysis will be described in the following section.

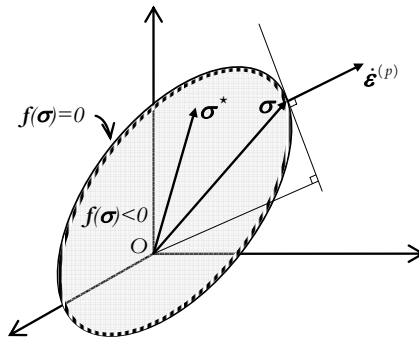


Figure 3.27. Plastic strain increment and yield condition $f(\boldsymbol{\sigma})$.

Extreme solutions and yield conditions

Since rigid plastic material behaviour is assumed there will be no deformations below the yield point. When the loading reaches the yield point, unlimited deformations are possible without changes in the load. If the corresponding strains satisfy a geometrically possible displacement field, then the body (or system) fails by yielding. Thus, the load carrying capacity is reached. To be able to determine the load carrying capacity, the principle of virtual work for a perfectly plastic body is used with extreme solutions. These basic theorems (extreme solutions/principles) of limit analysis were established by Gvozdev (1960), Hill (1951), and Drucker et al. (1952).

Lower bound theorem: An arbitrary load that is corresponding to a statically admissible state of stress everywhere at or below yield will not cause collapse of the body.

Upper bound theorem: An arbitrary load resulting from considering a kinematically admissible state of deformation that is, setting the work done by the external forces equal to the internal energy dissipation, not greater than or equal to the ultimate load

A statically admissible state of stress is in this context a state of stress that fulfils equilibrium and static boundary conditions. For a kinematically admissible state of deformation, the kinematic relations must be fulfilled.

For solutions where the lower- and upper bound theorem coincide, a uniqueness theorem was postulated and later on generalised by Sayir and Ziegler (1969).

Uniqueness theorem: Only one load can be found which satisfies:

- A statically admissible state of stress that corresponds to stresses on or within the yield surface.
- A kinematically admissible state of deformation that corresponds to strains/stresses according to the associated flow rule.

This means that loads satisfying the first condition are smaller or equal to the collapse load and loads satisfying the second condition are greater than or equal to the collapse load. Thus, a unique determination of the collapse load is achieved when conditions one and two give the same unique loads.

It is stated in Kaufmann (1998) that a complete solution, where the states of stress and deformation are compatible, is difficult or even impossible to achieve and that the ultimate load can usually be bracketed by the lower- and upper bound solutions. This is shown in Figure 3.28.

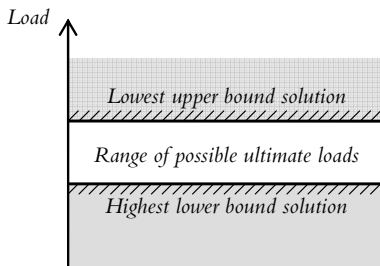


Figure 3.28. Illustration of the lower and upper bound solution.

To apply limit analysis on concrete structures, suitable failure criteria (yield conditions) must be postulated. Establishing an excessively detailed failure criterion for reinforced concrete will generate complexity and could also be misleading, because testing of plain concrete will give large scatterings in the results. Further, the crude assumption of rigid plastic material behaviour obeying the associated flow rule gives a drastic idealisation of the actual behaviour. Therefore a rather simple failure criterion is introduced using the modified Coulomb failure criterion. The modified Coulomb failure criterion was introduced by Chen and Drucker (1969) for brittle materials such as concrete blocks and rock. It is not within the scope of this thesis to elaborate this failure criterion. However, the yield condition for reinforced disks derived by Nielsen (1999), is shown in Figure 3.29. This yield condition is based on isotropic reinforcement ratio and

orthotropic alignment of the reinforcement. The reinforcement degree, Φ , is based on the ratio between the force per unit length that the reinforcement can carry and the force that the concrete can carry in pure compression, see also eq. (3.111). b_w is the thickness of the disk.

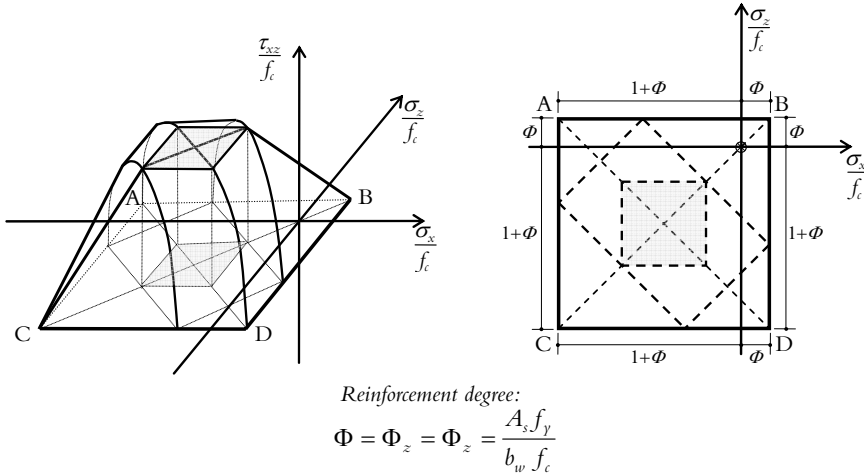


Figure 3.29. Yield condition for a concrete disk with isotropic reinforcement, based on Nielsen (1999).

It is possible to use limit analysis and concrete plasticity to estimate the load bearing capacities for reinforced concrete members. The best application refers to the lower bound solutions for safe design of the reinforcement. The next section describes the variable angle truss model in general and then the limit analysis approach to finding ultimate loads, based on Nielsen (1999) in particular.

It should be pointed out that besides the variable angle truss model, a different theory exists based on crack sliding. Accurate calculation based on this crack sliding theory must be carried out numerically. There are simplified approximations for this theory, but this is not considered in the work presented in this thesis.

Variable angle truss model

As the 45° Mörsh truss model continuously underestimates the shear resistance of a concrete member a different approach can be set by assuming a lower inclination of the compressive strut. If the inclination of the compressive strut is assumed to be at an angle θ then the new equilibrium conditions can be expressed as in Figure 3.30.

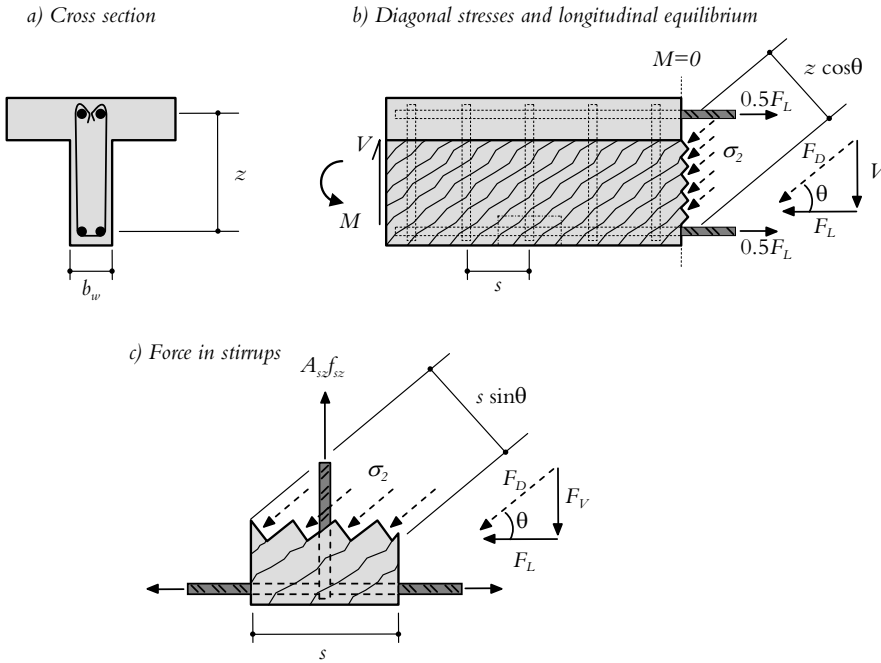


Figure 3.30. Geometry, forces, stresses and equilibrium for the variable angle truss model, based on Collins and Mitchell (1991).

The resultant of the principal diagonal (compressive) stresses, σ_2 , is the diagonal resultant, F_L , which can be derived from the equilibrium in the free body diagram in Figure 3.30 b. The diagonal resultant, F_L , is shown in eq. (3.80) and the principal compressive stress, σ_2 , is shown in eq. (3.81). The vertical component of the principal diagonal compressive stress is shown in Figure 3.30 c where an enlargement of the around the stirrup is shown. The vertical component equals $F_V = \sigma_2 b_w s \sin^2 \theta$. This vertical component, F_V , must be countered by the tensile force in the stirrup, $A_{sz} \sigma_{sz}$. Using eq. (3.81) the fact that $F_V = A_{sz} \sigma_{sz}$ gives the expression in eq. (3.82). The longitudinal equilibrium demands that the tensile force in the longitudinal reinforcement equals, F_L , which is expressed in eq. (3.83) by the shear force.

$$F_L = \frac{V}{\sin \theta} = \sigma_2 b_w z \cos \theta \quad (3.80)$$

$$\sigma_2 = \frac{V}{b_w z} \frac{1}{\sin \theta \cos \theta} = \frac{V}{b_w z} (\tan \theta + \cot \theta) \quad (3.81)$$

$$\frac{A_{sz} \sigma_{sz}}{s} = \frac{V}{z} \tan \theta \Rightarrow V = \frac{A_{sz} \sigma_{sz}}{s} z \cot \theta \quad (3.82)$$

$$F_L = V \cot \theta \quad (3.83)$$

There are now four unknowns; σ_2 (the principal diagonal compressive stress), $A_{sz}f_{sz}$ (the stress in the stirrup), F_L (tensile force in the longitudinal reinforcement) and the inclination of the diagonal compressive stress, θ and only three equilibrium equations. This is the Mörsh predicament mentioned in section 3.3.2, where Mörsh considered it impossible to solve θ mathematically.

However, assuming that the stirrups yield ($\sigma_{sz}=f_{sy}$) and by making an assumption about the level of compressive stress, σ_2 , in the concrete can determine the inclination, θ , by solving eq. (3.81) and (3.82) simultaneously.

$$\cot^2 \theta = \frac{\sigma_2 b_w s}{A_{sz} f_{sy}} \quad (3.84)$$

Alternatively, it can be assumed that the longitudinal reinforcement and the stirrups yield at the same time at failure and then determine V and θ by using eq. (3.83) and (3.82). These assumptions are used in plasticity methods, given by Thürlimann and Grob (1976) and Nielsen (1999).

Thürlimann and Grob (1976), apply a truss model with a variable angle, θ . It is assumed that both longitudinal tensile reinforcement and stirrups yield at shear failure. A smaller value on θ leads to less amounts of stirrups but at the same time increases the tensile force in the longitudinal reinforcement. The concrete part in the shear resistance, V_c , is successively decreasing towards zero as the stirrup amounts increase. This approach is not commented on further but more focus given to Nielsen and co-workers' approach to the shear resistance, described in Nielsen (1999).

Maximum shear resistance, transverse shear reinforcement

Lower bound solution:

For the lower bound solution, Nielsen (1999) idealized the following:

“The concrete beam is simply supported, loaded in 4 point bending and has both constant depth and constant width in the shear zone. The truss is considered to have a compressive stringer (the compressive zone) taking a compressive force C and a tensile stringer (tensile zone) taking a tensile force T . All shear reinforcement is aligned vertically to the longitudinal axis and closed stirrups are utilized”

An idealisation of the diagonal compressive stresses in the web is shown in Figure 3.31 along with assumed forces, stresses and set-up. Inclined shear cracks caused by the diagonal stress field are assumed to be parallel to the stress field and uniformly distributed carrying the following stresses in the x - z plane. The stresses can be expressed as

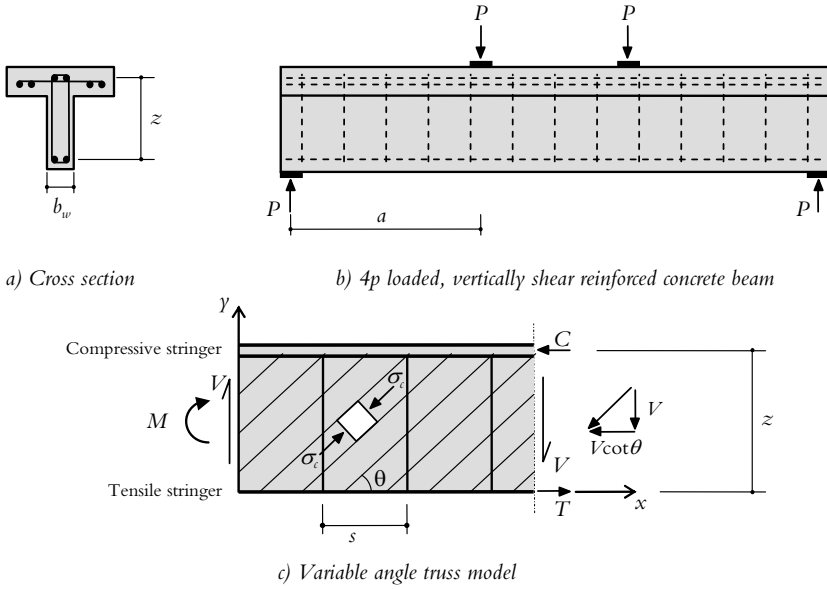


Figure 3.31. Beam loaded in shear, variable angle truss model, based on Nielsen (1999).

$$\sigma_x = -\sigma_c \cos^2 \theta \quad (3.85)$$

$$\sigma_z = -\sigma_c \sin^2 \theta \quad (3.86)$$

$$\tau = |\tau_{xz}| = \sigma_c \sin \theta \cos \theta \quad (3.87)$$

The shear stress, τ , is assumed to be constant in the same way as described in section 3.3.2 and thus related to the shear force V as

$$\tau = |\tau_{xz}| = \frac{V}{b_w z} \quad (3.88)$$

The forces in the stirrups ($A_{sz} \sigma_{sz}$) distributed over the concrete area are assumed to be related to an equivalent stirrup stress, see also Figure 3.30. This equivalent stirrup stress is expressed as

$$\sigma_z = \frac{A_{sz} \sigma_{sz}}{b_w s} = \rho_z \sigma_{sz} \quad (3.89)$$

where ρ_z is the shear reinforcement ratio. For vertically aligned stirrups, the equivalent stress contributions in x-direction and τ_{xz} are zero. Total stresses in concrete and stirrups are expressed as

$$\sigma_x = -\sigma_c \cos^2 \theta \quad (3.90)$$

$$\sigma_z = -\sigma_c \sin^2 \theta + \rho_{sz} \sigma_{sz} \quad (3.91)$$

$$\tau = \sigma_c \sin \theta \cos \theta \quad (3.92)$$

The boundary condition along the stringers demands that σ_z be zero. Solving eq. (3.92) with respect to σ_c and inserting the result in (3.90) and (3.91) using the boundary condition $\sigma_z = 0$ gives

$$\sigma_c = \frac{\tau}{\sin \theta \cos \theta} = \tau(\tan \theta + \cot \theta) \quad (3.93)$$

$$\sigma_x = -\tau \cot \theta \quad (3.94)$$

$$\rho_z \sigma_{sz} = \tau \cot \theta \quad (3.95)$$

Note that eq. (3.93) is the same expression as eq. (3.81). However, in order to be safe, the diagonal compressive stress must fulfil, $\sigma_c \leq f_{cc}$, and the shear reinforcement stresses, $\sigma_{sz} \leq f_{sy}$, where f_{sy} is the yield strength of the shear reinforcement. By assuming that the beam will not fail in the flexural tension or compression zone, the best lower bound solution is the largest solution that satisfies the limits described above.

$$\sigma_c = \tau(\tan \theta + \cot \theta) \leq f_{cc} \quad (3.96)$$

$$\sigma_{sz} \leq f_{sy} \quad (3.97)$$

Assuming that the limits above occur at the same time, yielding of the shear reinforcement and web compressive failure, gives the solution for τ and θ (similar to eq. (3.84)).

$$\frac{\tau}{f_{cc}} = \sqrt{\psi(1-\psi)} \quad (3.98)$$

$$\tan \theta = \sqrt{\frac{\psi}{1-\psi}} \quad (3.99)$$

Where, ψ is the ratio of maximum shear reinforcement contribution to the compressive strength of the concrete according to

$$\psi = \frac{\rho_z f_{sy}}{f_{cc}} \quad (3.100)$$

When plotting eq. (3.93) a circle will occur in the τ/f_{cc} , ψ - coordinate system. When $\psi=0.5$, the maximum value of τ/f_{cc} is 0.5. For $\psi>0.5$, the best lower bound solution is given for $\sigma_{sz} = 0.5 f_{cc}/\rho_z < f_{sy}$ which corresponds to a straight line where $\tau/f_{cc}=0.5$, this is shown in Figure 3.32. When $0 \leq \psi \leq 0.5$, then $0^\circ \leq \theta \leq 45^\circ$ and θ

is constant at 45° for $\psi > 0.5$. It is also stated in Nielsen (1999) that the solution has to be modified for small ψ -values and that the modification leads to the same solution as for the upper bound solution. The upper bound solution will be described in the following section. For the uniform loading case the reader is referred to Nielsen (1999).

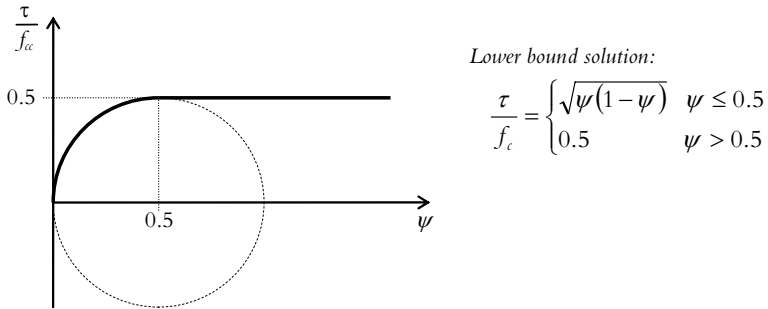


Figure 3.32. Lower bound solution for the maximum shear capacity, based on Nielsen (1999).

Upper bound solution:

The lower bound solutions are quite limited to certain simple cases, the upper bound solution on the other hand is possible for the most complicated cases. Again, the four point load case shown in Figure 3.31 is considered. The upper bound solution is given using a displacement field, where the part “I” is given a displacement u , see Figure 3.33. Part “II” is considered not to be moving at all. ψ is assumed to be constant. Assuming that the yield lines incline at an angle of β , the expression for the work done by part “I” is shown in eq. (3.101).

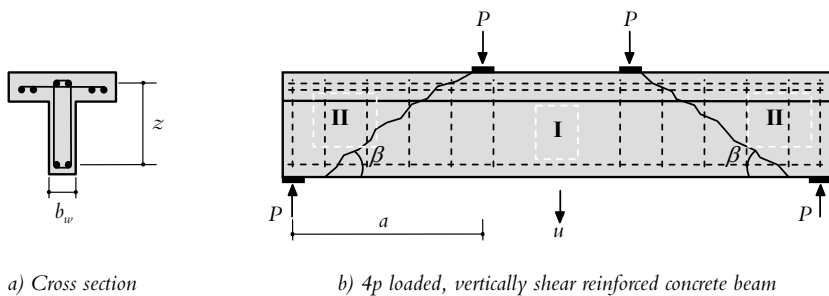


Figure 3.33. Four point shear loaded reinforced concrete beam, based on Nielsen (1999).

$$P \cdot u = \underbrace{\rho_z f_{sy} b_w z \cot \beta \cdot u}_{\text{stirups}} + \underbrace{\frac{1}{2} f_{cc} b_w (1 - \cos \beta) \frac{z}{\sin \beta}}_{\text{concrete}} \cdot u \tag{3.101}$$

In the expression of the work in eq. (3.101) it is assumed that the stringers do not contribute at all. The total work is the dissipation of the stirrups crossing the yield line and the dissipation in the concrete. The dissipation expression of the concrete is based on Nielsen (1999). Assuming constant shear and dividing with the concrete compressive strength gives the upper bound solution according to

$$\frac{\tau}{f_c} = \frac{P}{b_w z f_c} = \psi \cot \beta + \frac{1}{2} (1 - \cos \beta) \frac{1}{\sin \beta} \quad (3.102)$$

Minimising τ/f_c with respect to β gives the solution in eq. (3.103). This is the same solution as the lower bound solution given in eq. (3.98). The inclination of the yield line is given in eq. (3.104). It can also be shown that the inclination of the yield line corresponds to $\beta = 2\theta$, θ is determined by eq. (3.99).

$$\frac{\tau}{f_c} = \sqrt{\psi(1-\psi)} \quad (3.103)$$

$$\tan \beta = \frac{2\sqrt{\psi(1-\psi)}}{(1-2\psi)} \quad (3.104)$$

For eq. (3.103) to be valid, geometrical boundary condition implies that the yield line inclination has to be limited according to eq. (3.105).

$$\frac{z}{a} \leq \tan \beta \leq \infty \quad (3.105)$$

To obtain the lower limit of the geometrical boundary condition given in (3.105), the inclination for $\tan \beta = z/a$ is inserted into eq. (3.102). This gives a lower limit of the shear capacity, τ/f_c , with regards to the yielding shear reinforcement ratio to the compressive strength of the concrete, ψ , according to

$$\frac{\tau}{f_c} = \frac{1}{2} \left[\sqrt{1 + \left(\frac{a}{z}\right)^2} - \frac{a}{z} \right] + \psi \frac{a}{z} \quad (3.106)$$

The upper limit of the geometrical condition is given for $\beta = \pi/2$ ($\tan \beta = \infty$) and which is obtained for $\psi = 0.5$ and $\tau/f_c = 0.5$. Thus, by increasing the shear reinforcement beyond $\psi > 0.5$ will not contribute to the shear capacity. The solution of eq. (3.106), (3.103) and (3.98) is shown in Figure 3.32. The same upper bound solution is found in Nielsen (1999) by estimating the influence of the stringers, when using a displacement field accounting for “hinges” (H) at four points shown in Figure 3.32.

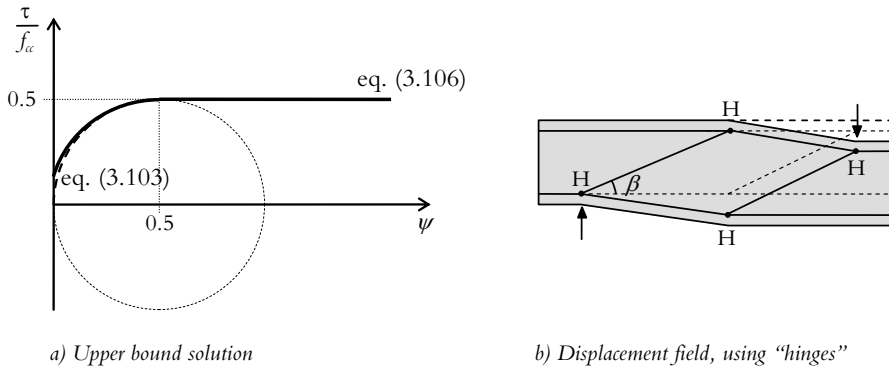


Figure 3.34. a) Upper bound solution for the maximum shear capacity. b) Influence of the longitudinal reinforcement (stringers), based on Nielsen (1999).

Maximum shear capacity, no shear reinforcement

Lower bound solution:

For concrete beams with no shear reinforcement, the derivation is similar to an ordinary strut and tie approach. For the derivation in Nielsen (1999), an ideal case is considered for a beam with rectangular cross section and subjected to concentrated loading. It is assumed that the arched region ABDE in Figure 3.35 is in uniaxial compression and that the loads and tensile force in the reinforcement is transferred through the regions AEF and BCD, which are under biaxial hydrostatic pressure. The hydrostatic pressure is also assumed to be equal to concrete strength, f_c . Maximum load is achieved when BD is at its largest. D lies within a circle with BE as its diameter, thus the maximum load is achieved when $CD = y_0 = h/2$. Geometry gives the distance BC and the lower bound solution in eq.(3.107) and (3.108) for the largest BC. The lower bound solution expressed in τ/f_c is given in eq. (3.109). Note that all derivations are made on the full depth of the beam.

$$BC = x_o = \frac{1}{2} \left(\sqrt{a^2 + h^2} - a \right) \tag{3.107}$$

$$P = b_w x_o f_c \tag{3.108}$$

$$\frac{\tau}{f_c} = \frac{P}{b_w h f_c} = \frac{x_o}{h} = \frac{1}{2} \left(\sqrt{1 + \left(\frac{a}{h} \right)^2} - \frac{a}{h} \right) \tag{3.109}$$

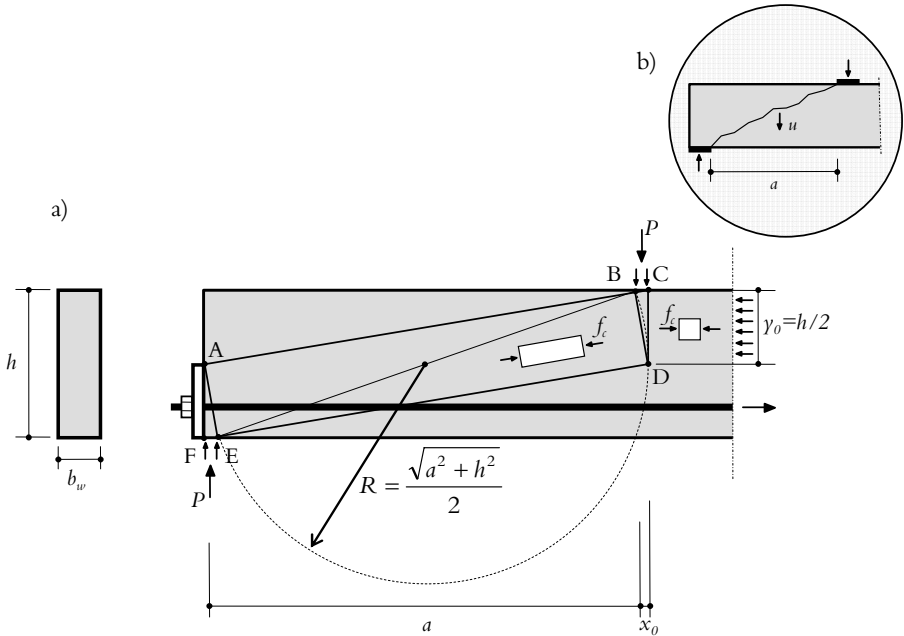


Figure 3.35. Lower (a) and upper (b) bound solution for a beam with no shear reinforcement, based on Nielsen (1999).

The force in the tensile reinforcement has to be larger than the compressive force and the tensile reinforcement area A_{sl} has therefore to fulfil the following conditions:

$$A_{sl}f_{sy} \geq 1/2 b_w h f_{cc} \quad (3.110)$$

$$\Phi = \frac{A_{sl}f_{sy}}{b_w h f_{cc}} \geq \frac{1}{2} \quad (3.111)$$

where f_{sy} is the yield strength of the longitudinal reinforcement and Φ is the longitudinal reinforcement degree.

Upper bound solution:

Using eq. (3.106) with $\psi = 0$ will give the upper bound solution, eq. (3.112), for the case of no shear reinforcement and for a rectangular cross section. In this case the internal lever arm, z , must be chosen as the total depth, h , of the beam. Eq. (3.109) and (3.112) are identical.

$$\frac{\tau}{f_{cc}} = \frac{1}{2} \left[\sqrt{1 + \left(\frac{a}{h}\right)^2} - \frac{a}{h} \right] \quad (3.112)$$

Influence of longitudinal reinforcement

In the previous solutions for the maximum shear capacity it is assumed that the longitudinal stringers remain rigid. In Nielsen (1999), the influence of the longitudinal reinforcement is considered for a shear reinforced beam with concentrated loading. In this approach the tensile reinforcement is considered to yield at the point of maximum moment and that the stirrups yield along the entire shear span. The statically admissible solution is given in eq. (3.113) and (3.114), considering the equilibrium in Figure 3.31 assuming that the stirrup stress is the yield strength of the shear reinforcement, eq. (3.95), and the tensile reinforcement is yielding, thus the tensile force is $T_y = A_{sl} f_{sy}$.

$$T_y = \frac{Pa}{z} + \frac{P}{2} \cot \theta \quad (3.113)$$

$$\tau = \frac{P}{b_w z} = \rho_z f_{sy} \cot \theta \quad (3.114)$$

Using the longitudinal reinforcement ratio, Φ in eq. (3.111), and the shear reinforcement ratio, ψ in eq. (3.100), together with eq. (3.113) and (3.114) gives the lower bound solution as long as the diagonal compressive is below the concrete compressive strength, f_c .

$$\frac{\tau}{f_c} = \psi \frac{a}{z} \left[\sqrt{1 + \frac{2\Phi}{\psi (a/z)^2}} - 1 \right] = \psi \left[\sqrt{\frac{2\Phi}{\psi} + \left(\frac{a}{z} \right)^2} - \frac{a}{z} \right] \quad (3.115)$$

This lower bound solution is of limited interest for small ψ and a/z (a/h) ratios, since it is not taking strut and tie action into consideration. A typical failure mechanism for this solution is shown in Figure 3.36 where the displacement is simply a rotation about the point A. The upper bound solution corresponds to the flexural capacity given in eq. (3.117).

$$\frac{\tau}{f_c} = \psi \frac{a}{z} \left[\sqrt{1 + \left(\frac{a}{h} \right)^2} - \frac{a}{h} \right] \quad (3.116)$$

$$\frac{\tau}{f_c} = \Phi \frac{z}{a} \quad (3.117)$$

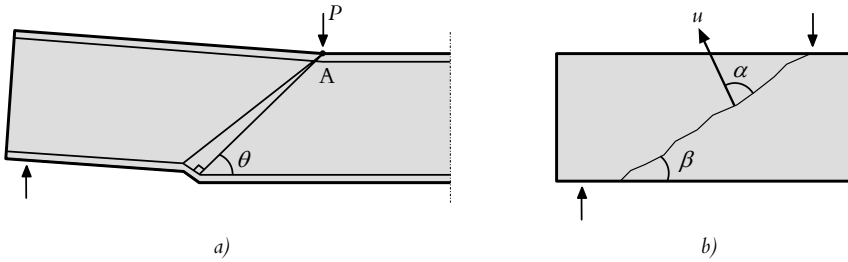


Figure 3.36. a) Failure mechanism when longitudinal reinforcement is yielding, b) Displacement used in upper bound solution. Based on Nielsen (1999).

However, for rectangular beams with no shear reinforcement the lower bound solution is different. It is stated in the previous part, for rectangular beams with no shear reinforcement subjected to concentrated loads, that $\Phi \geq 1/2$ in eq. (3.111). This implies that the maximum moment equals the flexural yield moment for $\Phi = 1/2$. Therefore the beam should theoretically have reached its flexural capacity when $\Phi < 1/2$. The lower bound solution for the case where $\Phi < 1/2$ is established by finding a value for γ_0 in Figure 3.35 that satisfies the equilibrium condition.

$$A_{sl}f_{sy} = b_w\gamma_0f_{cc} \Rightarrow \gamma_0 = \frac{A_{sl}f_{sy}}{b_w h f_{cc}} h = \Phi h \quad (3.118)$$

The lower bound solution is obtained by determining the load carrying capacity according to eq. (3.108) and calculating the corresponding x_0 value. The solution is given in eq. (3.119). For $\Phi = 1/2$ the solution is exactly as eq. (3.109). For $\Phi > 1/2$ the term $4\Phi(1-\Phi)$ should be replaced by 1 and thus correspond to eq. (3.109). The same result is obtained for the upper bound solution using the displacement u inclined at an angle α to the yield line given in Figure 3.36. Decreasing the shear capacity given in eq. (3.119) for different shear span to depth ratios is shown in Figure 3.37 for different longitudinal reinforcement degrees. It can be seen that the shear capacity is increasing as the longitudinal reinforcement degree Φ is increased until Φ reaches 0.5 when the solution is exactly the same as for eq. (3.109).

$$\frac{\tau}{f_{cc}} = \frac{1}{2} \left(\sqrt{4\Phi(1-\Phi) + \left(\frac{a}{h}\right)^2} - \frac{a}{h} \right) \quad \text{for } \Phi \leq \frac{1}{2} \quad (3.119)$$

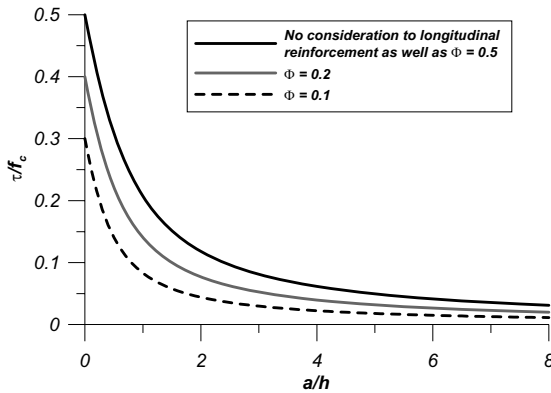


Figure 3.37. Shear capacity vs. shear span/depth ratio for different longitudinal reinforcement ratios.

Effective concrete compressive strength

In order to obtain a fair theoretical estimation compared to experimental results, the compressive strength needs to be reduced by an effectiveness factor, v_1 . The effectiveness factor for concrete compressive strength is given in Nielsen (1999) as a linear relationship based on empirical results. As an example the effectiveness factor for reasonable, safe values is expressed in the following as

$$v_1 = 0.7 - \frac{f_c}{200} \quad [\text{units in MPa}] \quad (3.120)$$

This effectiveness factor should be compared to the one given in EC2-1 (2004), see eq. (3.146) where additional reduction has been made. Eq. (3.120) is preferably used on normal concrete $f_c < 50$ MPa. Other reduction relationships exist for different kinds of concrete qualities, for these the reader is referred to Nielsen (1999).

Concluding remarks

Design methods based on plasticity theory developed by Nielsen and his co-workers at Technical University of Denmark have been adopted in Eurocode. The design procedure is based on lower bound solutions where the uniform loading and concentrated loading is combined by superpositioning. Eq. (3.82) is used for a shear reinforced beam with vertical stirrups, see also eq. (3.144). The shear resistance of a beam with no shear reinforcement is governed by flexure shear failure. When designing for shear resistance in Eurocode (or the second alternative in BBK), section 3.4.2., the shear resistance for a beam with no shear reinforcement is given by eq. (3.137). Here the non pre-stressed case is presented.

$$V_{Rd,c} = \left[C_{Rd,c} k (100 \rho_l f_{ck})^{1/3} \right] b_w d \quad (3.121)$$

Where, without further justification, $C_{Rd,c}$ is a coefficient derived from tests, k is the size factor depending on the effective depth, d . ρ_l is the influence of the longitudinal

reinforcement which could be compared to the longitudinal reinforcement degree, eq. (3.111), but without f_c and f_y .

Additional remarks

In the previous section, a perfect plastic behaviour of the reinforcing bars is assumed as well as that reinforcement only carries axial forces. Further, the bond between the reinforcement and concrete is assumed to be perfect. This means that there can not be any displacement between the reinforcement and concrete and that the change of stresses in the reinforcement bars can be utilised within an infinitely small bond (anchorage length). These idealisations of the reinforced concrete behaviour are quite rudimentary. Since in real a concrete structure, transverse shear stresses such as dowel action can occur, bond stresses between reinforcement and concrete are limited by the bond strength and tension stiffening effects occur. However, the assumptions made in the previous section make the analysis of concrete structures less complicated and the influence of these simplifying assumptions are in some cases negligible.

However, an analysis has been presented that takes the bond between reinforcement and concrete, tension stiffening effects and compression softening behaviour into consideration. The analysis is called Cracked Membrane Model (CMM) and was developed by Walter Kaufmann and Peter Marti at ETH in Zürich. This model is numerically intricate and requires numerical tools for solving the shear resistance. Therefore, this model is not further described in this thesis and the reader is referred to the literature in Kaufmann (1998) and Kaufmann and Marti (1998).

3.4 Shear design models

This section shows a curtailed description of the design codes for shear resistance according to Eurocode, ACI and the Swedish BBK. First the fixed angle methods are based on empirical relationships and the 45° Mörsh truss analogy. These design codes are the ACI and the BBK. Thereafter the design codes are based on the variable angle truss model being described, namely Eurocode and BBK. It should be mentioned that in BBK there exist two ways of designing the shear resistance. Design based on “addition” approach and the variable angle truss analogy. The latter is most identical to the Eurocode approach for calculating the shear resistance.

3.4.1 Fixed angle - Truss analogy

ACI

The design model for calculating shear strength in the American codes is taken from ACI (2008). The shear strength is based on average shear stress on a full effective cross section $b_w d$. The nominal shear strength is provided using above-mentioned superpositioning (“addition” approach) of the concrete shear strength to the contribution of the shear reinforcement as

$$V_n = V_c + V_s \quad (3.122)$$

where V_c is the nominal shear strength of concrete calculated according to (3.123) and V_s is the nominal shear strength provided by the shear reinforcement according to (3.124) or (3.125) depending on the use of vertical or inclined stirrups respectively. The concrete contribution to the shear resistance is

$$V_c = 0.17\lambda\sqrt{f'_c}b_w d \quad (3.123)$$

where f'_c is the specified concrete compressive strength. Lack of both test and practical material data for high strength concrete $\sqrt{f'_c}$ is limited to 8.3 MPa, except for some special cases of pre-stressed concrete application which are not within the scope of this thesis. λ is a reduction factor of the compressive strength considering lightweight concrete, $\lambda = 1$ for normal concrete. b_w is the width of the web and d is the internal lever arm.

$$V_s = \frac{A_{sz}f_{sy}d}{s} \quad (3.124)$$

$$V_s = \frac{A_{sz}f_{sy}(\sin\alpha + \cos\alpha)d}{s} \quad (3.125)$$

Where A_{sz} is the reinforcement area within the longitudinal stirrup spacing s . f_{sy} is the yield strength and α is the inclination of the shear reinforcement. There are also limitations for the shear reinforcement contribution to the shear strength. To avoid

diagonal crushing of the compression chords and to limit diagonal cracking at service loads, V_s should not be greater than

$$V_c = 0.66\sqrt{f'_c} b_w d \quad (3.126)$$

When designing for shear, the maximum longitudinal spacing between shear assemblies should not exceed (3.127) for shear reinforcement perpendicular to the axis of the structure.

$$s_{\max} = d/2 \text{ or } 600 \text{ mm} \quad (3.127)$$

BBK (alternative 1)

Reinforced concrete without shear reinforcement

$$V_d \leq V_c + V_i \quad (3.128)$$

where V_d is the design shear load, V_c is the concrete contribution to the shear resistance and V_i is the result of having a variable effective depth .

For concrete members with constant cross section, the shear capacity for concrete, V_c , is

$$V_c = b_w d f_v \quad (3.129)$$

where b is the width of the beam, d is the effective height and f_v is the concrete nominal shear strength according to

$$f_v = \xi(1 + 50\rho_l)0.3f_{ct} \quad (3.130)$$

$$\xi = \left. \begin{array}{ll} 0.5 & d \leq 0.2m \\ 1.6 - d & 0.2 < d \leq 0.5m \\ 1.3 - 0.4 \cdot d & \text{for } 0.5 < d \leq 1.0m \\ 0.9 & d > 1.0m \end{array} \right\} \quad (3.131)$$

$$\rho_l = \frac{A_{sl}}{b_w d} \leq 0.02 \quad (3.132)$$

Where f_{ct} is the concrete tensile strength, limited to the value corresponding to f_{ctk} 2.7 MPa. A_{sl} is the area of longitudinal tensile reinforcement.

In the Swedish design code there is also an alternative way for calculating the concrete contribution to the shear resistance. This approach is identical to the EC2-1 (2004) approach described in section 3.4.2, eq. (3.137)-(3.142).

Reinforced concrete with shear reinforcement

The shear resistance of a concrete member reinforced in shear is calculated according to

$$V_d \leq V_c + V_s \quad (3.133)$$

where the concrete contribution is calculated by eq. (3.128) to eq. (3.133) and the value for ξ does not need to be below 1.0. Shear resistance from the shear reinforcement, V_s , is the sum of the components in the shear force direction of the shear reinforcement that are crossed by 45° section between compression and tensile chords, see Mörsch truss model. For reinforcement assemblies where the reinforcement is divided equally, s , in the longitudinal direction of the member.

$$V_s = A_{sz} f_{sz} \frac{0.9d}{s} (\sin \beta + \cos \beta) \quad (3.134)$$

A_{sz} is the cross sectional area of the reinforcement at a section of s . β is the angle between the reinforcement and the longitudinal axis of the member. The tensile strength of the reinforcement, f_{sz} , is equalled to the naked steel reinforcement tensile strength, f_{sy} , but is recommended to be limited to

$$f_{sy} = \frac{520}{1.15\gamma_n} \quad (3.135)$$

where γ_n is the partial coefficient considering the safety class at ULS.

Note that there is also an upper limit of the shear strength with the shear reinforced member, regarding compressive failure in the compression chord. The upper limit of the shear resistance is

$$V_d \leq 0.25b_w d f_{cc} \quad (3.136)$$

3.4.2 Limit analysis and variable angle – Truss analogy

Eurocode (EC2-1)

Strut and tie models are used for design in ultimate limit state considering continuity regions (cracked state). If approximate compatibility for strut and tie models is ensured then steel stresses and crack width control may be carried out in the service limit state. An example of this compatibility is in particular that the position and direction of important struts should be oriented according to linear elasticity theory.

Shear resistance for concrete and reinforced concrete members according to EC2-1 (2004) is divided into:

- $V_{Rd,c}$ shear resistance of members without shear reinforcement

- $V_{Rd,s}$ shear force sustained by yielding shear reinforcement
- $V_{Rd,max}$ maximum shear force limited by crushing of the compression struts

$V_{Rd,c}$ and $V_{Rd,s}$ is not combined as in “addition” approach methods, but are considered separately. $V_{Rd,max}$ should be verified when designing shear reinforced concrete members.

Concrete members with no design requirements for shear reinforcement

The following design is only valid for members not requiring shear reinforcement. However, minimum shear reinforcement should nevertheless be assigned according to eq. (3.149) and (3.150).

The concrete contribution to the shear resistance

$$V_{Rd,c} = \left[C_{Rd,c} k (100 \rho_l f_{ck})^{1/3} + k_1 \sigma_{cp} \right] b_w d \quad (3.137)$$

with a limiting minimum of

$$V_{Rd,c} = (v_{min} + k_1 \sigma_{cp}) b_w d \quad (3.138)$$

where f_{ck} is the characteristic concrete compression strength in MPa

$$k = 1 + \sqrt{\frac{200}{d}} \leq 2.0 \quad \text{with } d \text{ in mm} \quad (3.139)$$

$$\rho_l = \frac{A_{sl}}{b_w d} \leq 0.02 \quad (3.140)$$

A_{sl} is the tensile reinforcement area at a point $\geq (l_{bd} + d)$ beyond the considered section

b_w is the smallest width of the cross section in the tensile area in mm.

σ_{cp} is the prestressing stress (not considered in this thesis)

Following values for $C_{Rd,c}$, v_{min} and k_1 are recommended values given in EC2-1 (2004), national annexes may provide different values for different countries.

$$C_{Rd,c} = \frac{0.18}{\gamma_c} \quad (3.141)$$

$$v_{min} = 0.035 k^{3/2} \cdot f_{ck}^{1/2} \quad (3.142)$$

k_1 is set to 0.15

It should also be noted that the above described approach for calculating the concrete shear resistance is also suggested in the Swedish design code BBK (2004) as an alternative to eq. (3.129). However, similar to the EC2-1 (2004) approach, the $V_{Rd,c}$ cannot replace eq. (3.129) or be incorporated in eq. (3.133).

Concrete members requiring shear reinforcement

This design is based on a truss model where the inclined compression struts are aligned at an angle θ and the shear reinforcement at an angle α , the truss model is shown in Figure 3.38. N is the horizontal resultant of the truss forces, compression chord (concrete) and tensile chord (shear reinforcement). F_{td} and F_{cd} is the design value for the tensile force in the longitudinal reinforcement and concrete compression force in the longitudinal direction of the member, respectively. z is the internal lever arm and if the details of the reinforcement are unknown, then $z=0.9d$ is normally used. Note that the inclination of the compression chords should be limited. National annex values for different countries exist but the recommended limitation is $21.8^\circ \leq \theta \leq 45^\circ$, ($0.4 \leq \tan \theta \leq 1$).

$$N = V(\cot \theta - \cot \alpha) \quad (3.143)$$

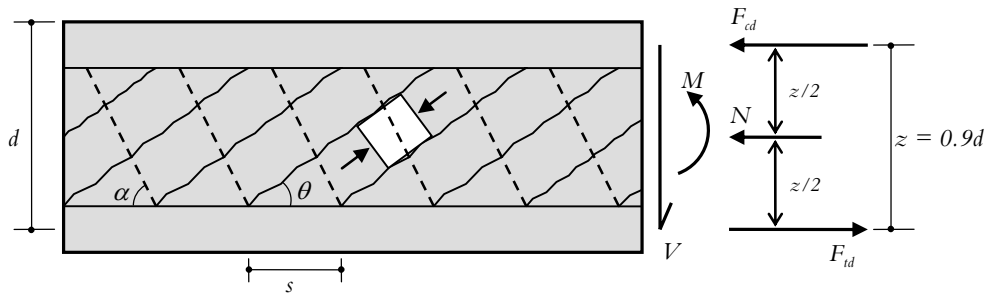


Figure 3.38 Truss model for shear reinforced concrete members.

For the case where the shear reinforcement is orthogonal to the longitudinal reinforcement ($\alpha=90^\circ$), the smallest of V_{rd} according to (3.144) and (3.145).

$$V_{Rd,s} = \frac{A_{sz}}{s} z f_{yd} \cot \theta \quad (3.144)$$

$$V_{Rd,max} = \frac{\alpha_{cw} b_w z \nu_1 f_{cd}}{\cot \theta + \tan \theta} \quad (3.145)$$

Where A_{sz} is the cross sectional area of the shear reinforcement, s is the stirrups' distance and f_{yd} is the design yield strength of the shear reinforcement. ν_1 is a reduction factor for concrete cracked in shear, national annex variations may exist but the recommended value is suggested in eq. (3.146) (for $f_{yd} > 0.8f_{yk}$). This "effectiveness" factor is also mentioned in eq. (3.120).

$$\nu_1 = 0.6 \left[1 - \frac{f_{ck}}{250} \right] \text{ with } f_{ck} \text{ in MPa} \quad (3.146)$$

α_{cw} is a coefficient considering the state of stress in the compression chord for pre-stressed members. If no pre-stressing is considered then $\alpha_{cw}=1$.

For shear reinforcement inclined at an angle α the following expressions are used to calculate the shear resistance, the minimum of eq. (3.147) and (3.148) should be chosen.

$$V_{Rd,s} = \frac{A_{sz}}{s} z f_{yd} (\cot \theta + \cot \alpha) \sin \alpha \quad (3.147)$$

$$V_{Rd,max} = \alpha_{cw} b_w z v_1 f_{cd} \frac{(\cot \theta + \cot \alpha)}{1 + \cot^2 \theta} \quad (3.148)$$

When designing for shear, the maximum longitudinal spacing between shear assemblies should not exceed eq. (3.149) and for bent up bars eq. (3.150).

$$s_{max} = 0.75d(1 + \cot \alpha) \quad (3.149)$$

$$s_{max} = 0.6d(1 + \cot \alpha) \quad (3.150)$$

BBK (alternative 2)

This approach is exactly the same approach as for the EC2-1 (2004) described above. The only exception lies within the limitation of the maximum longitudinal spacing between the shear reinforcement bars.

When designing for shear, the maximum longitudinal spacing between shear assemblies should not exceed eq. (3.151).

$$s_{max} = 0.75d(1 + \cot \alpha) \leq 1.5d \quad (3.151)$$

3.4.3 Evaluation of design models

In this chapter a database of 64 reinforced concrete beams is used to compare the different design models stated in the previous section. This database of beams is based on the collection done by Lima and Barros (2007). All of the values used in this comparison are based on the experimentally obtained mechanical properties of the concrete and steel. The only exception is the tensile strength of concrete used in BBK (2004), which was calculated based on the tested compressive strength using the equation below. It should be noted that the second alternative in BBK is not included in this chapter since the solution is the same as the one in Eurocode.

$$f_{ct} = 0.21 f_{ck}^{2/3} \quad (3.152)$$

Where f_{ct} is the tensile strength of concrete and f_{ck} is the experimentally obtained compressive strength of concrete. Eq. (3.152) is based on the model used in *Betonghandbok* (1990).

Figure 3.39 shows the ratio between the experimental shear resistances divided by the shear resistances estimated by the ACI design. All of these values are plotted against the amount of shear reinforcement multiplied with the yield strength of the shear reinforcement. Here it can be noticed that ACI design give safe values for beams with no shear reinforcement, although in the worst case it underestimates the shear resistance by a factor of three. When it comes to shear reinforced beams the ACI design is mostly on the safe side but some of the estimations overestimate the shear resistance. The ACI shear design is the simplest of all the design approaches (compared to Eurocode and BBK) and for illustrational purposes a simplification of the estimated shear resistance has been made in Figure 3.39. Here the total shear resistance, V_u in eq. (3.122) and the experimentally obtained shear resistance, have been plotted against the $A_s f_y / s$ ratio. The ACI shear resistance in Figure 3.39 is calculated based on a rectangular cross section with a width of $b_w = 180$ mm, effective height of $d = 419$ mm and a compressive strength of $f_c = 40$ MPa. Here it can be noticed that, ACI gives a fairly safe estimation of the shear behaviour. There is however a wide scatter in the experimental results. It should be stated that, in real design the estimations should be lower taking partial safety factors into consideration. The estimation of the ACI shear design is of course based on similar kinds of beams as in the database, see section 3.3.3. The overall ratio between experimental and predicted shear resistance are 1.61 in average and with a coefficient of variance (COV) of 33%.

Results from a similar approach as in Figure 3.39, but this time, based on the shear design in BBK are shown in Figure 3.40. The overall ratio between experimental and predicted shear resistance for the design based on BBK are 1.19 with a COV of 39%. Comparing BBK to ACI for the concrete contribution to the shear resistance, V_c it is clear that BBK both overestimates and underestimates the results compared to the experimental values. When the members have shear reinforcement the results between BBK and ACI are quite similar, although the BBK design has a slightly higher tendency to underestimate the shear resistance than the ACI design.

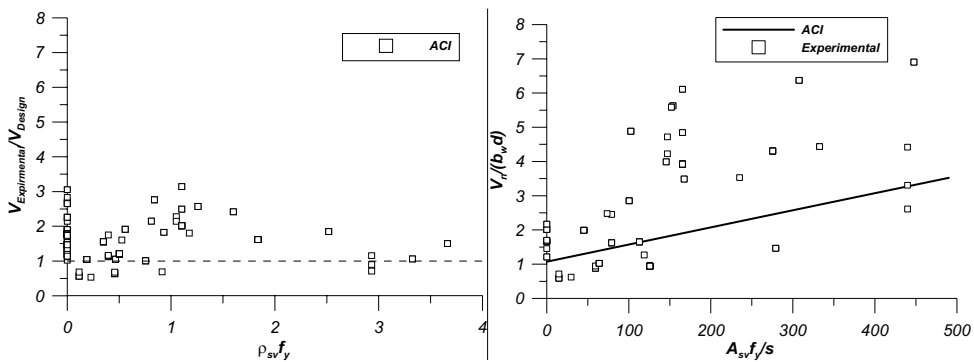


Figure 3.39. To the left, Experimental values normalised to predicted ACI (2008) design. To the right, ACI (2008) based on generic design and experimental values.

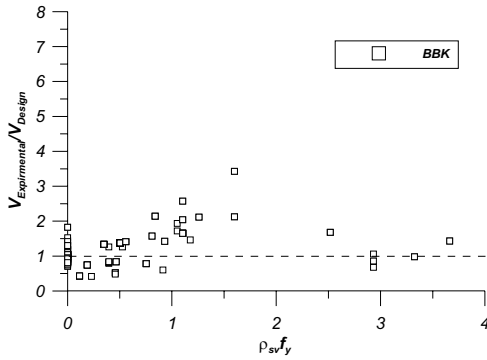


Figure 3.40. Experimental shear resistance normalised to BBK (2004) design.

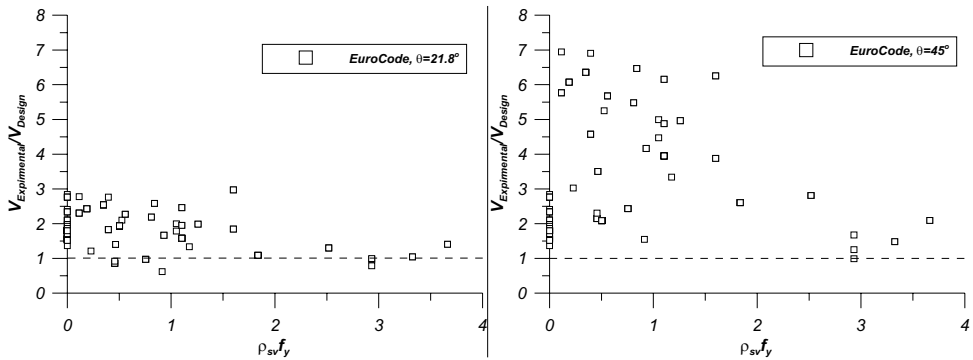


Figure 3.41. Experimental shear resistance normalised to EC2-1 (2004), $\theta = 21.8^\circ$ to the left and $\theta = 45^\circ$ to the right.

Shear design in Eurocode, EC2-1 (2004), uses the variable angle truss approach for shear reinforced beams. In this approach, the inclination of the diagonal compressive stresses has a lower and upper limit ($21.8^\circ \leq \theta \leq 45^\circ$). Eurocode shear resistance predictions based on the lower and upper limit compared to experimental results is shown in Figure 3.41. The concrete contribution, V_c , for beams containing no shear reinforcement is estimated safely by the Eurocode shear design. For beams containing shear reinforcement the inclination of θ has a significant influence. Choosing the lower limit of θ gives fairly safe estimations with a few overestimations of the shear resistance compared to the experimental results. By choosing the upper limit of θ all values are safe, but with heavy underestimations of the shear resistance by a factor up to seven. The ratios between experimental and predicted shear resistance are

For $\theta = 21.8^\circ$, 1.82 in average with a COV of 25%

For $\theta = 45^\circ$, 2.89 in average with a COV of 57%

Regarding all of the shear designs, the BBK design has the closest estimation ($V_{experimental}/V_{design}$) of the concrete contribution compared to experimental results. ACI and Eurocode are the shear designs that underestimate the concrete contribution the most, although Eurocode has no estimation ratio close to 1.

The reason for under- or overestimating the shear resistance contribution by the concrete, V_c , originates in the founding assumptions and theoretical approach for each design together with the large scattering of concrete. Figure 3.42 shows the three different shear designs for the concrete contribution according to Eurocode, ACI and BBK. These calculations are carried out for a rectangular beam with an effective depth of $d = 419$ mm, width b_w 180 mm and with maximum longitudinal reinforcement ratio $\rho_l = 0.02$. Estimated shear resistance is plotted against different concrete compressive strengths, f_{ck} , ranging up to 80 MPa. Note that the compressive strength in BBK is based on the concrete tensile strength, f_{ct} , according to eq. (3.152). The shear design model in BBK gives the less conservative values and reaches the maximum shear resistance at $f_{ck} = 47$ MPa, eq. (3.130). Shear design based on ACI is more conservative and the maximum shear resistance at $f_{ck} = 68.9$ MPa, ($\sqrt{f_{ck}} = 8.3$ MPa). The most conservative approach is given by the Eurocode. These tendencies are also shown in Figure 3.39, Figure 3.40 and Figure 3.41.

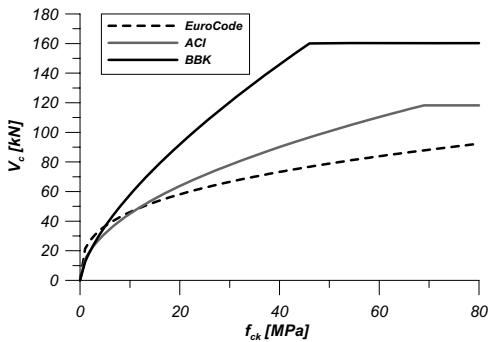


Figure 3.42. Concrete contribution, V_c , for Eurocode, ACI and BBK shear design.

The shear reinforcement contribution to the shear resistance is described by a straight line in all the shear design models. For $\theta = 45^\circ$, Eurocode and BBK give the same results. However as the inclination of θ is reduced to the lower limit of 21.8° the estimated shear resistance in Eurocode increases. A typical shear resistance based on the shear reinforcement is shown in Figure 3.43 for different effective depths. Calculations are based on $f_{ck}=30$ MPa, $f_y=500$ MPa, $\rho_{sv}=0.005$ and $b_w=180$ mm.

The upper limit of the total shear resistance is based on web compressive failure. All of the design models have different limitations given in eq. (3.148) for Eurocode, eq. (3.126) for ACI and eq. (3.136) for BBK. These upper limits of the shear resistance are plotted against the compressive strength for the concrete, Figure 3.43. Calculations in Figure 3.43 are based on the same mechanical and geometrical properties described

above, but here the effective height is chosen to $d=419$ mm. BBK is again the less conservative approach with a linear behaviour of the maximum shear resistance. This means that the upper limit is directly proportional to the concrete compressive strength. Both ACI and Eurocode have proportionalities to the compressive strength where the upper limit goes towards an asymptote while BBK has a linear proportionality. ACI has the most conservative approach in the web compressive failure and BBK has the least conservative approach. It can be seen in Figure 3.43, that Eurocode and BBK have similar upper limits up to a compressive strength of approximately 30 MPa for $\theta = 45^\circ$.

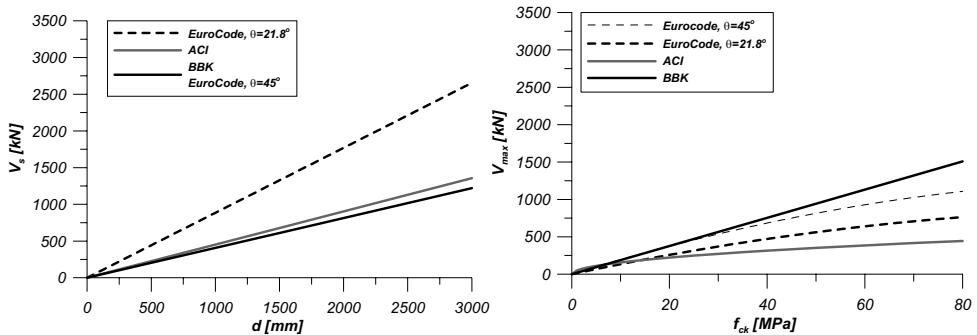


Figure 3.43. To the left, typical shear resistance, V_s . To the right, upper limit, V_{max} .

Concluding remarks

From the results of the ratios between experimental and predicted shear resistance for shear reinforced concrete beams it is clear that the use of Eurocode, assuming an inclination of 45° , will give highly conservative predictions. By lowering the assumed inclination to 21.8° the predictions become closer to the experimentally obtained shear resistance. Comparing the results from the Eurocode design assuming the smallest inclination to the ACI and BBK design it is shown that the BBK gives the best predictions on average but has the highest coefficient of variance.

For concrete beams without internal shear reinforcement the predictions based on Eurocode do not give any unsafe shear resistances and the predictions are similar to the design based on ACI. On the other hand, design based on BBK gives unsafe predictions. This is strongly related to the influence of the concrete strength (e.g. concrete compressive strength) in each model where the Eurocode is the most conservative approach and BBK the least.

It can be concluded that design based on Eurocode should be used for conservative prediction and that design based on BBK should be used for less conservative predictions. However, the choice of the inclination in Eurocode highly influences the predictions, where the lowest limit still gives conservative predictions. In addition, it seems as though the concrete contribution has a significant influence on the shear resistance.

It should be noted that this comparison is made on beam specimens tested from a non-cracked state up to failure. For estimations of beams having pronounced diagonal cracking the influence of the concrete contribution to the shear resistance should be that significant.

Further, the evaluation of the different shear design codes are based on experimentally obtained mechanical properties and no reduction by partial factors were used. Considering reduction factors, although not shown in this thesis, should increase the conservatism in all of the described shear design approaches.

4 Flexure and shear design for MBC strengthening

4.1 Introduction

This chapter is divided into two design proposals for MBC strengthening of concrete structures. The first design refers to flexural strengthening of concrete slabs and beams and the second design to shear strengthening of concrete beams. Section 4.2 consider flexural strengthening and the proposed design is compared to the experimental results in Paper I. Section 4.3 discusses shear design based on existing design models for concrete structures such as the 45° truss models, the variable angle truss model and the modified compression field theory, all previously described in chapter 3. The proposed shear design models for the MBC system are compared to the experimental results in Paper II.

4.2 Flexural design

This section of the thesis is basically an example of how to estimate the flexural resistance of a concrete beam strengthened with the MBC system. A straight forward approach is adopted based on plane section analysis but with a modified geometry to suite the MBC strengthening application. A, to some extent, similar approach can be found in Täljsten (2002) for epoxy bonded strengthening systems.

There are however some limitations in this design. Firstly, no consideration has been taken to the bond-slip behaviour between the strengthening layer and the base concrete. Secondly, full composite action between mineral-based bonding agent and CFRP grid is assumed. The reason or motivation for this relates to the experimental investigations presented in Paper I, Paper II and Blanksvärd (2007). All of the results indicate full composite action by fibre rupture at ultimate.

Before establishing the flexural design for MBC strengthened concrete beam, different possible failure modes are discussed.

4.2.1 Possible failure modes

When strengthening a concrete beam or a one-way slab in flexure, there are seven possible failure modes that can take place in the ultimate limit state. Assumed possible failure modes are shown in Figure 4.1 and listed below.

1. Compressive failure by exceeding the ultimate compressive strain in the concrete compressive zone. This kind of failure mode is considered as brittle.
2. Yielding of the tensile reinforcement. This failure mode is more ductile.
3. Yielding of the compressive reinforcement. This failure mode is considered as relatively ductile.

4. Tensile failure in the longitudinal tows in the CFRP. This failure mode is also considered as brittle.
5. Anchorage failure in the bond zone of the MBC strengthening system, depending where the failure occur it might be either ductile or brittle.
6. Peeling failure of the MBC system at the cut-off end to the base concrete. This failure mode is considered as brittle.
7. Delamination or bond slip in the transition zone between the mineral-based bonding agent and the CFRP grid. This failure mode is considered as ductile.

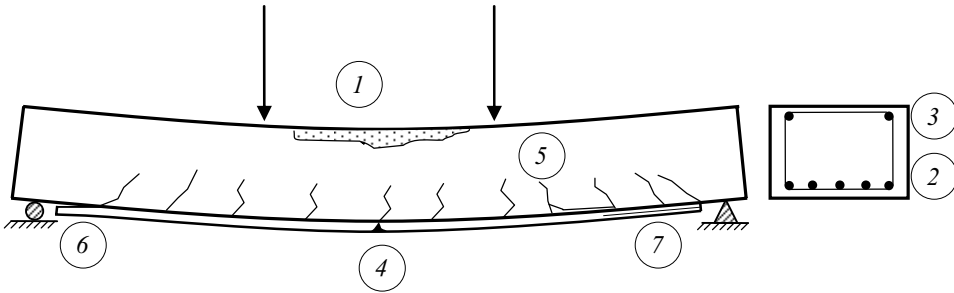


Figure 4.1. Possible failure modes for a reinforced concrete beam strengthened with the MBC system.

As mentioned above, failure modes 1-4 is considered in this design proposal while failure modes 6-7 are not considered. It should also be mentioned that, if applicable, the failure modes should behave in a ductile manner for designing concrete structures for flexural strengthening. By having a ductile failure mode, large deformation will occur before the ultimate failure. This failure behaviour gives earlier forewarning than a brittle failure mode which mostly occurs suddenly.

4.2.2 Stresses and strains for different failure modes

If the concrete beam is already subjected to initial stresses and strains, due to e.g. dead load and static permanent loads, these strains can be calculated using the flexural approach described in chapter 3.1. Knowing the initial strains and the assumed failure modes, the following failure mode combinations can be identified for double reinforced cross sections.

1. Failure in longitudinal CFRP tows and yielding of the compression reinforcement.
2. Failure in longitudinal tows of the CFRP and no yielding of the compression reinforcement.
3. Crushing of concrete and yielding of the compression reinforcement.
4. Crushing of concrete and no yielding of the compression reinforcement.

Note, that the tensile reinforcement is assumed to be yielding at the ultimate limit state since the yield strain in steel is lower than the ultimate strain in the CFRP, see chapter 2. Further, the contribution of the mineral-based bonding agent is considered to be zero since it has similar properties to concrete and thus will be cracked at the ultimate limit state.

The sectional equilibrium is obtained in the same manner as given in section 3.1, but in this case additional reinforcement is placed on the bottom of the beam in the tensile zone. The new strengthened cross section together with longitudinal strains, stresses and forces are shown in Figure 4.2. Note, it is assumed that the CFRP grid in the MBC system is situated in the centre of the bonding agent and that the thickness of the latter is, t_{MBC} . The flexural capacity for each failure mode, stated above, has to be calculated based on longitudinal equilibrium. The initial strains are here named $\epsilon_{c,0}$ for the initial compressive strain and $\epsilon_{t,0}$ for the initial tensile strain.

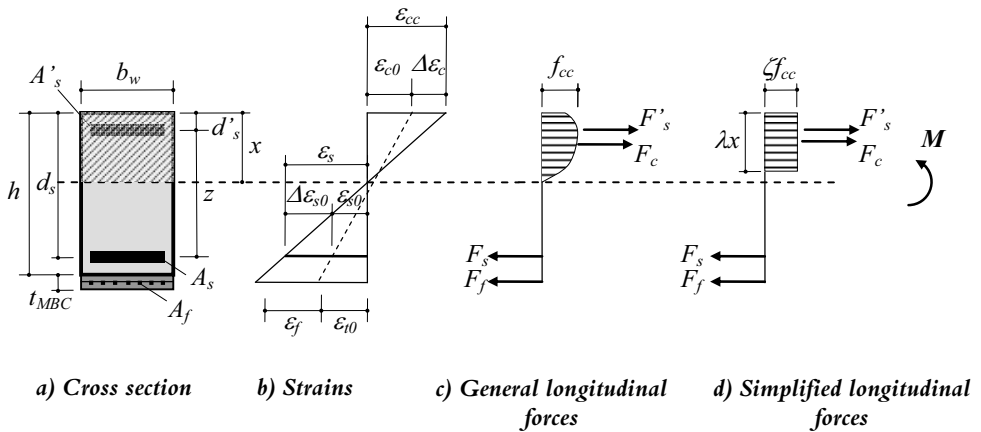


Figure 4.2. Stress-strain relationship for a reinforced concrete beam with rectangular cross section.

Calculation of the flexural capacity for a strengthened cross section depends on the failure mode. Failure mode 1 and 2 both consider fibre failure in the longitudinal CFRP tows but distinguish between whether the compressive reinforcement is yielding or not. Failure mode 3 and 4 consider the upper limit of the flexural capacity due to crushing of concrete and again distinguish between whether the compressive reinforcement is yielding or not when the concrete is crushed.

In the following sections, the calculation procedures for the flexural capacity are compiled for both failure modes 1, 2, 3, and 4.

| Failure mode 1 | Failure mode 2 |
|--|---|
| <p>- Failure in longitudinal CFRP tows and yielding of the compression steel reinforcement</p> | <p>- Failure in longitudinal CFRP tows and NO yielding of the compression steel reinforcement</p> |
| <p>1. Solve the longitudinal equilibrium in Figure 4.2 d</p> | |
| <p>Since both the strains in the longitudinal CFRP tows and the compressive reinforcement are known, the solution becomes</p> $\zeta f_{\alpha} b_w x + A'_s f'_y = A_s f_y + A_f \varepsilon_f E_f \quad (4.1)$ | <p>Since the strain level in the compressive reinforcement is unknown, the longitudinal equilibrium has to be solved by using plane section analysis.</p> $\zeta f_{\alpha} b_w x + A'_s \underbrace{\frac{x - d'_s}{h - x} (\varepsilon_f + \varepsilon_{t0})}_{f'_s} E_s = A_s f_y + A_f \varepsilon_f E_f \quad (4.2)$ |
| <p>2. Calculate the distance to the neutral axis by developing step 1</p> | |
| $x = \frac{A_s f_y + A_f \varepsilon_f E_f - A'_s f'_y}{\zeta f_{\alpha} b_w} \quad (4.3)$ | <p>The solution will be a quadratic equation that can be solved by</p> $C_1 x^2 + C_2 x + C_3 = 0 \quad (4.4)$ <p>Where the constants are:</p> $\begin{aligned} C_1 &= \zeta f_{\alpha} b_w \\ C_2 &= -\zeta f_{\alpha} b_w h - A'_s (\varepsilon_f + \varepsilon_{t0}) E_s \\ &\quad - A_s f_y - A_f \varepsilon_f E_f \\ C_3 &= A'_s (\varepsilon_f + \varepsilon_{t0}) E_s d'_s \\ &\quad - (A_s f_y - A_f \varepsilon_f E_f) h \end{aligned} \quad (4.5)$ |
| <p>3. The flexural capacity is obtained by solving the flexural equilibrium in Figure 4.2 d.</p> | |
| $\begin{aligned} M &= A'_s f'_y (\lambda x - d'_s) + A_s f_y (d_s - \lambda x) \\ &+ A_f \varepsilon_f E_f \left(h + \frac{t_{MBC}}{2} - \lambda x \right) \end{aligned} \quad (4.6)$ | $\begin{aligned} M &= A'_s \underbrace{\frac{x - d'_s}{h - x} (\varepsilon_f + \varepsilon_{t0})}_{f'_s} E_s (\lambda x - d'_s) \\ &+ A_s f_y (d_s - \lambda x) \\ &+ A_f \varepsilon_f E_f \left(h + \frac{t_{MBC}}{2} - \lambda x \right) \end{aligned} \quad (4.7)$ |

| Failure mode 3 | Failure mode 4 |
|--|--|
| <p>- Crushing of concrete and yielding of the compression reinforcement</p> | <p>- Crushing of concrete and NO yielding of the compression reinforcement</p> |
| <p>1. Solve the longitudinal equilibrium in Figure 4.2 d knowing that the strain in the concrete will reach the ultimate stage, ε_{cu}, by crushing of the compressed concrete.</p> | |
| <p>The strain in the longitudinal CFRP tows is not known and has to be solved by using plane section analysis.</p> $\zeta f_{\alpha} b_w x + A'_s f'_y = A_s f_y \quad (4.8)$ $+ A_f \left(\frac{h + \frac{t_{MBC}}{2} - x}{x} \varepsilon_{cu} - \varepsilon_{i0} \right) E_f$ | <p>Since both the strains in the compressive reinforcement and in the longitudinal CFRP tows are unknown, the longitudinal equilibrium has to be solved by using plane section analysis.</p> $\zeta f_{\alpha} b_w x + A'_s \left(\frac{x - d'_s}{x} \varepsilon_{cu} \right) E_s = A_s f_y \quad (4.9)$ $+ A_f \left(\frac{h + \frac{t_{MBC}}{2} - x}{x} \varepsilon_{cu} - \varepsilon_{i0} \right) E_f$ |
| <p>2. Calculate the distance to the neutral axis by developing step 1. The solution will be a quadratic equation that can be solved by</p> | |
| $C_1 x^2 + C_4 x + C_5 = 0 \quad (4.10)$ <p>Where the constants are</p> $C_1 = \zeta f_{\alpha} b_w \quad (4.12)$ $C_4 = A'_s f'_y - A_s f_y + A_f (\varepsilon_{cu} + \varepsilon_{i0}) E_f$ $C_5 = -A_f \varepsilon_{cu} E_f \left(h + \frac{t_{MBC}}{2} \right)$ | $C_1 x^2 + C_6 x + C_7 = 0 \quad (4.11)$ <p>Where the constants are</p> $C_1 = \zeta f_{\alpha} b_w$ $C_6 = A'_s \varepsilon_{cu} E_s - A_s f_y + A_f (\varepsilon_{cu} + \varepsilon_{i0}) E_f$ $C_7 = -\varepsilon_{cu} \left[A'_s E_s d'_s + A_f E_f \left(h + \frac{t_{MBC}}{2} \right) \right] \quad (4.13)$ |
| <p>3. The flexural capacity is obtained by solving the flexural equilibrium in Figure 4.2 d, knowing the distance to the neutral axis</p> | |
| $M = A'_s f'_y (\lambda x - d'_s) + A_s f_y (d_s - \lambda x) \quad (4.14)$ $+ A_f \left(\frac{h + \frac{t_{MBC}}{2} - x}{x} \varepsilon_{cu} - \varepsilon_{i0} \right)$ $\cdot E_f \left(h + \frac{t_{MBC}}{2} - \lambda x \right)$ | $M = A'_s \left(\frac{x - d'_s}{x} \varepsilon_{cu} \right) E'_s (\lambda x - d'_s) \quad (4.15)$ $+ A_s f_y (d_s - \lambda x)$ $+ A_f \left(\frac{h + \frac{t_{MBC}}{2} - x}{x} \varepsilon_{cu} - \varepsilon_{i0} \right)$ $\cdot E_f \left(h + \frac{t_{MBC}}{2} - \lambda x \right)$ |

4.2.3 Strain relationships for the cross section

The flexural capacity is now established for the identified failure modes in the previous section. However, the failure type depends on the reinforcement design and how much strengthening (CFRP) is applied. In order to know what failure mode affects the structural element in the ultimate limit state the following strain relationships for the compressive steel reinforcement are established using plane section analysis. The strain relationship for the compressive reinforcement in a reinforced concrete beam can be expressed as

$$\varepsilon'_s \geq \varepsilon_c - \frac{d'_s}{d_s}(\varepsilon_s - \varepsilon_c) \quad (4.16)$$

Where ε'_s is the strain in the compressive reinforcement and ε_c is the largest compressive strain in the concrete. In the ultimate limit state this strain relationship takes the following form

$$\varepsilon'_s \geq \varepsilon_{cu} - \frac{d'_s}{d_s}(\varepsilon_s - \varepsilon_{cu}) \quad (4.17)$$

For a MBC strengthened cross section with initial strains, the strain relationship will take the following form

$$\varepsilon'_s \geq \varepsilon_{cu} - \frac{d'_s}{h + \frac{t_{MBC}}{2}}(\varepsilon_f + \varepsilon_{t0} + \varepsilon_{cu}) \quad (4.18)$$

When the strain relationship for the compressive reinforcement is established a comparative parameter for the strengthening, ρ_f , needs to be established based on the strain in the compressive reinforcement. This comparative parameter is obtained in the same manner as for calculating the reinforcement ratio, thus taking the area of fibres and dividing it to the cross section area. Since this parameter depends on the strain relationship in the compressive reinforcement, two different parameters (ρ_{f1} and ρ_{f2}) have to be calculated depending on whether the compressive reinforcement is yielding or not.

Yielding of the compressive reinforcement

Longitudinal equilibrium of the cross section and assuming that the compressive reinforcement is yielding will give the following expression

$$\zeta f_{ac} b_w x + A'_s f'_y E_s = A_s f_y + A_f \varepsilon_f E_f \quad (4.19)$$

Since the concrete is assumed to reach its ultimate limit state, the strain relationship for the cross section based on plane sections can be expressed as

$$\varepsilon_f = \left(\frac{h + \frac{t_{MBC}}{2} - d_s}{d_s} \right) \varepsilon_{cu} + \frac{h + \frac{t_{MBC}}{2}}{d_s} \varepsilon_s - \varepsilon_{t0} \quad (4.20)$$

To reduce complicated expressions the following parameter is introduced, also based on plane section analysis.

$$\frac{x}{d_s} = \frac{\varepsilon_{cu}}{\varepsilon_{cu} + \varepsilon_s} = \nu_1 \quad (4.21)$$

Rearranging eq. (4.19) to obtain $A_{f\bar{p}}$, inserting eq. (4.20) and (4.21) and dividing the expression by b_w and d_s will give the following expression for the comparative parameter when the compressive reinforcement is yielding.

$$\rho_{f1} = \frac{\zeta f_{\alpha} \nu_1 + \rho'_s f'_y E_s - \rho_s f_y}{\left[\varepsilon_{cu} \left(\frac{h + \frac{t_{MBC}}{2}}{\nu_1 d_s} - 1 \right) - \varepsilon_{t0} \right] E_f} \quad (4.22)$$

Where ρ'_s is the compressive reinforcement ratio and ρ_s is the tensile reinforcement ratio.

No yielding of the compressive reinforcement

The longitudinal equilibrium is obtained in the same way as above.

$$\zeta f_{\alpha} b_w x + A'_s \varepsilon'_s E_s = A_s f_y + A_f \varepsilon_f E_f \quad (4.23)$$

Since the strain in the compressive reinforcement, ε'_s is not known, this strain will then be obtained by plane section analysis and using eq. (4.21) as

$$\varepsilon'_s = \left(1 - \frac{d'_s}{d_s \nu_1} \right) \varepsilon_{cu} \quad (4.24)$$

Using the equation above together with the longitudinal equilibrium in eq. (4.23) will give the following expression for the comparative parameter when the compressive reinforcement is not yielding. Again strengthening and reinforcement ratios are used by dividing by b_w and d_s .

$$\rho_{f2} = \frac{\zeta f_{cc} v_1 + \rho'_s \left(1 - \frac{d'_s}{d_s v_1} \right) \varepsilon_{cu} E_s - \rho_s f_y}{\left[\varepsilon_{cu} \left(\frac{h + \frac{t_{MBC}}{2}}{v_1 d_s} - 1 \right) - \varepsilon_{t0} \right] E_f} \quad (4.25)$$

Development of failure modes

Normally, depending on the type of failure mode, three different cross sections are differentiated when designing concrete elements in flexure. The desirable development of the flexural failure mode is for the tensile reinforcement to reach yielding before the concrete is crushed, so-called normally-reinforced cross section. The second type of cross section is the balanced cross section, where the reinforcement reaches yielding at the same time as the concrete crushes. The third type of cross section is the over-reinforced cross section, when the reinforcement is not yielding at all and the concrete is crushed before yielding of the reinforcement. Note that a secondary failure of the normally-reinforced cross section is crushing of the concrete. These three types of cross sections are shown in Figure 4.3 based on load-deflection response of a reinforced concrete beam. Depending on the amount of strengthening the failure mode of normally-reinforced concrete is more or less hard to achieve since the CFRP used is a brittle (linear elastic) material and the failure mode will be more like a balanced or over-reinforced cross section. The comparative parameters for the strengthening ratio related to the three different cross section types are further elaborated in the following sections.

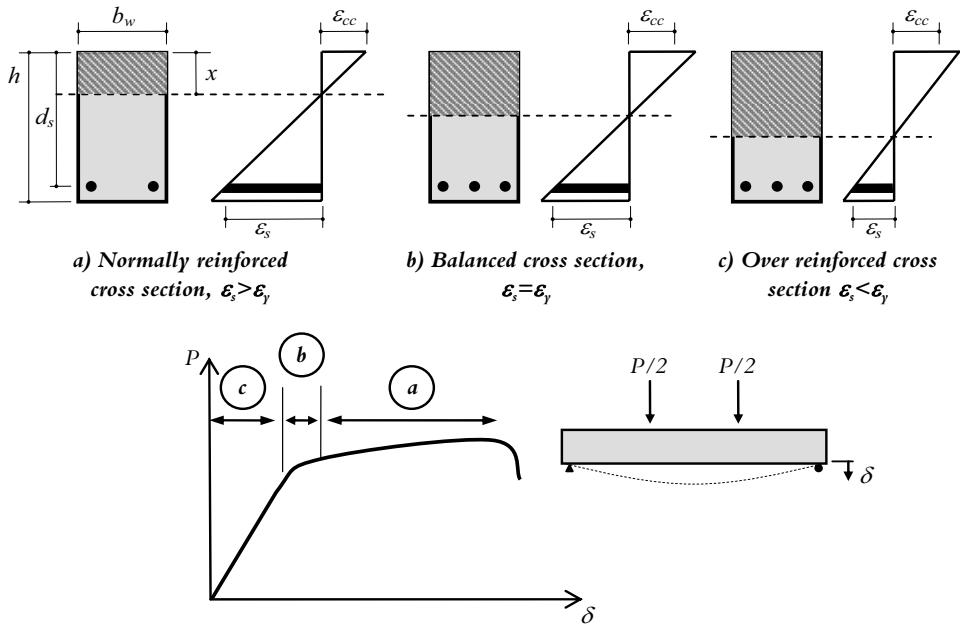


Figure 4.3. Typical load-deflection response of a reinforced beam subjected to flexural loading. a) Normally-reinforced cross section, b) balanced cross section and c) over-reinforced cross section.

Normally-reinforced cross section

A normally-reinforced cross section strengthened with the MBC system will fail by rupture of the longitudinal CFRP tows before the concrete is crushed. The longitudinal equilibrium equation gives

$$\zeta f_c b_w x + A'_s f'_s = A_s f_y + A_f \epsilon_f E_f \quad (4.26)$$

Rearranging the equation above to correspond to the comparative parameter (strengthening ratio, ρ_{fn}) for the normally-reinforced cross section will give the following expression

$$\rho_{fn} = \frac{\zeta f_c \frac{x}{d_s} + \rho'_s f_s - \rho_s f_y}{\epsilon_f E_f} \quad (4.27)$$

Since the strain and the stress in the compressive reinforcement are unknown, calculating the comparative parameter has to be solved in an iterative process. First, assume a stress level in the compressive reinforcement and calculate the distance to the neutral axis. Use Hooke's law to calculate the corresponding strain.

$$f'_s = E_s \varepsilon'_s \quad (4.28)$$

This strain has to be verified by using plane section analysis to obtain the compressive strain due to the calculated distance to the neutral axis according to

$$\varepsilon'_s = \frac{x - d'_s}{h + \frac{t_{MBC}}{2} - x} (\varepsilon_f + \varepsilon_{t0}) \quad (4.29)$$

When convergence is obtained then use eq. (4.27) to calculate the comparative parameter, ρ_{fb} .

Balanced cross section

For a balanced cross section, the concrete is crushed at the same time as the longitudinal CFRP tows rupture. The longitudinal equilibrium equation gives

$$\zeta f_{cc} b_w x + A'_s f'_y = A_s f_y + A_f \varepsilon_f E_f \quad (4.30)$$

The strain in the compressive reinforcement can be expressed using plane section analysis as

$$\varepsilon'_s = \frac{x - d'_s}{h + \frac{t_{MBC}}{2}} (\varepsilon_f + \varepsilon_{t0} + \varepsilon_{cu}) \quad (4.31)$$

This expression can be simplified to

$$\varepsilon'_s = \left(1 - \frac{d'_s}{\left(h + \frac{t_{MBC}}{2} \right) v_2} \right) \varepsilon_{cu} \quad (4.32)$$

where

$$v_2 = \frac{x}{h + \frac{t_{MBC}}{2}} = \frac{\varepsilon_{cu}}{\varepsilon_f + \varepsilon_{t0} + \varepsilon_{cu}} \quad (4.33)$$

Using eq. (4.32) and (4.30) and dividing by b_w and d_s will give the expression for the comparative parameter, ρ_{fb} , (strengthening ratio for balanced cross section).

$$\rho_{fb} = \frac{\zeta f_{cc} \frac{hv_2}{d'_s} + \rho'_s \left(1 + \frac{d'_s}{\left(h + \frac{t_{MBC}}{2} \right) v_2} \right) \varepsilon_{cu} E_s - \rho_s f_y}{\varepsilon_f E_f} \quad (4.34)$$

Over-reinforced cross section

For an over-reinforced cross section the concrete is crushed and the longitudinal CFRP tows are not ruptured. Using longitudinal equilibrium will give the following expression

$$\zeta f_{cc} b_w x + A'_s \varepsilon'_s E_s = A_s f_y + A_f \varepsilon_f E_f \quad (4.35)$$

Again, using the plane section analysis will give the strain in the compressive reinforcement and longitudinal CFRP tows according to

$$\varepsilon_f = \left(\frac{h + \frac{t_{MBC}}{2}}{x} - 1 \right) \varepsilon_{cu} - \varepsilon_{t0} \quad (4.36)$$

$$\varepsilon'_s = \left(1 - \frac{d'_s}{x} \right) \varepsilon_{cu} \quad (4.37)$$

The simplified expressions will take the form

$$\varepsilon_f = \left(\frac{h + \frac{t_{MBC}}{2}}{d'_s v_3} - 1 \right) \varepsilon_{cu} - \varepsilon_{t0} \quad (4.38)$$

$$\varepsilon'_s = \left(1 - \frac{1}{v_3} \right) \varepsilon_{cu} \quad (4.39)$$

where

$$v_3 = \frac{x}{d'_s} = \frac{\varepsilon_{cu}}{\varepsilon_{cu} - \varepsilon'_s} \quad (4.40)$$

Using eq. (4.38) and (4.39) in (4.35) together with dividing by b_w and d_s will give the expression for the comparative parameter, ρ_{f0} (strengthening ratio for over-reinforced cross section).

$$\rho_{f_0} = \frac{\zeta f_{ac} \frac{d'_s v_3}{d_s} + \rho'_s \left(1 - \frac{1}{v_3}\right) \varepsilon_{cu} E_s - \rho_s f_y}{\left[\varepsilon_{cu} \left(\frac{h}{d'_s v_3} - 1 \right) - \varepsilon_{t0} \right] E_f} \quad (4.41)$$

4.2.4 Failure mode criteria

In order to determine the different types of failure, the following criterias has to be met for the four failure modes respectively

1. *Failure in longitudinal CFRP tows and yielding of the compression reinforcement*

$$\rho_{f_1} \leq \rho_{f_1} \leq \rho_{f_b}$$

“To obtain fibre rupture and yielding of the compressive reinforcement, the strengthening ratio (ρ_{f_1} , CFRP rupture and yielding) should be smaller than the balanced cross section but larger than the normally-reinforced cross section”

2. *Failure in longitudinal tows of the CFRP and no yielding of the compression reinforcement*

$$\rho_{f_2} \leq \rho_{f_1}, \rho_{f_b}$$

“To obtain fibre rupture without yielding of the compressive reinforcement, the strengthening ratio (ρ_{f_2} , CFRP rupture without yielding) should be smaller than both the balanced and normally-reinforced cross section”

3. *Crushing of concrete and yielding of the compression reinforcement*

$$\rho_{f_1} \geq \rho_{f_b}, \rho_{f_0}$$

“For crushing of the concrete as well as yielding of the compression reinforcement, the strengthening ratio (ρ_{f_1} , CFRP rupture and yielding) should be larger than both the balanced and normally-reinforced cross section”

4. *Crushing of concrete and no yielding of the compression reinforcement*

$$\rho_{f_0} \leq \rho_{f_2} \leq \rho_{f_b}$$

“For crushing of the concrete without yielding of the compression reinforcement, the strengthening ratio (ρ_{f_2} , CFRP rupture without yielding) should be higher than the balanced cross section but smaller than the over-reinforced cross section”

4.2.5 Simplified design – Concrete members with no compressive reinforcement

For concrete members without compressive reinforcement, the failure modes described above are not valid to the same extent. For this type of concrete member, e.g. slabs, only two types of failures exist, assuming full composite action.

1. Failure in the longitudinal CFRP tows
2. Crushing of concrete

The cross section together with strain development and longitudinal forces for a concrete member having only tensile reinforcement is shown in Figure 4.4, assuming plane section analysis.

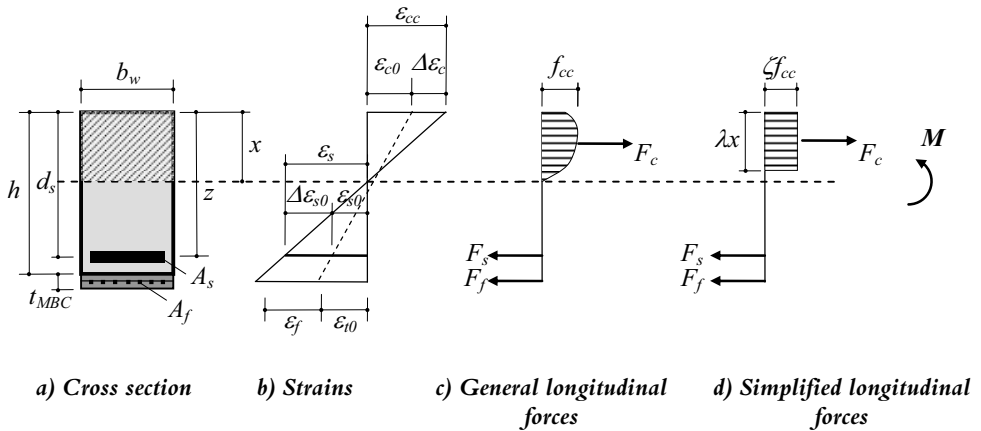


Figure 4.4. Stress-strain relationship for a tensile reinforced concrete beam with rectangular cross section.

Calculating the flexural capacity for this type of concrete members is carried out in the same manner as for the concrete members having both tensile and compressive reinforcement. As mentioned previously, for the most common types of reinforced concrete beams or slabs, the tensile reinforcement will yield before the ultimate strain is reached in the CFRP. Therefore, it is assumed that the tensile reinforcement has reached its yield limit at the ultimate state of flexural loading.

Different failure modes

| Failure mode 1 - Failure in longitudinal CFRP tows | Failure mode 2 - Crushing of concrete |
|---|--|
| 1. Solve the longitudinal equilibrium in Figure 4.4 d. | |
| Here, the strains in the longitudinal CFRP tows are known. $\zeta f_{\alpha} b_w x = A_s f_y + A_f \varepsilon_f E_f \quad (4.42)$ | Here, the strain in the concrete is reaching the ultimate strain, ε_{cu} . $\zeta f_{\alpha} b_w x = A_s f_y \quad (4.43)$ $+ A_f \left(\frac{h + \frac{t_{MBC}}{2} - x}{x} \varepsilon_{cu} - \varepsilon_{t0} \right) E_f$ |
| 2. Calculate the distance to the neutral axis by developing step 1. | |
| $x = \frac{A_s f_y + A_f \varepsilon_f E_f}{\zeta f_{\alpha} b_w} \quad (4.44)$ | $C_1 x^2 + C_8 x + C_9 = 0 \quad (4.45)$ Where the constants are $C_1 = \zeta f_{\alpha} b_w$ $C_8 = -A_s f_y + A_f (\varepsilon_{cu} + \varepsilon_{t0}) E_f \quad (4.46)$ $C_9 = -A_f \varepsilon_{cu} E_f \left(h + \frac{t_{MBC}}{2} \right)$ |
| 3. The flexural capacity is obtained by solving the flexural equilibrium in Figure 4.4 d, knowing the distance to the neutral axis. | |
| $M = A_s f_y (d_s - \lambda x) \quad (4.47)$ $+ A_f \varepsilon_f E_f \left(h + \frac{t_{MBC}}{2} - \lambda x \right)$ | $M = A_s f_y (d_s - \lambda x) \quad (4.48)$ $+ A_f \left(\frac{h + \frac{t_{MBC}}{2} - x}{x} \varepsilon_{cu} - \varepsilon_{t0} \right)$ $\cdot E_f \left(h + \frac{t_{MBC}}{2} - \lambda x \right)$ |

Failure mode criterion

In order to obtain the current failure mode, it is necessary to investigate which kind of reinforced cross section that is at hand. The different reinforced cross sections are described in Figure 4.3. It is therefore of interest to find a factor describing the “balanced cross section” and the maximum reinforced cross section

$$\rho_{bal} = \frac{\zeta}{1 + \frac{\varepsilon_f - \varepsilon_{t0}}{\varepsilon_{cu}}} \quad (4.49)$$

$$\rho_{max} = \frac{A_s f_{sy} + A_f \varepsilon_f E_f}{b_w h f_{cc}} \quad (4.50)$$

Where ρ_{bal} is the reinforcement ratio for balanced cross section and ρ_{max} is the reinforcement ratio for maximum reinforced cross section. A reinforcement ratio that, at the highest, corresponds to ρ_{bal} can be considered as a “normally-reinforced cross section”. This is also the control for which failure mode that is current, thus, failure mode 1 is current if the following relationship is valid.

$$\rho_{bal} \geq \rho_{max} \quad (4.51)$$

Keeping this ratio will ensure that ductile failure will occur which is a desirable failure mode since large deflections precede the ultimate collapse of the concrete member.

4.2.6 Estimation of flexural capacity of one-way slabs

In Paper I, a one-way slab was strengthened with the MBC system. This section uses the simplified design approach proposed above to calculate the flexural capacity of the strengthened slab. The reason for this is that the slab did not have any compressive reinforcement. First the geometry of the test specimens strengthened with the MBC system will be shown. Thereafter, the tested material properties and last the calculation procedure will be shown with a short discussion of the results. Note, a full elaboration of the experimental program is shown in Paper I.

Geometry and test set-up

The evaluated slabs had a rectangular cross section and were 4 m long, 1 m wide and had a depth of 100 mm. The slabs were only reinforced in tension, by having 10 Ø8 mm of tensile reinforcement. The distance d_s to the tensile reinforcement was 76 mm. All of the slabs were subjected to four point bending shown in Figure 4.5.

Strengthening of the reinforced slabs was carried out by using the MBC system and utilising one and two layers of CFRP grid. All of the strengthening was performed on the slabs while they were supported, thus no initial strains were induced to the system. The total thickness of the strengthening system, t_{MBC} , was 10 mm.

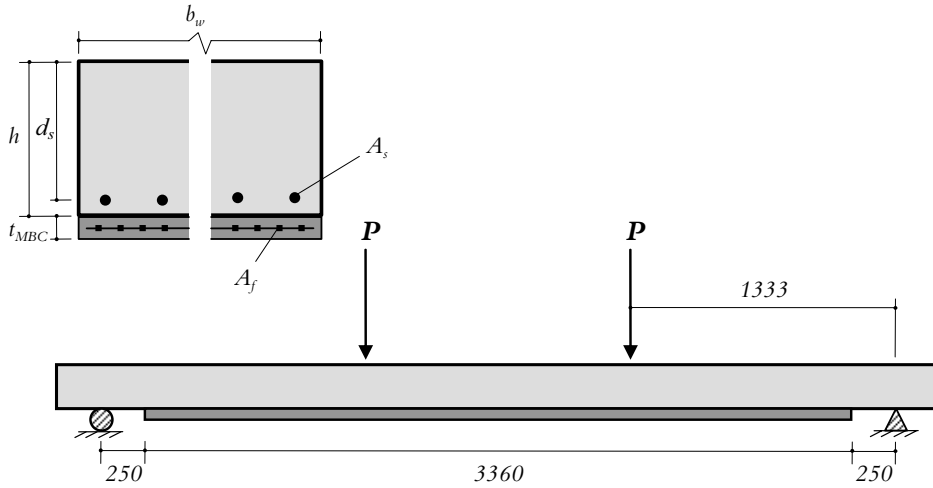


Figure 4.5. Test set-up and geometry of strengthened beam specimens.

Material properties

In this test four materials were used, concrete, steel reinforcement, a polymer modified mortar and CFRP grid. All of the mechanical properties for the longitudinal CFRP tows together with the total fibre amount for the cross section, A_f , are listed in Table 4.1, note that since the distances between tows are 45 mm a total of 22 tows are valid for the cross section. The mechanical properties for the tensile reinforcement are shown in Table 4.2. The concrete used in this test series had a compressive strength of 49.4 MPa and the ultimate compressive strain is assumed to be 0.0035.

Table 4.1. Material properties for longitudinal CFRP tows and total fibre area, A_f .

| | Tow spacing [mm] | E_f [GPa] | ε_f [‰] | Tow area [mm ²] | A_f [mm ²] |
|------|----------------------------|----------------|------------------------|---------------------------------------|-----------------------------|
| Grid | 45 | 404 | 10.5 | 0.9184 | 20.2 |

Table 4.2. Material properties for tensile reinforcement and total steel area, A_s .

| | \varnothing [mm] | E_s [GPa] | f_y [MPa] | A_s [mm ²] |
|-------|-----------------------|----------------|----------------|-----------------------------|
| Steel | 8 | 210 | 483 | 502.7 |

Flexural capacity

Since there is no compressive reinforcement in these slabs the two failure modes in the simplified approach will be failure in the longitudinal CFRP tows or crushing of the concrete. Note that the reduction factors for the simplified compressive stress distribution in the concrete are set to $\lambda = 0.4$ and $\zeta = 0.8$ as recommended by BBK (2004).

Failure mode 1 – Failure of the longitudinal CFRP grid tows

For the specimen strengthened with one layer of CFRP grid, the distance to the neutral axis is obtained from eq. (4.44).

$$x = \frac{A_s f_y + A_f \varepsilon_f E_f}{\zeta f_{cc} b_w} = \frac{502.7 \cdot 483 + 20.2 \cdot 10.5 \cdot 404}{0.8 \cdot 49.4 \cdot 1000} = 8.31 \text{ mm}$$

Insertion in eq. (4.47) gives the flexural capacity

$$\begin{aligned} M &= A_s f_y (d_s - \lambda x) + A_f \varepsilon_f E_f \left(h + \frac{t_{MBC}}{2} - \lambda x \right) = \\ &= 502.7 \cdot 483 \cdot (76 - 0.4 \cdot 8.31) + 20.2 \cdot 10.5 \cdot 404 \left(100 + \frac{10}{2} - 0.4 \cdot 8.31 \right) = 26.6 \text{ kNm} \end{aligned}$$

Using the same approach for the specimen strengthened with two layers of CFRP grid (twice the fibre amount) will give the following results:

$$x = 10.5 \text{ mm}$$

$$M = 34.6 \text{ kNm}$$

Failure mode 2 – Crushing of concrete

Use eq. (4.46) and (4.45) to obtain the distance to the neutral axis. When the distance to the neutral axis is known use eq. (4.48) to obtain the flexural capacity. The results are shown in Table 4.3.

Table 4.3. Distance to neutral axis and flexural capacity.

| | C_1 [N/mm] | C_4 [N] | C_5 [N/mm] | x [mm] | M [kNm] |
|------------------|-----------------|--------------|-----------------|-------------|--------------|
| 1 layer of CFRP | 39520 | -214212.7 | -2999806.7 | 11.8 | 39.85 |
| 2 layers of CFRP | 39520 | -185643.1 | -5999613.3 | 14.89 | 51.25 |

Determining failure mode

In order to determine current failure type of the cross section eq. (4.49) and (4.50) has to be used. For the slab with one layer of CFRP grid the following ratios are obtained.

$$\rho_{bal} = \frac{\zeta}{1 + \frac{\epsilon_f - \epsilon_{f0}}{\epsilon_{cu}}} = \frac{0.8}{1 + \frac{10.5 - 0}{3.5}} = 0.20$$

$$\rho_{max} = \frac{A_s f_{sy} + A_f \epsilon_f E_f}{b_w h f_{cc}} = \frac{502.7 \cdot 483 + 20.2 \cdot 10.5 \cdot 404}{1000 \cdot 100 \cdot 49.4} = 0.06$$

Applying the same procedure for the slab strengthened with two layers of MBC will render the following ratios:

$$\rho_{bal} = 0.20$$

$$\rho_{max} = 0.08$$

As shown above the relationship given in eq. (4.51) is valid for both of the evaluated slabs. Failure mode 1, failure of the longitudinal CFRP tows, is the governing type of failure. This was also the failure mode observed in the experimental study.

Results and discussion

All of the results from the experimental investigations are shown in Paper I. Table 4.4 shows the estimated and the experimentally–obtained ultimate flexure capacity. Both of the tested slab specimens failed by rupture of the longitudinal CFRP tows which was the governing failure mode achieved in the proposed estimations. Comparing the experimental to estimated flexural capacities it is clear that the proposed flexural design gives excellent estimations for the slabs. The ratio between experimental and estimated values was close to one. Seemingly, the proposed simplified model provides fair estimations. However, the more detailed model needs to be verified by additional test series performed on beam and slab specimens with different geometries and reinforcement schemes.

Table 4.4. Experimental and estimated flexural capacity.

| | Experimental <i>M</i> [kNm] | Estimated <i>M</i> [N] | Experimental/ Estimated [-] | Failure mode |
|------------------|--|---------------------------------------|--|-------------------------|
| 1 layer of CFRP | 26.7 | 26.6 | 1.00 | 1 |
| 2 layers of CFRP | 34.0 | 34.6 | 0.98 | 1 |

4.3 Shear design

4.3.1 Introduction

There exists a set of guidelines for strengthening concrete structures in shear, using FRPs bonded to the concrete surface using epoxy adhesives. Such guidelines can be found in ACI Committee 440 (2008), Monti and Liotta (2007), CNR (2005), Fib bulletin 14 (2001), CSA (2002), and Täljsten (2002).

Most of these guidelines practice the “addition” approach, see chapter 3, by adding the shear resistance contribution of the FRP (V_f) to the steel (V_s) and concrete shear resistance (V_c) according to

$$V_u = V_c + V_s + V_f \quad (4.52)$$

In all of these guidelines much focus is placed on the V_f contribution, especially since epoxy bonded strengthening system often exhibits debonding as a limiting failure mode besides fibre rupture.

However, using the “addition” approach makes it even more important that the proposed design is based on the same truss approach, for example, using the sum of V_c (based on regression) and V_s (based on the 45° Mörsh truss approach) as in ACI (2008) and BBK (2004). It can be argued that the V_f contribution is independent of the existing concrete structure. But, using a truss to model the ultimate shear resistance then the compressive strut should have the same inclination. In this thesis, the total shear capacity of a strengthened beam is modelled using the same truss model. V_f should then be applied based on the same truss approach, as it is in ACI Committee 440 (2008) where all forces are calculated based on a 45° truss. Using the design based on the variable angle truss model as in EC2-1 (2004) based on concrete plasticity could involve some difficulties regarding the basic assumptions on the limits of the inclination of the compressive strut, θ . This relates to the elastic brittle behaviour of the FRP compared to the yielding behaviour of steel shear reinforcement. However, since the concrete contribution is neglected for members with shear steel reinforcement there is some inherit safety in the design. This is further discussed in Paper V.

A comparison of different analytical approaches based on the most common shear design proposals for epoxy bonded strengthening systems is given in Sas (2008). In this comparison a database of over 200 beams strengthened in shear by epoxy bonded FRP was surveyed and the results indicate a wide scattering of the experimental versus predicted shear resistance. The variation in the results is strongly dependent on the background for calculating the shear resistance. The models surveyed in Sas (2008) were primarily based on either regression or the variable angle truss approach. However, since one of the limiting factors in epoxy bonded systems is the bond between the composite and the concrete, one explanation for the scattered results could then be in the description of the bond limitations. For fully wrapped beams, where the influence of bond is less significant better approximations are made. The MBC system does not behave in accordance with the epoxy based strengthening

systems, all tests in Paper I and II indicate full composite action. Therefore, bond has not been an issue and the behaviour of the MBC system is similar to reinforced concrete.

As previously mentioned, existing guidelines for FRP strengthening of concrete structures only considers epoxy bonded strengthening systems. To the author's knowledge there are no design guidelines for the MBC strengthening system presented in this thesis. There are however suggestions on how to estimate the shear capacity for strengthened beams using the textile reinforced mortar (TRM) and textile reinforced concrete (TRC). These systems have previously been described in chapter 2. The proposed model for the TRM system is given in Triantafillou and Papanicolau (2006), and the model is based on the variable angle truss model. Thus the inclination of the concrete compressive strut can be chosen arbitrarily. The shear design model for the TRC system is also based on the variable angle truss and is given in Rilem report 36 (2006). None of the models can directly be translated for MBC system design, since they have limiting factors for the effective strain based on textile fabrics. The verification of the design models for the TRM and TRC system is only validated for the V_f contribution. This means that the shear resistance of the concrete member is not taken into consideration in the verification. This is done by having a non-strengthened reference specimen corresponding to the V_c+V_s contribution in eq. (4.52), then this contribution is subtracted from the ultimate load of the strengthened specimen and V_f is obtained. A similar approach for the MBC system is given in Paper II.

In the coming sections, four different shear design proposals are given for the MBC system. These proposals are based on the same design proposals for concrete as given in chapter 3. The modified shear design proposals based on "addition" approach, variable angle truss approach and the full MCFT are merely stated here and for the derivations the reader is referred to Paper II and V. The simplified MCFT (SMCFT) is based on the derivations in chapter 3 and is further elaborated for the MBC adaptation in this section. Estimations of the different design proposals are compared to experimental results in section 4.3.6. Geometry and acting stresses and forces for a MBC strengthened cross section are presented in Figure 4.6.

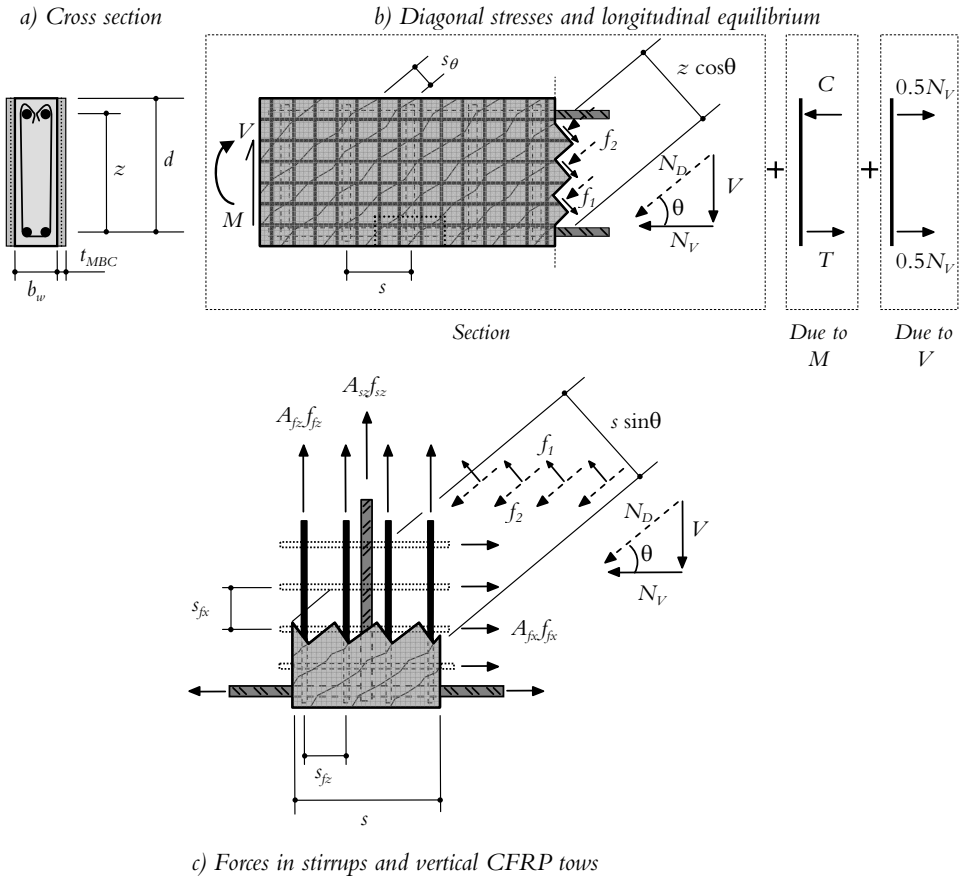


Figure 4.6. Geometry, stresses and forces for a MBC strengthened cross section

4.3.2 “Addition” approach based on 45° truss analogy

The background for the “addition” approach has been discussed in chapter 3. The concrete, V_c , and steel, V_s , contribution to the shear resistance can be calculated using, e.g. ACI (2008) or BBK (2004) see also chapter 3. Based on the 45° Mörsh truss, the following expression is obtained for the contribution of the CFRP grid in the MBC system, noting that the MBC strengthening system is applied on both sides.

$$V_f = 2 \frac{A_{fz} f_{fz}}{s_{fz}} z \quad (4.53)$$

Where z is the internal level arm, A_{fz} is the fibre amount, s_{fz} is the internal distance and f_{fz} is the stress in the transverse grid tows, see also Figure 4.6.

“Addition approach” and variable angle truss approach

In Paper II a different approach similar to many of the existing shear design proposals for an epoxy bonded strengthening system has been suggested by the author. This design is based on the “addition” approach, eq. (4.54), and in this proposal the inclination of the compressive strut, θ , could be set arbitrarily, eq. (4.55). Also the contribution of the mineral-based bonding agent, eq. (4.56), to the shear resistance is added.

$$V_u = \underbrace{V_c + V_s}_{\text{reinforced concrete}} + \underbrace{V_f + V_{MBA}}_{\text{MBC strengthening}} \quad (4.54)$$

$$V_f = \frac{2\varepsilon_{fz,ef} E_{fz} A_{fz} h_{ef} \cot(\theta)}{s_{fz}} \quad (4.55)$$

$$V_{MBA} = \frac{1}{3} t_{MBC} h_{ef} f_{MBA,t} \quad (4.56)$$

where $\varepsilon_{fz,ef}$ is denoted the effective strain for the transverse grid tows and this is further explained in section 4.3.5 together with a discussion of the influence of the mineral-based bonding agent to the shear resistance. E_{fz} is the modulus of elasticity for the transverse grid tows. h_{ef} is the effective height of the MBC system. There has been no investigation regarding the influence using different heights (depths) in this thesis and since the strengthening system has always been applied over the entire sides of the beam the effective height is set to be equal to the internal lever arm z . t_{MBC} is the thickness of the mineral-based bonding agent. Note, a factor 2 has to be applied when strengthening both sides of the beam. $f_{MBA,t}$ is the tensile strength of the mineral-based bonding agent.

Since the angle of the compressive strut could be set arbitrarily this model should belong in the variable angle truss approach. However, in the variable angle truss approach the concrete contribution to the shear resistance is not considered and therefore this design approach has to be seen as a separated approach where the resistance of the reinforced concrete beam is calculated separately from the shear resistance of the MBC strengthening. This is further discussed in the result and discussion chapter below.

4.3.3 Variable angle truss approach

The variable angle truss approach does not consider the shear resistance of concrete and the inclination of the compressive strut, θ , is set as an additional unknown. Since the inclination is not known the following limitations are given for concrete beams with steel shear reinforcement, $21.8^\circ \leq \theta \leq 45^\circ$ ($2.5 \leq \cot \theta \leq 1$). In this study, these limitations are considered to be valid for a MBC strengthened concrete member. The shear resistance of internal steel shear reinforcement and FRP grid based on the variable angle truss model is

$$V_u = V_s + V_f = \left(\frac{A_{sz} f_{sz}}{s} + 2 \frac{A_{fz} f_{fz}}{s_{fz}} \right) z \cot \theta \quad (4.57)$$

Where s is the internal distance of the steel reinforcement, see Figure 4.6.

4.3.4 Modified compression field theory

Adapting the modified compression field theory (MCFT), described in chapter 3, for the MBC system mainly originates in altering the constitutive and geometrical relationships. The applied equilibrium equations are basically the same but with a new CFRP material being added. Using the modified compression field theory is more intricate than to use the proposed shear design based on the “addition” approach or the variable angle truss approach. In the MCFT described in chapter 3, there are basically 15 equations that need to be solved and further controlled for convergence. These 15 equations have to be altered to obtain equilibrium considering the addition of a CFRP grid to the geometry. The derivations are presented in Paper V and the summary of the modified equations is shown in Figure 4.7.

Using the suggested equations in Figure 4.7 to obtain the shear resistance described in the “solution technique for MCFT” section in chapter 3 for concrete members subjected to both shear and flexure will give the steps shown below. Note that the contribution of the longitudinal CFRP tows to the resistance of the concrete member has been neglected; this is further discussed in the section describing the simplified MCFT below.

1. Choose a value for the principal strain, ε_1 .
2. Estimate the inclination of principal compressive stress, θ .
3. Calculate the diagonal crack width, w , using eq. (9) and (10) in Figure 4.7. Where the longitudinal and transverse average crack spacing, s_{mx} and s_{mz} , are calculated using the following equations based on the CEB-FIP code (1972) when using deformed reinforcing bars.

$$s_{mx} = 2 \left(c_x + \frac{s_x}{10} \right) + \frac{d_{bx}}{10 \rho_x} \quad (4.58)$$

$$s_{mz} = 2 \left(c_z + \frac{s}{10} \right) + \frac{d_{bz}}{10 \rho_z} \quad (4.59)$$

Where c_x and c_z are the maximum clear cover distance in the longitudinal and the transverse direction respectively. s is the stirrup distance and s_x is the internal distance between the longitudinal reinforcement. For small distances between the longitudinal reinforcement, the contribution of the latter can be ignored. d_{bx} and d_{bz} are the diameter of the reinforcing bars, while ρ_x and ρ_z are the reinforcement ratio, in the longitudinal and transverse direction respectively.

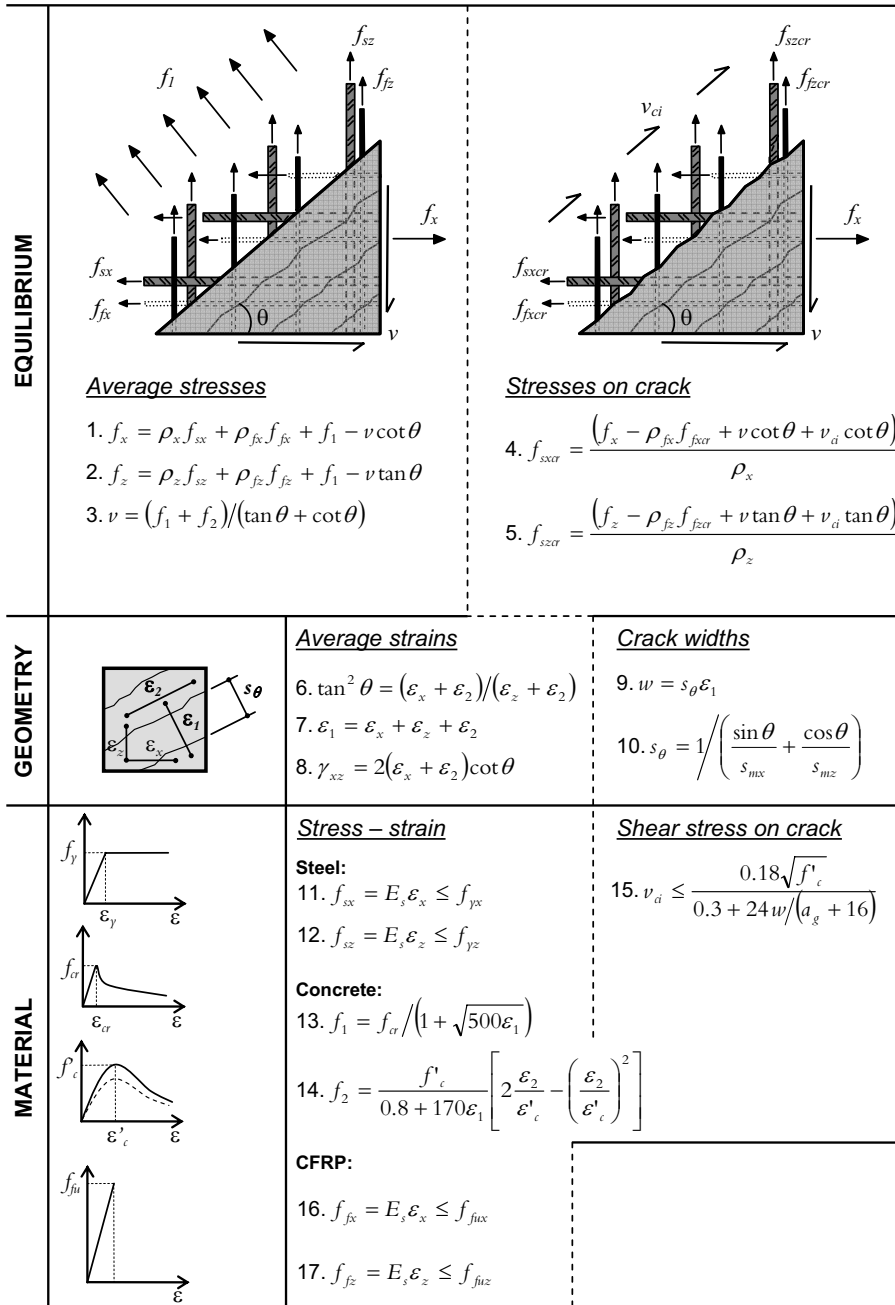


Figure 4.7. Equilibrium, geometry and material relationships for the MCFT adapted to a MBC strengthened concrete member.

4. Estimate a level of the transverse strain, ϵ_z , and check that the stress level in the stirrups, f_{sz} , and in the transverse CFRP tows, f_{fz} , does not exceed the limiting stresses according to:

$$f_{sz} = E_s \epsilon_z \leq f_{sy} \quad (4.60)$$

$$f_{fz} = E_{fz} \epsilon_z \leq f_{fz,ef} \quad (4.61)$$

Where $f_{fz,ef}$ is the effective strength of the CFRP, see section 4.3.5

5. Calculate the principal tensile stress according to eq. (13) in Figure 4.7. When assuming a principal tensile strain $\epsilon_t \leq \epsilon_{ot}$, a linear relationship of f_t is assumed according to Hooke's law, see also Figure 4.7. Note that the two sets of stresses in Figure 4.7, stresses between and across the crack, must be statically equivalent. This limitation is also known as the "crack check" (Bentz, 2000), and for these two sets of stresses to produce the same vertical component the requirement in equation (4.62) need to be fulfilled. Here the stresses across the crack are substituted against the ultimate stresses, f_{sy} for the stirrups and $f_{fz,ef}$ for the transverse CFRP tows.

$$f_1 = v_{ci} \tan \theta + \frac{A_{sz}}{s b_w} (f_{sy} - f_{sz}) + 2 \frac{A_{fz}}{s_{fz} b_w} (f_{fz,ef} - f_{fz}) \quad (4.62)$$

Where, v_{ci} , is the shear stress across crack due to aggregate interlocking shown in eq. (15) in Figure 4.7, note that a_g is the maximum aggregate size.

6. The total shear resistance, V , can be calculated using the equilibrium in Figure 4.6 b and c and is given as

$$V = \underbrace{f_1 b_w z \cot \theta}_{\text{concrete}} + \underbrace{\frac{A_{sz}}{s} f_{sz} \cot \theta}_{\text{stirrups}} + 2 \underbrace{\frac{A_{fz}}{s_{fz}} f_{fz} \cot \theta}_{\text{vertical CFRP tows}} \quad (4.63)$$

7. The principal compressive stress, f_2 , is calculated using Mohr's circle of stress and the shear stress is assumed to be constant over the cross section. The principal compressive stress and the shear stress are then obtained as

$$f_2 = (\tan \theta + \cot \theta) v - f_1 \quad (4.64)$$

$$v = V / (b_w z) \quad (4.65)$$

8. Calculate the strength of the diagonal compression stress field, f_{2max} , by using eq. (14) in Figure 4.7.
9. Check that the calculated principal compressive stress is lower or equal to the strength of the diagonal compression field, $f_2 \leq f_{2max}$. If this requirement is not fulfilled, then go back to step (1) and choose a smaller ϵ_t .

10. Calculate the transverse and longitudinal strains, ε_x and ε_z , along with the principal compressive strain, ε_2 , by elaborating eq. (6), (7) and (14) in Figure 4.7. The strains are then obtained as

$$\varepsilon_2 = \varepsilon'_c \left(1 + \sqrt{1 + f_2/f_{2\max}} \right) \quad (4.66)$$

$$\varepsilon_x = \frac{\varepsilon_1 \tan^2 \theta + \varepsilon_2}{1 + \tan^2 \theta} \quad (4.67)$$

$$\varepsilon_z = \frac{\varepsilon_1 + \varepsilon_2 \tan^2 \theta}{1 + \tan^2 \theta} \quad (4.68)$$

11. Calculate the stresses corresponding to the strains obtained in step (10), f_{sz} and f_{fz} respectively. Then check that the estimation of the strain ε_z and corresponding stresses, f_{sz} and f_{fz} , in step (4) is valid. If not, revise step (4) and proceed until the estimation corresponds to the calculated values.
12. Use a plane section analysis (described in chapter 3) and find the strain distribution that corresponds to the specified moment due to the shear force. Then use the longitudinal strain obtained in step (10) and control that convergence is fulfilled. If this requirement is not fulfilled, revise the assumed inclination θ and return to step (3) until convergence is obtained.

Note that the longitudinal strain obtained in step (10) is assumed to be located at $z/2$ (mid-depth of beam) for a beam containing internal steel shear reinforcement and at the same level as the tensile reinforcement for beams with no internal steel shear reinforcement.

Simplified modified compression field theory

Adapting the simplified MCFT for the MBC strengthening system is basically performed similar to the MCFT by altering the geometrical relationships and considering the constitutive relationship for the CFRP. Keep in mind that the background to the simplified MCFT is given in chapter 3 and that this section will only show the alterations made to suit MBC strengthening. The major alterations are done to the transverse- and longitudinal equilibrium. Thus as a conservative approach the values describing the tensile behaviour of concrete (the β value), the inclination of the compressive strut (θ value), and the effective crack spacing (s_{xe}) are assumed to be unchanged when adding a linear elastic material such as the CFRP.

The motivation for assuming the same behaviour of the β , θ , and s_{xe} is based on the fact that the simplified MCFT is basically a linear analysis and the CFRP material behaviour is linear elastic up to failure.

The shear stress on the MBC strengthened cross section can be expressed as

$$v = v_c + v_s + v_f = \beta \sqrt{f'_c} + (\rho_z f_{sz} + 2\rho_{fz} f_{fz}) \cot \theta \quad (4.69)$$

Where ρ_z is the shear reinforcement ratio, f_{sz} is the stress in the transverse steel reinforcement, ρ_{fz} is the transverse CFRP tow ratio and f_{fz} is the stress in the transverse CFRP tows. Assuming that the shear stress is constant over the effective cross section, the shear force is calculated as

$$v = \frac{V}{b_w d} \quad (4.70)$$

The expressions for the β , θ and s_{xe} values are repeated from chapter 3 as

$$\beta = \frac{0.4}{1 + 1500\varepsilon_x} \cdot \frac{1300}{1000 + s_{xe}} \quad (4.71)$$

$$\theta = (29 + 7000\varepsilon_x) \cdot (0.88 + s_{xe}/2500) \leq 75^\circ \quad (4.72)$$

$$s_{xe} = \frac{35s_x}{a_g + 16} \geq 0.85s_x \quad (4.73)$$

The effective crack spacing can be assumed to be 300 mm for concrete members having sufficient shear reinforcement ($\rho_z f_{yz} > 0.06 \sqrt{f'_c}$) to control the crack spacing, this reduces the crack spacing term in eq. (4.71) to unity. For members containing no shear reinforcement the crack spacing s_x is proposed to be 0.9d.

Longitudinal strain

The representative longitudinal strain, ε_x , is conservatively taken at mid-depth of the concrete member when using the MCFT. An additional conservative approach where it is simple to obtain the longitudinal strain is to take one half of the tensile strain in the flexural reinforcement, ASCE-ACI 445. (1998). For a reinforced concrete beam subjected to both flexural and shear loading the longitudinal equilibrium could be taken from Figure 4.6 and Figure 4.8 assuming an equivalent truss. The total longitudinal force due to bending moment and shear can be expressed as

$$N_{tot} = T + 0.5N_v = T + 0.5V \cot \theta \quad (4.74)$$

Where the tensile force T depends on the bending moment and can be taken as

$$T = \frac{M}{z} \quad (4.75)$$

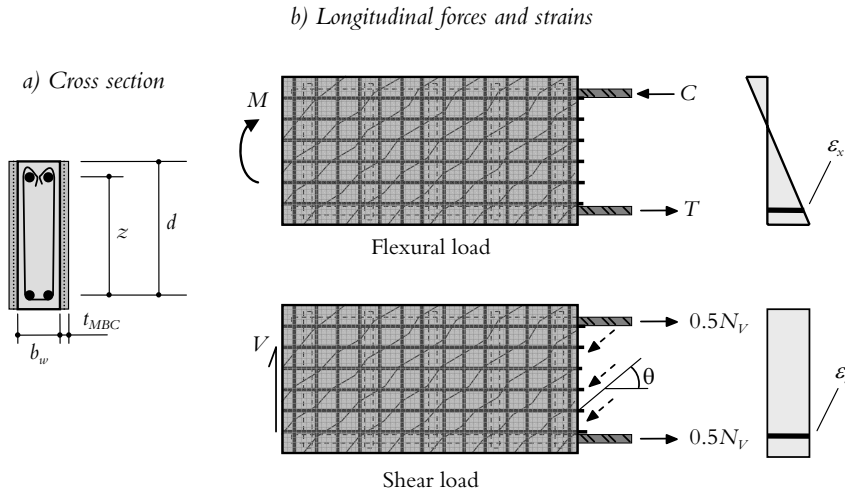


Figure 4.8. Determination of strains due to flexural and shear loading.

Knowing the longitudinal tensile force, the longitudinal strain could be expressed as

$$\varepsilon_x = \frac{\frac{M}{z} + 0.5V \cot \theta}{2(E_s A_s + E_{fx} A_{fx})} \quad (4.76)$$

The area of the longitudinal CFRP tows, A_{fx} , that contributes to the longitudinal tensile force due to the bending moment is not exactly known and depends on the longitudinal strain development. However, the fibre area for each single longitudinal tow is so far maximum 1 mm^2 and a typical $\rho_{fx} E_{fx}$ relationship is $38 - 90 \text{ MPa}$. The area and $\rho_{fx} E_{fx}$ relationship for the tensile reinforcement in the concrete beams in Paper II, $A_s \sim 2400 \text{ mm}^2$ and $\rho E_s \sim 5600$. By comparing these values it is clear that the influence of the longitudinal CFRP tows on the longitudinal strain is negligible. In addition, the results in Blanksvård (2007) did not show any significant influence of the longitudinal CFRP tows to the longitudinal strain development. Note, for deep beams with low amounts of flexural reinforcement or for disks with low reinforcement amounts, the contribution of the longitudinal CFRP tows should be included. In these cases a more detailed analysis must be made. However, existing beams to be strengthened in shear should have sufficient flexural reinforcement and therefore the assumption of neglecting the contribution of the longitudinal CFRP tows is valid.

The solution procedure for calculating the shear resistance according to the simplified MCFT adapted to a MBC strengthened concrete beam is:

- Step 1 Estimate a value for the longitudinal strain, ε_x .
- Step 2 Calculate the effective crack spacing, s_{xe} .

- Step 3 Calculate the β and θ according to eq. (4.71) and (4.72).
- Step 4 Calculate the shear stress, ν according to eq.(4.69).
- Step 5 Calculate the shear force, V . (4.70).
- Step 6 Calculate the longitudinal strain, ε_x , according to eq. (4.76). Compare this value to the estimates value in step 1. Return to step 1 until convergence is obtained.

4.3.5 Additional remarks

Effective strain

The strain development along a shear crack has, for a rectangular beam, a more or less parabolic shape which is shown in Blanksvärd (2007) and illustrated in Figure 4.9. As shown in chapter 2, the tensile behaviour of CFRP is linear elastic up to the ultimate failure. Therefore, after reaching the ultimate strength the CFRP will rupture. This is not the case for steel which has a yielding plateau. To counter for the elastic properties of the CFRP an effective strain is introduced in eq. (4.77). The strain reduction factor, η , is based on the ratio between the maximum shear stresses and the average shear stresses for a rectangular cross section, Popov (1999), see eq. (4.78). For further discussion of effective strains for cracked cross sections, the reader is referred to Carolin and Täljsten (2005), here an investigation of different stiffness showed that the reduction factor should be in the range of 0.5 – 0.7.

$$\varepsilon_{fz,ef} = \eta \varepsilon_{fuz} \quad (4.77)$$

$$\eta = \frac{\nu_{average}}{\nu_{max}} = \frac{V/A}{3V/(2A)} = \frac{2}{3} \quad (4.78)$$

where ε_{fuz} is the failure strain of the transverse CFRP tows, ν is the shear stress, V is the shear force and A is the area of the cross section.

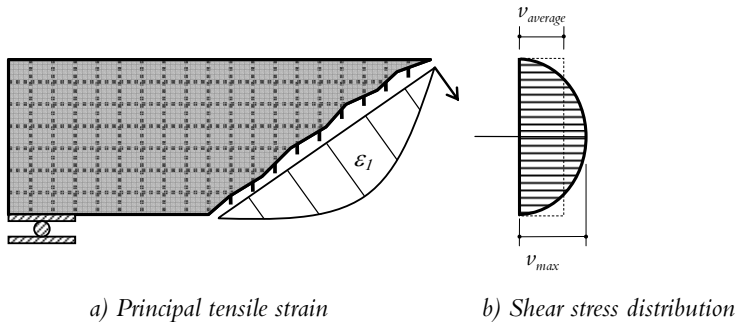


Figure 4.9. a) Principal strains across a shear crack and b) shear stresses over the cross section.

Shear resistance of the mineral-based bonding agent

Considering a rectangular cross section, Figure 4.9, for a non-cracked section the maximum shear stress in the cross section is $\tau_{max} = 3V/(2A)$. The maximum shear stress is located in the point of gravity and has the same size as the maximum principal tensile stress. In *Betonghandbok* (1990) it is stated that no shear reinforcement is needed if the principal tensile stress is less than $0.5 f_{ct}$. By using this expression for the maximum shear stresses, the shear contribution for the mineral-based strengthening system, assuming the mineral-based bonding agent performs in the same way as for concrete, can be expressed as

$$v_{max} = \frac{3V}{2A} \Rightarrow V \leq \frac{2A}{3} \frac{1}{2} f_{ct} \quad (4.79)$$

$$\Rightarrow V_{MBA} = \frac{1}{3} t_{MBC} f_{MBA,t} \approx$$

This could also be compared to the reduction of the formal shear strength, f_v , in BBK (2004), see chapter 3. Where the formal shear strength is a function of dowel effect, size and tensile strength of concrete and in the suggested reduction factor is 0.3, see the background on the BBK development in chapter 3.

Another engineering approach to handle the increase in the cross section by using the MBC system is to assume that the increase in the width of the member is proportional to the elastic modulus by a factor η_{MBA} , shown in eq. (4.80). By multiplying this factor to the thickness of the MBC, t_{MBC} , and adding this to the original width, b_w , of the base concrete member will give a new increased effective width of the strengthened member, b'_w , shown in eq. (4.81).

$$\eta_{MBA} = \frac{E_{MBA}}{E_c} \quad (4.80)$$

$$b'_w = b_w + 2\eta_{MBA} t_{MBC} \quad (4.81)$$

where E_{MBA} is the modulus of elasticity for the mineral-based binder and E_c is the modulus for the base concrete. However, the thickness of the MBC system is often quite small in most MBC applications. This, and also the fact that most commercially available binders have a similar modulus of elasticity as the base concrete, will give that the contribution of the binder to the shear resistance is small or negligible. Anyway, neglecting the contribution of the binder in the MBC is a conservative approach for design.

Web compressive failure

The web compressive failure is not considered in the proposed shear design for MBC strengthened structures. However, it is recommended to use the same upper bound for

the shear resistance as the ones used in concrete design models, e.g. ACI (2008), BBK (2004) and EC2-1 (2004).

4.3.6 Estimation of shear capacity for reinforced concrete beams

Background

In this section, an extended summary from the results in Paper V is presented. Therefore, the reader is also referred to Paper V for more details of the test set-up, geometries and mechanical properties of the materials used in the study. However, in order for the reader to be able to read through this section without going back and forth to paper V for all details, the basics of the test set-up, geometries and mechanical properties are stated in the following.

Test set-up and geometries

Reinforced concrete beams with a rectangular cross section were used in this study, the depth (h) of the beams was 500 mm and the width (b_w) was 180 mm. The beams were flexurally reinforced with 2413 mm² reinforcement bars in the bottom (A_s) and 402 mm² in the top (A'_s). The distance to the bottom reinforcement was 419 mm (d_s) and the distance to the top was 38 mm (d'_s). The beams were subjected to four point bending and the shear span was set to 1250 mm. One of the shear spans had no internal shear reinforcement but was strengthened with the MBC system having a thickness of 20 mm (t_{MBC}). The other shear span was heavily reinforced with internal steel shear reinforcement. Geometries and test set-up are shown in Figure 4.10.

In total, 7 beams were evaluated. Two non-strengthened reference beams, three beams strengthened using a CFRP grid (M) with a carbon fibre amount of 159 g/m², one beam using a CFRP grid (L) with a carbon fibre amount of 98 g/m² and one beam using a CFRP grid (S) with a carbon fibre amount of 66 g/m².

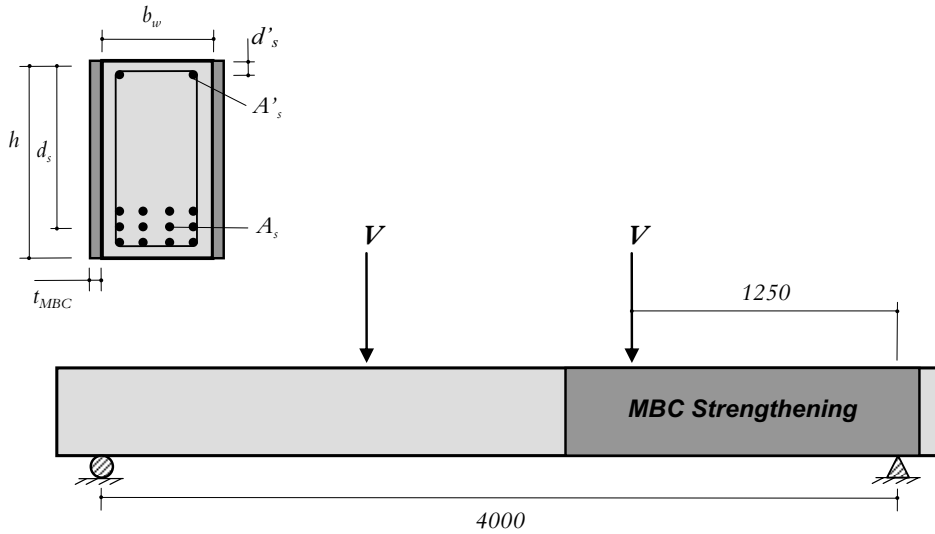


Figure 4.10. Test set-up and geometries of shear beams.

Material properties

The concrete compressive strength for the beam specimens varied between 32.5 to 44.8 MPa. The material properties for the fibres in the transverse CFRP tows are shown in Table 4.5. The flexural reinforcement had a yield strength of 555 MPa and a yield strain of 2.79% while the yield strength of the shear reinforcement were 601 MPa and the yield strain of 2.84%.

Table 4.5. Material properties for transverse CFRP tows.

| Grid | s_{fz} [mm] | E_{fz} [GPa] | ϵ_{fz} [‰] | $\epsilon_{fz,ef}$ [‰] | A_{fz} [mm ²] |
|--------|------------------|-------------------|------------------------|---------------------------|--------------------------------|
| Grid S | 25 | 366 | 14.0 | 9.4 | 0.2395 |
| Grid M | 45 | 404 | 11.1 | 7.4 | 0.9184 |
| Grid L | 72 | 454 | 8.3 | 5.6 | 1.071 |

Results and discussion

Results from the different design approaches are shown in Figure 4.11 as well as the ratio between experimental and predicted shear resistance for reference beams and beams strengthened using the different CFRP grids. Note that in the calculations the reduced effective strain was used. Further, the concrete contribution in the “addition” approach is based on both ACI and BBK shear design. For the variable angle truss approach the inclination of the compression strut, θ , is chosen to be the least conservative 21.8°. The design approach to give the best prediction is the one based on

MCFT, where the ratio between experiments and predictions are in average 1.16 with a COV of 6%. The second best ratio is given by the “addition” approach based on BBK design with an average of 1.22 and with a COV of 15%. The third best predictions are given by the simplified MCFT (SMCFT) with an average of 1.72 and a COV of 10%. The fourth best was the “addition” approach based on the ACI design with an average of 1.96 and with a COV of 24%. The most conservative approach is the variable angle truss model based on Eurocode where the concrete contribution is not considered. Although assuming the least conservative inclination of the compressive strut the ratio between experiments and predictions was incredible high, 4.70 with a COV of 48%.

On the other hand, both the full MCFT and the simplified MCFT give estimates of the compressive strut inclination. In the “addition” approach this inclination is assumed to be 45° and in the variable angle truss approach this inclination is merely guessed. The experimental shear inclination is compared to the compressive strut inclinations estimated by the MCFT approaches in Table 4.6 together with the experimental and predicted shear resistance. The experimental results are also shown in Paper II and Paper V for strengthened and non-strengthened beam specimens.

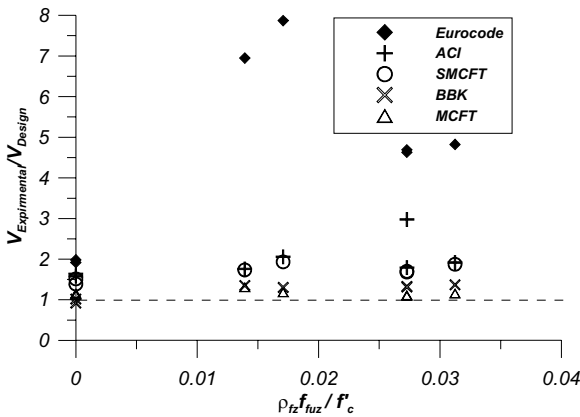


Figure 4.11. Ratio between experimental and predicted shear resistance of MBC strengthened beams with no internal shear reinforcement.

The simplified MCFT estimates the crack inclination quite well for all the specimens while the full MCFT requires lower inclinations in order to obtain longitudinal equilibrium. Although the simplified MCFT gave really good estimations of the shear crack inclination, the predicted shear resistance was quite conservative for both strengthened and non-strengthened beams.

Table 4.6. Experimental and predicted shear crack inclination.

| Specimen | Grid | f'_c [MPa] | $\rho_{fuz}f_{fuz}/f'_c$ [-] | V_{exp} [kN] | V_{exp}/V_{SMCFT} | V_{exp}/V_{MCFT} | θ_{Exp} | θ_{SMCFT} | θ_{MCFT} |
|----------|------|-----------------|---------------------------------|-------------------|---------------------|--------------------|----------------|------------------|-----------------|
|----------|------|-----------------|---------------------------------|-------------------|---------------------|--------------------|----------------|------------------|-----------------|

| | | | | | | | | | |
|----------|---|------|-------|-------|------|------|----|------|------|
| C40s0 | - | 37.2 | 0 | 123.5 | 1.47 | 1.12 | 30 | 35.0 | 35.4 |
| C40s0* | - | 36.3 | 0 | 126.7 | 1.51 | 1.15 | 34 | 34.9 | 35.0 |
| C40s0-Ma | M | 40.2 | 0.027 | 244.9 | 1.78 | 1.11 | 36 | 38.1 | 26.0 |
| C40s0-Mb | M | 40.2 | 0.027 | 241.9 | 1.76 | 1.10 | 32 | 38.1 | 26.0 |
| C40s0-S* | S | 32.5 | 0.017 | 208.1 | 1.93 | 1.18 | 34 | 36.3 | 21.7 |
| C40s0-M* | M | 35.1 | 0.031 | 251.9 | 1.87 | 1.16 | 34 | 37.7 | 23.3 |
| C40s0-L* | L | 44.8 | 0.014 | 206.4 | 1.73 | 1.31 | 31 | 37.0 | 22.3 |

Concluding remarks

Note that the proposed design in Paper II, based on the “addition” approach and the variable angle truss model, is not shown in Figure 4.11. This model would basically be the variable angle truss approach similar to the Eurocode design but adding the concrete contribution by using, e.g. ACI or BBK. Mixing different truss analogies with the additional unknown inclination of the compressive strut is probably not the best approach for designing MBC strengthened concrete structures in shear.

The cross sectional enlargement by adding a mineral-based bonding agent can give a contribution to the shear resistance. This influence would be prominent for slender beams with thick layers of the mineral-based bonding agent. The mineral-based bonding agent used in this survey had 80% of the base concrete properties so for these sets of beams, based on both eq. (4.79) and (4.80), the shear resistance contribution would be in the range of 10-15% for the base concrete. However, since the contribution of the mineral-based bonding agent to the shear strength is not fully investigated a safe design would be to neglect this contribution.

The predicted inclinations of the compressive strut for simplified MCFT were quite good when compared to the experimentally measured crack inclinations. While the full MCFT gave lower estimations for the MBC strengthened specimens. Firstly, it should be mentioned that the experimentally obtained crack inclination is a crude measurement taken as the inclination from the flexural crack initiated in the bottom of the beam to the propagated shear crack at the top of the beam. Secondly, the inclination predicted by the simplified MCFT is based on a conservative regression while the full MCFT is based on both transverse and longitudinal equilibrium. Therefore, the prediction of the inclinations in the full MCFT has better accordance to the shear crack at the mid-depth of the beams when compared to the experimental shear crack propagation. In addition, the shear crack predictions based on MCFT depend on the assumed flexural contribution to the longitudinal equilibrium. In the full MCFT performed in this thesis, the flexural contribution is based on a stiffness approach while for the simplified MCFT this contribution is based on a simple truss.

Although the design approach based on the full MCFT gives the best shear resistance predictions in this series it is still an iterative process that could be time consuming. Based on the results on this series of rectangular beams, design based on the “addition” approach is quite easy to carry out, which make them suitable for “back on the envelope” predictions. The simplified MCFT involves one iterative step but is also

capable of predicting the inclination of the compressive strut and provides conservative predictions of the shear resistance.

It can therefore be concluded, that the use of the “addition” approach based on the ACI is the less time consuming approach while giving quite conservative predictions. The “addition” approach based on BBK involves a few more steps but predicts the concrete contribution to the shear strength in closer accordance to experiments. The simplified MCFT involves one iterative step and gives predictions similar to the ones based on ACI, but provides estimates on the shear crack inclination. If a more detailed analysis is required then the full MCFT can provide reasonable estimations of the shear resistance and both longitudinal and transverse strains.

5 Discussion and Conclusions

5.1 Discussion

From the research presented, it has been found that concrete structures can be strengthened by the use of mineral-based composites (MBC). The strengthening effect is comparable to epoxy based FRP systems. The primary focus in the thesis has been to investigate the strengthening effect on a component and structural level. No development of new materials has been made and important questions such as long term effects and bond still remain to be answered. Bond in this regard refers to the transition zone between the base concrete and mineral-based binder and also the bond between the CFRP grid and binder. The most important findings are summarised and discussed below.

For flexurally strengthened slabs (Paper I), the ultimate flexural resistance was increased by up to 100% compared to the non-strengthened reference specimen. The failure mode for the strengthened slabs was rupture of the longitudinal fibres. Efforts to increase the mechanical bond by sanding the surface of the CFRP grid have a negative effect on the ultimate failure load. This premature failure is believed to depend on a too good bond in the vicinity of opening cracks, introducing stress concentrations. Comparing the strengthening effect of the MBC system to the epoxy bonded strengthening system using carbon fibre sheets, it is clear that the MBC system provides a similar or higher flexural load capacity. However, the failure mode for the epoxy bonded system differentiated from the MBC system by having a combination of debonding and fibre rupture. It is probable that the MBC system would not be as competitive to the epoxy bonded system in flexural strengthening if beam/slab specimens with less width had been used. From the small scale tests performed in Paper I it was found that using a binder with a higher modulus of elasticity give higher flexural capacity compared to the use of binders with lower stiffness.

From the investigation on shear strengthening of beams (Paper II and Paper VI), it was shown that increasing the carbon fibre amount in the grid increases the shear resistance. Using a binder with low modulus of elasticity generates shear cracks at lower shear loads compared to using a binder with higher stiffness. The experimental program for shear strengthening performed in this thesis contains a vast measuring set-up using both strain gauges and photometric measurements. Strain gauge readings from the internal shear reinforcement showed that the strains were reduced for specimens strengthened with the MBC system compared to non-strengthened specimens. The strain gauge readings on the vertical CFRP tows showed that high local strains were obtained in the vicinity of shear cracks. This further indicates good bond between the CFRP grid and the binder.

The strain gauge readings from the gauges mounted on the stirrups also monitored an important behaviour. For beam specimens with a low amount of internal shear reinforcement, low strains were measured up to a certain cracking load and as the shear crack propagated, the strain in the stirrup increased rapidly with increasing shear load. For the strengthened specimens the cracking load was increased which indicates that the MBC system is active also at low shear loads. When the amount of internal shear reinforcement was increased the difference between the cracking load for a strengthened specimen compared to a non-strengthened specimen was less pronounced. Specimens with increased amounts of internal shear reinforcement will have a better capacity for redistributing the stresses in the concrete. Since strain gauge readings provide only local measurements the use of photometric strain monitoring gave useful insight in the global behaviour of the shear strengthened beams. The photometric strain reading showed that the principal tensile strains were reduced for the MBC strengthened specimen compared to non-strengthened ones, even for lower shear loads. This also indicates that the crack widths are reduced for MBC strengthened specimens.

Since the MBC system inherits the properties of its constituents and that most mineral based binders are quasi-brittle it is possible to create a high performance MBC by the use of strain hardening cementitious composites such as ECC (engineered cementitious composites). Paper IV shows the combination of using an ECC binder and CFRP grids and their tensile behaviour as a MBC system. Using the ECC as a binder compensates for the brittleness of the CFRP and prevents premature failure of the grid by reducing locally high crack openings. This is caused by the crack bridging effect of the short fibres in the ECC. A full utilisation of the ductility in the ECC is however not achieved due to the fact that the CFRP grid will reach its ultimate strain first. It should also be mentioned that the ECC was never used in structural applications such as flexural and shear strengthening in this research.

A design proposal for MBC strengthening in flexure and shear is given in chapter 4 and Paper V. There are however some limitations on these design proposals, no consideration to the effects of bond was considered. For the shear design proposal no consideration was taken to the discontinuity regions and this is mainly because most strengthening is applied in the continuity regions of shear beams. Further only rectangular and constant cross sections were considered in order to maintain simplicity, transparency and accordance to the chosen shear beam specimens.

The simplified flexural design proposal was validated on the experimental results in paper I on strengthened slabs with excellent predictions. The detailed flexural design proposal needs to be validated against further tests on beams and slabs with compressive reinforcement. It was not possible to validate the proposed failure mode criterion because no tests were performed on these kinds of specimens.

The proposed shear design approach is based on existing shear design codes for reinforced concrete together with a more detailed analysis based on the modified compression field theory. The reason for doing so is that designing concrete in shear has been the topic for many researchers since the late 1800s and the progress has been

limited, probably because shear in concrete is an intricate problem. By having the basis in accepted shear analogies such as the 45° truss and the variable angle truss model it is easier to implement or superimpose the MBC strengthening system. All of the proposed models including the concrete contribution to the shear strength gave reasonable results compared to the experimentally obtained shear resistances. Further, it is assumed that neglecting the contribution of the mineral-based binder to the shear resistance will give conservative results. In addition, the reduction factor considering the linear elastic behaviour of the CFRP is based on non-cracked cross sections. An analysis of a cracked section would probably result in a larger reduction of the ultimate strain. However, based on the fact that all predictions were conservative it is assumed that the suggested reduction factor could be used for safe design.

5.2 Conclusion

The conclusions are made by answering the research questions stated in the first chapter of this thesis.

Can MBC systems be used for concrete repair and strengthening?

Yes, the MBC system has a friendly working environment with low risks for the manual worker. It is easy to apply and can favourably be shotcreted to the base concrete. It can also be applied on moist surfaces and the system is diffusion open. All of the results from both flexural and shear strengthening indicate increased load bearing capacities.

It has also been shown that the MBC system used for shear strengthening concrete beams will provide shear crack reductions and lower the strains in the shear reinforcement.

Can MBC systems obtain a comparable strengthening effect as for externally epoxy bonded CFRP systems?

Yes, the flexural response of the MBC system is highly competitive compared to epoxy bonded carbon fibre sheets for strengthening slabs.

For shear strengthening purposes the MBC system obtains comparable load bearing capacities to an epoxy bonded system with carbon fibre sheets applied in a transverse direction covering the entire side.

Is it possible to estimate the ultimate load bearing capacity for MBC strengthened concrete members by using existing design or slightly modified design models?

Yes, the proposed flexural design to estimate the flexural capacity for slabs strengthened with the MBC system gave excellent predictions. It is clear that using a simple approach based on the assumption that plane sections remain plane and longitudinal equilibrium renders reasonable results. The simplified flexural design proposal showed excellent results based on the results obtained from the one way slab specimens with no compressive reinforcement. However, there was no validation on the more detailed flexural design proposal but nevertheless, it is assumed that this model would give fair

estimations. This is based on the fact that the plane section analysis is valid for most cases of flexural loading.

All of the proposed models based on existing theories such as the 45° truss analogy, the variable angle truss model and the modified compression field theory gave more or less reasonable results. For non-cracked members it is recommended to use the shear design approach based models including the concrete contribution such as the “addition” approach and the ones based on modified compression field theory.

5.3 Suggestions on future research

The research carried out so far on the topic of mineral-based composites have shown promising results regarding both the behaviour and possibilities to estimate the flexural and shear resistance of strengthened concrete structures. Although, the research questions stated in the beginning of the thesis have been answered, one question often leads to a second question and so on. This is also the case in my work where new questions have aroused new areas of research. This section proposes different fields for future research. The proposals for future research are divided into the three interconnected levels that were stated in Paper IV and here shown in Figure 5.1, namely *material level*, *component level* and lastly the *structural level*.

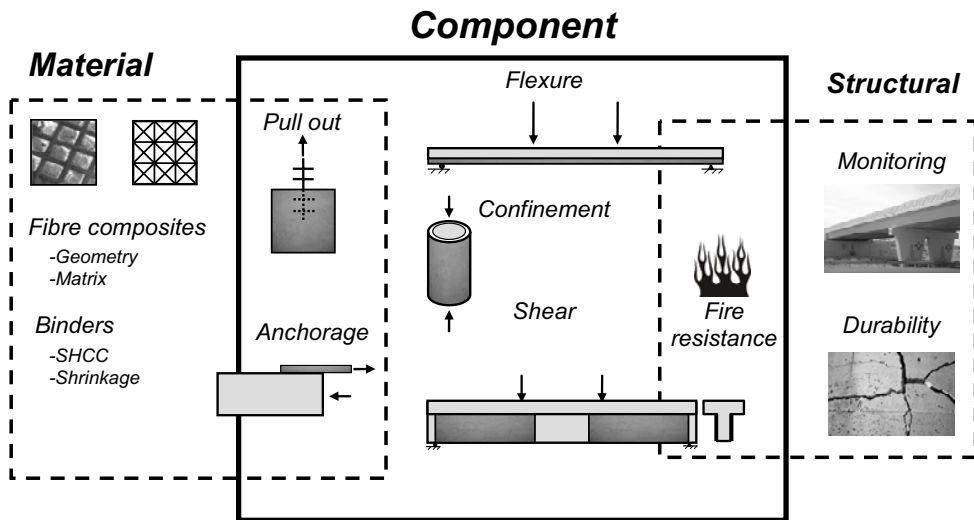


Figure 5.1. Future research on material, component and structural level.

Material level: Future research should be carried out on optimising the fibre composite and binders. For the fibre composite, increasing the fibre amount should also lead to further increasing the load bearing capacity of the MBC strengthening. Since impregnating the grid with an epoxy matrix gives a stiff and brittle FRP, when handled

and applied, a new more elastic polymer matrix should be developed ensuring the possibilities of bending the grid around corners. For strengthening biaxially loaded structures the grid geometry could be refined going from a two directional grid to a three or multi-directional grid depending on the actual state of stress. The bond stress development between the CFRP grid and binder should also be further investigated together with required development length to obtain full composite action.

Further, the shrinkage of the binder and its influence on the quality of the application need to be investigated. This is important in order to avoid edge lifting or early age cracking.

Component level: Component level refers here to testing of structural elements, e.g. beams, slabs, columns etc. The research on component level also covers a theoretical understanding of the structural behaviour. It would therefore be interesting to carry out additional tests on beams with T-sections. Here the challenge would lie within studying the anchoring of the MBC system in the compressive zone. This could be tested by investigating the influence of the effective depth of the beams, see Figure 5.2. As the effective depth increases, the influence of the anchorage should decrease. For a beam with a small effective depth, the available anchorage length is smaller. In addition, mechanical systems for anchoring the grid in the flanges before applying the binder could be investigated in order to overcome some of the presumed anchorage problems.

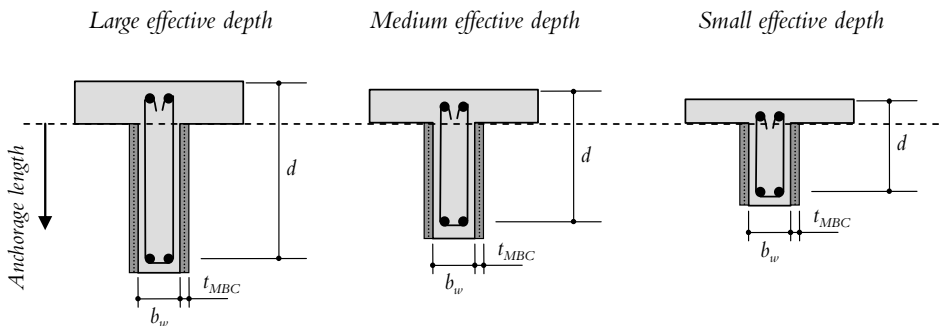


Figure 5.2. Large, medium and small effective depth on a T-cross section.

The results in this thesis regarding the reduction of principal strain indicate that the MBC system can be used as crack reinforcement in prefabricated concrete elements or newly-built concrete structures. An interesting aspect in this respect should be to use only the non corrosive CFRP grid as reinforcement and thus decreasing the demand for concrete cover.

The proposed design models for shear strengthening are only developed for rectangular beams. In order to be more generic, the models need to be developed for beams with T-cross sections. In order to do proper design, partial coefficients need to be investigated regarding both the models and the CFRP grid. In addition, as the materials used in the MBC system are developed and enhanced, the proposed shear models need to be adjusted accordingly.

Structural level: Structural level here refers to field applications and industrial implementation. The research carried out within this thesis could be regarded as applied science and should therefore be able to be implemented in civil engineering. One aspect, not considered at all in this thesis is the long term behaviour of the MBC system. Here investigations of creep, shrinkage and degradation should be made. Although spanning over a long time, this could preferably be done on a real structure in need of repair or strengthening. Before applying the MBC system a monitoring program should be established considering the strains in the CFRP, deflections of the structure, temperature movement, degradation etc. Full scale, in-situ tests in this regard would be a step closer to getting a better understanding of problems that may occur outside laboratory environments.

Finally, my opinion is that the research has just begun in this field and that there is unbroken land to be explored for many other researchers. The prospects for an increased use of mineral based composites are great.

References

Cited references listed in alphabetical order

ACI Committee 224. (1992) *Cracking of Concrete Members in Direct Tension*, Report ACI 224.2R-92, American Concrete Institute, USA

ACI Committee 318. (2008) *Building code requirements for structural concrete (318M-08)*. American Concrete Institute, Farmington Hills (MI, USA)

ACI-ASCE Committee 326. (1962) *Shear diagonal tension*. ACI Journal, 59(3), pp. 277-333.

ACI Committee 440. (2008) *Guide for the design and construction of externally bonded FRP systems for strengthening concrete structures*. American Concrete Institute, ACI 440.2R-08, Detroit, pp. 76.

Aho, Timo., Kinnunen, Jukka., Lyöri, Veijo., Kilpelä, Ari., Duan, Guoyong and Kostamovara, Juha (2007). *A new time of flight sensor for measuring strain in large structures*. Sustainable Bridges. Assessment for Future Traffic Demands and longer Lives, Edited by J. Bien, L. Elfgrén and J. Olofsson, Dolnoslaskie Wydawnictwo Edukacyjne, Wrocław, ISBN 978-83-7125-161-1, pp 181-190.

ASCE-ACI 445. (1998) *Recent Approaches to Shear Design of Concrete Structures*. Journal of Structural Engineering, 124(12), pp. 1375-1417.

Agopyan, V., Savastano, H., V.M. and Cincotto, M.A. (2005) *Developments on vegetable fibre-cement based materials in São Paulo, Brazil: an overview*. Cement and Concrete Composites 27, pp. 527-536.

Al-Amoudi, O.S.B., Abiola, T.O and Maslehuddin, M. (2006) *Effect of superplasticizer on plastic shrinkage of plain and silica fume cement concretes*. Construction and Building Materials, 20, pp. 642-647.

Al-Saleh, S.A and Al-Zaid, R.Z. (2006) *Effects of drying conditions, admixtures and specimen size on shrinkage strains*. Cement and Concrete Research, 36, pp. 1985-1991.

Banthia, N and Gupta, R. (2006) *Influence of polypropylene fiber geometry on plastic shrinkage cracking in concrete*. Cement and Concrete Research, 36, pp. 1263-1267.

Baumann, T. (1972) *Zur frage der netzbewehrung von flächentragwerken*. Bauingenieur, 47, pp. 367-377.

BBK 04. (2004) *Boverkets handbook about concrete structures* (in Swedish). ISBN: 91-7147-816-7.

Bentz, D.P., Geikerb, M.R and Hansen, K.K. (2001) *Shrinkage-reducing admixtures and early-age desiccation in cement pastes and mortars*. Cement and Concrete Research, 31, pp. 1075-1085.

Bentz, E.C. (2000) *Sectional Analysis of Reinforced Concrete Members*. PhD Thesis, Department of Civil Engineering, University of Toronto, 2000, 310 pp.

Bentz, E.C., Vecchio, F.J., and Collins, M.P. (2006) *The simplified MCFT for calculating the shear strength of reinforced concrete elements*. ACI Structural Journal, 103(4), pp. 614-624.

Beeldens, A., Van Gemert, D., Ohama, Y. and Czarnecki, L. (2003) *From microstructure to macrostructure: an integrated model of structure formation in polymer modified concrete*. Proceedings 4th Asia Symposium on Polymers in Concrete ASPIC 2003, Chuncheon, Korea, May 1-3, 2003, pp. 211-219.

Betonghandbok (1990) *Construction* (In Swedish). Second edition. Solna: AB Svensk byggtjänst, ISBN: 91-7332-533-7.

Betonghandbok (1994) *Material* (In Swedish). Second edition. Solna: AB Svensk byggtjänst, ISBN: 91-7333-266-6.

Beton Kalender Teil 1. (1990) Verlag Ernst & Sohn, Wiesbaden, Germany.

Beushausen, H. and Alexander, M.G. (2005) *Failure mechanisms and tensile relaxation of bonded concrete overlays subjected to differential shrinkage*. Cement and Concrete Research, 36, pp. 1908-1914.

Betongrapport nr 9. (2002) *Fiberkompositer (FRP) för betongkonstruktioner* (In Swedish). Swedish Concrete Association. ISBN: 91-973445-2-4.

Blanksvärd, T. (2007) *Strengthening of concrete structures by the use of mineral based composites*. Licentiate thesis 2007:15, Luleå University of Technology, department of civil and environmental engineering, ISBN: 91-85685-07-3.

Bolander, J.E and Berton, S. (2004) *Simulation of shrinkage induced cracking in cement composite overlays*. Cement and Concrete Research, 26, pp. 861-871.

- Branson, D.E. (1977) *Deformation of concrete structures*. McGraw-Hill, Inc., U.S., ISBN: 0-07-007240-X, 546 pp.
- Carolin, A. (2003) *Carbon Fibre Reinforced Polymers for Strengthening of Structural Elements*. Doctoral thesis 2003:18, Luleå University of Technology, department of civil and environmental engineering, ISBN: 91-89580-04-4.
- Carolin, A and Täljsten, B. (2005) *Theoretical Study of Strengthening for Increased Shear Bearing Capacity*. Composites for Construction, 9, pp. 497-506.
- Carolin, A., Täljsten, B., and Hejll, A. (2005) *Concrete beams exposed to live loading during carbon fiber reinforced polymer strengthening*. Composites for Construction, 9(2), pp. 178-186.
- Carlswärd, J. (2006) *Shrinkage cracking of steel fibre reinforced self compacting concrete overlays – Test methods and theoretical modelling*. Luleå University of Technology, Division of Structural Engineering, Doctoral thesis 2006:55.
- CEB-FIP (1972) *Model code for concrete structures: CEB-FIP International recommendations*. 3rd edition, Comité Euro-International du béton, Paris, pp. 348.
- Chen, W. F., and Drucker, D. C. (1969) *Bearing capacity of concrete block and rock*. ASCE, Engineering mechanics division, 95(4), pp. 955-978.
- CNR (2005). *Instructions for design, execution and control of strengthening interventions through fiber reinforced composites*. CNR-DT 200/04, Consiglio Nazionale delle Ricerche, Rome, Italy (English version, (2005).
- Collins, M. P. (1998) *Procedures for calculating the shear response of reinforced concrete elements: A discussion*. Structural Engineering, 124(12), pp. 1485-1488.
- Collins, M. P. and Mitchell, P. (1991) *Prestressed concrete structures*. New Jersey: Prentice-Hall, inc. ISBN: 0-13-691635-X.
- CSA (1994). *Design of concrete structures*. Canadian Standards Association, CSA A23.3-94, pp. 200.
- CSA. 2002 *Design and Construction of Building Components with Fibre-Reinforced Polymers*. Canadian Standards Association, CAN/CSA-S806-02, Toronto, Canada, pp. 187.
- CSA (2004). *Design of concrete structures (CSA A23.3-4)*. CSA Committee A23.3, Canadian Standards Association. Mississauga, pp. 214.

Curbach, M., Graf, W., Jesse, D., Sickert, J. U., and Weiland, S. (2007) *Segmentbrücke aus textilbewehrtem Beton: Konstruktion, Fertigung, numerische Berechnung*. Beton- und Stahlbetonbau, 102(6), pp. 342-352.

Curbach, M., and Jesse, F. (2009) *Eigenschaften und Anwendung von Textilbeton*. Beton- und Stahlbetonbau, 104(1), pp. 9-16.

Cuypers, H., Wastiels, J., Van Itterbeeck, P., De Bolster, Orłowsky, E. J and Raupach, M. (2006) *Durability of glass fibre reinforced composites experimental methods and results*. Composites Part A: Applied Science and Manufacturing, 37, pp. 207-215.

Drucker, D. C., Greenberg, H. J., and Prager, W. (1952) Extended limit design theorems for continuous media. Quarterly of Applied Mathematics, 9, pp. 381-389.

EC 2-1. (2004) *Eurocode 2: Design of concrete structures – Part 1: Common rules for building and civil engineering structures*. prEN 1992-1, CEN (Comité Européen de Normalisation), European Committee for Standardisation, Central Secretariat, Brussels. December 2004

Fib Bulletin 3 (1999) *Structural Concrete – Textbook on behaviour, design and performance*. Volume 3, manual textbook, ISBN 978-2-88394-043-7, pp. 292.

Fib bulletin 14. (2001) *Design and use of externally bonded fibre reinforced polymer reinforcement (FRP EBR) for reinforced concrete structures"* Technical report, TG 9.3, July 2001, ISBN 2-88394-054-1, 138 pp.

Fischer, G., and Li, V. C. (2007) *Effect of fiber reinforcement on the response of structural members*. Engineering Fracture Mechanics, 74, pp. 25-272.

Fukuyama, H. and Sugano, S. (2000) *Japanese seismic rehabilitation of concrete building after the Hyogoken Nanbu earthquake*. Cement and Concrete Composites, 22(1) pp. 59-79.

Garcés, P., Fraile, J., Vilaplana-Ortego, E., Cazorla-Amorós, D., Alcocel, E. G and Andión, L. G. (2005) *Effect of carbon fibres on the mechanical properties and corrosion levels of reinforced portland cement mortars*. Cement and Concrete Research, 35, pp. 324-331.

García Santos, A., Rincón, J. M., Romero, M and Talero, R. (2005) *Characterization of a polypropylene fibered cement composite using ESEM, FESEM and mechanical testing*. Construction and Building Materials, 19, pp. 396-403.

Grace, N. F., Abdel-Sayed, G., and Ragheb, W. F. (2002) *Strengthening of concrete beams using innovative ductile fiber-reinforced polymer fabric*. ACI Structural Journal, 99(5), pp. 692-700.

Groth, P. (2000) *Fibre Reinforced Concrete*. Doctoral thesis 2000:4, Luleå University of Technology, division of structural engineering, ISSN: 1402-1544.

- Grzybowski, M. and Shah, S.P. (1990) *Shrinkage cracking of fiber reinforced concrete*, ACI Materials Journal, 87, pp. 138–148.
- Gutiérrez, R.M., Díaz, L.N and Delvasto, S. (2005) *Effect of pozzolans on the performance of fiber-reinforced mortars*. Cement and Concrete Composites, 27, pp. 593–598.
- Gvozdev, A. A. (1960) *The determination of the value of the collapse load for statically indeterminate systems undergoing plastic deformation*. Mechanical sciences, 1, pp. 322–335. (English translation of the Russian of the Russian original published in; Proceedings in the conference on plastic deformations, December 1936, Akademiia Nauk SSSR, Moscow-Leningrad, 1938, pp. 19–38.)
- Han, D and Tsai, S. W. (2003) *Interlocked Composite Grids Design and Manufacturing*. Journal of composite materials, 37, pp. 287–316.
- Hedman, O. and Losberg, A. (1975) *Shear design of concrete structures* (In Swedish). Nordisk betong, 5, pp. 19–29.
- Hedman, O. and Losberg, A. (1978) *Design of concrete structures with regards to shear forces*. CEB Bulletin, 126, pp. 184–209.
- Hegger, J., and Voss, S. (2004) *Textile reinforced concrete under biaxial loading*. Proceedings of 6th Rilem Symposium on Fiber Reinforced Concrete (FRC), BEFIB 2004, Varenna, Italy, pp. 1463–1472.
- Hegger, J., Will, N., Bruckermann, O., and Voss, S. (2006) *Load-bearing behaviour of textile reinforced concrete*. Materials and Structures, 39, pp. 765–776.
- Hewlett, P. C. (1988) *Cement Admixtures, Uses and Applications*. Longman, Harlow, pp. 85–101.
- Hill, R. (1951) *On the state of stress in plastic-rigid body at the yield point*. The philosophical magazine, 42, pp. 868–875.
- Holt, E.E. (2001) *Early age autogenous shrinkage of concrete*. VTT Publications, Technical Research Centre of Finland, 446, ISSN 1235–0621. 184 pp.
- Hoult, N. A., Sherwood, E. G., Bentz, E. C. and Collins, M. P. (2008) *Does the Use of FRP Reinforcement Change the One-Way Shear Behavior of Reinforced Concrete Slabs?*. Journal of Composites for Construction, 12(2), pp. 125–133.
- Hsu, T. T. C. (1988) *Softened truss model theory for shear and torsion*. ACI structural journal, 85(6), pp. 624–635.

Jeppsson, J. (2003) *Reliability-based assessment procedures for existing concrete structures*. Division of Structural Engineering, Lund University, Lund, Doctoral thesis, report TVBK-1026.

Johansson, T. (2005) *Strengthening of concrete structures by Mineral Based Composites*. Research report 2005:10, Luleå University of Technology, Department of Civil and Environmental Engineering.

Jonasson, J.E. (1977) *Computer programs for non-linear analyses of concrete in view of shrinkage, creep and temperature* (in Swedish). Swedish Cement and Concrete Institute, Stockholm, Sweden, CBI Research Report 7:77.

Jonasson, J.E. (1978) *Analysis of creep and shrinkage in concrete and its application to concrete top layers*. Cement and Concrete Research, 8, pp. 441-454.

Joyce, M., and Brown, M. A. (1966) *W. B. Wilkinson (1819-1902) and his place in the history of reinforced concrete*. The Newcomen Society, 39, pp. 129-142.

Justnes, H and Oye, B. A. (1990) *The microstructure of polymer cement mortars*. Nordic Concrete Research publication No. 9.

Kabele P., Takeuchi S., Inaba K., and Horii H. (1999) *Performance of Engineered Cementitious Composites in Repair and Retrofit: Analytical Estimates*. Proceedings of HPFRCC 3 - The Third International RILEM Workshop Cachan: RILEM Publications, 1999, p. 617-627. ISBN 2-912143-06-3.

Kaufmann, W. (1998). *Strength and deformations of structural concrete subjected to In-plane shear and normal forces*. Institut für Baustatik und Konstruktion, ETH, Zürich, Doctoral thesis, pp. 147

Kaufmann, W. and Marti, P. (1998) *Structural concrete: Cracked Membrane Model*. Structural Engineering, 124(12), pp. 1467-1475.

Kockal, N.U and Turker, F. (2007) *Effect of environmental conditions on the properties of concretes with different cement types*. Construction and Building Materials, 21, pp. 634-645.

Hognestad, E. (1952) *Fundamental concepts in ultimate load design of reinforced concrete members*. ACI Journal Proceedings, 48(6), pp. 809-830.

Kupfer, H. (1964) *Erweiterung der Mörschen fachwerkanalogie mit hilfe des prinzipts vom formänderungsarbeit*. CEB Bulletin d'information, 40, pp. 44-57.

Langlois, V., Fiorio, B., Beaucour, A. L., Cabrillac, R., and Gouvenot, D. (2007) *Experimental study of the mechanical behavior of continuous glass and carbon yarn-reinforced mortars*. Construction and Building Materials, 21, pp. 198-210.

- Li, V. C. (1992) *Performance Driven Design of Fiber Reinforced Cementitious Composites*. In Proceedings of 4th RILEM International Symposium on Fibre Reinforced Concrete, Chapman and Hall, Ed. Swamy, R. N., pp. 12 – 30.
- Li, V. C. (2002) *Reflections on the research and development of engineered cementitious composites (ECC)*. Proceedings of the JCI International Workshop on Ductile Fiber Reinforced Cementitious Composites (DFRCC) – Application and Evaluation, DFRCC-2002, Takayama, Japan, October 21-22, pp. 1-21.
- Li, Z and Ding, Z. (2003) *Property improvement of Portland cement by incorporating with metakaolin and slag*. Cement and Concrete Research 33 579-584 (PII: S0008-8846(02)01025-6).
- Lepech, M. D., and Li, V. C. (2008) *Large-scale processing of engineered cementitious composites*. ACI Materials Journal, 105(4), pp. 358-366.
- Lima, J. L. T. and Barros, J. A. (2007) *Design models for shear strengthening of reinforced concrete beams with externally bonded FRP composites: a statistical vs reliability approach*. Proceedings in FRPRCS-8, Patras, Greece, July 16-18 (CD ROM).
- Meier, U. (1987) *Bridge repair with high performance composite materials*. Material und Technik, 4, pp. 125-128.
- Monti, G and Liotta, M.A. (2007) *Tests and design equations for FRP-strengthening in shear*. Construction and Building Materials, 21, pp. 799–809.
- Moody, K. G., Viest, I. M., Elstner, R. C. and Hognestad, E. (1954) *Shear strength of reinforced concrete beams part 1 – Tests of simple beams*. ACI Journal Proceedings, 51(12), pp. 317-332.
- Morrow, J. and Viest, I. M. (1957) *Shear strength of reinforced concrete frame members without web reinforcement*. ACI Journal, 53(9), pp. 833-869.
- Möller, B., Graf, W., Hoffmann, A., Sickert, J. U., and Steinigen, F. (2005) *Tragwerke aus Textilbeton - Berechnungsmodelle, Anwendungen*. Bautechnik, 82(1), pp. 882-795.
- Mörsch, E. (1908) *Der eisenbetonbau – seine theorie und anwendung*. 3. Auflage, Verlag Konrad Wittwer, Stuttgart, pp. 376.
- Mörsch, E. (1922) *Der eisenbetonbau - seine theorie und anwendung*. 5. Auflage, Verlag Konrad Wittwer, Stuttgart, pp. 460.
- Nielsen, M. P. (1999) *Limit analysis and concrete plasticity*. Second edition. Boca Raton, Florida, CRC Press LLC, ISBN: 0-8493-9126-1.

Nordin, H. (2003). *Fibre Reinforced Polymers in Civil Engineering*. Licentiate thesis 2003:25, Luleå University of Technology, department of civil and environmental engineering, ISBN: 91-89580-08-7.

Ohama, Y. (1998) *Polymer-based admixtures*. Cement and Concrete Composites, 20, pp. 189-212.

Pang, X., and Hsu, T. T. C. (1996) *Fixed angle softened truss model for reinforced concrete*. ACI structural journal, 93(2), pp. 197-207.

Pascal, S., Alliche, A and Pilvin, Ph. (2004) *Mechanical behaviour of polymer modified mortars*. Materials Science and Engineering A 380, pp. 1-8.

Peled, A., Cohen, Z., Pasher, Y., Roye, A., and Gries, T. (2008) *Influences of textile characteristics on the tensile properties of warp knitted cement based composites*. Cement and Concrete Composites, 30, pp. 174-183.

Prager, W. (1955) *Probleme der Plastizitätstheorie*. Birkhäuser Verlag, Basel and Stuttgart, pp. 100.

Popov, E. P. (1999) *Engineering Mechanics of Solids*. New Jersey: Prentice-Hall, inc. ISBN: 0-13-081534-9. pp. 430-432.

Qi, C., Weiss, J and Olek, J. (2003) *Characterization of plastic shrinkage cracking in fiber reinforced concrete using image analysis and a modified Weibull function*, Materials and Structures, 36, pp. 386-395.

Raupach, M., Orłowsky, J., Büttner, T., and Keil, A. (2006) *Recent developments of the usage of polymers in textile reinforced concrete*. Proceedings of the 5th Asian Symposium on Polymers in Concrete, Taramani, India, September 11-12, pp. 53-60.

Ray, I and Gupta, A. P. (1994) *Effect of latex and superplasticizers on Portland Cement Mortar in the fresh state*. Cement & Concrete Composites, 16, pp. 309-316.

Ray, I and Gupta, A. P. (1995) *Effect of latex and superplasticizers on Portland Cement Mortar in the hardened state*. Cement & Concrete Composites. 17, pp. 9-21.

Rilem report 36. (2006) *State-of-the-art Report of RILEM technical committee 201-TRC: Textile Reinforced Concrete*. Edited by Brameshuber, W. Rilem publications S.A.R.L, Bagnaux, France, ISBN: 2-912143-99-3.

Ritter, W. (1899) *Die bauweise Hennebique*. Schweizerische Bauzeitung, 17, pp. 41-43, 49-52 and 59-61.

- Roye, A and Gries, T. (2005) *Tensile behavior of rovings, textiles and concrete elements – possible to compare directly?* Composites in Construction 2005 – Third International Conference, Lyon, France, July 11.
- SB-MON. (2007) *Guideline for Monitoring of Railway Bridges*. Prepared by Sustainable Bridges – a project within EU FP6. Available from www.sustainablebridges.net.
- Sas, G. (2008) *FRP strengthening of RC beams and walls*. Licentiate thesis 2008:39, Luleå University of Technology, department of civil and environmental engineering, Sweden, pp. 107 +57.
- Sayir, M., and Ziegler, H. (1969) *Der verträglichkeitssatz der plastizitätstheorie und seiner anwendung auf räumlich unetstetige felder*. Zeitschrift für angewandte Mathematik und Mechanik, 20, pp. 78-93.
- Schorn, H., Raupach, M., Brameshuber, W., Höcker, H., Mäder, E., Arnold, B. J. A., Brockmann, T., Hempel, R., Orłowsky, J., and Plonka, R. (2004) *Betontechnologie und Dauerhaftigkeit von glasfaserbewehrten Bauteilen*. Beton- and Stahlbetonbau, 99(6), pp. 444-451.
- Schulze, J. (1999) *Influence of water-cement ration and cement content on the properties of polymer-modified mortars*. Cement and Concrete Research, 29, pp. 909-915.
- Schweite, H. E., Ludwig, U and Aachen, G. S. (1969) *The influence of plastics dispersions on the properties of cement mortars*. Betonstein Zeitung, 35(1) pp. 7-16.
- Shi, C., and Mo, Y. L. (2008) *High performance construction materials – science and applications*. World Scientific Publishing Company, ISBN: 98-127973-5-1.
- Song, P.S., Hwang, S and Sheu, B.C. (2005) *Strength properties of nylon- and polypropylene-fiber-reinforced concretes*. Cement and Concrete Research, 35, pp. 1546-1550.
- Stanf, H., and Li, V. C. (2004) *Classification of fibre reinforced cementitious materials for structural applications*. 6th RILEM Symposium on fiber-reinforced concretes (FRC) – BEFIB 2004, 20-22 September, Varenna, Italy, pp. 197-218.
- Sustainable Bridges (2004) *European Railway bridge demography*. Report, WP1-02-T-040601-Deliverable D 1.2, pp 1-15.
- Tepfers, R. (1998) *Bond of FRP reinforcement in concrete: A state-of-the-art in preparation*. ACI Special Publication, 180, pp. 493-504.

Thürlimann, B. and Grob, J. (1976) *Ultimate strength and design of reinforced concrete beams under bending and shear*. Institut für Baustatik und Konstruktion, ETH, Zürich, Bericht 63.2

Triantafillou, T. C. and Plevris, N. (1992) *Strengthening of R/C beams with epoxy bonded fiber composite materials*. Materials and structures, 25, pp. 201–211.

Triantafillou, T. C., Papanicolaou, C. G., Zissimopoulos, P., and Laourdekis, T. (2006) *Concrete confinement with textile reinforced mortar jackets*. ACI Structural Journal, 103(1), pp. 28–37.

Triantafillou, T.C and Papanicolaou, C.G. (2006) *Shear strengthening of reinforced concrete members with textile reinforced mortar (TRM) jackets*. Materials and Structures, 39(1), pp. 93–103.

Täljsten, B. (2002) *FRP Strengthening of Existing Concrete Structures: Design Guidelines*. Luleå University of Technology. ISBN: 91-89580-03-6.

Wagner, H. (1929) *Ebene blechwandträger mit sehr dünnem stegblech*. Zeitschrift für flügtechnik und motorluftschiffahrt, Berlin, 20 (8–12).

Wagner, H. B. (1965) *Polymer modified hydraulic cements*. In industrial and engineering chemistry, product research and development, 4(3) pp. 191–203.

Wagner, H. B and Grenely, D. H. (1978) *Interphase effects in polymer modified hydraulic cements*. Journal of Applied Polymer Science, 22(3) pp. 821–834.

Walraven, J. C. (1981) *Fundamental analysis of aggregate interlock*. ASCE, Structural division, 107, pp. 2245–2270.

Van Gemert, D., Czarnecki, L., Maultzsch, M., Schorn, H., Beeldens, A., Lukowski, P and Knapen, E. (2005) *Cement concrete and concrete–polymer composites: Two merging worlds: A report from 11th ICPIC Congress in Berlin, 2004*. Cement and Concrete Composites, 27, pp. 926–935.

Vecchio, F., and Collins, M. P. (1982) *The response of reinforced concrete to in-plane shear and normal stresses*. Publication 82-03, Department of Civil Engineering, University of Toronto, pp. 332.

Vecchio, F. J., and Collins, M. P. (1986) *The modified compression field theory for reinforced concrete elements subjected to shear*. ACI journal, 83(2), pp. 219–231.

Wendehorst, R. (1992) *Baustoffkunde*. Vincentz-Verlag, Weinheim, Germany.

von Mises, R. (1928) *Mechanik der plastischen formänderung von kristallen*. Zeitschrift für angewandte Mathematik und Mechanik, 8, pp. 161-185.

Wu, H. C and Teng, J. (2002) *Innovative Cement Based Thin Sheet Composites for Retrofit*. In CD third International Conference on Composites in Infrastructures, ed. San Francisco, CA, June 2002.

Wu, H.C. (2004) *Design Flexibility of Composites for Construction*. In International Conference on Fiber Composites, High Performance Concretes and Smart Materials, ed. V.S. Parameswaran, Chennai, India, pp. 421-432.

Wu, H. C and Sun, P. (2005) *Fiber Reinforced Cement Based Composite Sheets for Structural Retrofit*. BBFS 2005 - In International Symposium on Bond Behavior of FRP in Structures, ed. J.F. Chen and J.G. Teng, Hong Kong, 7-9 December, pp. 351-356.

DOCTORAL AND LICENTIATE THESES**DIVISION OF STRUCTURAL ENGINEERING
LULEÅ UNIVERSITY OF TECHNOLOGY****Doctoral Theses**

(Some are downloadable from: <http://epubl.ltu.se/1402-1544/index.shtml>)

- 1980 Ulf Arne Girhammar: *Dynamic Fail-Safe Behaviour of Steel Structures*. Doctoral Thesis 1980:060D. pp. 309.
- 1983 Kent Gylltoft: *Fracture Mechanics Models for Fatigue in concrete Structures*. Doctoral Thesis 1983:25D. pp. 210.
- 1985 Thomas Olofsson: *Mathematical Modelling of Jointed Rock Masses*. In collaboration with the Division of Rock Mechanics. Doctoral Thesis 1985:42D. pp. 143.
- 1988 Lennart Fransson: *Thermal ice pressure on structures in ice covers*. Doctoral Thesis 1988:67D. pp. 161.
- 1989 Mats Emborg: *Thermal stresses in concrete structures at early ages*. Doctoral Thesis 1989:73D. pp. 285.
- 1993 Lars Stehn: *Tensile fracture of ice. Test methods and fracture mechanics analysis*. Doctoral Thesis 1993:129D, September 1993. pp. 136.
- 1994 Björn Täljsten: *Plate Bonding. Strengthening of existing concrete structures with epoxy bonded plates of steel or fibre reinforced plastics*. Doctoral Thesis 1994:152D, August 1994. pp. 283.
- 1994 Jan-Erik Jonasson: *Modelling of temperature, moisture and stresses in young concrete*. Doctoral Thesis 1994:153D, August 1994. pp. 227.
- 1995 Ulf Ohlsson: *Fracture Mechanics Analysis of Concrete Structures*. Doctoral Thesis 1995:179D, December 1995. pp. 98.

-
- 1998 Keivan Noghabai: *Effect of Tension Softening on the Performance of Concrete Structures*. Doctoral Thesis 1998:21, August 1998. pp. 150.
- 1999 Gustaf Westman: *Concrete Creep and Thermal Stresses. New creep models and their effects on stress development*. Doctoral Thesis 1999:10, May 1999. pp. 301.
- 1999 Henrik Gabrielsson: *Ductility in High Performance Concrete Structures. An experimental investigation and a theoretical study of prestressed hollow core slabs and prestressed cylindrical pole elements*. Doctoral Thesis 1999:15, May 1999. pp. 283.
- 2000 Patrik Groth: *Fibre Reinforced Concrete - Fracture Mechanics Methods Applied on Self-Compacting Concrete and Energetically Modified Binders*. Doctoral Thesis 2000:04, January 2000. pp. 214. ISBN 978-91-85685-00-4.
- 2000 Hans Hedlund: *Hardening concrete. Measurements and evaluation of non-elastic deformation and associated restraint stresses*. Doctoral Thesis 2000:25, December 2000. pp. 394. ISBN 91-89580-00-1.
- 2003 Anders Carolin: *Carbon Fibre Reinforced Polymers for Strengthening of Structural Members*. Doctoral Thesis 2003:18, June 2003. pp. 190. ISBN 91-89580-04-4.
- 2003 Martin Nilsson: *Restraint Factors and Partial Coefficients for Crack Risk Analyses of Early Age Concrete Structures*. Doctoral Thesis 2003:19, June 2003. pp. 170. ISBN: 91-89580-05-2.
- 2003 Mårten Larson: *Thermal Crack Estimation in Early Age Concrete – Models and Methods for Practical Application*. Doctoral Thesis 2003:20, June 2003. pp. 190. ISBN 91-86580-06-0.
- 2005 Erik Nordström: *Durability of Sprayed Concrete. Steel fibre corrosion in cracks*. Doctoral Thesis 2005:02, January 2005. pp. 151. ISBN 978-91-85685-01-1.
- 2006 Rogier Jongeling: *A Process Model for Work-Flow Management in Construction. Combined use of Location-Based Scheduling and 4D CAD*. Doctoral Thesis 2006:47, October 2006. pp. 191. ISBN 978-91-85685-02-8.
- 2006 Jonas Carlswård: *Shrinkage cracking of steel fibre reinforced self compacting concrete overlays - Test methods and theoretical modelling*. Doctoral Thesis 2006:55, December 2006. pp. 250. ISBN 978-91-85685-04-2.
- 2006 Håkan Thun: *Assessment of Fatigue Resistance and Strength in Existing Concrete Structures*. Doctoral thesis 2006:65, December 2006. pp. 169. ISBN 978-91-85685-03-5.

-
- 2007 Lundqvist Joakim: *Numerical Analysis of Concrete Elements Strengthened with Carbon Fiber Reinforced Polymers*. Doctoral thesis 2007:07, March 2007. pp. 50+58. ISBN 978-91-85685-06-6.
- 2007 Arvid Hejll: *Civil Structural Health Monitoring - Strategies, Methods and Applications*. Doctoral Thesis 2007:10, March 2007. pp. 189. ISBN 978-91-85685-08-0.
- 2007 Stefan Woksepp: *Virtual reality in construction: tools, methods and processes*. Doctoral thesis 2007:49, November 2007. pp. 191. ISBN 978-91-85685-09-7.
- 2007 Romuald Rwamamara: *Planning the Healthy Construction Workplace through Risk assessment and Design Methods*. Doctoral thesis 2007:74, November 2007. pp. 179. ISBN 978-91-85685-11-0.
- 2008 Bjornar Sand: *Nonlinear finite element simulations of ice forces on offshore structure*. Doctoral thesis 2008:39, September 2008. pp. 241.
- 2008 Sofia Utsi: *Performance based concrete mix-design: aggregate and micro mortar optimization applied on self-compacting concrete containing fly ash*. Doctoral thesis 2008:49, November 2008. pp. 190. ISSN 1402-1544.
- 2009 Markus Bergström: *Assessment of Existing Concrete Bridges – Bending Stiffness as a Performance Indicator*. Doctoral thesis, March 2009. pp. 221. ISBN 978-91-86233-11-2.
- 2009 Tobias Larsson: *Fatigue assessment of riveted bridges*. Doctoral thesis, March 2009. pp. 165. ISBN 978-91-86233-13-6.
- 2009 Thomas Blanksvärd: *Strengthening of Concrete Structures by the Use of Mineral Based Composites – System and Design Models for Flexure and Shear*. Doctoral thesis, April 2009. pp. 221. ISBN 978-91-86233-23-5.

Licentiate Theses

(Some are downloadable from: <http://epubl.ltu.se/1402-1757/index.shtml>)

- 1984 Lennart Fransson: *Bärförmåga hos ett flytande istäcke. Beräkningsmodeller och experimentella studier av naturlig is och av is förstärkt med armering*. Licentiate Thesis 1984:012L. pp. 137.
- 1985 Mats Emborg: *Temperature stresses in massive concrete structures. Viscoelastic models and laboratory tests*. Licentiate Thesis 1985:011L, May 1985, rev. November 1985. pp. 163.

-
- 1987 Christer Hjalmarsson: *Effektbehov i bostadshus. Experimentell bestämning av effektbehov i små- och flerbostadshus.* Licentiate Thesis 1987:009L, October 1987. pp. 72.
- 1990 Björn Täljsten: *Förstärkning av betongkonstruktioner genom pålimning av stålplåtar.* Licentiate Thesis 1990:06L, May 1990. pp. 205.
- 1990 Ulf Ohlsson: *Fracture Mechanics Studies of Concrete Structures.* Licentiate Thesis 1990:07L, May 1990. pp. 66.
- 1990 Lars Stehn: *Fracture Toughness of sea ice. Development of a test system based on chevron notched specimens.* Licentiate Thesis 1990:11L, September 1990. pp. 88.
- 1992 Per Anders Daerga: *Some experimental fracture mechanics studies in mode I of concrete and wood.* Licentiate Thesis 1992:12L, 1ed April 1992, 2ed June 1992. pp. 81.
- 1993 Henrik Gabrielsson: *Shear capacity of beams of reinforced high performance concrete.* Licentiate Thesis 1993:21L, May 1993. pp. 109.
- 1995 Keivan Noghabai: *Splitting of concrete in the anchoring zone of deformed bars. A fracture mechanics approach to bond.* Licentiate Thesis 1995:26L, May 1995. pp. 123.
- 1995 Gustaf Westman: *Thermal cracking in high performance concrete. Viscoelastic models and laboratory tests.* Licentiate Thesis 1995:27L, May 1995. pp. 125.
- 1995 Katarina Ekerfors: *Mognadsutveckling i ung betong. Temperaturkänslighet, hållfasthet och värmeutveckling.* Licentiate Thesis 1995:34L, October 1995. pp. 137.
- 1996 Patrik Groth: *Cracking in concrete. Crack prevention with air-cooling and crack distribution with steel fibre reinforcement.* Licentiate Thesis 1996:37L, October 1996. pp. 128.
- 1996 Hans Hedlund: *Stresses in High Performance Concrete due to Temperature and Moisture Variations at Early Ages.* Licentiate Thesis 1996:38L, October 1996. pp. 240.
- 2000 Mårten Larson: *Estimation of Crack Risk in Early Age Concrete. Simplified methods for practical use.* Licentiate Thesis 2000:10, April 2000. pp. 170.
- 2000 Stig Bernander: *Progressive Landslides in Long Natural Slopes. Formation, potential extension and configuration of finished slides in strain-softening soils.* Licentiate Thesis 2000:16, May 2000. pp. 137.

-
- 2000 Martin Nilsson: *Thermal Cracking of young concrete. Partial coefficients, restraint effects and influences of casting joints*. Licentiate Thesis 2000:27, October 2000. pp. 267.
- 2000 Erik Nordström: *Steel Fibre Corrosion in Cracks. Durability of sprayed concrete*. Licentiate Thesis 2000:49, December 2000. pp. 103.
- 2001 Anders Carolin: *Strengthening of concrete structures with CFRP – Shear strengthening and full-scale applications*. Licentiate thesis 2001:01, June 2001. pp. 120. ISBN 91-89580-01-X.
- 2001 Håkan Thun: *Evaluation of concrete structures. Strength development and fatigue capacity*. Licentiate thesis 2001:25, June 2001. pp. 164. ISBN 91-89580-08-2.
- 2002 Patrice Godonue: *Preliminary Design and Analysis of Pedestrian FRP Bridge Deck*. Licentiate thesis 2002:18. pp. 203.
- 2002 Jonas Carlswård: *Steel fibre reinforced concrete toppings exposed to shrinkage and temperature deformations*. Licentiate thesis 2002:33, August 2002. pp. 112.
- 2003 Sofia Utsi: *Self-Compacting Concrete - Properties of fresh and hardening concrete for civil engineering applications*. Licentiate thesis 2003:19, June 2003. pp. 185.
- 2003 Anders Rönneblad: *Product Models for Concrete Structures - Standards, Applications and Implementations*. Licentiate thesis 2003:22, June 2003. pp. 104.
- 2003 Håkan Nordin: *Strengthening of Concrete Structures with Pre-Stressed CFRP*. Licentiate Thesis 2003:25, June 2003. pp. 125.
- 2004 Arto Puurula: *Assessment of Prestressed Concrete Bridges Loaded in Combined Shear, Torsion and Bending*. Licentiate Thesis 2004:43, November 2004. pp. 212.
- 2004 Arvid Hejll: *Structural Health Monitoring of Bridges. Monitor, Assess and Retrofit*. Licentiate Thesis 2004:46, November 2004. pp. 128.
- 2005 Ola Enochsson: *CFRP Strengthening of Concrete Slabs, with and without Openings. Experiment, Analysis, Design and Field Application*. Licentiate Thesis 2005:87, November 2005. pp. 154.
- 2006 Markus Bergström: *Life Cycle Behaviour of Concrete Structures – Laboratory test and probabilistic evaluation*. Licentiate Thesis 2006:59, December 2006. pp. 173. ISBN 978-91-85685-05-9.

-
- 2007 Thomas Blanksvärd: *Strengthening of Concrete Structures by Mineral Based Composites*. Licentiate Thesis 2007:15, March 2007. pp. 300. ISBN 978-91-85685-07-3.
- 2007 Alann André: *Strengthening of Timber Structures with Flax Fibres*. Licentiate Thesis 2007:61, November 2007. pp. 154. ISBN 978-91-85685-10-3.
- 2008 Peter Simonsson: *Industrial bridge construction with cast in place concrete: New production methods and lean construction philosophies*. Licentiate thesis 2008:17, May 2008. pp. 164. ISBN 978-91-85685-12-7.
- 2008 Anders Stenlund: *Load carrying capacity of bridges: three case studies of bridges in northern Sweden where probabilistic methods have been used to study effects of monitoring and strengthening*. Licentiate thesis 2008:18, May 2008. pp. 306. ISBN 978-91-85685-13-4.
- 2008 Anders Bennitz: *Mechanical Anchorage of Prestressed CFRP Tendons*. Licentiate thesis 2008:32, September 2008. pp. 293. ISSN 1402-1757.
- 2008 Gabriel Sas: *Shear strengthening of RC beams and walls*. Licentiate thesis 2008:39, December 2008. pp. 202. ISSN 1402-1757.

PAPER I

“Mineral-Based Bonding of Carbon FRP
to Strengthen Concrete structures”

BY

Björn Täljsten and Thomas Blanksvärd

Published in

Journal of Composites for Construction, Vol. 11, No. 2, April 1, 2007

Mineral-Based Bonding of Carbon FRP to Strengthen Concrete Structures

Björn Täljsten¹ and Thomas Blanksvärd²

Abstract: The advantages of fiber-reinforced polymer (FRP)-strengthening have been shown time and again during the last decade. Several thousand structures retrofitted with FRPs exist worldwide. There are various reasons why the retrofit is needed, but it is not uncommon for the demands on the structure to change with time, as buildings and civil structures usually have a very long life. The structures may have to eventually carry larger loads or fulfill new standards. In extreme cases, a structure may need repair due to an accident or to errors made during the design or construction phases, and must therefore be strengthened before it can be used. Different methods to retrofit with FRPs also exist, such as bonding of plates or sheets, with their use of epoxy as the bonding agent being the commonality. Epoxy provides very good bond to concrete and is durable and resistant to most environments in the building industry. However, epoxy may also create problems in the working environment, needs a minimum application temperature, and creates diffusion-closed surfaces. These drawbacks can be overcome if the epoxy can be replaced with a cementitious bonding agent. In this paper tests are presented where the epoxy has been replaced with a cement based bonding agent for retrofitting. Pilot tests show that very good composite action can be achieved and that only minor changes in the design procedure need to be taken.

DOI: 10.1061/(ASCE)1090-0268(2007)11:2(120)

CE Database subject headings: Concrete structures; Composite materials; Fiber reinforced polymers; Grid systems; Mortars.

Introduction

Background

There is a critical need to restore civil engineering infrastructures worldwide, in particular related to transportation because of age, deterioration, misuse of facilities, lack of regular repair and maintenance, and the use of inappropriate materials, construction techniques or both. There can also be a need due to the increased and changing loads on the structure. Technical innovations in the construction industry have progressed in recent years. The research and development of high performance and multifunctional construction materials have been improved to satisfy the need from industry and advanced technologies have been introduced to upgrade existing structures. Upgrading is here defined as the improvement of a structure's performance level, which can be divided into load carrying capacity, function, durability, or aesthetics. The following methods may apply to upgrade a structure, i.e., refined design and calculation methods, strengthening, replacement of structural parts, improvement of the durability, aesthetics or both by different methods, materials, and systems.

This paper focuses on strengthening. The anticipated design life of steel reinforced concrete structures is frequently shortened due to the altering load situation on the structure or the deterioration of the concrete structure, such as corrosion in steel reinforcement. In producing new concrete structures, numerous techniques to protect steel from corroding have been developed. Some examples include providing steel bars with a protective epoxy coating, decreasing the concrete porosity, increasing the requirements of the reinforcement cover, and cathode protection. These methods are more successful in suppressing or postponing the corrosion process than eliminating it (Yost et al. 2001). During the last decade, fiber reinforced polymers (FRPs) have been introduced into the building arena, with their main advantages being that they possess several physical properties of interest, viz. high tensile strength and high elastic modulus yet low weight. In addition, they do not corrode and are anticipated to have a longer life in a concrete structure than an ordinary steel reinforcement.

FRPs are today used for various applications, such as reinforcement in RC and PC structures, stay cables, and newly built structures. However, the most extensive application is by far in the repair and strengthening of existing structures. This strengthening technique may be defined as one in which composite sheets or plates of relatively small thicknesses are bonded, in most cases, to a concrete structure with an epoxy adhesive to improve its structural behavior and strength. The sheets or plates do not require much space and give a composite action between the adherents. The adhesive used to bond the fabric or laminate to the concrete surface is normally a two-component epoxy adhesive. The old structure and the newly adhered material create a new structural element with a higher strength and stiffness than the original. A critical parameter when strengthening an existing structure is the choice of bonding material between the FRP and concrete surface.

The use of epoxy as a bonding medium for the adherent has

¹Professor, Division of Structural Engineering, Luleå Univ. of Technology, 971 87 Luleå, Sweden; and, Division of Structural Engineering, Technical Univ. of Denmark, DTU-Building 116, Brovej, DK-2800 Kgs. Lyngby, Denmark. E-mail: bt@byg.dtu.dk

²MSc, Ph.D. Student, Division of Structural Engineering, Luleå Univ. of Technology, 971 87 Luleå, Sweden. E-mail: thomas.blanksvard@ltu.se

Note. Discussion open until September 1, 2007. Separate discussions must be submitted for individual papers. To extend the closing date by one month, a written request must be filed with the ASCE Managing Editor. The manuscript for this paper was submitted for review and possible publication on September 21, 2005; approved on July 5, 2006. This paper is part of the *Journal of Composites for Construction*, Vol. 11, No. 2, April 1, 2007. ©ASCE, ISSN 1090-0268/2007/2-120-128/\$25.00.

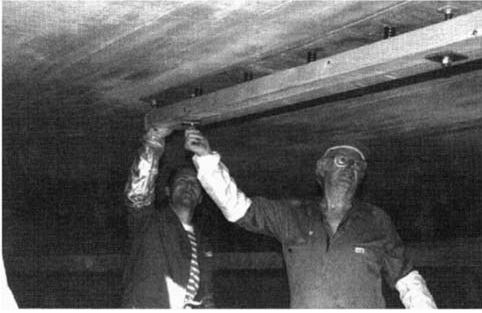


Fig. 1. Strengthening of a concrete bridge with steel plates—carried out in Sweden during the mid-1990s

proven to give excellent force transfer. Not only does epoxy bond to concrete, steel, and composites, it has also shown to be durable and resistant to most environments (Fukuyama and Sugano 2000; Nordin 2003). However, certain drawbacks can be identified when epoxy is used for plate bonding. Epoxy as a bonding agent may create problems in the work environment, it should have a minimum application temperature, often 10°C, and it creates sealed surfaces (diffusion-closed) that may imply freeze/thaw problems for concrete structures. In addition to this, high temperatures might cause problems to cold cured adhesives mostly used for FRP strengthening (Badanoiu and Holmgren 2003). To avoid some of these problems, the use of mineral-based composite (MBC) systems consisting of FRPs and a cementitious bonding agent is suggested. Upgrading civil structures with MBCs gives a more compatible repair or strengthening system with the base concrete. Applications and research in this field are limited; hence, this paper presents a unique pilot study where concrete slabs and small-scale concrete beams have been strengthened with carbon fiber-reinforced polymer (CFRP) grids and cementitious bonding agents.

History

Steel plates were initially used for plate bonding to strengthen concrete structural members. The method of strengthening existing concrete structures with the use of epoxy adhesives originated in the 1960s in France (L'Hermite 1967; Bresson 1971a,b), where tests on concrete beams with epoxy bonded steel plates were conducted. The use of this strengthening method was also reported in South Africa in 1964 (Dussek 1974). Since then, the application of epoxy bonded steel plates has been used to strengthen bridges and buildings in several countries, such as Switzerland (Ladner and Flueler 1974; Fässler and Derendinger 1980), the former Soviet Union (Steinberg 1973), the United Kingdom (Swamy and Jones 1980), Australia (Palmer 1979), the United States (Klaiber et al. 1987), Japan (Raithby 1980), and Sweden (Täljsten 1990), just to mention a few. Even though this method was widely used, it was not considered very successful because drawbacks such as corrosion, the need for overlap joints, the heavy working loads during installation, and the need for pressure on the adhesive during hardening could not be overcome. In 1995, one of the last applications to strengthen bridges with steel plates was carried out in Sweden where the steel plates were mounted onto a bridge, Fig. 1. This project was considered successful, but the disadvan-

tage of the technique still remained, viz. heavy plates, need for overlap plates, bolting, and bonding pressure during curing of the adhesive. An inspection of the bridge 8 years after strengthening showed no corrosion or degradation of the strengthening system.

The plate bonding method has gone through a revival in the last decade mainly because of the increased need to retrofit existing structures. However, another very important factor is the introduction of advanced composites to the civil engineering arena. Fiber composites and reinforced polymers offer unique advantages in applications where conventional materials cannot supply a satisfactory service life (Agarwal and Broutman 1990). The high strength to weight ratio and the excellent resistance to electrochemical corrosion of composites make them attractive materials for structural applications. In addition, composites are formable and can be shaped to almost any desired form and surface texture. An interesting application of the currently available advanced composite materials is the retrofitting of damaged or structurally inadequate buildings and bridges. In Switzerland, (Meier 1987) one of the first applications to use CFRP was executed at the end of the 1980s, and since then, several thousand applications have been carried out worldwide.

The great potential and considerable economic advantages in FRP strengthening clearly exist. However, if the technique is to be used effectively, a sound understanding of both the short- and long-term behaviors of the bonding system is required, as well as reliable information concerning the adhesion to concrete and composite. Of great importance is the execution of bonding work to achieve a composite action between the adherents, and to know the practical limits of any proposed strengthening method.

At Luleå University of Technology in Sweden, research has been conducted in the area of plate bonding. Beginning in 1988, this research is now continuing with FRP materials. Both comprehensive experimental work and theoretical work have been carried out. Laboratory tests have included strengthening for shear (Täljsten 2001), torsion (Täljsten 1998), and bending. Full-scale tests on strengthened bridges were also performed (Täljsten 1994; Täljsten and Carolin 1999; Täljsten 2000). In particular, the theory behind the development of peeling stresses in the adhesive layer at the end of the strengthening plate was studied, along with the theory of fracture mechanics to explain the nonlinear behavior in the joint (Täljsten 1994, 1996, 1997). In Sweden, FRP strengthening methods have been used in the field for almost 10 years, and both CFRP plate and sheet systems are used. Sweden is also one of the first countries in the world where a national code exists for FRP strengthening (Täljsten 2003).

Advantages and Disadvantages Using FRP in Construction

Background

Many technical solutions for structural problems and deficient concrete exist, and the final decision is always based on numerous

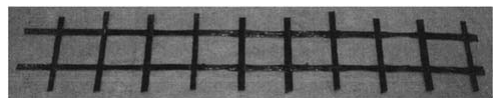


Fig. 2. CFRP grid used in Slabs 3, 4, and 6

Table 1. Data for the Reinforcement

| Reinforcement | E (GPa) | f_y (MPa) | ε (%) |
|---------------|------------------|------------------|----------------------|
| Steel | 209 ^a | 483 ^a | — |
| Fabric | 228 ^b | — | 1.50 ^b |
| Grid | 242 ^b | — | 1.43 ^b |

^aTested values.^bValues provided by the manufacturer.

factors, some of which include material cost, demand for mechanical strength and stiffness, impact resistance and resistance to vandalism, resistance against environmental effects, long-term properties such as relaxation and creep, application, and production methods. In some cases, the client may also not be familiar with the proposed solution and therefore chooses a more conventional method. Even though advanced composites have been used for retrofitting for more than a decade, many clients are still unfamiliar with the technology. All technologies contain advantages and disadvantages and CFRP retrofitting is no different. In particular some very important issues, strongly related to epoxy, that need to be given more attention are the following.

Long-term properties: Carbon fiber composites with an epoxy matrix are said to have very good long-term properties. However, since the materials have only been used in the building industry for approximately 10 years, not enough data to verify this exist. Still, the main concern is probably not the composite itself, but rather the adhesive layer. Experience from older steel plate bonding projects shows many of these structures to still be in use with no visible deterioration of the bond layer. If the right type of material is used, and the strengthening work is carried out carefully, 30 years of use should be no problem.

Working environment: Because epoxies are used to bond the plates or sheets to the structure, the working environment is very important. If these materials are not handled as prescribed, a risk for injuries to workers exists. However, with correct handling, the risk for injuries can be minimized.

Temperature and moisture dependence: The hardening process of thermosetting adhesives is moisture and temperature dependent. Therefore, it can be necessary in some environments to place heat to the structure.

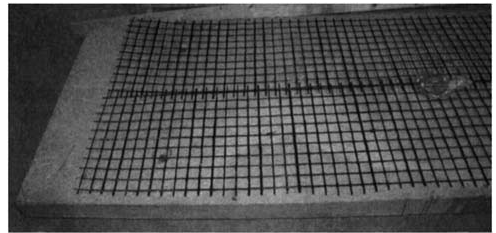
Diffusion openness: Thermosetting adhesives will seal the concrete surface. Combined with moisture and cold temperatures, this might lead to debonding due to freeze/thaw problems at the contact surface between the FRP and concrete.

One should also consider the relatively short time FRP retrofitting has been used in the construction industry. Its impact has been considerable. Not only have we obtained a new repair and strengthening method, but also introduced a totally new material to be added to steel, concrete, and wood. Its impact on the future is unknown, but probably larger than we can expect. To overcome some of the listed drawbacks with epoxy bonded FRP products, MBC bonding systems might be a part of the solution. In the following, this will be discussed in more detail.

Table 2. Material Data for the Bonding Agents

| Bonding agent | τ_a (MPa) | E_a (GPa) |
|---------------|-------------------|----------------|
| Cement based | >5.0 | 35.5 |
| Epoxy | >5.0 | 4.8 |

Note: All data presented are mean values from three tests.

**Fig. 3.** Concrete slab with the CFRP grid placed in position before applying the cementitious bonding agent

Mineral-Based Bonding Systems

Background

From several points of view, it would be very beneficial and interesting if the epoxy adhesive could be replaced with a mineral-based bonding agent, such as modified concrete. A drawback with epoxy is its toxicity; on the skin, thermosetting components can cause irritation and eczema. Inhalation of epoxy resin emissions should also be avoided. The hardeners have, as a rule, a pungent smell that can cause temporary irritation of the breathing passages.

It would also be beneficial to replace epoxy when retrofitting work is carried out in areas where the concrete needs to be diffusion open, i.e., wrapping of columns or similar applications. Low temperatures might also cause problems for thermosetting adhesives, where most formulas need at least 10°C to begin the exothermic hardening process. Here, it would be possible to apply the cement-based bonding agent at temperatures as low as 0°C, meaning that if the epoxy adhesive could be replaced with a mineral-based bonding agent, a more environmental friendly, diffusion open, and less temperature sensitive strengthening system could be obtained. However, these systems will most likely also have drawbacks. For example, plates or sheets will be complicated to bond, due to the low adhesion of the plates to the composite and the sheets due to inferior wetting of the fiber. Research with the use of short FRP fibers has been ongoing for some time now (e.g., Kesner et al. 2003; Li 1998; Rossi 1997). However, research with the use of long FRP fibers is limited. Research

**Fig. 4.** Bonding the CFRP fabric to Slab 5

Table 3. Data for Tests with Strengthened Slabs

| Slab | Reinforcement | Bond ^a | f_{cc} (MPa) | f_{ct} (MPa) | P_c (kN) | P_y (kN) | P_f (kN) |
|------|--|-------------------|-------------------|-------------------|---------------|---------------|---------------|
| 1 | — | — | 49.4 | 5.5 | 4 | 25 | 25 |
| 2 | Extra steel 4 no ϕ 8 ^a | — | 49.4 | 5.5 | 5 | 38 | 38 |
| 3 | 1 BPE NSMG 43 ^b | MBC | 49.4 | 5.5 | 4 | 32 | 35 |
| 4 | 1 BPE NSMG 43 ^b | MBC | 49.4 | 5.5 | 4 | 32 | 40 |
| 5 | BPE composite 200S ^c | Epoxy | 50.8 | 5.9 | 5 | 35 | 41 |
| 6 | 2 BPE NSMG 43 ^d | MBC | 50.8 | 5.9 | 10 | 40 | 51 |

^aExtra internal steel reinforcement.

^bOne layer of CFRP grid.

^cCFRP sheet.

^dTwo layers of CFRP grids.

studying cement overlays with textiles of carbon fabrics embedded in cement-based matrix to strengthen masonry walls has been carried out by (Kolsch 1998). The strengthening system prevents partial or complete collapse of masonry walls in the critical out-of-plane direction during a seismic event. A study to improve the bond between carbon fibers and cementitious matrices has been carried out by Badanoui (2001), where dry fiber fabrics were used. It was found that a pretreatment with silica fume and high amounts of polymers improved the bond behavior of carbon fiber to the cement, though more research in this field was also stressed. A very interesting pioneering work has been carried out

by Wiberg (2003). Large-scale tests of ordinary concrete beams strengthened with a cementitious fiber composite. The composite used was made of a polymer-modified mortar and unidirectional sheets of continuous dry carbon fibers applied by hand. Both flexural and shear strengthening were tested. From the tests, it was concluded that the method works, and that considerable strengthening effects could be achieved. In comparison with epoxy bonded carbon fiber sheets, the amount of carbon fiber needed to reach the same strengthening effect for the cementitious strengthening system was more than double. The reason for this is mainly due to problems with wetting the carbon fiber. This is also

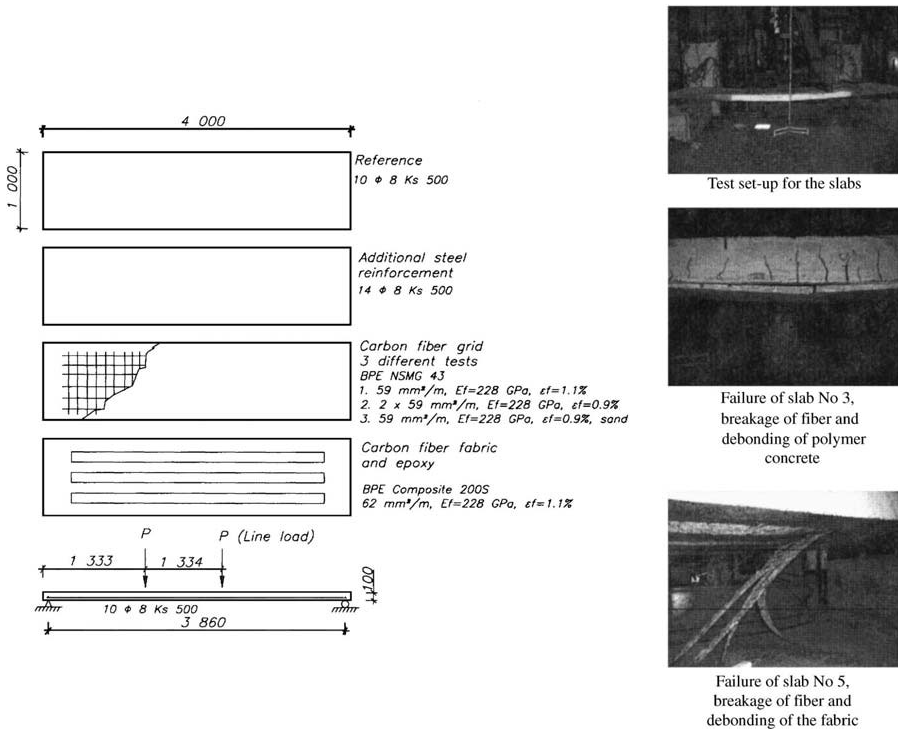


Fig. 5. Test setup for the pilot slab test

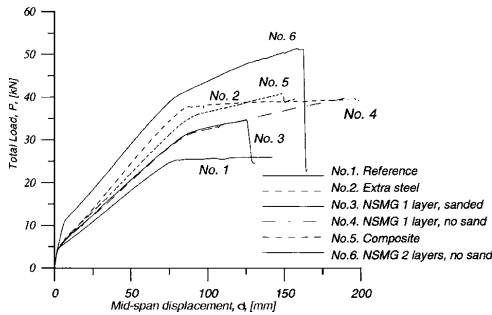


Fig. 6. Load-deflection curves for the slab pilot test

emphasized by Badanoiu and Holmgren (2003), where it was found that the load capacity of the cementitious carbon fiber composite is influenced by the amount of fibers in the tow. If the cementitious matrix can penetrate into the interior of the carbon fiber tow, a higher number of filaments will be active during loading, and thus lead to an increase in load carrying capacity.

Pilot Tests

At Luleå University of Technology, a research program is currently ongoing regarding the use of cementitious bonding agents with carbon fiber composites. In this paper, a brief description of two pilot test series carried out on strengthened concrete slabs and beams will be presented. The research focuses on the use of cementitious bonding agents as a replacement for epoxy adhesive. Compared to tests performed by earlier researchers, for example by Wiberg (2003), a different path to overcome problems with wetting the fibers was chosen. Instead of using dry fibers, a thin composite in the shape of a small rod (one dimensional), grid (two dimensional), or grid (three dimensional) is chosen. In both pilot tests, the same two-dimensional grid was chosen as reinforcement.

Testing of Slabs

The matrix for the grid in this particular case consists of epoxy; the grid is manufactured in a factory-controlled environment. The composite grid used in the test is shown in Fig. 2. In total, six slabs were tested, i.e., one reference slab, one with additional steel reinforcement, and three with carbon fiber grids. Here, one of the grids was sanded to increase the bond to the cementitious bonding agent, and for one of the tests the amount of carbon fiber

Table 5. Mechanical Properties of Concrete Cube Specimens for Beam Tests

| Specimen (slab) | Concrete batch | f_{cc} (MPa) | f_{ct} (MPa) |
|-----------------|----------------|----------------|----------------|
| 1 | 1 | 46.1 | 3.9 |
| 2 | 1 | 46.1 | 3.9 |
| 3 | 2 | 49.1 | 4.0 |
| Reference | 2 | 49.1 | 4.0 |

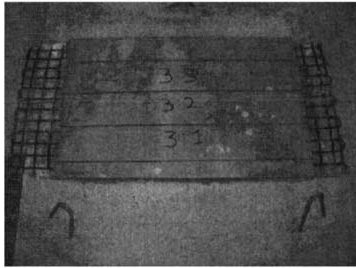
was doubled. In the last slab tested, traditional epoxy bonded carbon fiber sheets were used for strengthening. A comprehensive overview of properties for all tested slabs is recorded in Table 3. All slabs contained 10 ϕ 8Ks 500 standard steel reinforcement. Table 1 shows the material data of the carbon fiber grid and carbon fiber sheets together with the quality of the steel reinforcement. Here, E denotes the Young's modulus, f_y =yield stress for the steel, and ϵ =ultimate strain for the CFRPs. Table 2 contains the shear strength data, τ_a , for the cementitious bonding agent with the Young's modulus and the epoxy adhesive recorded with the bonding agent. The shear strength was measured by a ring torque test, see Becker (2003), and the obtained value for the epoxy adhesive is failure in the concrete substrate.

The square in the grid was 45 \times 45 mm with a cross-sectional area corresponding to 59 mm²/m in the loaded direction. The procedure for bonding the CFRP grid to the slab, Nos. 3, 4, and 6, was the following: The slab was first sand blasted and thoroughly cleaned, placed upside down to simplify the application procedure, and a thin layer of the cementitious mortar was then applied to it. The grid was then placed in position and the rest of cementitious mortar was applied. A thin plastic layer was placed over the slab to avoid early shrinkage. The cementitious bonding agent was allowed to harden in a controlled environment, +18 \pm 2 $^{\circ}$ C and 50% RH for 28 days before the slab was tested. The total thickness of the cementitious layer and the CFRP grid was approximately 8–10 mm. Fig. 3 shows the slab with the grid in position before applying the cementitious bonding agent. It should be mentioned that it would have been possible to apply the mortar upside down.

Slab 5 was strengthened with CFRP sheets and a normal bonding procedure was followed. The slab was first sandblasted, its surface cleaned properly, and a primer was applied. After the primer had hardened, a thin layer of epoxy was applied and the CFRP fabric mounted in the adhesive and a new layer of adhesive was applied. Fig. 4 shows the bonding procedure. Slab 5 was allowed to harden for 7 days in controlled environment, +18 \pm 2 $^{\circ}$ C and 50% relative humidity, prior to testing. The concrete compressive and splitting strength together with the surface strength (torque test) were measured in time for testing.

Table 4. Technical Data and Description of the Polymer Modified Mortars

| Mortar | Compressive strength | Bending tensile strength | Description |
|----------------|-------------------------------------|------------------------------------|--|
| StoCrete GM1 | 45 MPa (28 days) 35 MPa (7 days) | 9 MPa (28 days) 5 MPa (7 days) | One component, cement-based polymer and fiber reinforced powder material mixed with water |
| StoCrete TG3 | 64 MPa (28 days) | 10 MPa (28 days) | One component, cement-based polymer and glass fiber reinforced powder material mixed with water |
| StoCrete TS100 | 77 MPa (28 days) 70 MPa (7 days) | 11 MPa (28 days) 9 MPa (7 days) | One component, cement-based polymer reinforced and hydraulic hardening mortar—Can be applied with dry spraying |



Slab and beam geometry and markings prior to the sawing of the beams with the original and intact carbon fiber grid



Slab and beam geometry and markings prior to the sawing of the beams with the carbon fiber grid cut at the ends of the mortar

Fig. 7. Photos of the strengthened concrete slabs before they were sawed into beams

Table 3 illustrates the material data for the slabs. Here, f_{cc} =compressive strength and f_{ct} =splitting strength on 30 concrete cube specimens. P_c =cracking load for concrete and P_y =yield load for the slab. The failure load is denoted P_f . Additionally, Fig. 5 shows the load setup for the slabs. The distance between the supports is 3,860 mm; the distance between the support and the cut off length of the strengthening material is 140 mm.

In Fig. 5, all the slabs have the same size, though they have been strengthened by different methods. All slabs except the reference slab and Slab 6 with two CFRP grids were designed for the same failure load. Slab 2 is strengthened with 4 extra steel reinforcement bars, ϕ 8, Slabs 3 and 4 were strengthened with one single layer of CFRP grid, and for Slab 3 the grid was sanded prior to bonding, thus increasing the bond between the cementitious bonding agent and the grid. Slab 5 was strengthened by traditional epoxy bonded sheets. The cross-sectional area of the sheet is $62 \text{ mm}^2/\text{m}$. The last slab, Slab 6, was strengthened with two layers of CFRP grid.

The slabs were loaded with two line loads up to failure and the loading was deformation controlled with a load rate of 0.03 mm/s . This rate was doubled when the steel in the slab reached yielding. The load-deflection curves from the test are recorded in Fig. 6, where the total load is plotted as a function of the middeflection. In Fig. 6, note that the slab with the highest reinforcement content, i.e., Slab 6 with two layers of carbon fiber grid, sustained the highest load at failure. Slabs 2–5 were all designed for approximately the same flexural failure load. Slab 3

reached failure earlier than the other slabs due to fiber breakage, which was due to the bond between the grid and the cementitious bonding agent probably being too high, resulting in high stress concentrations. As a consequence a failure arose at a crack in the cementitious bonding material. In Slab 4, debonding between the CFRP grid created a small slippage between the cementitious bonding materials. This provided for a higher load as the stress concentrations were smeared out over a short distance, i.e., discrete stress concentrations could be avoided. However, in comparison with Slab 5, where sheets had been bonded with epoxy to the slab, a less stiff behavior could be noticed for the slabs with a single carbon fiber grid. This was probably because the epoxy bonded sheet prevents early cracking of the concrete as it is placed on the surface of the slab. The same effect cannot be obtained with the CFRP grid, as the grid is placed in the cementitious bonding material. Slabs 2, 4, and 5 reached approximately the same failure load. The slab with extra steel reinforcement, Slab 2, showed stiffer behavior than Slabs 3–5. The right-hand side in Fig. 5 shows a photo of failure modes for Slabs 3 and 5. For both of these slabs, debonding occurred after fiber breakage. This was not the case for Slabs 2, 4, and 6, where extensive cracking and large deflections preceded fiber breakage. This may also be noticed in Fig. 6, where large deflections were obtained for all these slabs. In addition Slab 6 obtained the highest failure load and was also the stiffest slab of the ones tested. Also the cracking and steel yielding loads were considerably higher for Slab 6 compared to the other slabs.

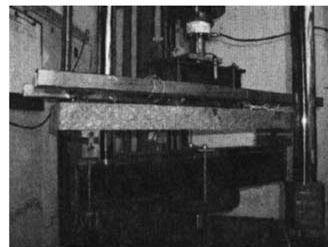
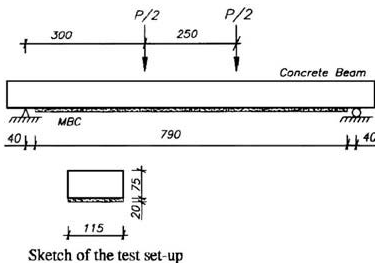


Fig. 8. Test setup in four-point bending

Table 6. Failure Load of the Evaluated Concrete Beams as an Average from Three Beams

| Beam (average from three beams) | F_{avr} (kN) | δ_{avr} (mm) |
|------------------------------------|-------------------|------------------------|
| Reference | 3.1 | 0.35 |
| TG3 beam | 7.8 | 12.7 |
| GM1 beam | 8.3 | 12.4 |
| TS100 beam | 8.4 | 14.6 |

Testing of Small-Scale Beams

This section presents a pilot study carried out at Luleå University of Technology where beams were strengthened with three different MBC systems. The main purpose with the test series was to investigate the bond and strengthening effect from the different used mortars. First, four concrete slabs were cast, three of which were slabs strengthened with a CFRP grid, the same type of grid presented in the previous pilot test. Here, three different cementitious bonding agents consisting of different types of commercially available polymer modified mortars were used and are described in Table 4.

The unstrengthened concrete slab acts as a reference to the strengthened specimens. Prior to the strength tests three beams were sawed out from the four different concrete slabs and then subjected to four-point beam bending. The base concrete in the slabs was cast as unreinforced slabs with a length and width of 1,000 mm and a thickness of 75 mm. The concrete slabs were cast in two different batches with two slabs in each set. Six concrete cubes for each batch were cast to evaluate the compressive and tensile strength of the concrete mixture for the different slabs. The motivation using slabs that then were sawed in smaller test beams was mainly that we wanted to minimize the effect of different concrete qualities. Mechanical properties of the concrete are shown in Table 5. The mortar systems also consist of a primer, StoCrete TH, whose purpose is to enhance the bond between the base concrete and the polymer modified mortars. This primer prevents moist transportation from the wet mortar to the dry base concrete, leading to lesser crack formations and improved bonding (Xiong et al. 2002).

In the test, the concrete slabs were cast and hardened for 7–9 days. The concrete surface was then sandblasted to remove the cement laitance for improved bonding between the base concrete and the polymer modified mortars (Naderi 2005). The concrete slabs had hardened for 11–13 days prior to the application of the

polymer modified mortars. The base concrete surface was the primed and the mortar and the CFRP grid were finally applied to the slabs. The photos in Fig. 7 show the strengthened concrete slabs, where the strengthened area just covers a part of the slab. The average bond length of the mortar was 790 mm, and the width and height of the beams sawn out from the slabs were 115 × 75 mm. The average thickness of the polymer modified mortar was 20 mm, with the CFRP grid placed in the center. The concrete and polymer modified mortar was then allowed to harden for 7 days prior to testing.

From each slab three beams were sawed out to obtain the geometry shown in Fig. 8, where the test setup also is recorded. Each beam was exposed to four-point bending tests. The distance between the two line loads was chosen smaller than the distance to the supports to minimize large-scale shear failure and end-peeling at the cut-off point of the strengthening material.

The midpoint deflection was measured with two LVDT gauges located on each side of the test beam. The presented deflections in the results are mean values of these two deflections. Since a smooth deflection of the strengthened beam was desired the deformation rate was controlled by the midpoint deflection of the beam and an average deformation rate was chosen to 0.02 mm/s. Table 6 presents the failure loads and the deflections for all the beams recorded. A typical failure for the test beams is shown in Fig. 9, where the polymer concrete was debonded from the CFRP grid at the time of fiber breakage. Up to this level the load transfer and the composite action was very high. Fig. 10 shows the load-deflection curves. It is quite clear from the load-deflection curves that the unreinforced reference beams did not provide any significant load carrying capacity. All strengthened beams increased the load carrying capacity considerably. The load-deflection curves look very similar among the three different MBC systems used. The beams initially reach the cracking load, the CFRP grid then becomes active, the next peak is due to slippage between the grid and the polymer mortar and this behavior proceeds up to failure, which was usually a combination of shear failure in the beams and breakage of the fiber grid. The failure was quite brittle for all beams tested, since no shear reinforcement was used for the small pilot beams. It might also be expected that there exists a size effect regarding the strengthening improvements and type of failure. However, this is beyond the scope of this study, and will be investigated in future research.

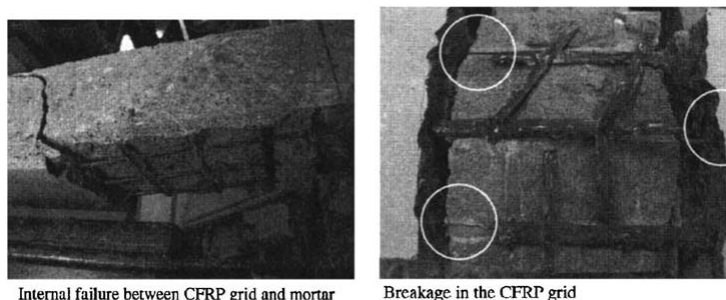


Fig. 9. Typical failure for the tested small-scale beams

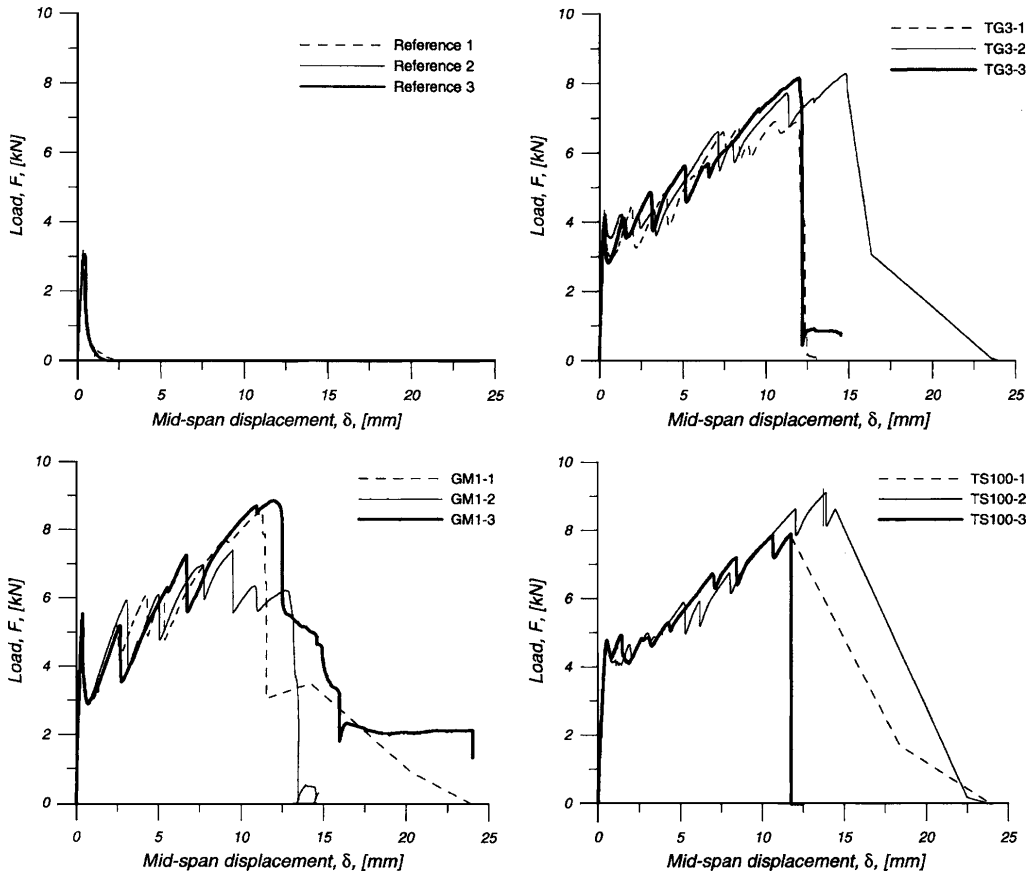


Fig. 10. Load-deflection curves for the tested small-scale beams

Conclusions

In this paper the use of cementitious bonding agents with advanced composite materials is discussed, and a new acronym is introduced MBC (mineral-based composites). Two pilot tests are presented and as seen from the results, the slabs strengthened with CFRP grids and bonded to concrete with a cementitious bonding agent are comparable to a slab strengthened with epoxy bonded carbon fiber fabrics and a slab with increased steel reinforcement. The failure mode for the slab strengthened with sanded CFRP grid and epoxy bonded fabric was quite brittle, whereas the failure mode for the other slabs was more ductile. In addition, the tested small-scale beams obtained a high strengthening effect and from the tests the stiffest mortar used gave the best strengthening effect. The tests were considered promising and are now being followed up with more comprehensive research at Luleå University of Technology in collaboration with Denmark Technical University, where larger beam structures are strengthened and studied both analytically and in laboratory tests.

Acknowledgments

The research presented in this paper has been funded by several organizations. Here the Swedish National Road Administration, the Development Fund of the Swedish Construction Industry, Skanska AB, and Sto Scandinavia shall be acknowledged.

Notation

The following symbols are used in this paper:

- E = Young's modulus (modulus of elasticity);
- E_a = Young's modulus for the bonding agent;
- F_{avr} = average failure load for small-scale concrete beams;
- f_{cc} = concrete uniaxial compressive strength;
- f_{cr} = concrete splitting (uniaxial tensile) strength;
- f_y = yielding stress for steel;
- P_c = crack load for concrete;
- P_f = failure load for concrete slab;

- P_y = yield load for concrete slab;
 δ_{avr} = average midpoint deflection for small-scale concrete beams;
 ε = ultimate strain for CFRP; and
 τ_a = shear strength for bonding agents.

References

- Agarwal, B. D., and Broutman, L. J. (1990). *Analysis and performance of fibre composites*, Wiley, New York.
- Badanoiu, A. (2001). "Improvement of the bond between carbon fibres and cementitious matrices." *Technical Rep No. 2001:1*, Concrete Structures, Dept. of Structural Engineering, Royal Institute of Technology, Stockholm, Sweden.
- Badanoiu, A., and Holmgren, J. (2003). "Cementitious composites reinforced with continuous carbon fibres for strengthening of concrete structures." *Cem. Concr. Compos.*, 25(3), 387–394.
- Becker, D. (2003). "Betongplattor förstärkta med kolfiberkomposit—En experimentell och teoretisk analys." Master's thesis, Dept. of Civil and Mining Engineering, Division of Structural Engineering, Luleå Univ. of Technology, Luleå, Sweden (in Swedish).
- Bresson, J. (1971a). "Nouvelles recherches et applications concernant l'utilisation des collages dans les structures." *Betong plaque, Annales de l'institut technique*, No. 278 (in French).
- Bresson, J. (1971b). "Realisation pratique d'un renforcement par collage d'armatures." *Annees de ITBTP*, 278, 50–52 (in French).
- Dussek, I. J. (1974). "Strengthening of bridge beams and similar structures by means of epoxy-resin bonded external reinforcement." *Transportation Research Record*, 785, Transportation Research Board, Washington, D.C., 21–24.
- Fässler, A., and Derendinger, P. (1980). *Die Sanierung der Gizenbrucke über die Muota*, Schweizer Ingenieur und Architekt, Sonderdruck aus heft 41/1980, 9 (in German).
- Fukuyama, H., and Sugano, S. (2000). "Japanese seismic rehabilitation of concrete building after the Hyogoken Nanbu earthquake." *Cem. Concr. Compos.*, 22(1), 59–79.
- Kesner, K. E., Billington, S. L., and Douglas, K. S. (2003). "Cyclic response of highly ductile fibre-reinforced cement-based composites." *ACI Mater. J.*, 100(5), 381–390.
- Klaiber, F. W., Dunker, K. F., Wipf, T. J., and Sanders, W. W., Jr. (1987). "Methods of strengthening existing highway bridges." Transportation Research Board, Washington, D.C.
- Kolsch, H. (1998). "Carbon fibre cement matrix (CFCM) overlay system for masonry strengthening." *J. Compos. Constr.*, 2(2), 105–109.
- Ladner, M., and Flueler, P. (1974). *Versuche an Stahlbeonbauteilen mit geklebter Armierung*, Schweizerische Bauzeitung, Heft 19, 9–16 (in German).
- L'Hermite, R. (1967). *L'application des colles et resins dans la construction*, La betong coffrage portant, Annales L'institut Technique, No. 239 (in French).
- Li, V. C. (1998). "Engineered cementations composites-tailored composites through micromechanical modelling, fibre reinforced concrete: Present and the future." *Canadian Society for Civil Engineering*, Montreal, 64–97.
- Meier, U. (1987). "Repair of bridges with high performance composite materials." *Mater. Tech. (Duebendorf, Switz.)*, 15(4), 125–128.
- Naderi, M. (2005). "Friction-transfer test for the assessment of in situ strength and adhesion of cementitious materials." *Constr. Build. Mater.*, 19(6), 454–459.
- Nordin, H. (2003). "Fibre reinforced polymers in civil engineering." Licentiate thesis 2003:25, Division of Structural Engineering, Luleå Univ. of Technology, Luleå, Sweden.
- Palmer, P. M. (1979). "Repair and maintenance of concrete bridges with particular reference to the use of epoxies." *Technical Rep. No. 14*, Main Roads Dept., Perth, Western Australia.
- Raithby, K. D. (1980). "External strengthening of concrete bridges with bonded steel plates." *Rep. No. 612*, Transportation and Road Research Laboratory, Crowthorne, Berkshire.
- Rossi, P. (1997). "High performance multimodal fibre reinforced cement composites (HPMRERCC): The LCPC experience." *ACI Mater. J.*, 94(6), 478–483.
- Steinberg, M. (1973). "Concrete polymer materials and its worldwide development." *J. Am. Concr. Inst.*, 12.
- Swamy, R. N., and Jones, R. (1980). "Technical Notes—Behaviour of plated reinforced concrete beams subjected to cyclic loading during glue hardening." *Int. J. of Cement Composites*, 2(4), 233–234.
- Täljsten, B. (1990). "Strengthening of concrete structures by adhesively bonded steel plates." Licentiate thesis 1990:06L, Luleå Univ. of Technology, Luleå, Sweden (in Swedish).
- Täljsten, B. (1994). "Plate bonding, strengthening of existing concrete structures with epoxy bonded plates of steel or fibre reinforced plastics." Doctoral thesis 1994:152D, Div. of Structural Engineering, Luleå Univ. of Technology, Luleå, Sweden.
- Täljsten, B. (1996). "Strengthening of concrete prisms using the plate-bonding technique." *Int. J. Fract.*, 82, 253–266.
- Täljsten, B. (1997). "Strengthening of beams by plate bonding." *J. Mater. Civ. Eng.*, 9(4), 206–212.
- Täljsten, B. (1998). "Förstärkning av betongkonstruktioner med stålplåt och avancerade kompositmaterial utsatta för vridning." *Research Rep. No. 1998:01*, Division of Structural Engineering, Luleå Univ. of Technology, Luleå, Sweden (in Swedish).
- Täljsten, B. (2000). "Förstärkning av befintliga betongkonstruktioner med kolfiberväv eller kolfiberlaminat, dimensionering, material och utförande." *Research Rep. No. 1999:12*, Division of Structural Engineering, Luleå Univ. of Technology, Luleå, Sweden (in Swedish).
- Täljsten, B. (2001). "Design guidelines—A Scandinavian approach." *Proc., Int. Conf. on FRP Composites in Civil Engineering*, CICE, Hong Kong, 153–164.
- Täljsten, B. (2003). *FRP strengthening of existing concrete structures. Design guideline*, 2nd Ed., Division of Structural Engineering, Luleå Univ. of Technology, Luleå, Sweden.
- Täljsten, B., and Carolin, A. (1999). "Strengthening of a concrete railway bridge in Luleå with carbon fibre reinforced polymers—CFRP: Load bearing capacity before and after strengthening." *Technical Rep. No. 1999:18*, Division of Structural Engineering, Luleå Univ. of Technology, Luleå, Sweden.
- Wiberg, A. (2003). "Strengthening of concrete beams using cementitious carbon fibre composites." Doctoral thesis, Royal Institute of Technology, Structural Engineering, Stockholm, Sweden.
- Xiong, G., Liu, J., Li, G., and Xie, H. (2002). "A way for improving interfacial transition zone between concrete substrate and repair materials." *Cem. Concr. Res.*, 32(12), 1877–1881.
- Yost, J. R., Goodspeed, C. H., and Schmeckpeper, E. R. (2001). "Flexural performance of concrete beams reinforced with FRP grids." *J. Compos. Constr.*, 5(1), 18–25.

PAPER II

“Shear Strengthening of Concrete
Structures with the Use of Mineral-Based
Composites”

BY

Thomas Blanksvärd, Björn Täljsten and Anders Carolin

Published in

Journal of Composites for Construction, Vol. 13, No. 1, February 1, 2009

Shear Strengthening of Concrete Structures with the Use of Mineral-Based Composites

Thomas Blanksvård¹; Björn Täljsten²; and Anders Carolin³

Abstract: Rehabilitation and strengthening of concrete structures have become more common during the last 10–15 years, partly due to a large stock of old structures and partly due to concrete deterioration. Also factors such as lack of understanding and the consequences of chloride attack affect the need for rehabilitation. In addition, more traffic and heavier loads lead to the need for upgrading. Existing externally bonded strengthening systems using fiber-reinforced polymers (FRP) and epoxy as bonding agents have been proven to be a good approach to repair and strengthen concrete structures. However, the use of epoxy bonding agents has some disadvantages in the form of incompatibilities with the base concrete. It is, therefore, of interest to substitute epoxy with systems that have better compatibility properties with the base concrete, for example, cementitious bonding agents. This paper presents a study on reinforced concrete beams strengthened in shear with the use of cementitious bonding agents and carbon fiber grids, denoted as mineral-based composites (MBC). In this study it is shown that the MBC system has a strengthening effect corresponding to that of strengthening systems using epoxy bonding agents and carbon fiber sheets. Different designs and material properties of the MBC system have been tested. An extensive monitoring setup has been carried out using traditional strain gauges and photometric strain measurements to obtain strains in steel reinforcement, in FRP, and strain fields on the strengthened surface. It has been shown that the use of MBC reduces strains in the steel stirrups and surface cracks even for low load steps as compared to a nonstrengthened concrete beam.

DOI: 10.1061/(ASCE)1090-0268(2009)13:1(25)

CE Database subject headings: Concrete structures; Composite materials; Fiber reinforced polymers; Grid systems; Mortars; Shear resistance.

Introduction

Concrete is a widely used building material for structures and is used in many different types of structures. Concrete is one of the oldest building materials and considerable advancements in developing concrete have progressed, in particular during the last 2 decades. Despite this, the construction industry is not renowned for research, development, and technical innovations, at least compared to such industries as car and aerospace. Nevertheless, a considerable amount of development and innovations are carried out in construction and the society is highly dependent on these innovations. For example, new systems, processes, or products that can lower the cost for maintenance, repair, and strengthening and at the same time prolong structural life, can save a considerable amount of money. Repairing and upgrading existing concrete structures is becoming more apparent due to reinforced concrete

(RC) and degradation, mistakes in the design or construction phases and changes in structural use. There are excellent methods for strengthening existing concrete structures. One such method uses fiber-reinforced polymers (FRPs) or dry fibers adhesively bonded to the concrete. The most commonly utilized FRPs are fibers made of carbon (C) or glass (G) and can be designed as laminates, bars, or sheets mounted on the surface or as near surface mounted bars in the concrete cover (Oehlers et al. 2007; Nordin 2003; Täljsten et al. 2003; Nordin and Täljsten 2006; Carolin and Täljsten 2003). Although strengthening systems using epoxy as the bonding agent have shown good results in terms of bonding and application there exist some drawbacks. These include: (1) regulations on how to handle the epoxy bonding agents, based on the risk for eczema and toxicity of the components; (2) low permeability and its diffusion tightness which, for example, can provoke freeze and thaw problems; (3) poor thermal compatibility to the base concrete, which may cause unfavourable constraints; and (4) the surface of the base concrete has to be dry and the temperature can normally not be under 10°C at the time of application.

Upgrading of civil structures with mineral-based composites gives a more compatible repair or strengthening system. In this paper mineral-based composite (MBC) is used synonymously with upgrading with FRP materials and a polymer-modified cement. Consequently, the use of polymer modified mortars should prevent some of the disadvantages with the organic resins such as epoxy. However, there are some uncertainties regarding the use of mortars as the bonding agent: (1) resistance and performance under low and high temperatures are to some extent unknown; (2) the bond in the transition zone between the base concrete and the FRP have not been very well examined, especially since the bond

¹Technology Licentiate, Division of Structural Engineering, Luleå Univ. of Technology, 971 87 Luleå, Sweden (corresponding author). E-mail: thomas.blanksvard@ltu.se

²Professor, Division of Structural Engineering, Luleå Univ. of Technology, 971 87 Luleå, Sweden; presently, Division of Structural Engineering, Technical Univ. of Denmark, DTU-Building 118, Brovej, DK-2800 Kgs. Lyngby, Denmark. E-mail: bt@byg.dtu.dk

³Lecturer, Division of Structural Engineering, Luleå Univ. of Technology, 971 87 Luleå, Sweden. E-mail: anders.carolin@ltu.se

Note. Discussion open until July 1, 2009. Separate discussions must be submitted for individual papers. The manuscript for this paper was submitted for review and possible publication on December 13, 2007; approved on June 20, 2008. This paper is part of the *Journal of Composites for Construction*, Vol. 13, No. 1, February 1, 2009. ©ASCE, ISSN 1090-0268/2009/1-25–34/\$25.00.

between the base concrete and the mortar can be influenced by the drying shrinkage; and (3) the durability regarding fatigue has not yet been tested.

The fibers utilized in combination with a cementitious bonding agent can be designed in different ways. To date, some of the most commonly used fibers are unidirectional dry fibers (Wiberg 2003), textiles in the form of meshes made from woven, knitted, or unwoven rovings of fibers in different directions (Peled et al. 1998; Peled and Bentur 2003; Triantafillou and Papanicolaou 2006; and Brückner et al. 2006), or FRPs where the fibers are assigned as a grid with two orthogonal directions (Blanksvärd 2007; Täljsten and Blanksvärd 2007; and Becker 2003). The possibilities of formability of the dry fibers and the textile meshes are higher compared to an FRP grid where the fibers are embedded into a matrix. On the other hand studies on the impregnation of the fibers in a roving with polymers (epoxy) results in a much higher bond strength compared to a cementitious bonding agent due to the low ability to penetrate the dry fiber roving (Dilthey et al. 2006; Raupach et al. 2006).

Mineral-Based Composites

The MBC system used in this research basically contains three material components: a cementitious binder, a CFRP grid, and a concrete surface primer. Generally, the surface of the base concrete needs to be roughened to remove the cement laitance and achieve a good bond between the base concrete and the mortar. Examples of roughening techniques are sandblasting or water jetting. In a laboratory environment or on smaller, defined, surfaces a hand layup method can be used to apply the MBC. This method includes prewetting the base concrete with water, where the time depends on the conditions of the base concrete and the climate conditions. This is further discussed in Carlswärd (2006). The best bond is obtained when the base concrete has just dried back from a saturated surface. Courard (2005) notes that a relative humidity (RH) of 80–90% in the transition zone gives the best bond. An excessively wet surface will result in a high local water/cement (w/c) ratio at the bond interface and a base concrete that is too dry will absorb too much moisture from the mortar. Prior to mounting the MBC system the base concrete surface has to be primed using a primer to reduce moisture transport from the wet mortar to the base concrete. The hand layup technique basically consists of the following: first, a layer of mortar is immediately applied to the primed surface; next the CFRP grid is placed on the first layer of mortar followed by an additional layer of mortar which is applied on the grid. A graphical representation of the hand layup MBC method, after sandblasting, is shown in Fig. 1. The system can also be applied by spraying.

Experimental Program

Method

The hand layup method was used for all of the evaluated specimens strengthened with the MBC system under laboratory conditions of 20°C and 60% RH. Sand blasting was used as the surface roughening technique. The general approach before the outcome of this study was to make small steps toward a better understanding of suitable materials to be used in the MBC system. In this study it was decided to investigate the strengthening effect in shear by using the MBC system. Hence, 23 concrete beams were

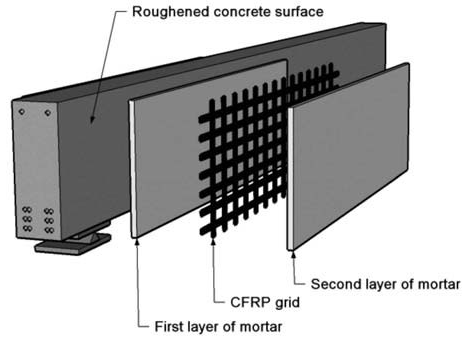


Fig. 1. Overview of MBC strengthening system

manufactured for shear strengthening purposes, comprising unstrengthened and strengthened concrete beam specimens. The varied parameters were: different mortar properties, different designs of the two-dimensional (2D) CFRP grid, different mechanical properties of the base concrete, different distances for the steel shear reinforcement, and different thicknesses of the cementitious bonding agent. To discern between the specimens, a classification scheme has been made based on the studied parameters (see Fig. 2). All beam specimens except for one, C40s0-M2-G2-t2, have a thickness of 20 mm. For comparison reasons one beam was strengthened using only mortar and no CFRP, and two beams were strengthened with epoxy bonded carbon fiber sheets. The epoxy bonded sheets were applied both vertically and horizontally along the beam axis.

Test Setup

The test setup chosen for all specimens was four-point loading. The experimental setup, geometries, and reinforcement scheme are reported in Fig. 3. To avoid local imperfections and ensure an in-plane loading, all four loading points were cast using gypsum as an intermediate layer between the concrete beam specimen and supports/loading points. The concrete beams are reinforced in shear in such a way that shear failure is directed to one half of the beam span, i.e., one span is over-reinforced. It is common for all

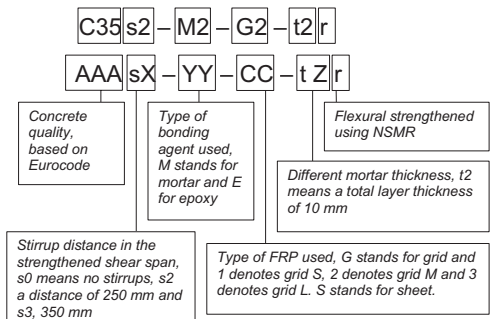


Fig. 2. Name convention for beam specimens

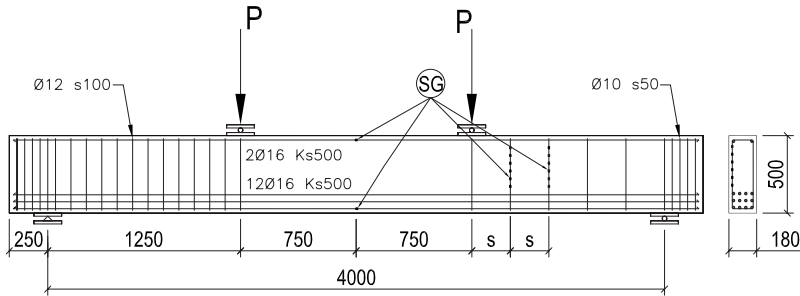


Fig. 3. Four-point beam bending test setup, geometry, and reinforcement scheme

of the concrete beams to be reinforced with 12 $\text{Ø}16$ steel bars at the bottom and two $\text{Ø}16$ at the top of the beam as tension and compression reinforcement. The shear reinforcement consists of $\text{Ø}10$ steel bars with a distance of 50 mm at the supports and $\text{Ø}12$ with the distance 100 mm in the heavily reinforced shear span. The material data are given in the next section. The densification of the shear reinforcement over the supports is to secure the anchorage of the longitudinal reinforcement. Further, the strengthened shear span of the beam specimens has three different designs of the shear reinforcement, which can be categorized as *no shear reinforcement*, stirrups with a distance $s=350$ mm, and stirrups with a distance $s=250$ mm. The first category mainly distinguishes the strengthening effects of the cementitious bonding agent and the MBC system. The other two mainly evaluate the influence of the interaction between steel shear reinforcement and the MBC strengthening system. Note that four beam specimens were also flexurally strengthened using near surface mounted reinforcement (NSMR) to increase the flexural capacity. This was necessary due to a very high shear force capacity in the strengthening beams to avoid flexural failure. In this study two CFRP bars were bonded into sawed grooves in the concrete cover (tensile side of the beams). For further information on the NSMR strengthening system the reader is referred to Nordin (2003), Täljsten et al. (2003), Nordin and Täljsten (2006), and Blanksvärd (2007).

Materials Used in Test

The primer used was a one component, cement based, and polymer reinforced powder material mixed with water. In total, three different commercially available mortars were evaluated in this study. All mortars are one component and based on cement. Their differences are mainly the different amount of polymers and reinforcing fibers. Table 1 gives an overview of all the evaluated mortars in the laboratory test, including material and mechanical

properties, mixing ratios, and grain size. The mixing ratios are given as mortar to water (m:w) in weight proportions. Tensile strength for the mortars is taken as bending tensile strength according to DIN EN 196-1 DIN EN (2005), manufacturer provided values. Both compressive and tensile strengths were taken for 28 days. Mortar 1 is a fast hardening repair and fine grain mortar. Mortars 2–3 are polymer modified and fiber reinforced with polypropylene fibers. The minimum layer thicknesses for the mortars are 3.0 mm (Mortars 1 and 2) and 6.0 mm (Mortar 3). Three different 2D CFRP grids were used to evaluate the response when incorporated in the MBC system. It is common for all of the different grids to have mechanical properties that are different in length and cross direction. The design of each CFRP grid is shown in Fig. 4. Notation for the grids is taken as Grid S, Grid M, and Grid L. S stands for a smaller distance between the tows; L has the largest distance in between the tows; and M has a tow distance in between S and L. All grids are commercially available and the manufacturer-provided mechanical and geometrical properties are reported in Table 2. It is important to distinguish the geometrical notation, length direction, and cross direction. Since the grids are delivered on a roll, the length direction is defined as the rolled direction. In Fig. 4 the length direction is placed vertically and the cross direction horizontally for all grids. The CFRP grids can be made infinitely long in the length direction, but due to manufacturing limitations, the length of the cross direction is limited to 1–2 m. The total carbon fiber amounts in the different grids are Grid S 66 g/m^2 , Grid M 159 g/m^2 , and Grid L 98 g/m^2 . For the beam specimens strengthened with carbon fiber sheets an epoxy adhesive was used with a tensile strength of 50 MPa and a modulus of elasticity of 2 GPa. The carbon fiber sheet used had a tensile strength of 3,500 MPa and a modulus of elasticity of 234 GPa. Further, the carbon fiber amount was 200 g/m^2 .

Three different concrete qualities were used for the base concrete in the beam specimens. These concrete qualities correspond

Table 1. Material and Mechanical Properties for Evaluated Mortars

| Mortar | Density (g/cm^3) | Maximum grain size (mm) | Mixing ratio (m:w) | Tensile strength ^a (MPa) | Compressive strength (MPa) | Modulus of elasticity (GPa) |
|--------|-----------------------------|-------------------------|--------------------|-------------------------------------|----------------------------|-----------------------------|
| 1 | 1.85 | 0.8 | 1:0.16 | 5.0 ^a | 22 | 18.0 |
| 2 | 1.89 | 1.0 | 1:0.16 | 9.0 ^a | 45 | 26.5 |
| 3 | 2.00 | 2.0 | 1:0.14 | 11.0 ^a | 77 | 35.0 |

^aBending tensile tests according to DIN EN 196-1.

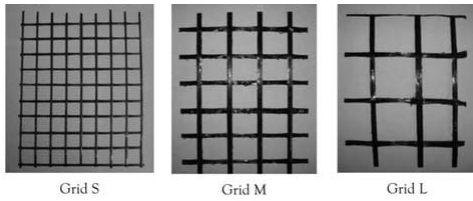


Fig. 4. Three different grids with different spacing and carbon amount for each tow direction

to C35, C40, and C55 (CEN 2004). The compressive strength for the different concrete qualities was tested on 150 mm cubes, cast at the same time as the beam specimens. The average value for the concrete compression strength was taken on 15 cubes for the respective concrete quality 48.9 MPa (C35), 55.7 MPa (C40), and 73.5 MPa (C55).

The longitudinal steel reinforcement had a yield strength of 555 MPa and a yield strain of 2.79%. The steel stirrups had a yield strength of 601 MPa and a yield strain of 2.84%. All tensile properties for the longitudinal reinforcement and the stirrups are average values based on five specimens each.

Regarding the mechanical properties of the CFRP bars used in the NSMR strengthening system the manufacturer values for the modulus of elasticity is 260 GPa, and for the strain at failure 0.8%.

Monitoring

A quite extensive measuring program was used to record the behavior of the beams tested. The monitoring measures included are load cells to measure the force, linear variable differential transformers (LVDT) for measuring deflections and settlements, electrical foil strain gauges (SG) for local strain measurements, and photometric strain measurement for global strain measurements. The loading was deformation controlled and the deformation rate was set to 0.01 mm/s, measured at the midpoint of the beam specimens. Note that this deformation controlled load does not imply test specimens marked with an asterisk in Table 3. These beams were load controlled at 10 kN/min. The support settlements were associated with the midpoint deflection readings in order to measure the absolute midpoint deflection of the beam specimens. Further, the midpoint deflection was measured on both sides on the beam specimens to record any out of plane rotation, and the midpoint deflections presented are taken as the mean value of these two LVDTs.

Strain Gauge Measurements

Two different types of (SGs) were used to measure strains on the CFRP grid and steel reinforcement. A gauge length of 5 mm was used (KFW-5-120-C1-11L3M2R) to measure strains on the steel reinforcement. In the case of measuring the strains on the CFRP grid the tows were quite narrow and a gauge length of 2 mm had to be used (KFWS-2N-120-C1-11L3M3R). All SGs are foil strain gauges with a waterproof coating. For the steel reinforcement, SGs were further protected against damage during handling with a protective tape wrapped around the SG and rebar. In all cases the SG wire was inserted into a plastic hose to minimize the influence of the concrete or mortar when embedded. It was common for all beam specimens to have strain readings in the compressed and tensile longitudinal steel reinforcement at the midsection of the beam. Six SGs were applied in the two stirrups closest to the load for beam specimens with shear steel reinforcement in the weakened or strengthened shear span. By applying strain gauges at these strategic points it is possible to monitor when the steel starts to yield both in real time during the loading and in the post analysis. These readings can then be compared to the crack pattern. Setup for the SG assessment is reported in Fig. 3. To compare the CFRP strain to the strain in the steel stirrups assessment asimilar to the SGs mounted on the stirrups was affiliated with the CFRP grid. By having SGs on the steel stirrups, CFRP, and use of photometric strain measurement (see below) it is possible to compare strains in the steel stirrups (internal concrete) to strains in vertical CFRP tows (internal MBC) as well as strain fields obtained by the photometric strain measurements. However, due to the design of the CFRP grid it was not possible to mount the SGs at exactly the same position as the steel reinforcement SGs. After casting the concrete beam specimens the steel stirrups were located using a metal detector and the SGs were mounted onto the nearest vertical CFRP tow corresponding to the stirrup with SGs applied. The first SG on the stirrup was applied 170 mm from the bottom of the beam, just above the tensile reinforcement, and the internal distance between the SGs were then 50 mm (see also Fig. 3).

A different method of mounting the SGs on the CFRP grid was also conducted for Specimen C40s0-M2-G2b, (see Table 3). This SG setup is reported in Fig. 5 and the strain gauges were applied on an assumed shear crack alignment of 30°. The SGs have been applied in pairs on both vertical (cross) and longitudinal (length) CFRP tows. These measurements can then be compared to the photometric strain measurements.

Photometric Strain Measurements

Traditional strain measurements using electrical foil strain gauges only measure local strains, while photometric strain measure-

Table 2. Manufacturer Provided Geometrical and Mechanical Properties for CFRP Grid

| Grid | Grid spacing (mm) | | Elastic modulus (GPa) | | Ultimate strength (MPa) | | Tow area (mm ²) | | t ^a (mm) |
|------|-------------------|-------|-----------------------|-------|-------------------------|-------|-----------------------------|--------|---------------------|
| | Length | Cross | Length | Cross | Length | Cross | Length | Cross | |
| S | 24 | 25 | 262 | 589 | 2,950 | 4,300 | 0.3570 | 0.2395 | 1.7 |
| M | 42 | 43 | 253 | 284 | 3,800 | 3,800 | 0.9184 | 0.9184 | 3.0 |
| L | 70 | 72 | 201 | 288 | 3,800 | 3,800 | 1.2684 | 1.0710 | 3.3 |

^aThickness of the CFRP tow.

Table 3. Test Matrix with Failure Loads and Failure Modes

| Beam | Bonding agent | CFRP | Stirrup distance | Failure load (kN) | Failure mode | Comments |
|---------------------------|---------------|-----------|------------------|-------------------|--------------|-------------------|
| C40s0 | — | — | — | 123.5 | S | Reference |
| C40s0 ^b | — | — | — | 126.7 | S | Reference |
| C40s0-M2 | Mortar 2 | — | — | 141.9 | S | Mortar |
| C40s0-M2-G2a ^c | Mortar 2 | Grid M | — | 244.9 | SR | MBC |
| C40s0-M2-G2b ^c | Mortar 2 | Grid M | — | 241.9 | SR | MBC |
| C40s0-M3-G2 | Mortar 3 | Grid M | — | 235.1 | SR | MBC |
| C40s0-E-S90 | Epoxy | Sheet 90° | — | 259.9 | SD | Epoxy, vertical |
| C40s0-E-S0 | Epoxy | Sheet 0° | — | 153.4 | S | Epoxy, horizontal |
| C40s0-M2-G1 ^b | Mortar 2 | Grid S | — | 208.1 | SR | MBC |
| C40s0-M2-G2 ^b | Mortar 2 | Grid M | — | 251.9 | SR | MBC |
| C40s0-M2-G3 ^b | Mortar 2 | Grid L | — | 206.4 | SR | MBC |
| C40s0-M1-G3 ^b | Mortar 1 | Grid L | — | 180.1 | SR | MBC |
| C35s0 | — | — | — | 130.6 | S | Reference |
| C35s3 | — | — | 350 | 346.0 | C+S | RC ^a |
| C35s3-M2-G2 | Mortar 2 | Grid M | 350 | 336.9 | C | MBC |
| C35s2-M2-G2r | Mortar 2 | Grid M | 250 | 370.5 | C | MBC+NSMR |
| C35s2-M2-G2-t2r | Mortar 2 | Grid M | 250 | 357.1 | C | MBC+NSMR |
| C55s0 | — | — | — | 158.8 | S | Reference |
| C55s3 | — | — | 350 | 318.9 | S | RC ^a |
| C55s2 | — | — | 250 | 361.4 | C | RC ^a |
| C55s2r | — | — | 250 | 399.5 | S | RC ^a |
| C55s3-M2-G2r | Mortar 2 | Grid M | 350 | 369.5 | C | MBC+NSMR |
| C55s2-M2-G2r | Mortar 2 | Grid M | 250 | 403.6 | C | MBC+NSMR |

^aReinforced concrete.

^bThe deformation rate during loading was not controlled, load controlled at 10 kN/min.

^ca, b specimen with similar strengthening system, a notates that the SG setup was applied along a presumed crack.

ments can indicate the global strain behavior of a specific surface. Photometric measurement entails taking images of a specific predefined area. The images are taken prior to loading and at certain load intervals during the test. All images are then analyzed by a tailor-made software developed at Luleå University of Technology that divides the images into different sections and calculates their point of gravity. Strains are then calculated by comparing the movements between the sections, prior to loading and at chosen load steps. For the software to work properly and give adequate results the photographed area needs to be given a random pattern. In this case the strengthened area was given this pattern through the use of an epoxy adhesive to adhere white and black sand

particles (0.55:0.45) to the surface. This random pattern was applied on the opposite side of the SG monitored side of the beam, (see Fig. 5). The photographic equipment consisted of a digital camera (Canon EOS 5D) and a professional lightning set. The method is called digital speckle photography (DSP), (see also Carolin et al. 2004 and Svanbro 2004).

Results and Discussion

In Table 3 all tested beam specimens, including type of bonding agent, type of strengthening system, and failure load, are reported. The shear span load is taken as the failure load, thus the total load divided by two. Identified failure modes are (S) for shear failure in concrete, (SR) for shear failure with rupture of CFRP, (SD) for shear failure and debonding of CFRP, and (C) for compression failure at the top of the concrete beam due to yielding of the tensile reinforcement. No debonding between the base concrete and the cementitious bonding agent was noticed in this experimental program. In this paper the writers have focused on the most essential parts from the experimental results. This includes the influence of the design of the CFRP grids and mortars for the specimens with no steel shear reinforcement and the interaction between the MBC strengthening system and steel shear reinforcement. A more comprehensive and detailed presentation is accounted for in Blanksvärd (2007). Specimens C35s0, C40s0, and C55s0 were basically performed as reference beams to evaluate the shear resistance when only using concrete without shear reinforcement. Similarly to these specimens, a larger shear crack

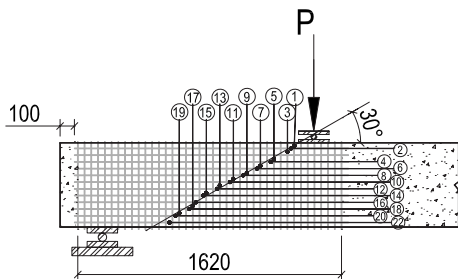


Fig. 5. SG setup for beam specimen C40s0-M2-G2a

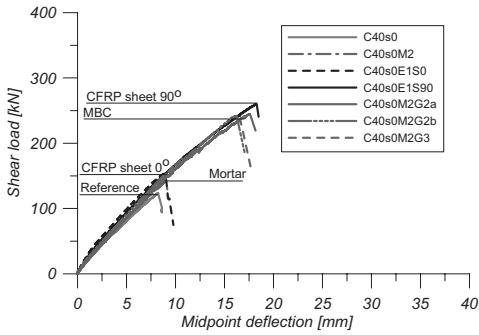


Fig. 6. Load and midpoint deflection for C40 beam specimens

arose just prior to the ultimate shear load. The failure was a typical shear crack aligned at 30–37°. Strengthening by the use of only Mortar 2 provides a 15% increase in shear bearing capacity compared to the nonstrengthened reference specimen.

The first visual shear cracks for the MBC strengthened specimens form in the center of the load span for a load higher than the reference beam and well before ultimate load. The geometry of the examined grid seems to have a small influence on the crack formation. However, using a grid with smaller tow distance (Grid S) seems to generate higher first crack load, due to a better crack redistribution. The first small visual shear crack appeared in a load range of 161–162 kN when using Grids M and L with Mortar 2. When using Grid S and Mortar 2 the first visual shear crack appears at a load above 171 kN. Using the mortar with the lowest mechanical properties (Mortar 1) in the MBC strengthening system leads to premature crack formations and lower failure load. Load and displacement for beams with concrete quality C40 are reported in Fig. 6. It is common for all beams corresponding to a concrete quality of C40, strengthened with the MBC system, that the failure mode was rupture of by of the vertical CFRP tow, [see Fig. 7(a)]. The MBC strengthening system provided such a good anchor that the strength in the vertical CFRP tows was fully utilized.

The beams with steel shear reinforcement in the strengthened shear span failed in flexure (yielding of the tensile reinforcement) and concrete crushing. These sets of beams are therefore evaluated for the load steps prior to compression failure. Note that the beam specimens with steel shear reinforcement with a distance of 300 mm and no MBC strengthening failed in shear yielding of the stirrups and for Specimen C55s3 one of the stirrups ruptured.

For nonstrengthened beam specimens with stirrups in the strengthened shear span the failure mode was similar, except for Specimen C55s2. First small bending cracks were initiated at lower load steps and the first visible shear crack appeared at 185 kN—C35s3, 150 kN—C55s3, 167 kN—C55s2, and 200 kN—C55s2r. As the loading proceeded the shear cracks increased in number and size. Note that the failure mode altered from crushing of the concrete in the compression zone for Specimen C55s2 to a shear failure for Specimen C55s2r which was strengthened in flexure with NSMR.

The failure mode for all of the MBC strengthened specimens with steel shear reinforcement in the strengthened shear span was similar with the ultimate failure mode of crushing the concrete in the compression zone. Reinforced concrete beams with a concrete corresponding to a quality of C55 have higher failure loads com-

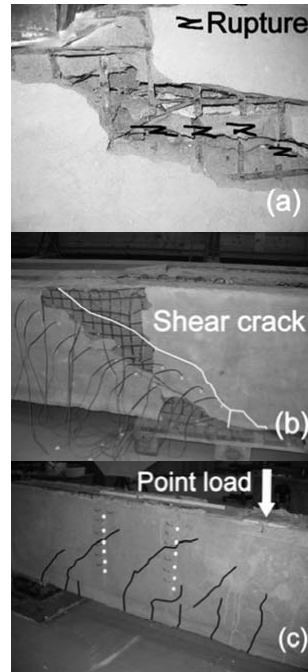


Fig. 7. Ultimate shear failures: (a) rupture of vertical CFRP tows; (b) ultimate shear crack and SGs; and (c) crack formations in strengthened shear span for specimen K30s3-M2-G2

pared to similar beams with a concrete quality corresponding to C35 (see Table 3). The interaction between the MBC strengthening system and the use of steel shear reinforcement is best visualized by the strain distribution using the results from both traditional SGs and from the photometric measurement (DSP).

Strain Gauge Measurements

Strain gauges mounted on the CFRP grid in the MBC strengthening system on beam Specimen C40s0-M2-G2b are reported in Fig. 5. Odd numbers represent strain gauges applied on vertical tows and even numbers represent strain gauges on horizontal tows. Strains along the presumed shear crack are reported in Fig. 8 for the vertical tows at three different load steps. The measured strains along the presumed shear crack of 30° are not evenly distributed but have local maxima and minimums. However, the highest strains are measured in the middle region along the measured line. Theoretically the strain distribution in the vertical direction should have a more parabolic behavior with the maximum strain in the center region of the beam or linearly increasing toward the bottom of the beam (Carolin 2003, Teng et al. 2006; and Monti and Liotta 2007). Note that the strain gauge line missed the ultimate shear crack but the strain gauges mounted near the bottom of the beam were close to the ultimate shear crack [see Fig. 7(b)]. The maximum vertical strain is approximately 5% which is far from the ultimate strain of the vertical CFRP tow. Strain readings from both the horizontal and vertical tows indicate that

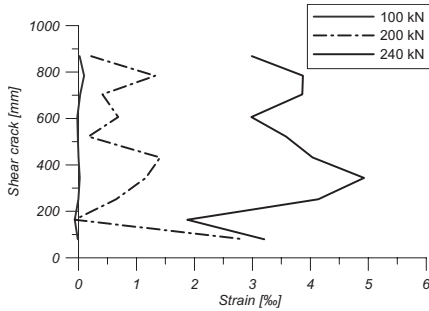


Fig. 8. Vertical strains measured at different load steps along presumed shear crack

the grid is not carrying high strain in the early stage of loading. However, a fast increase takes place in the final stage of loading, in agreement with the formation of cracks.

A comparison of the strains in the stirrup located at $2s = 700$ mm for both beam specimens with and without MBC strengthening is reported in Figs. 9(a and b) for the beam specimens with 350 mm between the stirrups and concrete quality C35. It is common for all strains to have low values monitored for load steps (<100 kN) prior to the failure load of Specimen C35s0 without stirrups. This specimen acts as a reference to the concrete contribution to the shear resistance. It is clear that the strains in the stirrups for the specimens with MBC strengthening have lower strains at the same load steps compared to nonstrengthened specimens. Based on the strain levels in Figs. 9(a and b) it should be noted hand to state that the MBC strengthening system reduces the strain levels in the stirrups even for lower load steps, for

example, 200 kN. Strains measured at a load level of 325 kN indicate that the monitored stirrup for the beam specimen without strengthening yield at discrete points. A comparison between the strains in the stirrups and in the vertical CFRP tows at approximately the same location is reported in Figs. 9(b and d). The strains in the vertical CFRP tows have locally higher strains for the first load steps, up to a shear load of 300 kN. For strain gauges applied at 668 mm from the load point origin, crack formations are noted as a high increase in local strain at a height in the beam of 300–350 mm, [see Fig. 9(d)]. Note that the shear crack has propagated crossing SGs on the vertical CFRP tows in the region of the locally high strains, [see Fig. 7(c)]. This high local strain reached beyond 15% prior to the failure load. This strain is higher than the ultimate strain of the vertical tow. Such strain levels indicate fiber rupture, but no visible proof of such an occurrence was evident during testing. Further, these locally high strains close to the formation of cracks also indicate a good bond between the CFRP grid and the mortar.

Specimens with an internal stirrup distance of 250 mm have significantly smaller strains in the stirrups than specimens with 350 mm stirrup distance, due to the increased reinforcement ratio. When comparing the strains in the stirrups between the specimens with a thinner layer of cementitious bonding agent to a specimen with thicker bonding layer no significant variations are noted. Measured strains in the stirrups indicate a fairly parabolic distribution in the stirrups.

Photometric Measurements

Using photometric strain monitoring provides an excellent overview of the global strain distribution for the monitored area. With photometric strain monitoring it is possible to measure crack formations and the strain field distribution. Fig. 10 shows the monitored principal strains at different load steps for an examined area

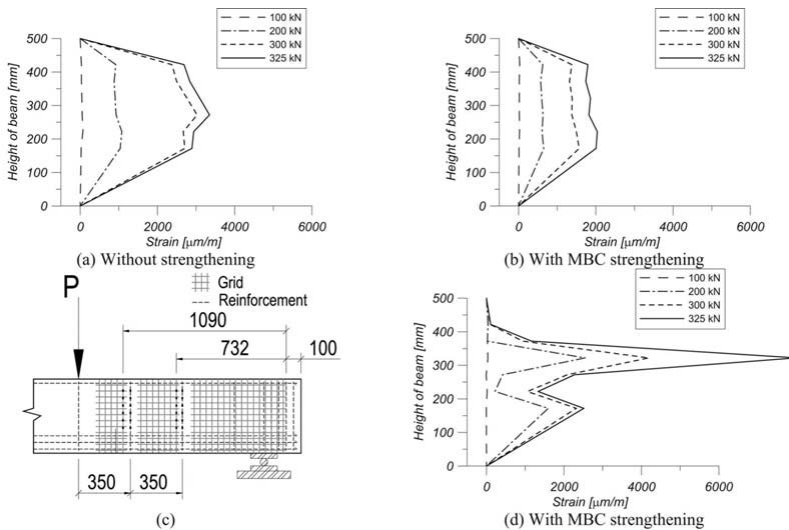


Fig. 9. Strains in stirrup at $2s = 700$ mm for specimen: (a) C35s3; (b) C35s3-M2-G2; (c) SG setup; and (d) strains in vertical CFRP tow at 668 mm from point load

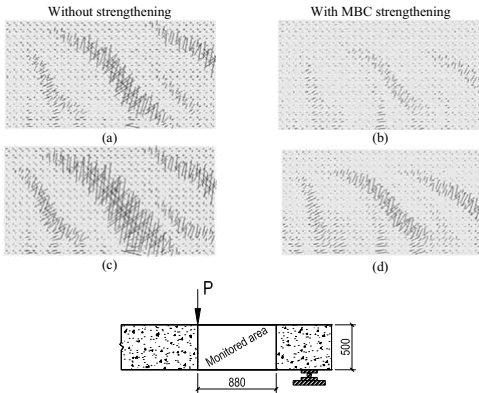


Fig. 10. Photometric strain measurements, principal strains: (a) K30s3 at 200 kN; (b) K30s3-M2-G2 at 200 kN; (c) K30s3 at 260 kN; and (d) K30s3-M2-G2 at 260 kN

of 880 × 500 mm. The monitored areas are close to the line load origin for beam specimens with a stirrup distance of 350 mm and concrete quality C35 both with and without the MBC strengthening system. The load steps were taken at shear span loads of 200 and 260 kN. By comparing the specimens with and without the MBC strengthening system it is clear that the MBC system reduces the strains even for the load of 200 kN. When the load is increased the MBC system still reduces the principal strains at a load of 260 kN compared to a nonstrengthened specimen.

There were no significant differences between the strains measured at the surface of the beam specimens with different mortar thicknesses at the first load steps. However, at a load step of 300 kN the beam specimen with a thinner layer of mortar had somewhat higher principal tensile strains along the major inclined crack. All of the reported principal strains in Fig. 10 have the same scale. Only the direction and relative size are given. For values on the principal strain the reader is referred to Blanksvärd (2007).

Shear Capacity of MBC

A straightforward estimation of the shear capacity at fiber rupture failure mode is developed for the MBC strengthening system. Since no tendencies toward debonding of the MBC system were noticed in this study, the debonding failure mode is not considered in this analytical approach. Further, the analytical approach is limited to considering rectangular beam cross sections. In this study a brief introduction to the background on the analytical approach is presented. The reader is referred to Blanksvärd (2007) for a more detailed description. For the total shear bearing capacity of the concrete beam, the superpositioning principle is applied according to

$$V_{TOTAL} = V_C + V_S + V_{FRP} + V_{MBA} \quad (1)$$

The concrete contribution, V_C , and the steel shear reinforcement, V_S , contribution to the shear capacity is not dealt with in this study. The shear capacity of the vertical CFRP, V_{FRP} , tows is shown in Eq. (2). This approach is based on the truss analogy for steel shear reinforcement (BBK 2004 and CEN 2004). The last

contribution, V_{MBA} , originates from the mineral-based bonding agent (mortar) because the cross section is enlarged and contributes to the shear capacity. The contribution of the vertical CFRP tows can be obtained analogously to the model on how to calculate the contribution of the steel shear reinforcement to the shear bearing capacity. V_{FRP} for the vertical CFRP tows can then be expressed as Eq. (2). Note that in Eq. (2) the factor of 2 originates because the MBC strengthening system is generally applied on both sides of the beam

$$V_{FRP} = \frac{2 \cdot \varepsilon_{ver,ef} \cdot E_{ver} \cdot A_{ver} \cdot h_{ef} \cdot \cot(\theta)}{s_{ver}} \quad (2)$$

where $\varepsilon_{ver,ef}$ =effective strain generalized over the shear crack; s_{ver} =distance between the vertical CFRP tows; h_{ef} =effective height on which the MBC system is taking shear forces; A_{ver} =area; E_{ver} =modulus of elasticity of the vertical CFRP tow; and θ =inclination of shear crack.

The effective strain can be expressed as Eq. (3), where a strain reduction factor is introduced which considers that carbon fibers are a linear elastic material that does not yield

$$\varepsilon_{ver,ef} = \eta \cdot \varepsilon_{ver,ult} \quad (3)$$

where $\varepsilon_{ver,ult}$ =ultimate strain in the vertical CFRP tows.

The strain reduction factor, η , is based on the ratio between the maximum shear stresses and the average shear stresses in a rectangular cross section (see also Popov 1999). For a further discussion of cracked cross sections the reader is referred to Carolin and Täljsten (2005)

$$\eta = \frac{\tau_{average}}{\tau_{max}} = \frac{V}{A} \cdot \frac{2}{3} \cdot \frac{A}{V} = \frac{2}{3} \quad (4)$$

Insertion of Eqs. (3) and (4) into Eq. (2) will give the shear bearing capacity of the vertical CFRP tows at fiber rupture

$$V_{FRP} = \frac{4 \cdot \varepsilon_{ver,ult} \cdot E_{ver} \cdot A_{ver} \cdot h_{ef} \cdot \cot(\theta)}{3 \cdot s_{ver}} \quad (5)$$

Considering a rectangular cross section, the maximum shear stress in the cross section is $\tau_{max} = 3V/(2A)$. The maximum shear stress is located in the point of gravity and has the same size as the maximum principal tensile stress. In BBK (2004) it is stated that no reinforcement is needed if the principal tensile stress is less than 0.5 f_{ct} . By using this in expression for the maximum shear stresses the shear contribution for the mineral based strengthening system, assuming the mineral-based bonding agent performs in the same way as for concrete, can be expressed as

$$\tau_{max} = \frac{3}{2} \cdot \frac{V}{A} \Rightarrow V \leq \frac{2 \cdot A}{3} \cdot \frac{1}{2} \cdot f_{ct} \Rightarrow V_{MBA} = \frac{1}{3} t_{MBA,tot} \cdot h_{ef} \cdot f_{MBA,t} \quad (6)$$

where $t_{MBA,tot}$ =total thickness of the mineral-based bonding agent. For side bonding on both sides of the beam this would be equal to $2t_{MBA}$. h_{ef} =effective height on which the MBC system is taking shear forces; and $f_{MBA,t}$ =tensile strength of the mineral-based bonding agent

A straightforward approach on validating the theory proposed for calculating the shear bearing capacity for the MBC strengthening system is to compare it to the experimental results. Using the experimentally obtained values for the material properties used in the MBC strengthening system and then applying Eqs. (5) and (6) will give an estimate of how well the analytical approach is performing. Experimentally obtained tensile properties for the

Table 4. Experimental versus Predicted Shear-Bearing Capacity for MBC System

| Specimen | $\varepsilon_{\text{ver,ult}}$ (%) | E_{ver} (GPa) | θ (°) | $f_{\text{MBA},j}$ (MPa) | V_{Pred} (kN) | V_{exp} (kN) | $V_{\text{pred}}/V_{\text{exp}}$ (kN) |
|--------------|---------------------------------------|---------------------------|-----------------|-----------------------------|---------------------------|--------------------------|--|
| C40s0-M2-G2a | 11.4 | 389 | 36 | 2.4 | 102.9 | 121.4 | 0.85 |
| C40s0-M2-G2b | 11.4 | 389 | 32 | 2.4 | 117.1 | 118.4 | 0.99 |
| C40s0-M2-G1* | 13.9 | 366 | 34 | 2.4 | 64.4 | 81.4 | 0.79 |
| C40s0-M2-G2* | 11.4 | 389 | 34 | 2.4 | 109.6 | 125.2 | 0.88 |
| C40s0-M2-G3* | 8.3 | 423 | 31 | 2.4 | 73.9 | 79.7 | 0.93 |

utilized materials are reported in Table 4 and in Blanksvärd (2007). A validation of the analytical approach is done on the beam specimens who had fiber rupture as the failure mode. This refers to the specimens without steel shear reinforcement in the strengthened shear span, all of the C40 specimens in Table 3.

However, in this case it is only interesting to evaluate the shear force contribution of the MBC system. Therefore, the experimentally obtained shear failure load is taken as the ultimate failure load of the MBC strengthened beam subtracted by the failure load of the reference beam without strengthening.

All of the experimental values are shown in Table 4. Note that the effective height z or h_{ef} has not been evaluated in this paper but it is set to the height of the beam. This assumption is based on the fact that the entire height of the beam was side bonded and that no debonding was observed for these specimens. The total thickness of the bonding agent is 40 mm for all of the specimens and the fiber area and tow distances for the different grids are reported in Table 2. Table 4 shows the predicted and experimental shear bearing capacity for the MBC strengthening system. The proposed analytical equations on how to calculate the shear bearing capacity of the MBC system seems to predict the ultimate experimental shear capacity satisfactorily. However, more research is needed to investigate the influences of the effective height and the behavior of the bonding agent.

Conclusion

Strengthening concrete structures with the presented MBC system can be favorable in comparison to existing external strengthening systems such as epoxy bonded CFRP. MBC systems are considered environmentally friendly and have a high compatibility with the base concrete. Furthermore it can be applied on moist surfaces and is open for diffusion.

The use of a CFRP grid with smaller tow distance generates a higher load for the appearance of the first inclined crack. The ultimate shear failure load increases when the fiber amount in the CFRP grid is increased. Using a mineral-based bonding agent (mortar) with low modulus of elasticity leads to premature cracking in the MBC strengthening system compared to the use of a mortar with higher stiffness.

The readings from strain gauges applied on vertical stirrups show tendencies toward a parabolic shape of the strain distribution along the stirrups. The strains in the stirrups for a certain load decrease with the use of MBC compared to the strains in a beam specimen without the MBC system. For vertical CFRP tows the strains do not clearly show a parabolic shape of the strain distribution along vertical CFRP tows. The tendency for these strain gauges is locally high strains located near crack formations which indicate a good bond between the CFRP grid and the mortar.

It is clear from the study of the principal strain that the strains are reduced for low load steps when using MBC strengthening

compared to nonstrengthened specimens. This is an advantage for design in a service limit state. At higher loads the MBC system still reduces the principal tensile strain. There are no significant differences at low load steps when using a thinner layer of bonding agent compared to using a thicker layer.

The proposed analytical model to estimate the shear resistance gives reasonable correlation to experimental values. It should also be noted that the measured strains in the vertical CFRP tows do not have a parabolic shape at load steps close to the ultimate load. At higher load steps, the strains are locally increased in the vicinity of forming shear cracks. The model is fairly transparent but the importance of effective height and different geometries (other than rectangular cross sections) needs to be further studied. Another important issue to be solved when estimating the bearing capacity is the strain development in the CFRP grid and its influence on the ultimate bearing capacity of the strengthening system.

In this particular research, only small variations in material or geometrical properties have been investigated. It is likely that more optimal systems can be developed with other configurations. The use and development of a mortar with higher fracture toughness together with the incorporation of more fibers or fibers with higher stiffness in the grid will probably enhance the performance of the MBC system. The reduction of principal strains when using the MBC strengthening system also indicates the potential of using the CFRP grid as crack reinforcement in the production of prefabricated concrete elements or in newly built structures.

In this paper, it is only the shear load carrying capacity for rectangular beams that has been studied and more detailed studies are needed on bonding between both the CFRP and the cementitious material and in the contact interface between the MBC and the base concrete.

Acknowledgments

The research presented in this paper has been funded by several organizations. The Swedish National Road Administration, The Development Fund of the Swedish Construction Industry, Skanska AB, and Sto Scandinavia are acknowledged.

Notation

The following symbols are used in this paper:

- A = cross-sectional area (m^2);
- A_{ver} = cross-sectional area of vertical CFRP tows (m^2);
- E_{ver} = Young's modulus for vertical CFRP tows (Pa);
- $f_{\text{MBA},j}$ = tensile strength of mineral-based bonding agent (Pa);
- h_{ef} = effective height of mineral-based bonding agent (m);

s_{ver} = distance between vertical CFRP tows (m);
 t_{MBA} = thickness of mineral-based bonding agent (m);
 V = shear force (N);
 V_C = shear capacity of concrete (N);
 V_{FRP} = shear capacity of FRP (N);
 V_{MBA} = shear capacity of mineral-based bonding agent (N);
 V_S = shear capacity of steel reinforcement (N);
 V_{TOTAL} = total shear capacity (N);
 z = effective height for bonded CFRP (m);
 $\varepsilon_{ver,ef}$ = effective strain for vertical CFRP tows (---);
 $\varepsilon_{ver,ult}$ = ultimate strain for vertical CFRP tows (---);
 η = strain reduction factor for CFRP (---);
 θ = shear crack angle (---);
 $\tau_{average}$ = average shear stress (Pa); and
 τ_{max} = maximum shear stress (Pa).

References

- BBK. (2004). *Boverkets handbook about concrete structures BBK 04*, Boverket, Sweden (in Swedish).
- Becker, D. (2003). "Concrete slabs strengthened with carbon fiber composites." Master's thesis, Luleå Univ. of Technology, Luleå, Sweden, 1402-1617 (in Swedish).
- Blanksvärd, T. (2007). "Strengthening of concrete structures by the use of mineral based composites." Licentiate thesis, Luleå Univ. of Technology, Luleå, Sweden.
- Brückner, A., Ortlepp, R., and Curbach, M. (2006). "Textile reinforced concrete for strengthening in bending and shear." *Mater. Struct.*, 39, 741-748.
- Carlsvärd, J. (2006). "Shrinkage cracking of steel fibre reinforced self compacting concrete overlays—Test methods and theoretical modelling." Doctoral thesis, Luleå Univ. of Technology, Luleå, Sweden.
- Carolin, A., Olofsson, T., and Täljsten, B. (2004). "Photographic strain monitoring for civil engineering." *Proc., FRP Composites in Civil Engineering, CICE 2004*, Adelaide, Australia, 593-600.
- Carolin, A., and Täljsten, B. (2003). "Theoretical study of strengthening for increased shear bearing capacity." *J. Compos. Constr.*, 9(6), 497-506.
- Comité Européen de Normalisation (CEN). (2004). "Eurocode 2: Design of concrete structures—Part 1: Common rules for building and civil engineering structures." *prEN 1992-1*, European Committee for Standardization, EC 2-1, Central Secretariat, Brussels, Belgium.
- Courard, L. (2005). "Adhesion of repair systems to concrete: Influence of interfacial topography and transport phenomena." *Mag. Concrete Res.*, 57(5), 273-282.
- Dilthey, U., Schleser, M., Möller, M., and Weichold, O. (2006). "Application of polymers in textile reinforced concrete—From the interface to construction elements." *Proc., 1st Int. RILEM Symp. Textile Reinforced Concrete*, RILEM, Aachen, Germany, 55-66.
- DIN EN. (2005). "Methods of testing cement—Part 1: Determination of strength." *DIN EN 196-1*, Deutsches Institut Für Normung.
- Monti, G., and Liotta, M. A. (2007). "Tests and design equations for FRP-strengthening in shear." *Constr. Build. Mater.*, 21, 799-809.
- Nordin, H. (2003). "Fibre reinforced polymers in civil engineering." Licentiate thesis, Luleå Univ. of Technology, Luleå, Sweden.
- Nordin, H., and Täljsten, B. (2006). "Concrete beams strengthened with prestressed near surface mounted CFRP." *J. Compos. Constr.*, 10(1), 60-68.
- Oehlers, D. J., Rashid, R., and Seracino, R. (2007). "IC debonding resistance of groups of FRP NSM strips in reinforced concrete beams." *J. Constr. Build. Mater.*, 22, 1574-1582.
- Peled, A., and Bentur, A. (2003). "Fabric structure and its reinforcing efficiency in textile reinforced cement composites." *Composites, Part A*, 34, 107-118.
- Peled, A., Bentur, A., and Yankelevsky, D. (1998). "Effects of woven fabric geometry on the bonding performance of cementitious composites." *Adv. Cem. Based Mater.*, 7, 20-27.
- Popov, E. P. (1999). *Engineering mechanics of solids*, Prentice-Hall, Upper Saddle River, N.J., 430-432.
- Raupach, M., Orlowsky, J., Büttner, T., Dilthey, U., and Schleser, M. (2006). "Epoxy impregnated textiles in concrete—Load bearing capacity and durability." *Proc., 1st Int. RILEM Symp.: Textile Reinforced Concrete*, RILEM, Aachen, 55-66.
- Svanbro, A. (2004). "Speckle interferometry and correlation applied to large-displacement fields." Doctoral thesis, Luleå Univ. of Technology, Luleå, Sweden.
- Täljsten, B., and Blanksvärd, T. (2007). "Mineral based bonding of carbon FRP to strengthen concrete structures." *J. Compos. Constr.*, 11(2), 120-128.
- Täljsten, B., Carolin, A., and Nordin, H. (2003). "Concrete structures strengthened with near surface mounted reinforcement of CFRP." *Adv. Struct. Eng.*, 6(3), 201-213.
- Teng, J. G., Yuan, H., and Chen, J. F. (2006). "FRP to concrete interfaces between two adjacent cracks: Theoretical model for debonding failure." *J. Solids Struct.*, 43, 5750-5778.
- Triantafyllou, T. C., and Papanicolaou, C. G. (2006). "Shear strengthening of reinforced concrete members with textile reinforced mortar (TRM) jackets." *Mater. Struct.*, 39, 85-93.
- Wiberg, A. (2003). "Strengthening of concrete beams using cementitious carbon fibre composites." Doctoral thesis, Royal Institute of Technology, Stockholm, Sweden.

PAPER III

“Strengthening of Concrete Structures
with cement based bonded composites”

BY

Thomas Blanksvärd and Björn Täljsten

Published in

Journal of Nordic Concrete Research, Vol. 38, No. 2, December, 2008

Strengthening of concrete structures with cement based bonded composites



Thomas Blanksvärd
Lic. Tech., Ph.D. Student
Luleå University of Technology
971 87 Luleå, Sweden
E-mail: thomas.blanksvard@ltu.se



Björn Täljsten
Ph.D., Professor
Technical University of Denmark
Brovej Building 118, 2800 Kgs. Denmark
E-mail: bt@byg.dtu.dk

ABSTRACT

Due to demands on higher loads, degradation, re-construction etc. there is a constant need for repair or strengthening of existing concrete structures. Many varying methods exist to strengthen concrete structures, one such commonly used technique utilizes surface epoxy bonded FRPs (Fibre Reinforced Polymers). The method is very efficient and has achieved world wide attention. However, there are some drawbacks with the use of epoxy, e.g. working environment, compatibility and permeability. Substituting the epoxy adherent with a cement based bonding agent will render a strengthening system with improved working environment and better compatibility to the base concrete structure. This study gives an overview of different cement based systems, all with very promising results for structural upgrading. Studied parameters are structural retrofit for bending, shear and confinement. It is concluded that the use of carbon FRPs provides the highest strengthening effect and that the fibres should be imbedded into a matrix for enhanced utilisation of inherent strain capacity.

Key words: Strengthening, Concrete, FRP, CFRP, Mortar, Fabric, Textiles, Grids, MBC.

INTRODUCTION

1.1 General

The use of reinforced concrete as a material for building structures is widely spread over the world due to its versatile applications. In general the construction industry is not known for development and technical innovations, at least not in comparison with industries such as the car and aerospace industries. Despite this, a considerably amount of research, development and innovations are carried out in construction and the society is highly dependent on these innovations. For example, systems or products that can lower the cost of maintenance and

prolong the structural life do not only save some of our beautiful heritage to future generations, but can also save a considerably amount of money.

The research and development of high performance and multifunctional construction materials have been improved to meet up with new demands and innovations. Advanced technologies have recently been focused on repair or upgrading of existing structures. The anticipated design life of steel reinforced concrete structures is frequently shortened due to alternation of the load situation on structures or deterioration, e.g. steel reinforcement corrosion. Traditional upgrading systems can consist of widening the cross section, external pre-stressing, span shortening etc. An alternative method to these traditional retrofitting methods is to bond a non corrosive material, such as FRP (Fibre Reinforced Polymers), to the surface of the structure. FRP materials have significant retrofitting potential and possess three physical properties of interest; high tensile strength, high elastic modulus and elastic-brittle stress-strain behaviour. One of the critical parameters in upgrading existing structures is the choice of bonding agent between the FRP and concrete surface, [1]. Strengthening systems with the use of continuous carbon fibres in an epoxy matrix bonded to concrete structures has proven to be successful, [2]. However, these methods present some important disadvantages regarding the use of organic resins (especially epoxies) which involve a hazardous working environment for the manual worker and have a low permeability, diffusion tightness and poor thermal compatibility with concrete, [3]. Upgrading civil structures with cement based bonding agents and high performance fibre materials give a more compatible repair or strengthening system with the base concrete. Consequently the use of cementitious bonding agents should prevent some of the disadvantages with the organic resins mentioned above. This study gives an overview of existing strengthening systems that use cement based bonding agents to adhere advanced fibre materials in order to upgrade existing concrete structures.

1.2 Materials

In this section only a brief introduction to the materials used in cement based strengthening systems is presented. It should be addressed that it is not the individual material properties that characterise the cement based composite, but the materials in combination and the synergy between them. A rough approach divides most of the cement based strengthening systems into two categories, fine grade *mortar* (bonding agent) and *fibre composites* (reinforcing for high tensile stresses).

Mortar: The bonding agents used in a cement based strengthening system are often fine grade (1 mm maximum grain size) mortars. To enhance the properties, e.g. workability, flowability, mechanical properties etc, of the mortars different mixtures and additives are used. Different additives can be polymers, superplasticizers and reinforcing fibres. The addition of different polymers enhances the properties of ordinary Portland cement. There are also a number of chemical admixtures, such as water reducing agents, ashes, aluminosilicate, superplasticizers, etc., that further improve the quality of mortar. All of the above mentioned improvements can enhance strength, shorten setting time, decrease autogenous shrinkage, control the alkali aggregate reaction and improve the durability, [4]. To increase the fluidity of fresh mortar and concrete for pumping, increase the strength and prolong the durability of hardened mortar and concrete, a small quantity of superplasticizers is often added to the mortar and concrete mixture. However, the single application of some superplasticizers can develop complications in the form of excessive bleeding, segregation and early loss of workability. Using them in combination with latex polymers could minimize these complications [5]. Other polymeric compounds can be re-dispersible polymer powder, water soluble polymer or liquid polymer.

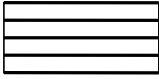

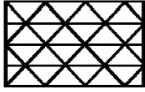
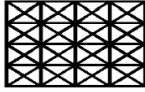
Another parameter that has a significant influence on the properties of the mortar is the mixture of ingredients. Compared with ordinary cement mortar, the properties of polymer modified mortar depend more on the polymer content or polymer to cement ratio (P/C) than the water to cement ratio (W/C) [6]. For example, three-point bending tests show that the maximum load is fairly constant for mortars with a P/C ratio 7.5 wt.% or lower. Increasing the P/C ratio between 10-15 % wt.% has shown to increase the flexural strength. However, a P/C ratio higher than 15 wt.% decreases the mechanical strength [7],[8].

Other ways to improve the performance of the mortars can be by adding reinforcing fibres. Especially for applications such as shotcreting, concrete upgrading and mining. The reason for adding fibres is primary to stabilize the micro-cracking. There are two main types of incorporating the fibres to the cement matrix, by the use of chopped or milled fibres or by the use of continuous fibres. The latter is more expensive and not easily mixed into the cement matrix. Chopped or milled fibres have less mechanical efficiency compared to continuous fibres but are more easily mixed in the mortar. Different types of fibres can be used, such as steel, alkali resistant glass, carbon, PP (polypropylene), PVA (polyvinyl alcohol) and natural fibres [9]-[13]. Drying shrinkage can be reduced by adding fibres in cement based materials. However, incorporating fibres in the material will generally reduce the compressive strength, thus increasing the permeability [14]. These insufficiencies can be bridged through the use of supplementary materials that will lead to a densification of the cement matrix. In the case of polypropylene reinforcing fibres, a suitable proportion of 2.0% is recommended; with an addition of 0.5% melamine formaldehyde dispersion, [15]. Adding silica fume will also improve the mechanical properties, such as compressive strength and flexural strength for cement matrices with steel and glass fibres [14]. When incorporating carbon fibres into the mortar a content of 0.5% of cement weight will give an optimum increase in flexural strength (general purpose pitch based carbon fibres), [13].

Fibre composites: The most common fibre composites consist of polymer fibres in matrices and additives. Different types of fibres consist of different materials, such as aramid, glass and carbon. The choice of material depends on the desirable properties of the composite, where carbon fibres have the highest strength and stiffness followed by aramid and glass fibres. The main function of the matrix is to transfer forces between fibres and to a lesser degree protect the fibres from the surrounding environment. The properties of the composite can be enhanced with the addition of additives, e.g. improve the bond between the composite and the strengthened material by a sizing compound, [16].

The fibres or fibre composites can be placed in different directions in the composite and thus form a large amount of FRP geometries with different mechanical properties. If the fibres are oriented in one direction the FRP becomes unidirectional. The fibres can also be woven or bonded in many directions, thus creating a bi or multi directional FRP. Table 1 shows different geometries for fibre composite strengthening materials. It should also be mentioned that 3D geometries are available. Depending on the type of fibre used, the FRP material can be referred to as CRFP (Carbon Fibre Reinforced Polymer), GFRP (Glass Fibre Reinforced Polymer) and AFRP (Aramid Fibre Reinforced Polymer). It is also possible combine these materials into a composite and then tailor-make the mechanical properties to correspond to the preferred characteristics.

Table 1. Different geometries for composite materials.

| | Mono-axial | Biaxial | Triaxial | Multi-axial |
|--------------|---|---|---|---|
| 1 Dimensions | Pultruded rod | - | - | - |
| 2 Dimensions |  |  |  |  |
| | Sheet | Weave/grid | Weave/grid | Weave/grid |

MINERAL BASED STRENGTHENING SYSTEMS

Strengthening concrete structures with continuous fibres or FRPs and cement based bonding agents must be done in well-defined steps. The process of optimising each and all of the incorporated materials into a composite with the most favourable strengthening properties are very complex. The components in the mineral based bonding agent as well as the materials and geometry of the fibres, or FRPs, play a significant role in the performance of the strengthening system. It is very hard to achieve a perfect penetration of the fibres or bond to FRPs in the mineral based matrix. Enhanced bonding of the fibre or FRP should be obtained when a non-linear geometry is introduced into the mineral based matrix. A special geometry may provide mechanical anchoring to the cement based matrix. As supported by many studies, in mineral based composites, the matrix does not fully penetrate in the spaces surrounding the fibre or FRP [13],[15]. In the following sections, four different approaches when designing cement based strengthening systems for concrete structures are described. The first system is Textile Reinforced Concrete (TRC) developed at the collaborative research centre at Dresden and Aachen University, Germany, in 1998. This strengthening system basically consists of woven fabrics bonded to the concrete surface with modified cement. The second system is called Fibre Reinforced Cement (FRC) and is being developed at Wayne State University, USA. This strengthening system consists of fibres impregnated with a cement matrix that results in a thin composite sheet. The third evaluated strengthening system is called Textile Reinforced Mortar (TRM), which is similar to the TRC system because it uses fibre textiles and mortar as a bonding agent. TRM is developed at the University of Patras, Greece. The fourth system and another way to strengthen concrete structures with FRPs and cementitious bonding agents is called Mineral Based Composites (MBC). This system has been developed at Luleå University of Technology, Sweden and presented in detail in this paper. This system uses a fibre composite grid bonded to the surface of a concrete structure to enhance its strength, stiffness or both. Common for all strengthening systems is the use of a cement based bonding agent. The main difference lies within the design of the fibre composites the manufacturing process and application technique.

2.1 Textile Reinforced Concrete (TRC)

The TRC strengthening technique is comprised of a cementitious matrix as the bonding agent and a textile fabric as reinforcement. The TRC system is mounted with a fine-grained, high strength concrete as the bonding agent. This high strength concrete has a maximum aggregate size of 1 mm. The reinforcing fibres are predominately made of AR-glass (alkali resistant glass fibres) produced into to a woven fabric, the use of carbon fibres or a combination with AR-glass has also been utilized. There can be many designs of the textile fabrics depending on the load case and positioning of the fabric. A maximum of four different fibre orientations can be obtained in the same multi-axial fabric; see also Figure 1. Fabrics with relatively complicated

yarn shapes, such as short weft knit, enhance the bonding and improve the composite performance [18]. Figure 1 shows a multiaxial textile fabric with filament bundles and stitching fibres.

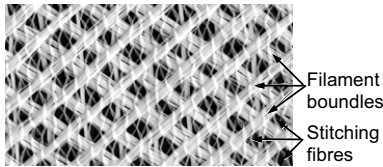


Figure 1. Multiaxial textile fabric used in textile reinforced concrete, tow spacing ~ 10 mm.

Strengthening in Shear

Shear strengthening of concrete beams with the TRC strengthening system has been performed at the Dresden University of Technology [19], [20]. The concrete beam specimens had a T-section and the test set-up was three point beam bending with a support span of 200 cm, see Figure 2. The concrete T-beams were symmetrically strengthened with the TRC system three sided wrapped around the bottom of the web extending 900 mm on each side from the middle of the beam. The TRC strengthening system was applied layer by layer. Fine-grained cement was used as the bonding agent and the fabric was laminated with a spatula in the wet cement matrix. The application of the TRC system is shown in Figure 3. The steel shear reinforcement was designed to ensure the redistribution of internal forces in the state of cracking and to simulate a reinforced concrete beam in need of strengthening. The flexural steel reinforcement was designed for a higher load than the shear reinforcement to avoid bending failure in the T-beam.

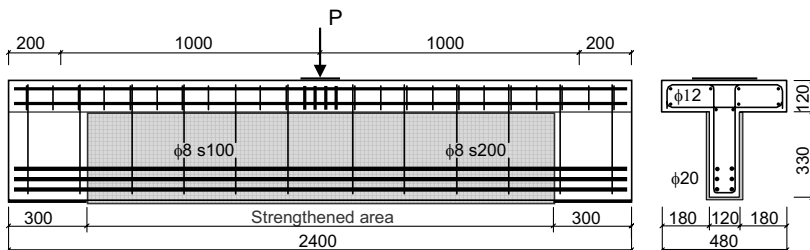


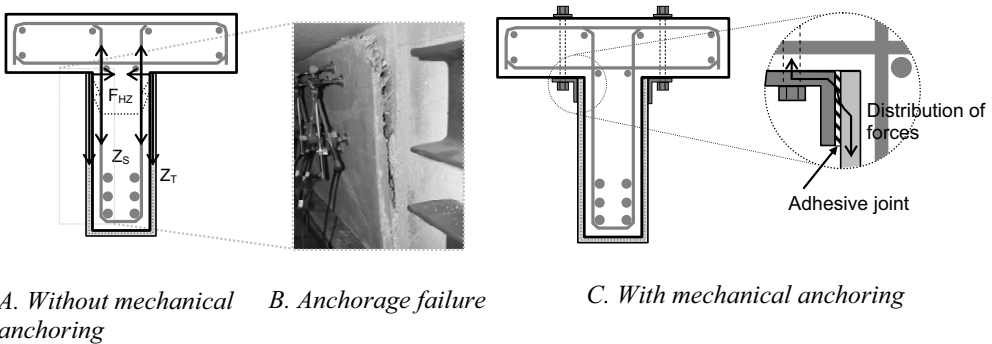
Figure 2. Test set-up and geometry of T-beams, strengthened area situated in the middle. Units in cm. after [19].



Figure 3. Mounting of the TRC strengthening system. To the left, the fabric is laminated onto the side of the beam. To the right, a layer of cement matrix is sprayed on to the surface of the fabric. Courtesy of A. Brueckner, Dresden University of Technology.

As seen in Figure 3, the fabric is wrapped around the web of the beam up to the underside of the flange. This strengthening methodology may cause insufficient anchorage of the TRC system, since there is no anchorage in the compressive zone. A mechanical anchorage would then be advantageous. In [19], the mechanical anchorage was designed with a steel L-section that was

bonded on both sides of the TRC system surface with an epoxy adhesive. Both anchored and unanchored strengthening was performed. Anchorage failure of a strengthened beam and strengthened T-beam cross sections with and without mechanical anchoring are recorded in Figure 4. The fabric used in these tests was a multiaxial textile with a weight per unit area of 470 g/m^2 . The AR-glass fibre inclination was $\pm 45^\circ$ to the load direction with the aim to be aligned with the principal stresses in the web. The applied textile fabric used in the system is shown in Figure 1. In total five concrete beams were strengthened with the TRC system. Two concrete beams were strengthened with two textile layers and one with four textile layers, all without mechanical anchoring. Two additional beam specimens were strengthened, one with three layers of fabric and one specimen with four layers of fabric, both with mechanical anchoring.



A. Without mechanical anchoring B. Anchorage failure C. With mechanical anchoring
 Figure 4. Strengthened T- section without mechanical anchoring. To the right, delamination failure of strengthening layer, from [19].

Strengthening of the T-beam cross section with TRC significantly increased the shear load capacity. However, when the number of textile fabric layers increases, so does the need for mechanical anchoring. The results indicate that the ultimate bearing capacity will roughly be the same for a T-beam strengthened with two layers compared to a specimen strengthened with four layers. The difference between two and four layers of textile fabric is in the initial stage of loading, where the four-layered strengthening displays higher stiffness until the propagation of the anchorage failure initiate. Typical anchorage failure is recorded in Figure 4 B. With mechanical anchoring, an increased stiffness and higher bearing capacity of the strengthened T-beam specimens are noticed. The strengthening effect of a TRC strengthened concrete beam compared to the average value of three non-strengthened reference T-beam is recorded in Table 2. The deformation rate of the loading in this study was set to 0.01 mm/sec . Table 2 shows that the strengthening effects are low and that debonding failure dominates if the textile is not anchored. However, by using anchoring a higher utilisation of the textile will be achieved and thus a higher strengthening effect. It should be noted that the strengthening effect is not drastically influenced by adding more textile layers. It should also be noted that the overall strengthening effect with or without anchoring is not that high (maximum 16%). The maximum strengthening effect was accomplished by using high amounts of fibres and mechanical anchorage. When using less layers of textiles and no mechanical anchorage the strengthening effect would be insignificant, taking into consideration the stochastic scattering of the failure loads.

It should be pointed out that the fibres were aligned in a $\pm 45^\circ$ and therefore are having a better utilisation of the fibres. Despite this, significant strengthening effect is absent although using mechanical anchorage.

Table 2. Strengthening effect of TRC, ultimate failure load divided by the average failure load of the reference beams, from [19].

| | 2 textile layers (without anchoring) | 4 textile layers (without anchoring) | 6 textile layers (without anchoring) | 2 textile layers (with anchoring) | 4 textile layers (with anchoring) | 6 textile layers (with anchoring) |
|----------------------|--|--|--|---|---|---|
| Strengthening effect | 1.01 | 1.01 | 1.07 | 1.06 | 1.09 | 1.16 |
| Failure mode | Fracture | Debonding | Debonding | Fracture | Fracture | Fracture |

Strengthening in flexure

It is also possible to use TRC for flexural strengthening, as reported in [21]. This study contains flexural strengthening of pre-deformed concrete slabs. For the flexural strengthening, a biaxial geometry of the fabrics was used. Three different fabric designs were evaluated. All of the textile reinforcement was mounted in three layers. The three fabric designs were AR-glass with a fibre area of 143 mm^2 , AR-glass fibre with polymer coating and a fibre area of 143 mm^2 , and carbon fibre with polymer coating and a fibre area of 50 mm^2 . The biaxial geometry of the fabrics was longitudinal and cross directional of the strengthened concrete beam. Mounting of the reinforcement can be seen in Figure 5. The test set-up was four-point beam bending with an effective span of 1.6 m. The height of the concrete slab was 100 mm and the concrete slab had flexural steel reinforcement. The results on the strengthened concrete specimen show that higher ultimate load carrying capacity and higher stiffness can be achieved. And also that a polymer coating of the fabrics increases the effectiveness of the textile fabric. It is also shown that for the same load carrying capacity only one-third of the carbon fibre area is needed compared to the AR-glass fibre area. The strengthening effects of the different TRC systems are recorded in Table 3. Strengthening of pre-damaged concrete structures utilizes the effectiveness of the fabrics more than strengthening of an undamaged concrete structure. The effectiveness of the fibres in pre-damages cross sections is based on the nature of bridging stresses over cracks in damaged zones. However, the effectiveness of the fibres with polymer coating is not concurrent to pre-damaged cross sections but is related to the strains and slip development in the textile and mechanical interlocking during loading, see also the discussion in the last chapter.



Figure 5. Mounting of the TRC strengthening system. Courtesy of A. Brueckner, Dresden University of Technology.

Table 3. Strengthening effect of flexural strengthened concrete beam with TRC system. Ultimate failure load divided by failure load of unstrengthened beam, from [21].

| | AR-glass, $A_f = 143 \text{ mm}^2$. No coating | AR-glass, $A_f = 143 \text{ mm}^2$. Polymer coating | Carbon fibre, $A_f = 50 \text{ mm}^2$. Polymer coating |
|----------------------|--|---|--|
| Strengthening effect | 1.51 | 1.86 | 1.86 |

There are numerous references on the development of TRC and for example computational models can be found in [22], analytical solutions of tensile response of the TRC in [17], stochastic modelling in [23] and bond mechanisms in [24].

2.2 Fibre Reinforced Cement (FRC)

This strengthening system is comprised of a fibre sheet or fabric that is impregnated with a cement based matrix. Combining the cement slurry and the different fibre geometries results in a thin composite sheet. Depending on the geometry of the fibres and the strengthening purpose, the composite plates can be made as thin as 2 mm, see Figure 6 C. Composites of ultra high performance, fibre reinforced cement plates have excellent durability and ductility properties during flexural tests, see Figure 6 A and B. The mounting of this strengthening system differs from the MBC and TRC strengthening systems. The sheet or fabric is cut into chosen dimensions and the fibre geometry is submerged into a cement slurry (matrix) for full penetration. The impregnated sheet or fabric is then removed from the slurry and immediately bonded to the concrete surface. The performance of this system is investigated in both confinement and flexural strengthening of concrete specimens [25], [26], and [27]. In the latter, the high tensile strength comes from the carbon fibre sheet and the ductility from multiple cracking of the cement based matrix, similar to the Engineered Cementitious Composites (ECC) [28]. The competitive product to cement based strengthening is epoxy bonded fibres; hence, comparing epoxy bonded products to the cement based composites would be of interest. In [26] and [27], both confinement and flexural strengthening were performed. The fibre material used in both studies was based on continuous carbon fibres without matrix.

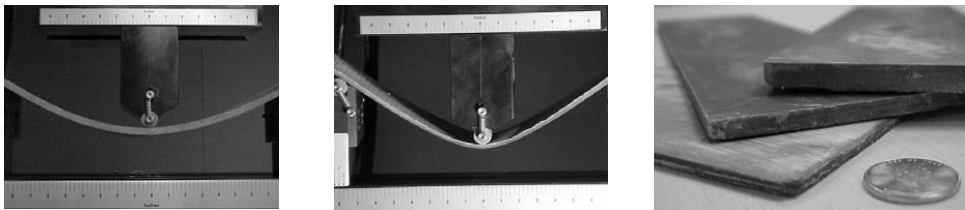


Figure 6. Composite plate with a thickness: A. 4.8 mm, B. 3.2 mm. C. Cement based composite plates with mono-axial fibre sheets, from bottom, 2, 3 and 4 mm of thickness. Courtesy of H.C. Wu.

Strengthening for Confinement

By using a carbon fibre sheet, concrete cylinders can be strengthened for confinement. The height of the cylinders was 203 mm with a diameter of 102 mm. The test set-up of the cylinders was in accordance to ASTM C39-96 (compression strength test on cylindrical specimens). The epoxy based strengthening system (CFRP) was wrapped around the cylinders and anchored with a bond length of 51 mm, the total thickness of this strengthening system was 2-3 mm. The cement based strengthening system (CFRC) was applied as described above with two layers of carbon fibre. The CFRC composite sheet was wrapped around the cylinder as with the CFRP strengthened specimens. However, the bond length of this system was 76 mm with an average thickness of 3 mm. Gaps of 38 mm were left at the bottom and top of the concrete cylinders for both strengthening systems, see Figure 7. The results indicate a higher compressive strength and higher ductility for the CFRP specimens. However, no major differences between the CFRP and the CFRC systems were noticed. The unconfined concrete cylinders had a compressive failure of 54 MPa and a deflection of 2 mm, whereas the compressive strength for CFRC strengthened specimens were 105 MPa with a deflection of 8 mm. Anchorage of the fibres is improved when wrapped. In this comparison it is much the properties of the carbon fibres that are shown, for fully anchored fibres.

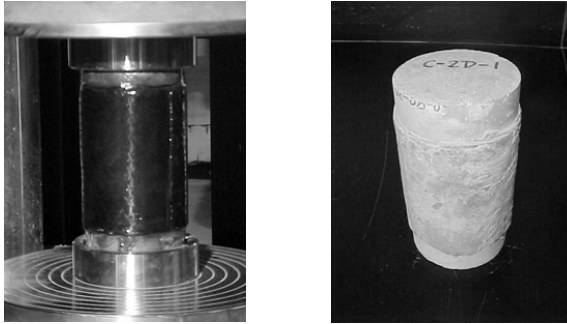


Figure 7. Confinement of concrete cylinders, to the left epoxy bonded CFRP and to the right CFRC wrapped specimen, courtesy of H.C. Wu.

Strengthening for flexure

Concrete beams have also been strengthened for flexure with the FRC system. Here, a comparison with epoxy bonded carbon fibres was conducted. The flexural test set-up is three-point bending according to ASTM C78-75 (rectangular beam specimen subjected to a three point load case with two shear spans and a maximum bending moment in the mid-point of the beam specimen). In comparison to the confinement strengthening, the fibre geometry changed from a sheet to a two dimensional/biaxial carbon fibre grid without any matrix. The volume content of fibres in the composite is 4.2% for both strengthening systems. Both CFRP and CFRC composites were bonded to the tensile side of the concrete beam. The test set-up for the CFRC beam can be seen in Figure 8. The non-reinforced and non-strengthened concrete reference beam displayed brittle failure due to lack of tensile reinforcement. An increase in both flexural strength and deflection occurred in both of the strengthening systems. However, the epoxy bonded strengthening system exhibited the highest increase in flexural strength. Failure of the beams with the epoxy bonded carbon fibres started with the formation of several cracks in the concrete as the load increased. The crack formulation gradually propagated to the bond zone between the concrete and epoxy adhesive. A typical peeling phenomenon then propagated through the transition zone between the base concrete and adhesive, with failure finally occurring as crushing of the concrete under the line load. Concrete beams strengthened with the CFRC system behaved differently with primarily one flexural crack and final failure due to rupture of the CFRP composite, see Figure 8. No bond problems were noticed in the transition zone between the base concrete and cement based bonding agent. The flexural strength of the CFRC system is inferior compared to the CFRP system, though larger than the non-strengthened reference beam. The strengthening effect, i.e. ultimate failure load of the strengthened specimen divided by the failure load of the reference beam for both confinement and flexural strengthening, is recorded in Table 4. It is not stated in [27], but the large difference in strengthening effects between the cement based and epoxy based flexural strengthening could be due to slippage of the fibres in the cement matrix. This better bond is also shown by one crack in the CFRC system and multiple cracking in the CFRP system. The fibres can be anchored by wrapping for the confinement strengthening. Fully anchoring the fibres will lead to similar strengthening effects when comparing the two strengthening systems for confinement. Slippage of the fibres originates from the poor bond/penetration of the cement matrix. A better bond to the fibres can be achieved when using epoxy bonding agents. This shows the importance of anchorage of the fibres in the cement based bonding agent. However in this case another aspect is not dealt with and that is the peeling stresses that occur in at the cut of end of the adhered system. In this case the system is applied beyond the supports and peeling stresses are prohibited.

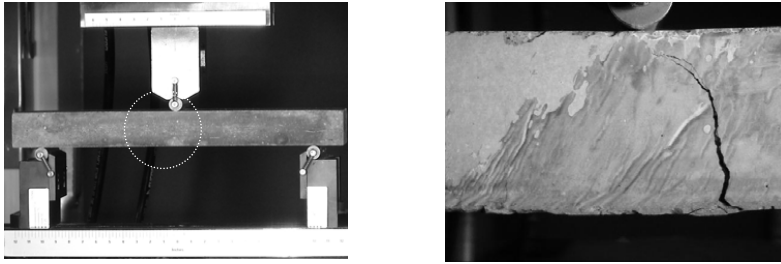


Figure 8. To the left, three point flexural test set-up and to the right, failure of CFRC beam, courtesy of H.C. Wu..

Table 4. Strengthening effect of both the FRC system and similar epoxy bonded strengthening system, ultimate failure values from [27].

| | Confinement/ Cement | Confinement/Epoxy | Flexural/Cement | Flexural/Epoxy |
|----------------------|---------------------|-------------------|-----------------|----------------|
| Strengthening effect | 1.85 | 1.94 | 2.03 | 4.65 |

2.3 Textile Reinforced Mortar (TRM)

This system is similar to the TRC strengthening system. The fibre textiles used for strengthening purposes are made of carbon fibre and the bonding agent is a polymer modified mortar. In this study, the evaluation of shear strengthened concrete beams was undertaken based on [29]. The base concrete beam specimens to be strengthened were 2600 mm long and with a cross section of 150 x 300 mm². The base concrete specimens were reinforced with steel rebars, both flexural and in the shear span. The steel reinforcement scheme is recorded in Figure 9 together with the four point bending test set-up. In [29], both epoxy and a cementitious bonding agent were used. This study had three variables; bonding agent (epoxy or mortar based), number of layers of textile (1 or 2 layers) and the alignment of the textiles. The alignment of the textiles was vertical or spirally applied at an angle of 10°.

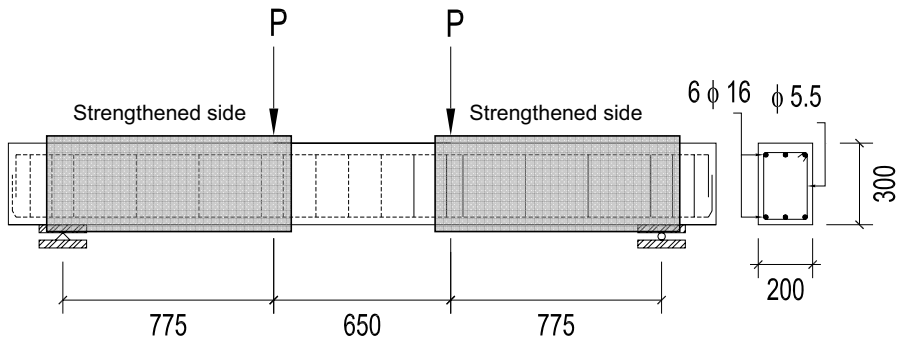


Figure 9. Reinforcement scheme for the base concrete specimens after [29].

The carbon fibre textile used in the strengthening system equalled the quantity of high strength rovings in the two orthogonal directions. Each roving is stitched together by a secondary polypropylene grid, similar to Figure 1. The width of the roving is 4 mm and the distance between them is 10 mm. The total weight of carbon fibres in the textile are 168 g/m², elastic modulus 225 GPa and tensile strength 3350 MPa.

Bonding agents used in the study were a structural epoxy adhesive and a polymer modified mortar. The two component epoxy adhesive had a tensile strength of 30 MPa and an elastic modulus of 3.8 GPa. The mortar consisted of a cementitious binder with the addition of polymers (10:1). Application of the mortar was done by a hand lay-up technique using a trowel to apply the mortar layers onto the base concrete surface and the textiles. The thickness of the mortar layers ranged from 1.5-2 mm, with the number of layers depending on the number of textile layers used.

All of the evaluated concrete beam specimens were statically loaded until failure with a displacement rate of 0.01 mm/sec. One non strengthened control beam was used as a reference. The beam specimens evaluated in this literature study are recorded in Table 5. Note that specimens R2, M2, M2-s and R1 indicated that the shear failure was suppressed and the ultimate failure was dominated by flexure. Common for all of the previously mentioned specimens is that the shear resistance was increased by a factor of approximately 2. Specimen M1, a strengthened reinforced concrete beam using one layer of carbon fibre textile bonded with mortar, failed in shear similar to the reference beam, but with a strengthening effect of 1.71. This was somewhat lower than the strengthened specimens using epoxy bonding agents. The shear failure using mortar bonded carbon fibres could be detected visually, which is not possible when using epoxy bonded fibres. This is a desirable property as it permits onsite damage control assessment when strengthening real structures [29]. It should also be noted that all of the strengthened specimens were wrapped and thus prohibited to fail by debonding of the strengthening system. If only side bonded, then anchorage problems and internal bond of the fibres could be evident. Especially for specimens with limited heights and therefore limited anchorage lengths, see also section 2.1.

Table 5. Summary of evaluated beam specimens, after [29].

| Specimen | Strengthening | Bonding agent | Peak force [kN] | Failure mode | Strengthening effect ^A |
|----------|--|---------------|-----------------|--------------|-----------------------------------|
| C | - | - | 116.5 | Shear | - |
| R2 | 2 layers of textile vertically wrapped | Epoxy | 233.4 | Flexure | 2.00 |
| M2 | 2 layers of textile vertically wrapped | Mortar | 243.8 | Flexure | 2.09 |
| M2-s | 2 layers of textile spirally wrapped | Mortar | 237.7 | Flexure | 2.04 |
| R1 | 1 layers of textile vertically wrapped | Epoxy | 261.9 | Flexure | 2.24 |
| M1 | 1 layers of textile vertically wrapped | Mortar | 200.1 | Shear | 1.71 |

^A Calculated as maximum peak load divided by peak load of the reference beam

2.3 Mineral Based Composites (MBC)

The MBC system used in this research contains basically three material components – a cementitious binder, a CFRP grid and a concrete surface primer. To achieve a good bond between the base concrete and the mortar, the surface of the base concrete needs to be roughened, e.g. sandblasting or water jetting, in order to remove the cement laitance. The

surface preparation method for all presented test specimens was sandblasting. In laboratory environment a hand lay-up method was used to apply the MBC. This method includes pre-wetting the base concrete with water for 1-3 days depending on the conditions of the base concrete and the surrounding climate. The moisture conditions in the transition zone between the base concrete and mortar are further discussed in [30], where it is found that the best bond is obtained when the base concrete has just dried back from a saturated surface. Prior to mounting the MBC system the base concrete surface has to be primed using a silt-up product (primer) to prevent moisture transport from the wet mortar to the base concrete. A first layer of mortar is immediately applied to the primed surface. Next, the CFRP grid is placed on the first layer of mortar followed by an additional layer of mortar being applied on top of the grid. The thickness of the mortar depends on the maximum grain size in the mortar. The hand-lay up method, after sandblasting, is shown in four steps in Figure 10. All of the evaluated specimens are strengthened with the MBC system using the hand lay-up method in laboratory conditions of 20°C and 60% relative humidity (RH).

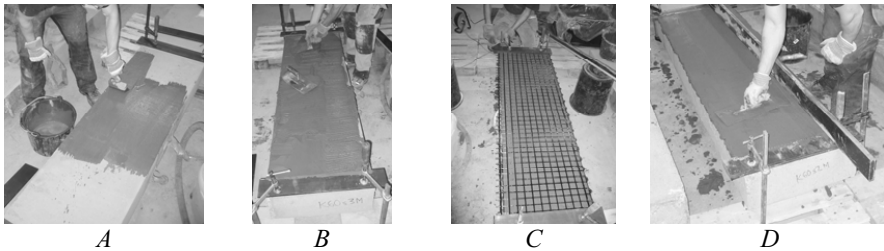


Figure 10. Hand lay-up of the MBC strengthening system. A) surface primer, B) first layer of mortar, C) placement of CFRP grid and D) last layer of mortar.

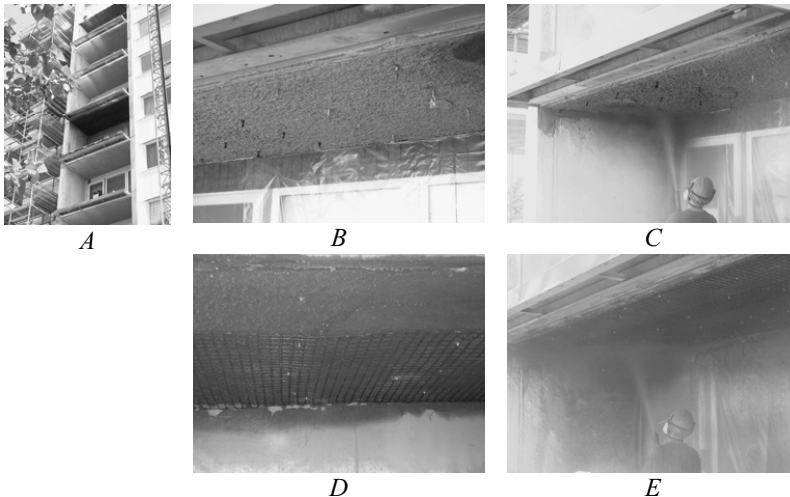


Figure 11. In-situ production method for the MBC strengthening system. A) Balconies to be strengthened, B) Concrete surface to be strengthened, studs applied, C) first layer of mortar is being sprayed, D) Mounting of the CFRP grid to the studs and E) Last layer of mortar is being sprayed.

When strengthening large structures, the hand lay-up method might be too time consuming and uneconomical depending on the size of the project. Figure 11 shows the strengthening of a balcony for flexure. The mortar is applied by shotcreting. These balconies were strengthened on the bottom side of the slab. This involves mounting the MBC system vertically from below. The production method generally consists of the same procedure as the laboratory hand lay-up method. However, to prevent the CFRP grid from falling down, a number of steel studs were nailed to the surface of the base concrete. The grid is fastened to these studs after the first layer of mortar has been applied. The first mortar layer is applied by spraying and the peak of the studs act as a maximum distance measurement to ensure that the right mortar layer thickness is being obtained. After attachment of the CFRP grid, a second layer of mortar is sprayed on. Prior to applying the mortar the surface was roughened by sandblasting and then primed. It is also possible to mount the grid to the studs and then apply the mortar by spraying directly onto the grid in one layer, thus reducing the workmanship by one step.

Strengthening for shear

In this study, 8 concrete beams were evaluated for shear strengthening purposes, comprising unstrengthened and strengthened concrete beam specimens. The strengthening consists of using epoxy bonded CFRP sheets, a cementitious bonding agent only and the MBC system. Beams strengthened with the use of epoxy bonding agents and CFRP sheets were performed by [31]. Set-up for all beam specimens were four-point bending. The geometries and reinforcement scheme are recorded in Figure 12. The concrete beams are reinforced in such a way that shear failure is directed to one of the shear spans. The design of the steel reinforcement is detailed below. This design of the reinforcement is motivated by the fact that due to the lack of shear reinforcement in one span, the beams only need to be strengthened in this span. Thus, the other shear span is heavily reinforced with steel stirrups. Common to all of the concrete beams is that they are reinforced with 12 Ø16 steel bars at the bottom and 2 Ø16 at the top of the beam as flexural and compression reinforcement. The shear reinforcement contains Ø12 steel bars with a distance 50 mm at the supports and Ø12 with the distance 100 mm in the heavily reinforced shear span. The densification of the shear reinforcement over the supports is supposed to prevent crushing and peeling failures and secure the anchorage of the longitudinal reinforcement. All of the steel reinforcements have the characteristic yield strength of 500 MPa. For a more comprehensive study the reader is referred to [32]. The latter includes a vast monitoring set-up using strain gauges and photometric measurement. [33] and [32] also contain the interaction between the MBC system and steel shear reinforcement and crack propagation for different magnitudes of shear load. The beam specimen strengthened with the epoxy based system utilizes vertically applied unidirectional carbon fibre sheets (200g/m²). Beams strengthened with the MBC system utilize three different CFRP grids, see Table 6. One of the beam specimens was strengthened using only mortar. The mortar used in this study had a maximum grain size of 1 mm, tensile strength of 5.4 MPa, modulus of elasticity 26.5 and compression strength of 45.0 MPa. The failure mode and strengthening effect for the studied beam is reported in Table 7. Four specimens were loaded by a deformation control of 0.01 mm/sec and specimens noted with a * which were load controlled at 10 kN/min.

Table 6. Manufacturer provided properties of the fibres in vertical CFRP tows.

| CFRP grid | Total fibre amount (g/m ²) | Transverse fibre amount (g/m ²) | Elastic modulus (MPa) | Tensile strength (MPa) | Tow distance (mm) |
|-----------|--|---|-----------------------|------------------------|-------------------|
| 1 | 66 | 32 | 589 | 4300 | 24 |
| 2 | 98 | 51 | 288 | 3800 | 70 |
| 3 | 154 | 84 | 284 | 3800 | 44 |

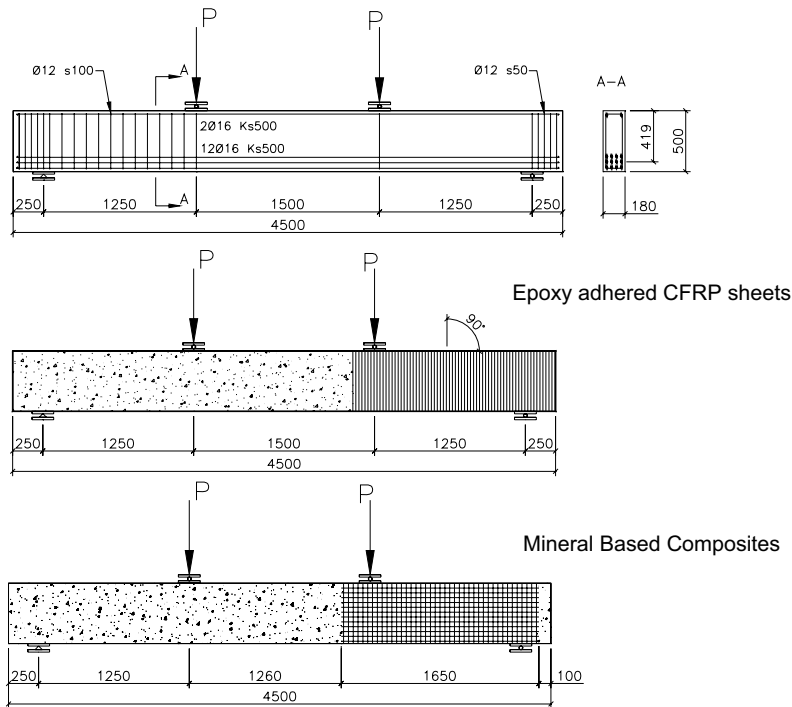


Figure 12. Test set-up and geometry for the reference and strengthened beams.

Table 7. Summary of beams strengthen for shear with MBC

| Specimen | Strengthening | Bonding agent | Peak force (kN) | Failure mode | Strengthening effect ^A |
|----------|------------------|---------------|-----------------|-------------------|-----------------------------------|
| R | - | - | 123.5 | Shear | - |
| R* | - | - | 126.7 | Shear | - |
| M | Only mortar | Mortar | 141.9 | Shear | 1.15 |
| MG3 | MBC with grid 3 | Mortar | 244.9 | Rupture of fibres | 1.98 |
| ES | Epoxy with sheet | Mortar | 259.9 | Debonding | 2.10 |
| MG1* | MBC with grid 1 | Mortar | 208.1 | Rupture of fibres | 1.68 |
| MG2* | MBC with grid 2 | Mortar | 206.4 | Rupture of fibres | 1.67 |
| MG3* | MBC with grid 3 | Mortar | 251.9 | Rupture of fibres | 1.99 |

^A Calculated as maximum peak load divided by peak load of the reference beam

Using mortar only to increase the cross section will contribute to the shear capacity with 15%. Using a grid with a higher fibre amount will generate a higher strengthening effect. The geometry of the studied grid seems to have little influence of the crack formation. However, using a grid with small tow distance will generate a higher first crack load. This should probably depend on the faster redistribution of tensile stresses. There is no large variation in strengthening effect when comparing the MBC system to the epoxy bonded carbon fibre sheet. It should be noticed that the fibre amount in the epoxy bonded sheets is almost 138% higher in the vertical direction compared to the MBC system. However, the failure mode for the sheets was debonding and ultimate strength of the fibres was not fully utilized.

Strengthening for flexure

The CFRP grid used in this study is the same as grid 3 in Table 6. Six slabs were tested, one reference slab, one with additional steel reinforcement, one with a carbon fibre sheet and three with the MBC system. Three different designs regarding the CFRP grid in the MBC strengthening were utilized. In one of the strengthened specimens an ordinary design of the grid was used, see section 2.3. In another, sand was adhered to the surface of the grid to enhance the mechanical interlocking to the mortar. In the last specimen, two layers of grid were used to increase the total fibre amount. The experimental set-up for the slabs was four point beam bending, with a distance of 3860 mm between the supports and 1333 mm to the line loads from the supports. Strengthening schemes and experimental set-up are shown in Figure 13. All the slabs have the same dimensions (4000 x 1000 mm), though they have been strengthened by different methods. The slabs were flexural reinforced with 10 ϕ 8 Ks 500 standard steel reinforcement. Table 6 shows the manufacturer provided material properties of the CFRP grid and carbon fibre sheet together the laboratory tested quality of the steel reinforcement.

Slab No 1 was a reference, steel reinforced concrete beam without any strengthening. Slab No 2 was strengthened with 4 extra steel reinforcement bars, ϕ 8. Slabs No 3, 4 and 6 were strengthened with the MBC system. The internal tow distance of the grid was 44 x 44 mm with a total cross sectional area corresponding to 21 mm²/m in the tensile bending direction. Note slab No 3 had a sanded surface on the grid and that slab No 6 had dual layers of CFRP grid. The total thickness of the cementitious layer and the CFRP grid was approximately 10 mm. Slab No 5 was strengthened with three carbon fibre sheets with a cross sectional area corresponding to 62 mm²/m of the slab in the bending tensile direction.

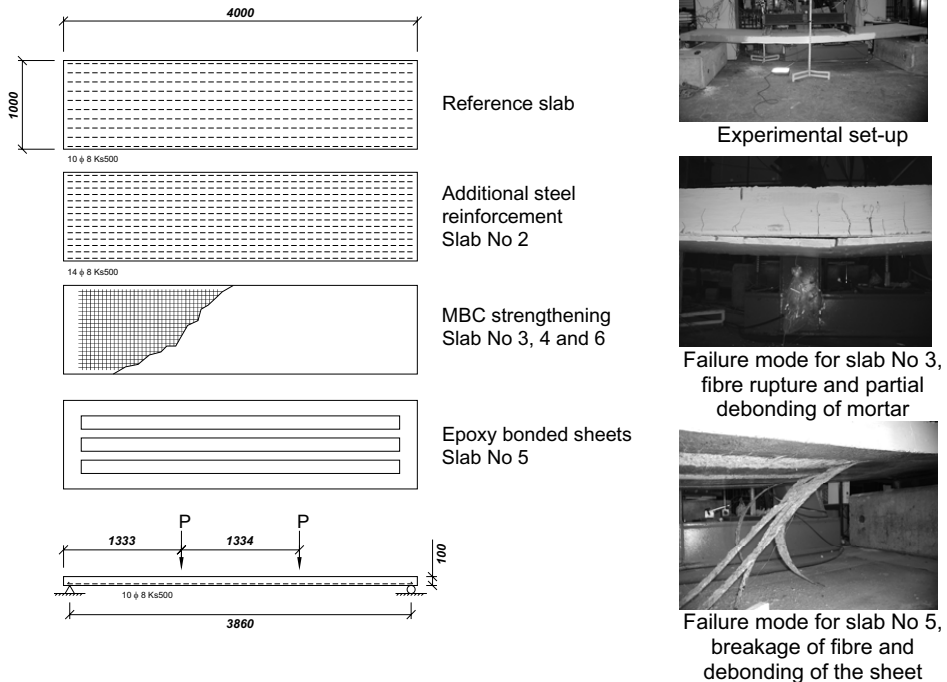


Figure 13. Experimental set-up of evaluated beam specimens.

Table 8. Material properties for steel and composites.

| Material | Tensile strength (MPa) | Elastic modulus (GPa) |
|--------------------|------------------------|-----------------------|
| Steel ϕ 8 | 483 | 209 |
| CFRP grid | 3800 | 253 |
| Carbon fibre sheet | 3600 | 228 |

The slabs were loaded with two line loads up to failure and the loading was deformation controlled with a load rate of 0.03 mm/s. This rate was doubled when the steel in the slab reached yielding. A summary of the beam specimens is shown in Table 9, note that the slab with two layers of carbon fibre grid (No 6), sustained the highest load at failure. Slab No. 3 reached failure earlier than the other slabs due to fibre breakage, which was due to the bond between the sanded grid and the cementitious bonding agent probably being too high, resulting in high stress concentrations. As a consequence, a failure arose at a crack in the cementitious bonding material. In slab No. 4, debonding between the CFRP grid created a small slippage between the cementitious bonding materials. This provided for a higher load since the stress concentrations were smeared out over a short distance, i.e. discrete stress concentrations could be avoided. Slabs No. 2, 4 and 5 reached approximately the same failure load. The slab with extra steel reinforcement, No. 2, showed stiffer behaviour than slabs No. 3, 4 and 5. The right-hand side in Figure 13 shows a photo of failure modes for slabs No 3 and No 5. For both of these slabs, debonding occurred after fibre breakage. This was not the case for slabs No. 2, 4 and 6, where extensive cracking and large deflections preceded fibre breakage. This may also be noticed in Figure 13, where large deflections were obtained for all these slabs. In addition slab No 6 obtained the highest failure load and was also the stiffest slab of the ones tested. Also the cracking and steel yielding loads were considerably higher for slab No 6 compared to the other slabs. Here it should also be noted that slab No 6 had a lower fibre content at the cross sectional area in the tensile direction. For a more detailed analysis of this study the reader is referred to [34].

Table 9. Summary of flexural strengthened beam specimens.

| Slab | Strengthening | Bonding agent | Peak force (kN) | Failure mode | Strengthening effect |
|------|--|---------------|-----------------|--------------------------------|----------------------|
| 1 | ---- | ---- | 25 | | - |
| 2 | Extra steel 4 no ϕ 8 ^a | ---- | 38 | Large deflection/yielding | 1.52 |
| 3 | MBC, sanded grid | Mortar | 35 | Fibre rupture | 1.40 |
| 4 | MBC, ordinary grid | Mortar | 40 | Large deflection/Fibre rupture | 1.60 |
| 5 | Epoxy bonded sheet | Epoxy | 41 | Fibre rupture/debonding | 1.64 |
| 6 | MBC, 2 layers of grid | MBC | 51 | Large deflection/Fibre rupture | 2.04 |

DISCUSSION AND CONCLUSION

It is not entirely reasonable to compare the different achieved strengthening effects between the different cement based strengthening systems. The reason for this originates in the experimental set-up design and size of the specimens. One major influencing parameter is the design of the steel reinforcement in the base concrete. But, it can clearly be stated that these strengthening systems all give a contribution to the load bearing capacity but with different strengthening effects. All evaluated tests on large scale specimens were deformation controlled and the deformation rate ensured similar redistribution of stresses and strains in the specimens. Nevertheless, a summary of flexural and shear strengthened specimens for all systems are shown in Table 10. The summarised specimens and strengthening system are all based on the best performing specimens with fibre rupture as failure mode. However, the failure mode was not stated for the flexural strengthened specimen using the TRC system. From Table 10 it can be concluded that for flexural strengthening all systems generated similar strengthening effects using approximately the same amount of carbon fibres in the tensile direction. However the FRC system was applied on small scale specimens with no steel reinforcement, for these specimens the size effect is not considered. Regarding the shear strengthening the TRM and MBC systems provided almost similar strengthening effects, for failure mode in shear, with the use of almost the same amount of carbon fibres. It should also be noted that the TRM system was wrapped around the beam and therefore prohibited to fail by debonding while the MBC system was side bonded. In retrofitting of existing structures fully wrapping is often not possible. For the TRC system in shear using glass fibres, an excessive amount of glass fibres is needed to generate a very small strengthening effect.

When using textile fabrics, there is a limitation on how many layers that can be used effectively. Using too many layers will create anchorage problems and generate debonding. This is especially apparent for shear strengthening with insufficient anchorage length in the compressed zone. However, using mechanical anchorage can delay and even avoid debonding. Using non impregnated sheets, grids or textiles will generate larger slips and inferior effective strain over the roving cross section. The reason for this is that total penetration of the cement based bonding agent in the fibre roving is difficult or even impossible to achieve. Using impregnated fibres (fibres imbedded in a matrix) will create a more effective strain distribution in the FRP tow. A better utilisation of the fibres will be achieved by stress transfer of the matrix and a mechanical interlocking in the mortar. Also the connection points between tows/rovings become more rigid which ensures less slippage and thus further enhance the mechanical interlocking. Another aspect of full utilisation of the fibres is the inclination of the fibres to the cracks. If the direction of fibre rovings or tows are applied perpendicular to the principal stress direction (crack inclination) a better utilisation should be achieved. This should have been the case for the shear strengthened TRC specimens. But in this case the choice of fabrics was the limiting parameter.

By wrapping the non impregnated fibres around the beam (as the case for shear strengthening using the TRM system) will create an infinite anchorage for the textiles and therefore a higher strengthening effect. This complete wrapping of the beam may become difficult to achieve in retrofitting an in-situ structural beam. By comparing the use of different fibre material then it is clear that the use of carbon fibre has the greatest structural advantage and the total amount of fibres to reach the same bearing capacity will be much lower. However, wrapping is not possible when using an epoxy impregnated carbon fibre grid due to the rigidity and brittleness of the matrix. Using textiles makes wrapping around corners much easier. Using a semi elastic matrix, e.g. latex, which still ensures rigid connection points but allows wrapping around corners could be a beneficial solution for ensuring rigidity, anchorage and effectiveness of the fibres.

The epoxy based systems have a slightly better performance compared to the cement based system, due to the superior bond between epoxy and the fibres. However, the MBC system for flexural strengthening needed a smaller carbon fibre area, in the tensile direction, to generate a higher bearing capacity compared to the epoxy bonded sheets. Increasing the bond between mortar and fibres by the use of sand, bonded to the surface of the CFRP grid, will cause high stress concentration and premature fibre rupture for flexural strengthening.

It should also be mentioned that none of the mortars used in the presented cement based systems for shear strengthening had any chopped or milled fibres, e.g. PVA, PP, glass, carbon etc. By using a mortar with chopped or milled reinforcing fibres should postpone large crack openings by the crack bridging ability of these fibres and thus create a more durable structure in service limit state. If the base concrete has a large chloride penetration depth then these cement based bonding agents should provide a more sustainable repair or upgrading system due to their permeability and the chloride peak would therefore equilibrate. For fully covered concrete surfaces the use of impermeable epoxy based systems may create durability problems for the steel reinforcement. Regarding the long term behaviour for the case of using the MBC strengthening, commercially available mortars with proven sustainability were employed. CFRPs have good long term behaviour if protected against UV radiation, which is the case when embedded into a cement matrix. Note, that it may be difficult to achieve fully resistant glass fibres in an alkaline environment. Another important aspect to be considered is the bond between cement based bonding agent and base concrete. Here, the preparation of the surface of the base concrete is crucial thus removing all poor concrete to ensure ultimate bonding characteristics. Complicated or poor anchoring details could also be a source of shortened service life of the strengthening systems.

Cost and labour effective application techniques have to be established to be able to successfully implement the strengthening system for structural retrofit. One example of effective application techniques are shotcreting the system, which can be done for the MBC and TRC systems. No industrialised application techniques have been recorded for the TRM and FRC systems.

Table 10. Summary of strengthening effects for evaluated systems.

| Strengthening system | Strengthening | Failure mode | Fibre type | Fibre amount | Strengthening effect |
|----------------------|---------------|---------------|------------|-----------------------|----------------------|
| TRC | Flexural | - | Carbon | 50 mm ² | 1.86 |
| FRC | Flexural | Fibre rupture | Carbon | 40 mm ² | 2.03 |
| MBC | Flexural | Fibre rupture | Carbon | 42 mm ² | 2.04 |
| TRC | Shear | Fibre rupture | Glass | 2820 g/m ² | 1.16 |
| TRM | Shear | Fibre rupture | Carbon | 168 g/m ² | 1.71 |
| MBC | Shear | Fibre rupture | Carbon | 154 g/m ² | 1.99 |

REFERENCES

1. Rizkalla, S. Hassan, N & Hassan, T. "Design recommendations for the use of FRP for reinforcement and strengthening of concrete structures". *Progress in Structural Engineering and Materials*, Vol. 5, No. 1, February 2003, pp. 16–28.
2. Nordin, H., & Täljsten, B. "Concrete beams strengthened with prestressed near surface mounted CFRP". *Composites for Construction*, Vol. 10, No. 1, January 2006, pp. 60-68.
3. Holmgren, J., & Badanoiu, A. "Cementitious composites reinforced with continuous

- carbon fibres for strengthening of concrete structures”. *Cement and Concrete Composites*, Vol. 25, No. 3, April 2003, pp. 387-394.
4. Li, Z., & Ding, Z. “Property improvement of Portland cement by incorporating with metakaolin and slag”. *Cement and Concrete Research*, Vol. 33, No. 4, 2003, pp. 579-584.
 5. Hewlett, P.C. “Cement Admixtures, Uses and Applications”. Longman Scientific and Technical (2nd ed), 1988, pp 85-101.
 6. Ohama, Y. “Polymer-based admixtures”. *Cement and Concrete Composites*, Vol. 20, No. 2, April 1998, pp. 189-212.
 7. Van Gemert, D., Czarnecki, L., Maultzsch, M., Schorn, H., Beeldens, A., Lukowski, P., & Knapen, E. “Cement concrete and concrete–polymer composites: Two merging worlds: A report from 11th ICPIC Congress in Berlin, 2004”. *Cement and Concrete Composites*, Vol. 27, No. 9-10, October 2005, pp. 926-935.
 8. Pascal, S., Alliche, A., & Pilvin, Ph. “Mechanical behaviour of polymer modified mortars”. *Materials Science and Engineering A*. Vol. 380, No. 1-2, August 2004, pp. 1-8.
 9. Groth, P. “Fibre Reinforced Concrete”. Doctoral thesis, Luleå University of Technology, division of structural engineering. 2000.
 10. Cuypers, H., Wastiels, J., Van Itterbeeck, P., De Bolster, Orlowsky, E. J., & Raupach, M. “Durability of glass fibre reinforced composites experimental methods and results”. *Composites Part A: Applied Science and Manufacturing*, Vol. 37, 2006, pp. 207-215.
 11. Agopyan, V., Savastano, H., V.M., & Cincotto, M.A. “Developments on vegetable fibre–cement based materials in São Paulo, Brazil: an overview”. *Cement and Concrete Composites*, Vol 27, 2005, pp. 527-536.
 12. Li, V.C., & Fisher, G. “Reinforced ECC – An evolution in from materials to structures”. *In the first FIB Congress*, Osaka, Japan, October 2002, pp. 105-122.
 13. Garcés, P., Fraile, J., Vilaplana-Ortego, E., Cazorla-Amorós, D., Alcocel, E. G., & Andión, L. G. “Effect of carbon fibres on the mechanical properties and corrosion levels of reinforced □odellin cement mortars”. *Cement and Concrete Research*, Vol. 35, 2005, pp. 324-331.
 14. Gutiérrez, R.M., Díaz, L.N., & Delvasto, S. “Effect of pozzolans on the performance of fibre –reinforced mortars”. *Cement and Concrete Composites*, Vol. 27, 2005, pp. 593-598.
 15. García Santos, A., Rincón, J. M., Romero, M., & Talero, R. “Characterization of a polypropylene fibered cement composite using ESEM, FESEM and mechanical testing”. *Construction and Building Materials*, Vol. 19, 2005, pp. 396-403.
 16. Paipetis, A., & Galiotis, C. “Effect of fibre sizing on the stress transfer efficiency in carbon/epoxy model composites”. *Composites Part A: Applied Science and Manufacturing*, 27, 1996, pp. 255-267.
 17. Mobasher, B., Pahilajani, J., & Peled, A. “Analytical simulation of tensile response of fabric reinforced cement based composites”. *Cement and Concrete Composites*, Vol. 28, 2006, pp. 77-89.
 18. Peled, A. “Textile cement based composites, effects of fabric geometry, fabric type and processing”. *Composites in Construction 2005 – Third International Conference*, Lyon, France, July 2005.
 19. Brueckner, A., Ortlepp, R., & Curbach, M. “Anchoring of shear strengthening for T-beams made of textile reinforced concrete (TRC)”. *Materials and Structures*, Vol 41, No 2, March 2008, pp. 407-418.
 20. Brueckner, A., Ortlepp, R., & Curbach, M. “Textile reinforced concrete for strengthening in bending and shear”. *Materials and Structures*, Vol 39, No 8, October

- 2006, pp. 741-748.
21. Weiland, S., Ortlepp, R., & Curbach, M. (2006) "Strengthening of predeformed slabs with textile reinforced concrete". *Proceedings of the second International fib-Congress CEB-FIP*, Naples, June 2006.
 22. Holler, S., Butenweg, C., Noh, S. Y., & Meskouris, K. "Computational model of textile-reinforced concrete structures". *Computers & Structures*, Vol. 82, 2004, pp. 1971-1979.
 23. Chudoba, R., Vořechovský, M., & Konrad, M. "Stochastic modelling of multi-filament yarns. I. Random properties within the cross-section and size effect". *Solids and Structures*, Vol. 43, 2006, pp. 413-434.
 24. Häußler-Combe, U., & Hartig, J. "Bond and failure mechanisms of textile reinforced concrete (TRC) under uniaxial tensile loading". *Cement & Concrete Composites*, Vol 29, No 4, April 2007, pp. 279-289.
 25. Wu, H.C., & Teng, J. "Innovative Cement Based Thin Sheet Composites for Retrofit". Third International Conference on Composites in Infrastructures, San Francisco, US, June 2002.
 26. Wu, H.C. "Design Flexibility of Composites for Construction". In *International Conference on Fiber Composites, High Performance Concretes and Smart Materials*. Parameswaran, India, 2004, pp. 421-432.
 27. Wu, H.C., & Sun, P. (2005) "Fiber Reinforced Cement Based Composite Sheets for Structural Retrofit". *International Symposium on Bond Behavior of FRP in Structures*, Hong Kong, December 2005, pp. 351-356.
 28. Li, V.C. "On engineered cementitious composites". *Advanced Concrete Technology*, Vol 1, No 3, August 2003, pp. 215-230.
 29. Triantafillou, T.C., & Papanicolaou, C.G. "Shear strengthening of reinforced concrete members with textile reinforced mortar (TRM) jackets". *Materials and Structures*, Vol 39, No 1, April 2006, pp. 93-103.
 30. Carlsvärd, J. "Shrinkage cracking of steel fibre reinforced self compacting concrete overlays – Test methods and theoretical modelling". Doctoral thesis, Luleå University of Technology, Division of Structural Engineering, 2006.
 31. Carolin, A. (2003) "Carbon Fibre Reinforced Polymers for Strengthening of Structural Elements". Doctoral thesis, Luleå University of Technology, 2003
 32. Blanksvärd, T. "Strengthening of concrete structures by the use of mineral based composites". Licentiate thesis, Dept. of Structural Engineering, Luleå University of Technology, Luleå, 2007, 300 pp.
 33. Blanksvärd T., Carolin A. and Täljsten B., (2008), "*Shear crack propagation in MBC strengthened concrete beams*". Proceeding of the fourth International Conference on FRP Composites in Civil Engineering, Zurich, Switzerland, 22-24 July 2008, CD-Publication and extended abstracts.
 34. Täljsten, B., & Blanksvärd, T. "Mineral based bonding of carbon FRP to strengthen concrete structures". *Composites for Construction*, Vol 11, No 2, March 2007, pp. 120-128.

PAPER IV

“From material level to structural use of mineral based composites – An overview”

BY

Katalin Orosz, Thomas Blanksvärd, Björn Täljsten and
Gregor Fisher

Submitted to

Journal of Materials and Structures in March 2009

From material level to structural use of mineral based composites- An overview

Katalin Orosz^{1,2}, Thomas Blanksvärd³, Björn Täljsten^{1,3} and Gregor Fischer¹

1. Technical University of Denmark, Dept. of Civil Engineering, Kgs. Lyngby, Denmark
2. Norut Narvik Ltd, Group Material Technology, Narvik, Norway
3. Luleå University of Technology, Div. of Structural Engineering, Luleå, Sweden

Abstract This paper surveys different material combinations and applications in the field of mineral based strengthening of concrete structures. Focus is placed on mechanical behaviour on material and component levels in different cementitious composites; with the intention of systematically map the applicable materials and material combinations for mineral based strengthening. A comprehensive description of a particular strengthening system developed in Sweden and Denmark, denominated as Mineral Based Composites (MBC), together with tests from composite material properties to structural elements is given. From tests and survey it can be concluded that the use of mineral based strengthening system can be used to increase the load bearing capacity of the strengthened structure. The paper concludes with suggestions on further development in the field of mineral based strengthening.

Keywords: concrete, mortar, strengthening, mineral based composites (MBC), fibre reinforced polymers (FRP), strain hardening cementitious composites (SHCC), cracking, bond

1 Introduction

The existing civil engineering infrastructure is a very important element of the economical potential of a majority of the countries worldwide. A large number of today's buildings, transportation systems, and utility facilities are built with reinforced concrete and many of these systems are currently reaching the end of their expected service life. Additionally, increased loads and traffic flows, reuse and ongoing deterioration even affect the durability of structures that are less than 20 years old.

There exist several repair and strengthening methods that can be applied to existing concrete structures for this purpose, such as cross section enlargement of critical elements, span shortening with additional supports, external/internal post tensioning, and steel plate bonding or strengthening with fibre reinforced polymer (FRP) composites. Since the end of the 1980s, the use of FRP has been researched and applied increasingly for the rehabilitation of existing concrete structures. Externally epoxy-bonded FRP systems have been proven to be an effective strengthening method in repairing or strengthening structures and a large amount of literature is published on

this topic; see e.g. [1-7]. FRP reinforcements can be used in numerous ways to strengthen a structure. E.g., by bonding plates or sheets with a high quality epoxy to the surface of concrete, timber or even steel structures. There are also methods to wrap columns for enhanced ductility and strengthening systems where FRP rods are embedded in the concrete surface. Systems replacing the epoxy with polymer-modified mortars have been recently developed. E.g., continuous fibre sheets can be embedded in a layer of mortar to provide e.g. confinement to a column; however, lately these sheets have been replaced by textiles due to bond issues related to difficulties with penetration as described in [8]. Biaxial or multidimensional FRP textiles are used in textile reinforced concrete (TRC) [9, 10] systems or, textile reinforced mortar (TRM) jacketing, see e.g. [11].

In this paper a state-of-the-art report using mineral based FRP strengthening systems are presented together with information about recent research at Luleå University of Technology (LTU), Sweden, and Technical University of Denmark (DTU). The literature survey is selective to published applications in which a fibre component has been used together with a cementitious bonding agent, referred to as “mineral based strengthening” in general. The authors also involved research and results from the field of ductile cementitious mortars which could be used together with an FRP component resulting in a high-performance strengthening material. The research significance within this paper is the mapping of possible design of different mineral based strengthening systems. In addition, a systematic mapping of the novel strengthening system named mineral based composites (MBC), developed at LTU and DTU, going from material science to composite behaviour as well as some outlines for applications to existing structures are presented.

2 Definition and development of mineral based strengthening systems

“Mineral based strengthening” in a broader perspective may be referred to any kind of a strengthening system in which a fibre component is embedded into a mineral based binder to repair or strengthen existing concrete structures. Mineral based strengthening in this context would include applications as surveyed in Section 3 from textile reinforced mortar/concrete through fibre reinforced cement to FRP grid applications.

Mineral based strengthening systems are originally derived from other externally bonded FRP systems. The most commonly used adhesive to bond the FRP element to the surface of the structure (mainly concrete) is the epoxy adhesive. The use of epoxy has proven to give excellent force transfer. It bonds to the majority of surfaces (concrete, steel, timber, etc.) and shows to be durable and resistant to many different environments. However, some drawbacks can be identified. Firstly, epoxy as a bonding agent may create problem in the working environment, secondly, epoxy is recommended to have a minimum application temperature, often above 10°C, and thirdly, epoxy creates diffusion-closed (sealed) surfaces which may imply moisture and freeze/thaw problems for concrete structures. There might also be bond problems

applying epoxy to wet or humid surfaces. To avoid some of these problems alternative strengthening systems have been researched and are currently being developed.

In mineral based strengthening systems, the traditional epoxy bonding agent to adhere the FRP to the concrete surface is being replaced by cementitious matrices to bond the fibre material to the concrete surface. Mineral based strengthening systems are made by replacing part of the cement hydrate binder of conventional mortar with polymers which, with the addition of fibre composites, become a high-performance external strengthening system for existing concrete structures.

3 Concept of mineral based strengthening

Mineral based strengthening systems are dealt with in three different levels. At the material level, the raw materials used in a mineral based composite system such as binders (different quasi-brittle or strain hardening mortars), FRP reinforcement (dry fibres, textiles, grids) and the most important properties of those are defined (Fig. 1). At the component level, larger strengthened elements are discussed, e.g. beams strengthened in flexure and shear. At the level of structural behaviour, field applications can be mentioned.

The intersection between material and component level would contain the different interactions between constituents and the effects of those on the structural behaviour (bond transfer mechanisms, fibre bridging and strain hardening).

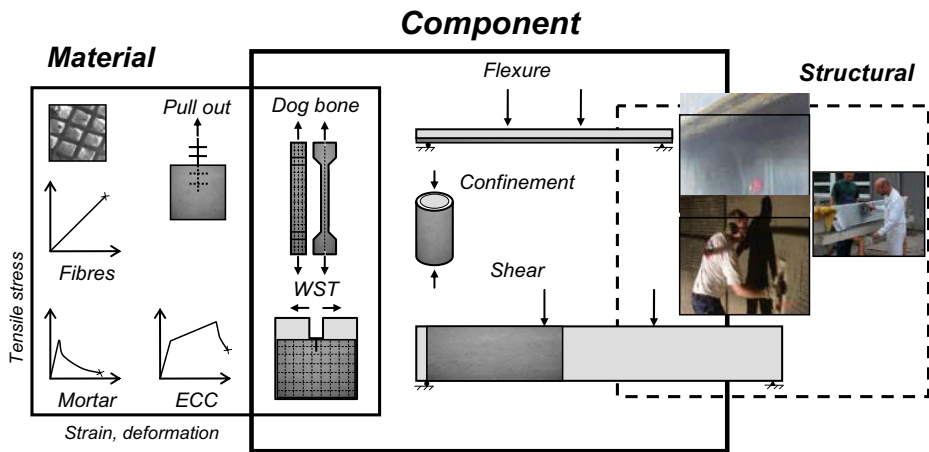


Fig. 1 From material to structural level

3.1 Materials for mineral based strengthening

A list of requirements is proposed in [11] which should be met for a successful and efficient mineral based strengthening. The mortar phase should have very low shrinkage deformations, high workability (application should be possible using a

trowel, or shotcreted); high viscosity (application should not be problematic on vertical or overhead surfaces); low rate of workability loss (application of each mortar layer should be possible while the previous one is still in a fresh state); and sufficient shear (hence tensile) strength, in order to avoid premature debonding. In case E-glass fibre textiles are used, the mortar-based matrix should be of low alkalinity. Li, [12], also adds a few requirements on the “future concrete” which the authors feel relevant for a concrete-like repair and strengthening material as well: the “concrete” should be highly ductile with the ability of “yield” like a metal when overloaded to prevent unpredictable and sudden failure; highly durable and sustainable. These justify involving ductile mortars into the MBC system.

Mapping of the materials that have been or are promising to be used in mineral based strengthening systems is shown in Fig. 2. The integrated materials in the mineral based strengthening systems can be divided in two main groups, binders and fibre composites. The components used in practical applications are detailed in the following.

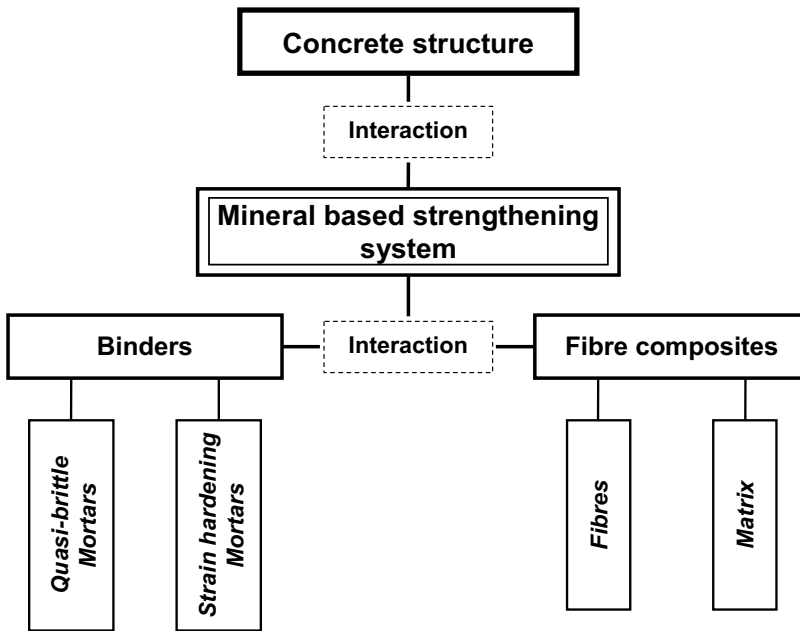


Fig. 2 Overview of the constituents and possible interaction in mineral based strengthening systems

3.1.1 Binders

Binders in practical applications are either quasi-brittle, conventional polymer-modified or more ductile, strain hardening mortars.

Quasi-brittle mortars

Polymer-modified mortar (PMM) is the most widely used [13], suitable mortar in a mineral based strengthening system. Polymeric admixture, or cement modifier, is defined as an admixture which consists of a polymeric compound that acts as a main ingredient when modifying or improving the properties such as strength, deformation, bond strength, or durability of mortars and concretes. The polymer-modified mortars or concretes therefore contain two types of binder, the hydraulic cement and the polymeric admixture. Polymeric admixtures can be latexes, powdered emulsions, water soluble polymers and liquid resins. Adding polymeric compounds to the fine-grained mortar phase is also common to enhance mechanical properties of textile reinforced concrete (TRC) or mortar. In [14], improved interfacial bond is achieved by a secondary polymeric cohesive matrix within the mortar phase. In general, the properties of a polymer-modified mortar (or concrete) depend significantly on the polymer content or polymer-cement (P/C) ratio rather than the water-cement ratio compared with ordinary cement mortar [16].

Increasing the P/C ratio to about 10-15% by weight has shown to increase the flexural strength. A P/C ratio higher than 15% by weight decreases the mechanical strength [16, 17]. Another source, [18] states that an addition of polymeric dispersion up to even 20% by weight results in a higher tensile strength of the (textile reinforced) concrete.

To further enhance the properties of a PMM, e.g. workability, flowability, mechanical properties etc. of the mortars, superplasticizers, silica fume, fly ash and reinforcing fibres can be used.

Fibres in the matrix can be chopped or milled fibres. The fibres must be easily dispersed in the mixture, must have suitable mechanical properties, and must be durable in the highly alkaline cement matrix. They are randomly (in a good mix, uniformly) distributed throughout the mortar/concrete. Continuous fibres are more effective in increasing strength in a certain direction compared to randomly distributed short fibres, but they are not easily mixed into the cement matrix and their high cost does not allow them to be widely used. Different types of fibres are currently used such as steel, glass, carbon, polyvinyl-alcohol (PVA), polypropylene, nylon and natural fibres depending on the structural needs. Using a small percentage of carbon fibre addition (~0.5%), a considerable increase in flexural strength is achieved relative to unreinforced mortar [19]. Other researchers have investigated new type of fibres, such as ceramic fibres [20]. The results show that the flexural strength of mortar can be increased and also the durability of this ceramic fibre reinforced mortar is much better than that of alkali-resistant (AR) glass fibre. The use of steel fibres is the most common solution to enhance toughness of a steel fibre reinforced concrete (conventional FRC). For enhanced ductility, first cracking strength or ultimate tensile strength, other types of fibres may be more suitable. The addition of small volume fractions of synthetic fibres (up to 2%) to the mortar can improve the toughness of the mortar [21]. Among these fibres, the polypropylene fibres are very popular in concrete and the nylon fibres are recently becoming more widely used [22]. The propylene fibres reinforce the concrete performance under flexure, tension, impact blows and

plastic shrinkage cracking. On the other hand, the nylon fibres improve the performance after the presence of cracks and sustained high stresses. In [23], both types of fibres were compared and the results showed a better improvement of the properties when using the nylon fibres than the polypropylene fibres. Other researches [24, 25] are focusing on the use of recycled PET (polyethylene terephthalate). PET fibres made from beverage bottles were used successfully up to 3% in (normal) concrete [24]. Another study on the durability in aggressive environments of a PET-reinforced concrete [25] emphasizes the sustainability and environmentally friendliness of such concretes since the PET fibre has a long decomposition time (over 100 years to completely degrade).

Some supplementary materials should be used for counteracting the insufficiencies brought about by the addition of fibres, such as increase in porosity or decrease in compressive strength. E.g., substitute a part of the cement (20%) by silica fume increases the compressive strength of the resulting mortar and provides a reduction of porosity, which leads to an increase of the flexural strength. Adding silica fume in concretes also increase the interfacial bond strength and interfacial fracture energy by about 100% due to its smaller particle size and thereby the ability to increase the density of the microstructure of a mix [26, 27].

In concrete prepared with ordinary Portland cement, the interfaces between the hydrated cement matrix and the aggregates are the weakest link [28]. The incorporation of industrial by-products such as fly ash in concretes can significantly enhance basic properties in both the fresh and hardened states [29, 30]. It is well known that blending cement with fly ash or other supplementary cementing materials improves the rheological properties of the fresh concrete and the engineering properties of hardened concrete [31-33]. Fly ash in textile reinforced concrete is widely used to densify the grain structure [34] resulting in an improved bond between textile and concrete. Superplasticizers can also be used to improve consistency and workability.

Strain hardening mortars

Engineered Cementitious Composites (ECC) is another type of binder which can be used together with an FRP component [35]. Both in the case of repair and strengthening, the failure mechanisms that lead to the need for repair/retrofit of a structure often involve fracture. This can be overcome by materials with improved toughness, ultimate tensile strength and ductility, which justifies involving ECC into the FRP strengthening. This micromechanically designed material invented in the early 1990's represents a particular class of HPRCC (High-Performance Fibre Reinforced Cementitious Composites), exhibiting strain hardening behaviour and multiple cracking during the inelastic deformation process [36]. Since its introduction, ECC has undergone major evolution in both material development and the range of applications. Recently, it is often referred to as SHCC (strain hardening cementitious composites) due to its tensile (pseudo-) strain hardening effect of (steel reinforced) ECC, see more in detail later, which has been previously documented by Fischer and Li [37].

Besides common ingredients of cementitious composites such as cement, sand, fly ash, water and additives, ECC utilizes short, randomly oriented polymeric fibres (e.g. polyethylene, polyvinyl alcohol) at moderate volume fractions (1.5-2%). In contrast to some other types of fibres, there is a strong chemical bond between PVA and mortar which needs to be reduced [38]. This is done by a chemical coating applied on the fibre surface and additional fly ash in the mix in order to prevent premature PVA fibre rupture and thus achieve a more ductile failure mode, characterized by pull-out from the cement matrix.

The tensile strain capacity of ECC is several hundred times that of normal concrete [12] and the fracture toughness of ECC is similar to that of aluminium alloys [39]. Furthermore, the material remains ductile even when subject to high shear stresses [40]. The compressive strength of ECC ranges from 40-80 MPa depending on mix composition, the high end similar to that of high strength concrete. ECC has typically an ultimate tensile strength of 5-8 MPa and a strain capacity ranging from 3% to 5%.

There are a number of characteristics of ECC that make it attractive as a repair material. According to Li [41], the unique feature of ECC is its ultra high ductility. This implies that structural failure by fracture is less likely in comparison to normal concrete or steel fibre reinforced concrete (FRC). As a consequence, ECC has been used in a wide range of applications where ductility and/or energy absorption performance or damage tolerance of the material is an important criterion (seismic and non-seismic structural applications, see e.g. [42-46]). In contrast to quasi-brittle repair materials, ECC can eliminate premature delamination of the strengthening layer or surface spalling in an ECC/concrete repaired system [47]. Spall resistance of ECC in the surroundings of a corroded rebar in slabs has been investigated by Kanda et al. [48], where ECC accommodated the expansion by a “plastic yielding” process through radial microcracking [12]. Interface defects can be absorbed into the ECC layer, and arrested without forming spalls, thus extending the service life [39]. Suthiwarapirak et al. [49] showed that ECC has significantly higher fatigue resistance than that of commonly used repair materials such as polymer mortars. It also has a good freeze-thaw resistance and restrained shrinkage crack control [42]. ECC-reinforced shear beams behaved in a ductile manner even without additional (steel) shear reinforcement and remained ductile even for short span shear elements which typically fail in a brittle manner with normal concrete [50]. Under shear, ECC develops multiple cracking with cracks aligned normal to the principal tensile direction. Because the tensile behaviour of ECC is ductile, the shear response is correspondingly ductile. ECC as a strengthening material also offers excellent crack control. When an ECC structural element is loaded in flexure or shear beyond the elastic range, the inelastic deformation is associated with microcracking with continued load carrying capacity across these cracks [41]. The microcrack width is dependent on the type of fibre and interface properties (generally less than 100 micron when PVA fibre is used). The tight crack width in ECC has advantageous implications on structural durability [12]. When used as strengthening or repair material, fine cracks also prevent penetration of substances [51]. The spacing between multiple cracks in a typical ECC is on the order

of several mm, while the crack widths are limited to the order of 200 μm . In standalone applications, maximum crack width in ECC is a material property independent of the embedded reinforcement, unlike in RC or conventional FRC in which cracks widths are influenced by the steel reinforcement [12]. However, crack distribution of ECC as repair material is more concentrated adjacent to an existing crack in the base substrate [12].

“Flowability” or “self-compactability” of ECC refers to the ability the material that it can flow under its own weight and fill the formwork properly. Despite the presence of (short, chopped, randomly oriented, typically PVA or PE) fibres, a self-compacting ECC is able to fill in each corner of the formwork without external vibration required [52]. This would also ensure a good bond to the embedded reinforcement (such as steel or FRP).

3.1.2 Fibre Composites

Commonly used FRP reinforcements are shown in Fig. 3. FRP rods are typically used as internal reinforcement or for near-surface mounted reinforcement (NSMR). Other pultruded profiles used are thin composite plates with a typical cross section of 1.4 x 80 mm, however none of these systems will be detailed within this paper. Uniaxial fibres or fibre sheets, textiles and grids used together with mineral-based bonding agents are other types of FRP reinforcement systems, these systems are described more in detail below.

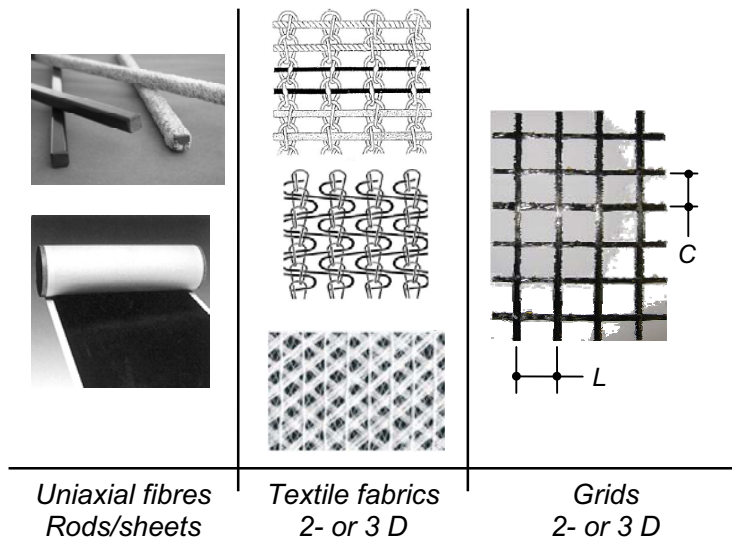


Fig. 3 Different types of fibre composites

Fabrics, textiles (knitted, woven or unwoven)

Different kinds of fibres used as FRP reinforcement and their mechanical properties are detailed e.g. in [53, 54]. There exist a few continuous long fibre applications, where non-impregnated unidirectional fibres may be embedded in a mortar phase [22], but the impregnation of continuous fibre sheets with mortars is very difficult resulting in a poor bond between fibre and mortar [8]. Fibres used in most mineral based strengthening systems usually come in the form of a textile or fabric (woven or knitted) or grid (with rigid joints), where the latter is impregnated and held together by an epoxy resin which also shapes the composite.

Fabrics are unidirectional or multidirectional FRP composites. They are widely used in textile reinforced concrete systems. The most commonly used textiles are the bidirectional woven fabrics, in which the yarns are woven together crossing them orthogonally, having a width of 300-600 mm, in large spools cut at the workplace. The density of the yarns directly affects the penetrability of the adhesive into the fabric; higher density leads to lower penetrability as the mechanical interlock acts through the fabric openings [11]. Woven fabrics are easy to adapt to any surface which makes them very suitable for wrapping (U-warp or full wrap) or confinement. The flexible shape also represents some disadvantages. The reinforcing efficiency is lower than that in straight yarns due to the crimped geometry of the woven fibres; however, this crimped geometry is advantageous in providing mechanical anchoring between the woven fabric and the cement matrix in a polymer-modified mortar. Fabrics having relatively complicated yarn shapes may enhance the bonding and improve the composite performance [11]. However, very complex textile geometries may cause premature failure of some of the yarns resulting in lower strength than the nominal strength of the fibrous phase would be, as reported in [55].

Bi- and triaxial grids with rigid joints

An FRP grid is a multidirectional prefabricated composite. For externally bonded reinforcement, grids are made of continuous fibres alternating in two directions and impregnated with a resin to form a 2D-cross laminate grid structure with rigid joints. The resin is usually epoxy and its role is to hold the fibres together and shaping the composite. The fibre amount and grid spacing often vary in the two perpendicular directions. FRP grids are typically produced in large rolls and then cut into the required dimensions. Compared to woven fabrics, FRP grids have improved mechanical properties and in general, have more rigid connection points. The improved performance is due to the aligned fibres in a certain (pre-defined) direction and that there are no unpenetrated fibres or fibre bundles which would prematurely fail (further discussed in Section 4.2 under TRC). Thinner grids are flexible and can be adapted to curved surfaces.

4 Existing mineral based strengthening systems

4.1 Continuous dry fibres

The use of continuous dry fibres are published in [56] where a pre-treatment with silica fume and high amounts of polymers improved the bond between carbon fibres and cementitious matrices. It was found that a pre-treatment with silica fume and relatively high amounts of polymers improved the bond behaviour of carbon fibre to the cement. Another report [57] has been published on large-scale tests of ordinary concrete beams strengthened with a cementitious fibre composite where the strengthening composite consisted of a unidirectional sheet of continuous dry carbon fibres and a polymer-modified mortar, applied by hand lay-up method. Both flexural and shear strengthening were investigated. From the tests it was concluded that the method works and that considerable strengthening effects can be achieved. However, in comparison with epoxy bonded carbon fibre sheets using the same amount of carbon fibre, the strengthening effect for the mineral based composite strengthening system was approximately half. The reason for this is most likely due to the reduced interfacial bond strength between the mortar and the carbon fibre reinforcement. This is also emphasized by [58], where it was found that the loading capacity of the cementitious carbon fibre composite is influenced by the amount of fibres in the tow. If the cementitious matrix penetrated into the interior of the carbon fibre tow, a higher number of filaments would be active during loading, leading to the increase in load carrying capacity.

Another way of using continuous dry fibres, usually in the form of sheets is the fibre reinforced composites (FRC) strengthening system (which may also use dry fabrics), as described by e.g., [59]. Depending on the geometry of the fibres and the strengthening purpose, the composite plates can be made as thin as 2 mm. The sheet or fabric is cut into chosen dimensions and the fibre geometry is submerged into cement slurry (matrix) for a better penetration. The impregnated sheet or fabric is then removed from the slurry and immediately bonded to the concrete surface. An improved penetration of the matrix into the fibres can be achieved by using multiple layers of continuous carbon fibres where all single layers were impregnated in cementitious slurry before bonded to the concrete surface. This procedure was also suggested in [52], however not executed.

4.2. Textile reinforced mortar (TRM) or textile reinforced concrete (TRC)

Textile Reinforced Concrete (TRC) is made from a cementitious matrix and layers of oriented, continuous fibres (technical textiles) as for reinforcement. Here TRC is only discussed as a strengthening material and not as a material also suitable for stand-alone applications such as thin shells. The most commonly used bonding agent for applying the textile on the structure is the fine grained concrete or mineral based mortar which has a grain size of less than 1 mm, and provides high strength and

flowable consistencies. Less than 2 mm of concrete or mortar thickness is needed between textile layers due to the small maximum aggregate size of the concrete mix [9]. Alkali-resistant glass (AR-glass) or carbon is used most often as the fibrous material. The fibres can be in the form of a woven textile or be unidirectional and held together by a yarn in the perpendicular direction in order to make the material easier to work with. The fabrics can be manufactured with a maximum number of four reinforcing directions depending on the load direction [9] and can therefore be tailored (the filaments are intentionally aligned in the direction of the tensile stresses leading to an increase in their effectiveness). There are several designs of textile fabrics depending on the load case and the positioning of the fabrics. Most fabrics are bi- or multi-axial warp knits and woven fabrics since they offer a great flexibility of properties and are suited for many cases.

In a TRC strengthening system, the transfer of the bond forces from one layer to another through the bonding joint must be guaranteed to ensure a full composite action. The bond behaviour of TRC is a complex property that depends both on the textile and the matrix. Due to the reinforcement geometry, only the outer filaments are directly in contact with the concrete, hence the load bearing capacity of a TRC depends mainly on the proportion of the outer to the inner filaments, and just a certain part of the tensile strength of the concrete can be activated due to the limited contact surface [14, 60]. Significant improvement in load capacity can be achieved if the textile is previously penetrated with liquid polymers [18, 60] or epoxy resins [18]. However, there is a risk that in an impregnated textile, a higher number of activated filaments would lead to abrupt failure of all filaments when the tensile strength of those is exceeded [18]. The same study also highlights that the tensile strength of a TRC (dogbone) specimen can be increased most effectively by both impregnating the textiles with polymers and adding polymer modifiers to the concrete.

TRC systems exhibiting mechanisms of distributed cracking and strain hardening behaviour (see Chapter 5.) have been used for stand-alone structural applications such as extremely thin and slender structures [61], or for repair and strengthening of existing structural members [9, 10]. Confinement strengthening of short columns both with epoxy and cement-based mortars has been investigated by [8]. Effectiveness of the TRM jacketing compared to the epoxy-impregnated counterparts resulted in a reduced effectiveness (80% for strength and 50% for ultimate strain). The strengthening effect increased with the number of confining layers and was highly dependent on the tensile strength of the applied cement mortar. Failure was more ductile in case of the TRM jacketing than in the epoxy-bonded jackets due to the slowly progressing fracture of individual fibre bundles. Shear strengthening of concrete beams has been examined in [62] on six identical RC beams with different bonding agents (epoxy and cement matrix), one or two layers of textile in different arrangements (conventional wrapping and spirally applied textiles). Two layers of mortar-impregnated textile reinforcement in the form of either conventional jackets or spirally applied strips were sufficient to increase the shear capacity of the beams tested more than 100% over the unstrengthened beam, preventing sudden shear failures and allowing activation of flexural yielding (as was the case with the resin-

based jacket). The TRM system, however, was found to be about 50% less effective than the FRP-strengthened beam. Other experiments [9, 10, 63] have been carried out on T-beams which were designed with minimum shear reinforcement but a great amount of longitudinal flexural reinforcement in order to prevent flexural failure. The strengthening fabric was a multiaxial textile applied as a U-wrap in an angle of 45° to the load direction, aligned with the principal stresses in the web of the T-beam to be strengthened. Varying parameters were the number of textile layers (2-6) placed with or without mechanical anchorage in the compression zone. The adhesive tensile load carrying capacity is crucial in the performance of the system – this determines how many layers can be anchored to the web without any additional mechanical anchorage. Tests revealed the importance of mechanically anchoring of the reinforcement. A load increase could be achieved with a few layers of textile even without anchorage to the compressive zone, however, when the adhesive tensile bond between the web and the reinforcement was exceeded, the TRC layers peeled away and therefore the reinforcement fails.

4.3 Mineral Based Composites (MBC)

MBC (mineral based composites) is defined as a system in which a FRP grid is applied onto the surface of the structure to be strengthened with a cement-based mortar as bonding matrix. MBC “inherits” the properties and behaviour of its constituents, e.g. brittleness or tension softening behaviour when the linear elastic fibre material is used together with quasi-brittle cementitious binders. However, its behaviour can significantly be changed/alterd and the material can be enforced to exhibit more ductility, multiple cracking or strain hardening in tension in a modified MBC where the mortar is a PVA-reinforced engineered cementitious composite (ECC) [64, 65]. In the recent development of MBC, two strengthening approaches meet and result in a high-performance hybrid strengthening material. One is finding the most suitable combinations of a FRP reinforcement and an existing mortar (which, depending on the application may be ordinary or polymer-modified mortar), and the other one is to strengthen/develop the mortar itself with different short fibres (in practice, mostly PVA) or involve existing, ductile mortars in order to improve the interaction between grid and mortar, tensile properties of the composite, crack spacing and crack widths, ductility and also if possible, fracture energy.

The FRP in MBC applications is normally a two-dimensional carbon fibre grid. As matrix, polymer-modified quasi-brittle mortars (PMM) are typically used. Between the two components little or no chemical bond exists. Therefore the bond strongly relies on mechanical bond, contrary to epoxy-based FRP systems. The pre-cut CFRP grid with varying grid spacing and thickness is embedded between two relatively thin layers of mortar.

To achieve a good bond between the base concrete and the mortar, the surface of the base concrete needs to be roughened, e.g. by sandblasting or water jetting, in order to remove the cement laitance. The surface preparation method normally is sandblasting. The strengthening layers can be applied by hand (hand lay-up) or shotcreting when strengthening large surfaces. The hand lay-up method includes pre-

wetting the base concrete with water for 1-3 days depending on the conditions of the base concrete and the surrounding climate. The moisture conditions in the transition zone between the base concrete and mortar are further discussed in [66], where it is found that the best bond is obtained when the base concrete has just dried back from a saturated surface. Prior to mounting the MBC system the base concrete surface has to be primed using a silt-up product (primer) to prevent moisture transport from the wet mortar to the base concrete. A first layer of mortar is immediately applied to the primed surface. Next, the CFRP grid is placed on the first layer of mortar followed by an additional layer of mortar being applied on top of the grid. The thickness of the mortar depends on the maximum grain size in the mortar.

Reliability of the system highly depends on the bond in two interface layers, between the concrete substrate and the first layer of mortar and in the between the grid in the mortar, see in [67].

5 Mineral based strengthening at material level

On the interface between the base concrete and the strengthening layer interface, such as between the fibre composite and the mortar, bond is crucial for the performance of the strengthening system. In a TRC or MBC system, bond between FRP and mortar relies mostly on mechanical interlocking (physical bond). If the mortar contains PVA fibres, a chemical bond is also being built up within the mortar phase. Good (but not overly strong) bond together with the deformation compatibility of the mortar and PVA fibres, results in fibre bridging and as a consequence, multiple cracking and overall strain hardening, resulting in a “stronger” and more ductile mortar. These mechanisms are detailed below.

5.1 Bond between base concrete and strengthening layer

When an existing RC element is to be strengthened, the tensile force developed in the strengthening layer must be introduced into the original concrete of the member by bond forces. Failure can initiate from an interfacial defect causing delamination of the whole strengthening layer in the case of a “weak” bond and spalling in the case of an overly “strong” bond [36].

Bond strength in a mineral based system generally depends on the adhesion in the interface, friction, aggregate interlocking and possibly, time-dependent factors [53].

The sensitivity of a structure to bond strength depends highly on what kind of load it is subjected to. The force transmission into the original concrete when strengthening for flexure occurs over a relatively large length (surface). In contrast, the force transmission via shear strengthening takes place only in the range behind the last shear crack [9]. As a result, significantly shorter anchorage lengths and “better bond”, and in some cases, additional anchoring is required for shear strengthening. An example is a TRC-reinforced T-beam strengthened for shear [9] where if the U-wrap around its web is not anchored into the slab via an L-shaped steel section the TRC reinforcement has a tendency to peel away from the web.

Incompatibility between the base concrete and the repair material in repair and/or strengthening systems can lead to the same bond problem and render the system ineffective resulting in debonding or spalling of the strengthening layer especially if the load is applied parallel to the bond line of the combined system. If there is an incompatibility in the elastic modulus of the base concrete and the mortar, it will result in the incompatibility of the deformations on the interface as the "weaker" material will have larger deformations [68]. If the load bearing capacity of the material or the bond at the transition zone is exceeded by the transferred load, failure will occur. Recommendations for the modulus of elasticity of the repair or strengthening material suggest a modulus at least 30% larger than the modulus of elasticity for the base concrete, [69]. When the bonding agent tensile load bearing capacity is exceeded in the interface between the base concrete and the strengthening layer, the strengthening would peel off the structure. To prevent debonding, it is usual to prescribe a minimum adhesive tensile strength of the original concrete substrate which, e.g. in German codes is 1.5 N/mm^2 [9]. If the surface is roughened adequately, by means of removing the deteriorated parts and sandblasting, a good bond can be guaranteed. Another parameter that influences the compatibility of the combined repair or strengthening system is the drying shrinkage. As the fresh repair or strengthening material has a tendency to shrink, the more or less older base concrete acts as a rigid foundation that restrains these movements. These differential movements cause tensile stresses in the repair or strengthening material and compressive stresses in the base concrete. Creep in this context can be an advantage since it releases parts of these stresses. Shrinkage incompatibility is more associated with cement based mortars while the polymer-modified mortars (PMC) show better shrinkage compatibility and epoxy mortars proved to have the best shrinkage compatibility [69].

5.2 Bond of FRP in a mortar

The mineral based strengthening systems are strongly dependent on the bond between fibre composite and mineral based binder. Using a non-impregnated textile fabric with a high density (high fibre filament amount) will make it hard for the mineral based binder to penetrate. This type of inferior bond or penetration of textile fabrics has been the focus for researchers developing the TRC system, [8, 11, 14]. Using an epoxy impregnated CFRP grid, as in the MBC system, relies on *physical bond* between CFRP and mortar. This physical bond can originate from direct mechanical anchorage (joints in the grid, transversal tows of the grid), frictional forces on the interface, aggregate or fibre interlock (if the mortar contains longer fibres) but there is no chemical bond between the FRP and the mortar as in an epoxy-bonded system there would be.

When using strain hardening mortars, there is a chemical bond between the mortar fine-grain aggregates and the PVA fibres which affects bonding of the embedded FRP reinforcement in the mortar. PVA has a high chemical bond and reaches its peak load at relatively small pullout length. During the extraction process, it has a tendency to break instead of pulling out from the mortar. In order to increase

the opening of an individual crack and enhance the composite stress-strain behaviour of PVA-ECC, the chemical and frictional bond of the PVA fibre is to be decreased, e.g. by means of particular surface treatment (coating) [39] or by modification of the fibre/matrix interface transition zone. Bond can be lessened e.g. by adding fly ash to the mix.

Bond characteristics influence the mechanism of load transfer between reinforcement and concrete, and therefore control the concrete (or mortar) crack spacing, crack width, required concrete cover to the reinforcement, and the reinforcement development length. The behaviour of strengthened concrete structures thus depends on the integrity of the bond. Most literature to date has been published about bond of FRP bars in concrete or other cementitious matrices. Very little literature is found on the bond of FRP grids to a cementitious material which is more complex because of the geometry of the grid, including the formation of the joints.

5.3 Multiple cracking – crack control through strain hardening materials

The deformation behaviour of cementitious composites (concrete, fibre reinforced concrete) and high performance fibre reinforced cement composites (HPFRCC) is typically distinguished according to their tensile stress-strain characteristics and post-cracking response [70]. In [71], it is shown that brittle matrices, such as plain mortar and concrete, lose their tensile load-carrying capacity almost immediately after formation of the first crack as illustrated in Fig. 4.

The addition of fibres in conventional fibre reinforced concrete (FRC) can increase the toughness of cementitious matrices significantly; however, their tensile strength and especially strain capacity and ductility beyond first cracking are not enhanced [72]. FRC is therefore considered to be a quasi-brittle material with tension softening behaviour, i.e. a decaying load and immediate localization of composite deformation at first cracking in the FRC matrix. In contrast, strain hardening fibre reinforced cementitious composites (SHCC), which is a particular class of HPFRCC (high performance fibre reinforced cementitious composites), are defined by an ultimate strength higher than their first cracking strength and the formation of multiple cracking during the inelastic deformation process. Under tension, it initially exhibits *multiple cracking with associated overall hardening*, which later changes to softening as fracture localizes [73]. The crack continues to open, and the embedded fibres are pulled out of the matrix (or break, depending on what matrix/fibre composition is used), which still generates some resistance against crack opening within the tensile softening regime. When all fibres are completely pulled out (or broken), no resistance is left, i.e. the tensile stress is equal to zero.

The contribution of a cementitious matrix to the load-deformation response of reinforced concrete or ECC is the so-called “strain hardening” or “plastic hardening”. Tensile softening vs. tensile hardening behaviour is illustrated in Fig. 4a. Textile reinforced concrete exhibits a similar hardening behaviour [74, 75], however the cracking process is clearly not as uniform as in an ECC (Fig. 4b). In the pre-cracking

regime (Stage I), the stresses are distributed until the first cracking strength of the concrete is reached. First cracking occurs at the point where the ultimate tensile strength of the concrete is reached and the FRP reinforcement will carry the entire applied load in the vicinity of the transverse crack location. The load carried by the concrete in the uncracked segments is transferred to the FRP reinforcement at the crack location via interfacial bond. After first crack formation (Stage IIa, “cracking formation”), the load-deformation curve shows a small increase in loading capacity as compared to that in Stage I due to the formation of additional transverse cracking. The member is softened by the formation of additional crack(s) and the load increase per deformation increment is decreasing with each crack until Stage IIb when a stabilized crack pattern is reached (post-cracking regime). When the final crack pattern is being formed, the slope of the stress strain relationship becomes steeper again, which mainly results from the Young’s modulus of the fibre reinforcement. Crack widths are also governed by the FRP reinforcement and the bond characteristics to the surrounding concrete matrix. At this stage of a stabilized crack pattern (Stage III) no further cracking occurs. Here, mainly the FRPs determine the stiffness of the member. Stage III is characterized either by slippage in the fibre tows instead of yielding of steel reinforcement, or by linear elastic deformations until the FRP ruptures in a brittle manner upon reaching its tensile failure strain, as detailed in [76]. In practice, final failure normally is a combination of fibre slippage and rupture [74].

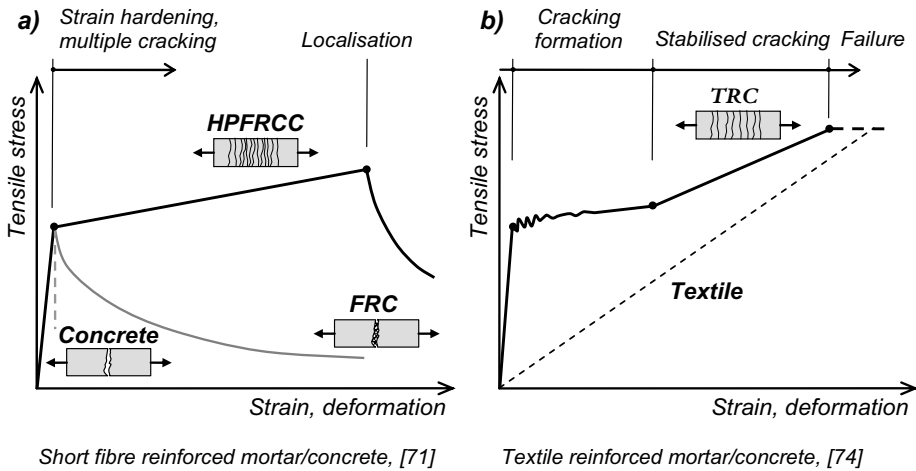


Fig. 4 (a) Strain hardening and strain softening mortars, (b) Tensile behaviour of TRC

Due to the more homogeneous nature (as a consequence of randomly distributed, well mixed short fibres) of ECC, there is a gradually increasing part of the curve smoother than for TRC because of the fibre bridging characteristics of the PVA fibres compared to those of a textile mesh. In ECC, there is no definite distinction

between stages IIa and IIb (crack saturation) [37]. The (pseudo) strain-hardening behaviour in ECC is achieved by sequential development of matrix multiple cracking [77]. “Multiple cracking” means that under tension, cracks are consecutively formed after first cracking, and become evenly and closely spaced. Deformation then is often expressed in terms of strain instead of crack opening displacement. Multiple cracking results in the improvement in “ductility, toughness, fracture energy, strain hardening, strain capacity and deformation capacity under tension, compression or bending” [78].

The strain hardening ensures that a structural element made of such a composite material will maintain its stability also after cracking. This is a significant difference between all conventional FRC and SHCC materials as shown in Fig. 4. Deformation of ECC is uniform on a macro-scale and considered as pseudo-strain, which is a *material property* [37], in contrast to other reinforced concrete-like materials such as conventional FRC. As a consequence of the strain hardening, the tensile strain capacity and ultimate strength *in the cracked state of ECC* are much higher than that of conventional (steel) fibre reinforced concrete.

5.3 Fibre bridging

Since the overall hardening behaviour highly relies on fibre bridging, it is important to know how high bridging stresses arise in the fibres. This would also limit and determine which materials are usable as reinforcing fibres. For very flexible fibres which have a high strain capacity (polymeric fibres), a snubbing effect (fibre dowel action arising when a fibre is not loaded in the direction of the initial straight fibre) may occur reducing the fibre critical length leading to premature failure. For elastoplastic fibres (steel), local yielding can happen, as for elastic-brittle fibres (carbon, glass) fibre failure may happen due to bending of fibres [40]. The fibre bridging analysis is about relating the single fibre bridging stress to the crack opening which is a function of fibre and interface properties and mode of failure [79]. Fibre properties may include the fibre modulus, ultimate tensile strength, fibre length, diameter, and the interface properties are the cohesive strength, fracture properties and frictional properties. The micromechanics of fibre bridging is described more in detail by [80]. In a composite, the embedded fibres in the mortar would often bridge a crack at an angle. Inclined fibre pullout would depend on a greater number of parameters, involving the inclination angle of the fibre to the matrix crack plane, local fibre/matrix interaction properties and possible aging effects (interfacial properties and fibre/matrix interaction changing with time) [80].

Fibre bridging after first cracking of the cement matrix is well detectable in PVA-reinforced mortars. For MBC systems, the mechanism is important because with adequately chosen mortars, a MBC system can be altered/improved resulting in a more efficient strengthening material under tension or shear.

6. Testing MBC systems

As previously shown in Fig. 1, the three (material, component and structural) levels of mineral based strengthening must be linked together. It is not within the scope of this paper to generalize about all existing mineral-based strengthening systems, however linking can be done and is presented for mineral based composites through experimental investigations carried out at LTU and DTU.

Mineral based composites are, as defined earlier, a particular instance of mineral based strengthening in which FRP grids are adhered to the concrete substrate by means of (quasi-brittle or strain hardening) mortars. By using ECC as the mortar phase in MBC, different force transfer mechanisms come into play which did not exist in the initial phase of MBC research where the mortar was a quasi-brittle PMM. In addition to that, MBC research has mostly focused on beams strengthened in flexure and shear, and much less attention has been paid to repairing structural members in which significant tensile forces may emerge. Before applying the MBC as a strengthening material in conditions where the structural member is subject to tensional or splitting forces (or bending combined with axial forces), it is necessary to properly characterize the tensile behaviour. Knowledge of related parameters such as the tensile strain – crack opening curve makes possible estimations e.g. about brittleness in compression and tension or shear capacity. Suitable test methods are being searched, which quantify the tensile properties of MBC directly (dogbone tests) or indirectly (WST, giving the splitting tensile strength).

This section will give insight in the MBC behaviour for tension, flexure and shear. Tests have been performed on the tensile behaviour of the MBC system, dogbone and wedge splitting tests (WST), along with flexural and shear strengthening, see Fig. 5 where all tests are shown.

6.1 Experimental set-up

A summary of tests conducted at LTU and DTU is shown in Fig. 5. Uniaxial tensile and wedge-splitting tests aim to characterize the tensile and fracture properties of the strengthening material. Shear and flexural strengthening (Fig. 8) involving MBC lead towards the structural level and applications as outlined in Fig. 1. Short descriptions of each test are summarized below, and further references are given to a more detailed description of each.

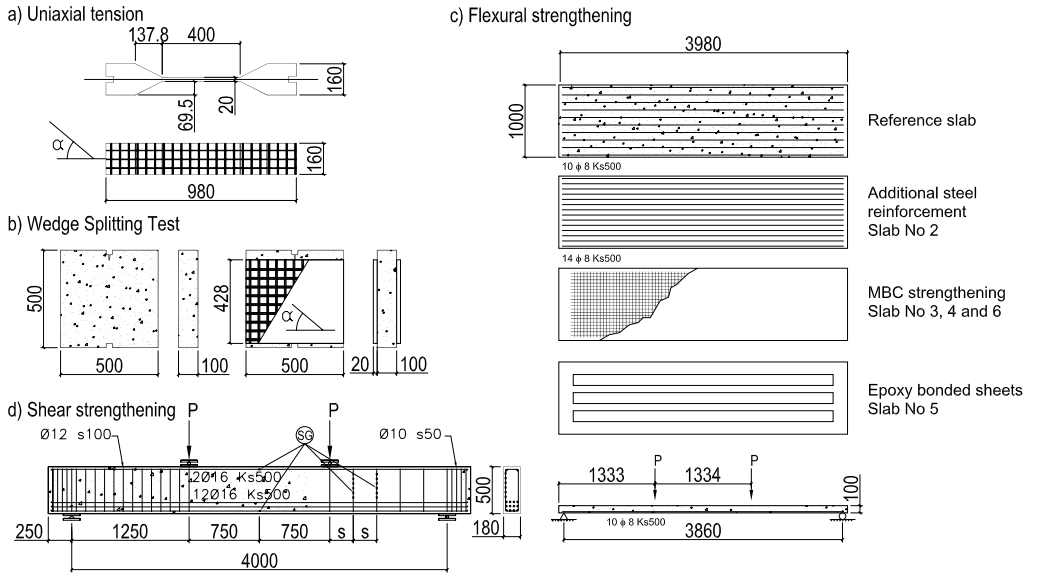


Fig. 5 Experimental tests for tensile and fracture behaviour: (a) uniaxial tensile test on dogbones, (b) wedge-splitting test, (c) flexural beams and (d) shear beams

6.2 Material properties

All the material properties for the materials used in the four different tests are summarized in Table 1 for the CFRP grids and Table 2 for the binders.

Table 1 Mechanical properties for the fibres in each tow of the CFRP grids used in experimental tests [54]

| Material | Direction | Tow spacing [mm] | Tensile strength [MPa] | E modulus [GPa] | Failure strain [%] |
|----------|--------------|------------------|------------------------|-----------------|--------------------|
| Grid S | Transverse | 25 | 5214 | 366 | 14.0 |
| Grid S | Longitudinal | 24 | 3546 | 278 | 12.5 |
| Grid M | Transverse | 43 | 4620 | 389 | 11.9 |
| Grid M | Longitudinal | 42 | 4219 | 404 | 10.5 |
| Grid L | Transverse | 72 | 3772 | 423 | 8.6 |
| Grid L | Longitudinal | 70 | 3877 | 320 | 12.8 |

Table 2 Material properties for binders used in experimental tests

| Material | Description | Tensile strength [MPa] | Compressive strength [MPa] |
|-----------------|-----------------------------------|-----------------------------------|---------------------------------------|
| PMM | Polymer-modified mortar | 2.4 | 53.2 |
| ECC | Engineered cementitious composite | 3.0 | 60.0 |

6.3 Linking material and component levels

6.3.1 Uniaxial tensile tests

New test method and test specimens have been developed for testing MBC under uniaxial tension in [65]. The bare strengthening material was tested, without considering the interaction with a real structure to be strengthened. Quasi-brittle polymer-modified mortars and ECC have been investigated together with an embedded CFRP grid in the mid-plane of the dogbone-shaped specimens, focusing on crack development and the influence of the applied mortar's ductility on the behaviour in tension.

Dimensions of the dogbone-shaped test specimens were 160 x 160 x 980 mm, with a representative test section of 400 x 160 x 20 mm. Two different grids with different grid spacings, and three chosen grid orientations (0° - longitudinally placed grid, 90° - transversally placed grid, 15° - rotated grid) were tested in different combinations, more in detail presented in [65]. The number of the CFRP tows in the representative test section, tensile direction, were 7 (small grid) and 4 (medium grid). The specimens were fixed in self-centering, custom-made clamps.

In Fig. 6a, quasi-brittle and ductile mortars are compared and related to the linear elastic behaviour of the pure CFRP grid. Behaviour of all specimens was nearly identical up to first cracking irrespective of which mortar is used. After first cracking, ECC specimens show a significant strain hardening behaviour with both small (S) and medium (M) grids which is represented as the contribution of the mortar compared to the shifted lines of the pure grid. The ECC specimens, after the first crack, show a further load increase until the peak load. These curves are smooth due to the fibre-bridging characteristics of the cracks in ECC. Curves of quasi-brittle mortars are more jagged and have a significant drop in load carrying capacity right after the first crack (and after further crack formation). This fact shows that the increased ductility of the ECC mortar has a positive effect on the interaction with the CFRP through the fibre bridging effect. It seems to prevent premature failure of the CFRP grid which was observed in the specimens with brittle mortars, with significantly reduced axial tensile strength.

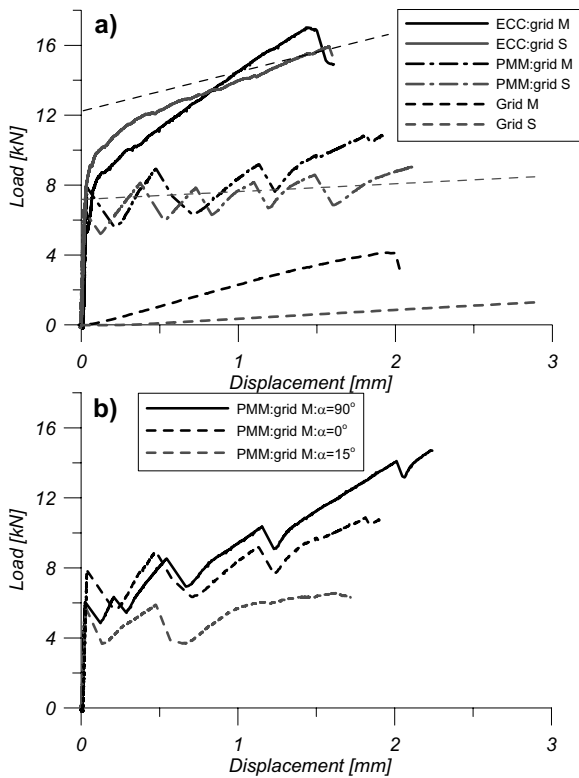


Fig. 6 (a) All dogbone specimens with grid S and M placed in longitudinal (0°) direction; (b) Effect of grid orientation (transverse (90°), longitudinal (0°) and rotated in 15°)

Fig. 6b illustrates the effect of the grid orientation. The apparent better performance of the grid when rotated transversally may be due to an epoxy surplus on the transversal tows resulting in improved mechanical anchorage or, more likely, due to the joint shape (between longitudinal and transversal tows of the grid) and associated deformation capacity of the grid joints when loaded in a certain direction.

6.3.2 Wedge splitting tests

Brittleness of concrete-like materials is usually evaluated by means of the post failure behaviour in tension governed by the stress versus crack width relation (σ - w), the so-called softening behaviour which is a basic property of a (conventional) concrete described by the tensile strength, the maximum crack width and the fracture energy, which corresponds to the area under the stress versus crack width curve. WST (wedge splitting test), originally introduced by [81] and further improved by [82] is a suitable method, traditionally used for brittle materials, for obtaining the splitting tensile strength along with the post-peak behaviour, and an estimation on the fracture energy.

WST is an extension of the uniaxial test because the MBC strengthening is

applied on a concrete surface. In a recently published study [64], behaviour of a CFRP grid reinforcement in two different directions (0° and 45° , respectively) together with quasi-brittle and ductile mortars has been investigated and evaluated through recording and comparing crack widths, crack patterns, splitting load versus crack opening displacement curves and fracture energy values for the MBC-strengthened concrete specimens. External dimensions of the plain concrete test specimen were 500 x 500 x 100mm, after strengthening with a representative test section of 400 x 420 x 140mm where 140mm is the total thickness after strengthening on both sides. The length of the starter notch together with the groove is 50mm. The bottom groove served to ease proper vertical positioning and acted as a line support for the heavy specimens. The CFRP grid was applied on both sides (ten tows bridging the crack on both sides, in the non-rotated position), placed between two 10 mm thick layers of mortar, applied on the concrete surface roughened with sandblasting and treated with a primer to enhance bond on the concrete-mortar interface. Tests were run deformation-controlled, i.e. through the crack opening displacement kept constant at 0.3 mm/min, by a clip gauge mounted at the tip of the notch in the midplane of the specimen. During the test, vertical load and crack opening displacement (COD) are recorded; hence the splitting load can be calculated.

The resulting splitting force vs. crack opening displacement plots show that the splitting tensile strength of concrete can be significantly improved with MBC strengthening, resulting in an increase of 30-110% in peak splitting load compared to the unstrengthened reference specimen (Fig. 7.) ECC has given significantly higher failure loads and similarly to the uniaxial tests, it prevented pronounced drops in load capacity. Ductility is significantly enhanced by all grid-mortar combinations resulting in an extreme increase of fracture energy which is directly proportional to the area under the curves.

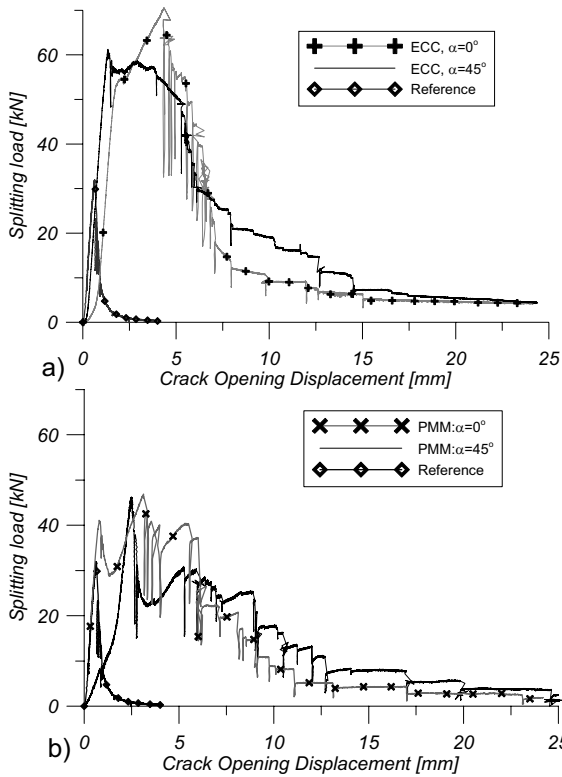


Fig. 7 Splitting force vs. COD curves for specimens with highest peak load per series, against reference specimen (plain concrete)

Bond provided by both mortars was excellent leading to CFRP rupture. By applying PVA-reinforced ductile ECC as bonding agent, improved performance, significantly higher fracture energy, multiple cracking and enhanced ductility were observed, caused by improved bond between grid and mortar due to the refined grain structure, the bridging effect of the embedded fibres working against crack opening and via direct mechanical interlock with the grid.

Compared to a uniaxial tensile test, WST also has provided information on the softening part of the curve after peak load, revealing tendencies in how fast or how gradually load capacity decreases until all crack bridging fibre tows and embedded fibres in the mortar are broken. The slopes of the F_s vs. COD curves reveal that the tensile ductility (recorded peak load and its tendency to decrease to zero) depends more on the grid orientation than on the mortar quality, unlike the increase in the energy absorption/fracture energy which seems to be “mortar-dependent” and is significantly higher for the ECC specimens.

6.4 Linking component and structural levels

6.4.1 Slabs strengthened in flexure

The test set-up and geometry for the slab specimens is shown in Fig. 5 and a more detailed overview and results are also published in [83, 84]. Three of the slabs were strengthened using the MBC system, one specimen with one CFRP grid, one specimens with a sanded CFRP for better mechanical anchorage and one specimen with double CFRP grid. In addition one specimen was strengthened using epoxy bonded carbon fibre sheets and yet one specimen containing four extra flexural steel reinforcement bars, the extra reinforcement was calculated to correspond to the strengthening. Thus, all of the specimens were designed to have similar failure loads, except the specimen with dual CFRP grid. The thickness of the strengthening layer was approximately 10 mm and a quasi-brittle mortar was used as binder. In all MBC strengthened specimens the CFRP grid had a fibre content of 159 g/m^2 (Grid M). For the epoxy based strengthening, the carbon fibre sheets had a fibre content of 200 g/m^2 . The total carbon fibre amount in the tensile direction of the specimens corresponded to $20 \text{ mm}^2/\text{m}$ (CFRP grid) and $62 \text{ mm}^2/\text{m}$ (carbon fibre sheet) respectively.

All of the strengthened slabs increased the ultimate bearing capacity in comparison to the non strengthened reference beam. Strengthened specimens using one layer of CFRP grid failed at a total load of 35 kN and specimens with epoxy bonded sheet failed at 41 kN while showing a stiffer behaviour compared to the latter. The specimen containing four extra flexural bars failed at a load of 38 kN, similar loads to the specimens with only one grid. However, the specimen with extra steel reinforcement showed stiffer response compared to both the specimens strengthened with sheets and one CFRP grid. It is also noted that sanding the surface of the grid (specimen No. 3) led to premature rupture of the CFRP grid. Strengthening the specimen with dual layer of CFRP grid will have a positive effect on the load bearing capacity. Thus this specimen (No. 6) had the highest ultimate load capacity of 51 kN. All of the specimens with the MBC system failed by fibre rupture while the epoxy based strengthening system failed by a mix mode of debonding and fibre rupture. Comparative load-displacement curves are plotted in Fig. 8.

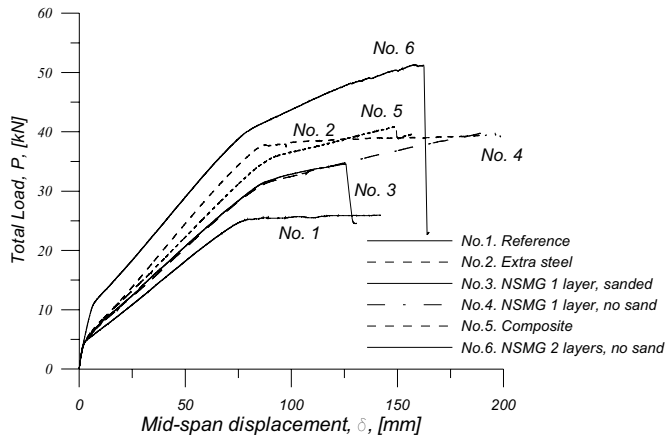


Fig. 8 Load vs. mid-span displacement of flexural strengthened specimens

6.4.2 Beams strengthened in shear

Beams strengthened in shear had a rectangular cross section and were 4.5 m long and had a height of 0.5 m. Again, these results are described in more detail in [54, 67]. Note, in Fig. 8, that the beams were heavily shear reinforced in one shear span and had inferior to no shear reinforcement in the other shear span. Thus, only the shear span containing no or little shear reinforcement was strengthened. In these experiments, the influence of different grids and internal steel shear reinforcement ratios were studied. In all test the quasi-brittle PMM was used as a binder of the strengthening system. The PMM was also used in the dogbone and WST tensile test. For testing the influence of different CFRP grids, the carbon fibre amount was varied from 66, 98 to 159 g/m² (Grid S, L and M). All of these specimens had no internal shear reinforcement in the strengthened shear span. For specimens with different internal shear reinforcement the different distances was $s = 350$ mm and $s = 250$ mm, see also Fig. 5. The internal shear reinforcement was monitored by six strain gauges mounted on both two stirrups closest to the load, see Fig. 5. In addition, six strain gauges were mounted on the vertical CFRP tows in the grid at the same locations as the strain gauges mounted on the stirrups.

All of the specimens with no internal shear reinforcement and strengthened with the MBC system failed by fibre rupture of the vertical tows. For strengthened specimens with different internal reinforcement amounts the failure mode changed from a brittle shear failure to a more ductile compressive/crushing failure. The ultimate loads for all specimens are summed in Table 3 together with compressive- and tensile strength of the concrete, and failure modes (S-shear failure and C-compression/crushing). From the results of the specimens strengthened with different grids it was clear that the specimens with highest carbon fibre amount had the highest load bearing capacity. Since the specimens containing internal shear reinforcement were heavily monitored by strain gauges, the shear behaviour and strain development from initial load stages could be measured. Here, the strain development in the stirrups

was reduced for beams strengthened with the MBC system. The strains monitored in the CFRP grid indicated that high strain concentrations were apparent in the vicinity of cracks.

Table 3. Ultimate shear loads and failure modes, along with description of tested shear beams

| Beam | CFRP | Stirrup distance [mm] | Failure load [kN] | Failure mode | Compressive strength [MPa] | Tensile strength [MPa] |
|---------------|-------------|------------------------------|--------------------------|---------------------|-----------------------------------|-------------------------------|
| C40s0 | - | - | 123.5 | S | 44.8 | 2.9 |
| C40s0* | - | - | 126.7 | S | 36.3 | 2.5 |
| C40s0-M | - | - | 141.9 | S | 53.6 | 2.8 |
| C40s0-Grid M | Grid M | - | 244.9 | S | 53.6 | 2.8 |
| C40s0-Grid M | Grid M | - | 241.9 | S | 53.6 | 2.8 |
| C40s0-Grid S* | Grid S | - | 208.1 | S | 32.5 | 2.7 |
| C40s0-Grid M* | Grid M | - | 251.9 | S | 35.1 | 3.0 |
| C40s0-Grid L* | Grid L | - | 206.4 | S | 44.8 | 2.5 |
| C35s0 | - | - | 130.6 | S | 47.0 | 2.7 |
| C35s3 | - | 350 | 346.0 | C+S | 47.6 | 3.1 |
| C35s3-Grid M | Grid M | 350 | 336.9 | C | 52.4 | 3.0 |

*The deformation rate during loading was not controlled but load controlled at 10 kN/sec

Typical strain readings from internal shear reinforcement and CFRP grid are shown in Fig. 9 for specimens with and without strengthening corresponding to specimens with concrete compressive strength of 47-52 MPa and internal stirrup distance of 350 mm (Specimens C35s3 and C35s3-Grid M in Table 3). Fig. 9a and b shows that strains in the (steel) stirrups are reduced in all MBC-strengthened beams even at relatively low load levels (100-200 kN) when compared to the non-strengthened ones. As the shear load increases, the favourable strain reduction of the MBC system is more pronounced for a strengthened specimen compared to a non strengthened specimen.

In the vertical CFRP tows, a significantly uneven strain distribution is visible, with locally high strains in the vicinity of forming shear cracks. These strains are increasing rapidly as the shear crack is opening.

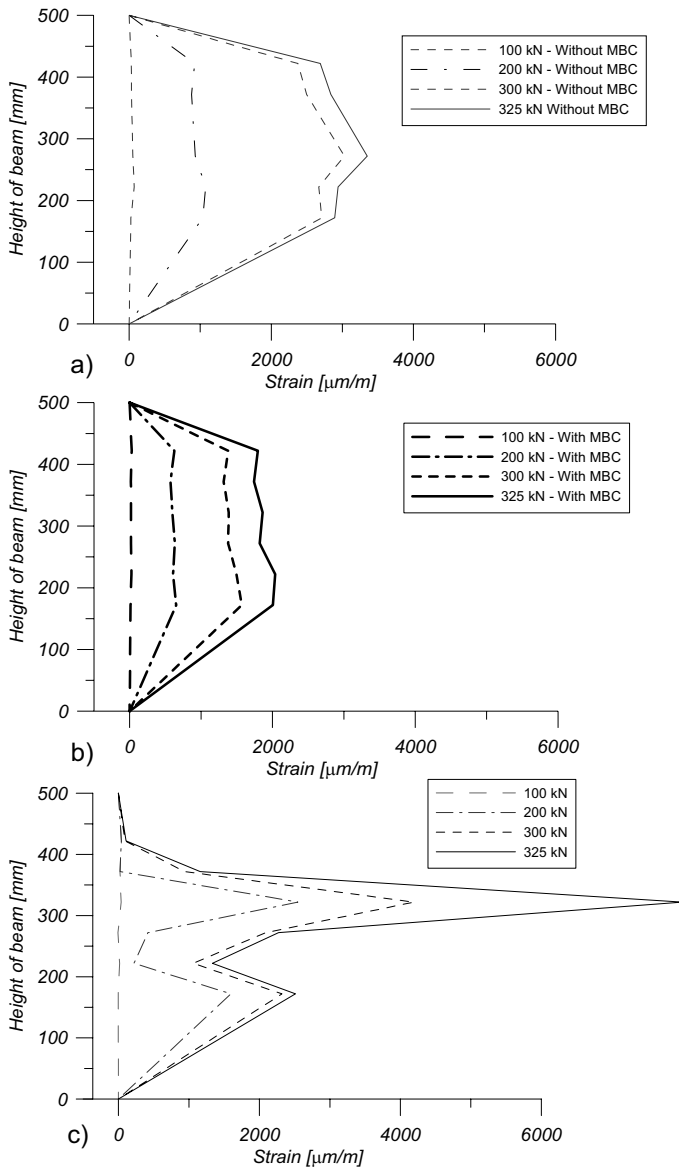


Fig. 9 Strain development at different shear loads, (a) in stirrups without MBC and (b) in stirrups with MBC and (c) strains in vertical CFRP tows

6.5 Field implementations

The MBC strengthening system should be able to be implemented in various field strengthening applications such as; harbour structures (less sensitive to moisture compared to epoxy bonded strengthening systems), large structures that requires

higher compatibility of the strengthening system to the base concrete structure, low temperature applications, applications that demand diffusion openness and for concrete applications that excludes the use of epoxies. In addition, the MBC system can be used in tunnelling or mining applications instead of using steel fibre reinforced shotcrete. In the latter, the combination of using ECC as a binder should further improve the ductility and crack bridging ability of the MBC system. Pilot studies for in-situ production techniques of the MBC system using quasi-brittle mortars as binders have been investigated in [83]. The results from this study clearly show that spraying the MBC system can be made in an easy and efficient manner. The application technique is done by mounting the CFRP grid on pre-attached studs and then the binder is being sprayed. The thickness of the MBC system is controlled by the chosen length of the studs.

6.6 Discussion and conclusions

Uniaxial tests have revealed that the most commonly used grid (medium-sized, M-grid) performs better when placed in transversal direction. This leads to the need of studying the effect of grid joint formations (i.e., the grid is “woven” out of two perpendicular tows of CFRP and the grid joint looks differently depending on the direction). The uneven distribution of the residual epoxy on the grid surface in the two perpendicular directions could also contribute to the direction-dependent performance.

Flexural specimens strengthened with MBC had higher ultimate load compared to the epoxy bonded sheets of comparing the fibre amount in the tensile direction. Although, the failure mode for the MBC was fibre rupture while the epoxy bonded carbon fibres failed by a mix mode of debonding and fibre rupture. However, trying to improve the bond between the mineral based binder and the CFRP grid by the use of sand-coated grids has negative effects on ultimate load bearing capacity. It appears that sanding the surface creates discrete increases in strain and leading to premature failure, this was however not monitored. But as shown in the shear strengthening in Fig. 9b, by the use of monitoring strains in the grid, discrete high strains occur in the vicinity of cracks.

All MBC-strengthened shear beams, which had no internal shear reinforcement, failed by rupture of the vertical tows in the grid. From this series of specimens it was concluded that increasing the fibre amount will also increase the ultimate failure load, to what extent is not within the scope of this paper. But increasing the fibre to a certain level should imply failure in the intermediate transition zone between binder and fibre composite. For beams with internal reinforcement the failure mode changed from a brittle shear failure to a more ductile compressive failure. For the specimens with internal reinforcement it could be seen from strain gauge monitoring that the MBC strengthening system reduced strains in the steel reinforcement even for low shear loads. Thus, this indicates that the MBC strengthening system can be used for crack width reduction in the service limit state.

MBC tests have shown that strain hardening mortars can be successfully used together with embedded FRP reinforcement and the fibre bridging behaviour of ECC “compensates” for the brittleness of the grid and prevents premature failure of it by

retaining fast and rigid deformations in the grid joints. This may enable a better utilization of the grid.

To the authors' knowledge, ECC has been implemented into the MBC system for the first time. Due to its fibre bridging mechanisms and strain hardening behaviour, ECC shall further be tested as a bonding agent for mineral based strengthening systems. Preliminary results from pullout tests carried out by the authors have shown that if the application method is correct and the mix is properly compacted around the CFRP grid, there is a nearly perfect bond on the interface even at short embedment lengths (45 mm) using both polymer-modified quasi-brittle mortars and ECC. Therefore in a real structural element, the failure mode is expected to be fibre rupture.

Traditionally, ECC has been used up to its maximum strain or deformation capacity (especially where energy dissipation is the major concern). In an ECC-based MBC, the FRP component is fully used up to its maximum potential; however the ECC is not because the FRP reinforcement fails prior to that the ECC would reach its maximum strain capacity. In a structural member made from pure ECC, the maximum strain capacity would be characterized by the highest yet sustainable crack density with evenly distributed fine cracks.

Despite the fact that when combined with FRP, the maximum strain capacity of the ECC is not fully utilized, ECC improves the MBC system significantly. Its main advantages are that it accommodates larger elongations than FRP therefore it will not be the weak link in strengthening; it enforces the failure mode to be more ductile [50] and prevents or reduces sudden brittle deformations. Its documented spalling resistance [47, 48] is also very attractive when designing externally bonded strengthening systems.

6.7 Future research for MBC

6.7.1 Materials

Strain hardening mortars together with FRP grids should be further tested especially in shear beams or other shear sensitive structures where it should yield a more predictable and ductile failure mode.

Tri- or other multiaxial grids could also be effectively used, in particular for shear strengthening. More flexible grids, in which the joints are not rigid using a more elastic matrix for impregnating the fibres, would most likely accommodate larger deformability of the grids for the use of e.g. wrapping. Also investigations of incorporating higher fibre amount in the CFRP grid should be made for further increase the load bearing capacity.

When using ECC as binder, further investigation is needed on whether (and to what extent) the large improvement in load capacity is due to a direct tensile contribution from the ECC or the fact that it is capable to retain grid joints from fast and brittle deformations breaking the grid or to slow down this process, hence preventing premature failure in the grid.

6.7.2 Structural behaviour and future applications

Influences on the bond in the transition zone between fibre composite and binder should be investigated when increasing the fibre amount in the FRP grids. The investigations done so far on the MBC system has shown no problems concerning the bond to the base concrete structure, future applications involving enhancing the load bearing capacity should be followed by an experimental program involving the bond to the base concrete.

For field applications the influence of shrinkage should also be made, especially when incorporating ECC as a binder. However, traditional precautions can be used when commercially available PMM is used as binders.

Regarding future applications, stay-in-place formwork could be one new approach. Especially for the combination of using concrete with low quality as a core material and then using high quality binders together with a FRP grid as a protective outer layer of remaining formwork.

To incorporate the MBC system for the use in civil engineering structures design guidelines should be developed for estimating the load bearing capacity.

7 Discussion and general conclusions in mineral based strengthening

7.1 Guidelines

One of the most important aspects for implementing these mineral based systems for the use in real structures is that there exist engineering design methods for calculating the load bearing capacity. To the authors' knowledge, there exists no general and commonly accepted design for the mineral based system. These guidelines should be made on a sound physical basis dealing with both the favourable aspects at the service limit state (crack bridging and crack reducing effects) together with the load bearing increase in the ultimate limit state.

7.2 Production methods and procedures

For strengthening larger surfaces, sprayed ECC together with FRP grid reinforcement may be a solution. Although this paper has not dealt with sprayable ECC there has been publications about the topic, see e.g. [85]. As the tensile strength of the pure ECC is not significantly different from that of a concrete, combining it with FRP would be useful when the tensile stresses significantly exceed the upper load bearing capacity of an additional pure ECC strengthening layer.

7.3 Suitable materials

Perhaps it is an advantage to strengthen a structure using a textile for increasing the ductility at ultimate failure load due to the relatively poor bond between binder and fibre composite. However, for service limit state a full utilization of interfacial bond between FRP and mortar is desirable to maintain economy. This justifies the applicability of grid-type reinforcement if the shape of the cross-section allows a grid to be used. It is important to emphasize that epoxy coating, compared to the textiles used in TRC, significantly improves the interaction between mortar and FRP because of the difficulties of the mortar to penetrate dry fibre bundles.

An alternative to TRC when ductility is an issue is strain-hardening mortars together with grids as published in [64, 65]. Strain-hardening mortars also offer the advantage of a more ductile and predictable failure mode which would be beneficial for strengthening shear sensitive structures.

It is assumed that ECC, when combined with grids, would be able to ensure a more even stress distribution among the grid tows along a crack line because of its fibre bridging effect. Then the peak strains in the adjacent grid tows (as shown e.g. in Fig. 9b) would be reduced and redistributed to the neighbouring tows hence making the failure more predictable.

New matrices could also be introduced for impregnating the FRP component. A common method for strengthening columns or beams is wrapping with textiles or continuous sheets/dry fibres. However, wrapping is not possible when using an epoxy impregnated carbon fibre grid due to the rigidity and brittleness of the matrix. Using textiles makes wrapping around corners much easier [84]. Using a semi-elastic matrix, e.g. latex, which still ensures rigid connection points but allows wrapping around corners, could be a beneficial solution for ensuring rigidity, anchorage and effectiveness of the fibres.

7.4 Interactions

Further research should be directed to the influence of bonding, both between base concrete and binder along with the transition zone and between binder and fibre composite. In MBC, having perfect bond between fibre composite and quasi-brittle binder could lead to premature failure in the FRP. In TRC, bond between textile and mortar is significantly weaker and there is a limitation of how many layers of textile can be used effectively without anchorage problems (if there is no additional mechanical anchorage) and debonding. This also limits the maximum fibre amount applicable in a certain direction and therefore the maximum strengthening effect achievable by a TRC system.

Penetration of the FRP component has been a problematic issue with several existing systems (e.g. dry fibres/sheets, TRC). Using non-impregnated sheets, grids or textiles will generate larger slips and inferior effective strain over the roving cross section with possibly overloaded yarns. Using impregnated fibres (fibres imbedded in an epoxy matrix) will create a more effective strain distribution in the FRP tow such as in case of FRP grids.

7.5 Other issues

Further research should also be directed to the durability and fatigue aspects of mineral based strengthening. In seismic regions, ductility and energy dissipation capacity is of importance; in this regard ECC-based systems which use additional fibre composites as reinforcement could be further developed and investigated.

Acknowledgements The research work presented in this paper was performed at the Technical University of Denmark and Luleå University of Technology, financed by the Norwegian Research Council through the strategic institute program RECON at Norut Narvik Ltd, the Swedish road administration and the development fund of the Swedish construction industry. Sto Scandinavia should also be acknowledged for supplying materials in the experimental studies.

References

1. Carolin A (2003) Carbon fibre reinforced polymers for strengthening of structural elements. Doctoral thesis. Luleå University of Technology, Luleå, Sweden
2. Täljsten B (2006) FRP Strengthening of Existing Concrete Structures. Design Guideline, Luleå University of Technology, Luleå, Sweden
3. Meier U (1987) Bridge repair with high performance composite materials. *Material und Technik* 4:125-128
4. Triantafillou TC (1998) Shear strengthening of reinforced concrete beams using epoxy-bonded FRP composites. *ACI Struc J* 95(2):107-115
5. Nanni A (1995) Concrete repair with externally bonded FRP reinforcement. *Concr Int*, June 1995, pp 22-26
6. Ohuchi H, Ohno S, Katsumata H, Kobatake Y, Meta T, Yamagata K, Inokuma Y, Ogata N (1994) Seismic strengthening design technique for existing bridge columns with CFRP. In: Park R (ed) *Proceedings of the Second International Workshop on Seismic Design and Retrofitting of Reinforced Concrete Bridges*, Queenstown, New Zealand, pp 495-514
7. Chajes MJ, Januska TF, Mertz DR, Thomson TA, Finch WW (1995) Shear strengthening of reinforced concrete beams using externally applied composite fabrics. *ACI Struc J* 92(3):295-303
8. Triantafillou TC, Papanicolaou CG, Zisimopoulos P, Laourdekis T (2006) Concrete confinement with textile reinforced mortar jackets. *ACI Struc J* 103(1):28-37
9. Brückner A, Ortlepp R, Curbach M (2007) Anchoring of shear strengthening for T-beams made of textile-reinforced concrete (TRC). *Mat Struc* 2007(41):407-418
10. Brückner A, Ortlepp R, Weiland S, Curbach M (2005) Shear strengthening with textile reinforced concrete. In: *Third International Conference Composites in Construction*, Lyon, France, pp 1307-1314
11. Triantafillou TC, Papanicolaou CG (2005) Textile Reinforced Mortars (TRM) versus Fibre Reinforced Polymers (FRP) as Strengthening Materials of Concrete Structures. In: Shield CK, Busel JP, Walkup SL, Gremel DD (ed) *ACI SP-230 7th International Symposium on Fibre-Reinforced (FRP) Polymer Reinforcement for Concrete Structures*, American concrete Institute, pp 99-118

-
12. Li VC (2005) Engineered Cementitious Composites. In: Presentations at ConMat'05 (Vancouver, Canada, August 2005).
Available at:
[http://www.engineeredcomposites.com/publications/Conmat05/Li\(ECC\).pdf](http://www.engineeredcomposites.com/publications/Conmat05/Li(ECC).pdf).
Accessed 10 Jan 2009
 13. Mirza J, Mirza MS, Lapointe R (2002) Laboratory and field performance of polymer modified cement-based repair mortars in cold climates. *Construction and Building Materials*, Elsevier Science Ltd., v. 16, 2002, pp 365-374
 14. Raupach M, Orlowsky J, Büttner T, Keil A (2006) Recent developments of the usage of polymers in textile reinforced concrete. In: *Proceedings of the 5th Asian Symposium on Polymers in Concrete*, Taramani, India, pp 53-60
 15. Ohama Y (1998) Polymer-based admixtures. *Cem Concr Compos* 20(2):189-212
 16. Van Gemert D, Czarnecki L, Maultzsch M, Schorn H, Beeldens A, Lukowski P, Knapen E (2005) Cement concrete and concrete-polymer composites: Two merging worlds: A report from 11th ICPC Congress in Berlin, 2004. *Cem Concr Compos* 27(9):926-935
 17. Pascal S, Alliche A, Pilvin Ph (2004) Mechanical behaviour of polymer modified mortars. *Mat Sci Eng*380(1-2):1-8
 18. Schleser M, Walk-Laufer B, Raupach M, Dilthey U (2006) Application of Polymers to Textile-Reinforced Concrete. *J Mat Civ Eng* 18(5):670-676
 19. Garcés P, Fraile J, Vilaplana-Ortego E, Cazorla-Amorós D, Alcocer EG, Andi6n LG (2005) Effect of carbon fibres on the mechanical properties and corrosion levels of reinforced Portland cement mortars. *Cem Concr Res* 35:324-331
 20. Peled A, Bentur A (2000) Geometrical characteristics and efficiency of textile fabrics for reinforcing cement composites. *Cem Concr Res* 30:781-790
 21. Wang Y, Wu HC, Li VC (2000) Concrete reinforcement with recycled fibres. *J Mat Civ Eng* 12:314-319
 22. Song PS, Hwang S, Sheu BC (2005) Strength properties of nylon and polypropylene-fibre-reinforced concretes. *Cem Concr Res* 35:1546-1550
 23. Silva DA, Betioli AM, Gleize PJP, Roman HR, G6mez LA, Ribeiro JLD (2005) Degradation of recycled PET fibres in Portland cement-based materials. *Cem Concr Res* 35:1741-1746
 24. Ochi T, Okubo S, Fukui K (2007) Development of recycled PET fiber and its application as concrete-reinforcing fiber. *Cem Concr Compos* 29(6):448-455
 25. Betioli AM, Silva DA (2005) Evaluation of Durability of PET Fibers Under Diverse Aggressive Environments. In: *10DBMC International Conference On Durability of Building Materials and Components*, Lyon, France pp 1-7
 26. Wu K, Zhou J (1988) The influence of the matrix-aggregate bond on the strength and brittleness of concrete. In: *Mindess S, Shah SP (ed) Bonding in Cementitious Composites, Symposium Proceedings*, vol. 114, Materials Research Society, Pittsburgh, USA, pp 29-34
 27. Mitsui K, Li Z, Lange DA, Shah SP (1994) Relationship between microstructure and mechanical properties of the paste-interface. *ACI Mater J* 91:30-39
 28. Wong YL, Proon CS, Zhou FP (1999) Properties of fly ash-modified cement mortar-aggregate interface. *Cem Concr Res* 29(12):1905-1913
 29. Ahmed I (1993) *Use of waste materials in highway constructions*. Noyes Data Corporation, New Jersey, USA, 114 p
 30. Chandra, S (1997) *Waste materials used in concrete manufacturing*. Noyes Publications, Westwood, USA, 651 p

-
31. Urban M (2003) Properties of hardened self-compacting concrete with fly ash. In: Proceedings of the 3rd International Scientific Conference on Quality and Reliability in Building Industry, Levoča, Slovak Republic, pp 533-538
 32. Feldman RF, Carette GG, Malhotra VM (1990) Studies on mechanism of development of physical and mechanical properties of high-volume fly ash-cement pastes. *Cem Concr Compos* 12(4): 245-251
 33. Rudzionis Z, Ivanauskas E (2004) Investigations in properties of self-compacting concrete modified by fly ash admixture. In: Zavadskas EK, Vainiunas P, Mazzolani FM (ed) Proceedings of the 8th International Conference Modern Building Materials, Structures and Techniques, Vilnius, Lithuania, pp 151-156
 34. Mobasher B, Peled A, Pahilajani (2004), "Pultrusion of fabric reinforced high flyash blended cement composites". In: Proceedings, RILEM Technical Meeting, BEFIB, pp 1473-1482
 35. Xu S, Li Q (2007) An Experimental Study on Bending Behavior of Cementitious Composites Reinforced in Combination with Carbon Textile and Short-cut PVA Fiber. In: Grosse, CU (ed) *Advances in Construction Mat* 2007, pp 237-254
 36. Li VC (1998) Repair and retrofit with Engineered Cementitious Composites. In: Proceedings FRAMCOS-3 Fracture Mechanics of Concrete Structures, AEDIFICATIO Publishers, Freiburg, Germany, pp 1715-1726
 37. Fischer G, Li VC (2002) Influence of Matrix Ductility on the Tension-Stiffening Behavior of Steel Reinforced Engineered Cementitious Composites (ECC). *ACI J Struc* 99(1):104-111
 38. Wang S, Li VC (2003) Tailoring of PVA Fibre/Matrix Interface For Engineered Cementitious Composites (ECC). In Proceedings, Fibre Society 2003 Symposium in Advanced Flexible Materials and Structures: Engineering With Fibre, Loughborough, UK, pp 91-92
 39. Maalej M, Hashida T, Li VC (1995) Effect of Fibre Volume Fraction on the Off-Crack Plane Energy in Strain hardening Engineered Cementitious Composites. *J Am Cer Soc* 78(12):3375, 1995
 40. Li VC, Chan YW (1994) Determination of Interfacial Debond Mode for Fibre Reinforced Cementitious Composites. *ASCE J Eng Mech* 120(4):707-719
 41. Li VC (2002) Reflections on the Research and Development of Engineered Cementitious Composites (ECC). In: Proceedings of the JCI International Workshop on Ductile Fibre Reinforced Cementitious Composites (DFRCC) - Application and Evaluation (DRFCC-2002), Takayama, Japan, pp 1-21.
 42. Li VC, Fischer G, Kim Y, Lepech M, Qian S, Weimann M, Wang S (2003) Durable Link Slabs for Jointless Bridge Decks Based on Strain hardening Cementitious Composites. Michigan Department of transportation Research Progress Report, Michigan, USA
 43. Fukuyama H, Matsuzaki Y, Nakano K, Sato Y (1999) Structural Performance of Beam Elements with PVA-ECC. In: Reinhardt HW, Naaman A (ed) Proceedings of High Performance Fibre Reinforced Cement Composites 3 (HPRFCC 3), Chapman & Hull, pp 531-542
 44. Parra-Montesinos G, Wight JK (2000) Seismic Response of Exterior RC Column-to-Steel Beam Connections. *ASCE J Struc Eng* 126(10):1113-1121
 45. Yoon JK, Billington SL (2004) Cyclic Response of Unbonded Post-Tensioned Precast Columns with Ductile Fibre-reinforced Concrete. *ASCE J Bridge Eng* 9(4):353-363

-
46. Fischer G, Li VC (2003) Intrinsic Response Control of Moment Resisting Frames Utilizing Advanced Composite Materials and Structural Elements. *ACI Struc J* 100(2):166-176
 47. Lim YM, Li VC (1997) Durable Repair of Aged Infrastructures Using Trapping Mechanism of Engineered Cementitious Composites. *J. Cem Concr Compos* 19(4):373-385.
 48. Kanda T, Saito T, Sakata N (2003) Tensile and anti-spalling properties of direct sprayed ECC. *J Adv Concr Tech* 1(3):269-282
 49. Suthiwarapirak P, Matsumoto T, Kanda T (2002) Flexural Fatigue Failure Characteristics of an Engineered Cementitious Composite and Polymer Cement Mortars. *JSCE J Mat Conc Struc Pav*, 718(57):121-134
 50. Li VC (2002) Large Volume, High-Performance Applications of Fibres in Civil Engineering. *J App Pol Sci* (83):660-686
 51. Kamal A, Kunieda M, Ueda, N, Nakamura H. (2008) Evaluation of crack opening performance of a repair material with strain hardening behavior”, *Cem Concr Compos* 30(10):863-871
 52. Invention Title: Self-compacting Engineered Cementitious Composites (Self-compacting ECC) Inventors: Li VC, Kong J
Available at: http://ace-mrl.engin.umich.edu/NewFiles/invention/sc_abstract.html.
Accessed 10 Jan 2009
 53. ACI 440.2R-02 (2002) Guide for the Design and Construction of Externally Bonded FRP Systems for Strengthening Concrete Structures. ACI Committee Report, 45p
 54. Blanksvård T (2007) Strengthening of concrete structures by the use of mineral based composites. Licentiate thesis, Luleå University of Technology, Luleå, Sweden
 55. Peled A, Bentur A, Yankelevsky D (1998) Effects of woven fabric geometry on the bonding performance of cementitious composites - Mechanical performance. *Adv Cem Bas Mat* (7):20-27
 56. Badanoiu A (2001) Improvement of the bond between carbon fibres and cementitious matrices. Technical report. Royal Institute of Technology, Stockholm, Sweden
 57. Wiberg A (2003) Strengthening of concrete beams using cementitious carbon fibre composites”, Doctoral thesis, Royal Institute of Technology, Stockholm, Sweden, 2003
 58. Badanoiu A, Holmgren J (2003) Cementitious composites reinforced with continuous carbon fibres for strengthening of concrete structures, *J Cem Concr Compos* 25:387-394
 59. Wu HC, Sun P (2005) Fibre Reinforced Cement Based Composite Sheets for Structural Retrofit. In: Chen JF, Teng JG (ed) International Symposium on Bond Behavior of FRP in Structures, BBFS 2005, Hong Kong, pp 351-356
 60. Keil A, Raupach M (2007) Improvement of the Load-Bearing Capacity of Textile Reinforced Concrete by the Use of Polymers. In: Proceedings of Ohama Symposium, 12th International Congress on Polymers in Concrete ICPIIC'07, Chuncheon, Korea, pp 873-881
 61. Brockmann T, Bramshuber W (2005) Matrix Development for the Production Technology of Textile Reinforced Concrete (TRC) Structural Elements. In: Proceedings of the 3rd International Conference on Composites in Construction, Lyon, France, pp 1165-1172
 62. Triantafillou TC, Papanicolau CG (2006) Shear strengthening of RC members with textile reinforced mortar (TRM) jackets. *RILEM Mat Struc* 39:1-9

-
63. Curbach M (2005) Verstärkung von Balken und Plattenbalken mit textilbewehrtem Beton. Published in SFB 528 Textile Bewehrungen zur Bautechnischen Verstärkung und Instandsetzung, pp 433-462
 64. Orosz K, Täljsten B (2008) Development of a new test method for Mineral Based Composites - Wedge splitting test. In: Proceedings of the 2nd International Conference on Concrete Repair, Rehabilitation and Retrofitting (ICRRR2008), Cape Town, South Africa
 65. Täljsten B, Orosz K, Fischer G (2007) Crack development in CFRP reinforced mortar - an experimental study. In: Smith ST (ed) Proceedings of the Asia-Pacific Conference on FRP in Structures (APFIS 2007), pp 671-676
 66. Carlsvärd J (2006) Shrinkage cracking of steel fibre reinforced self compacting concrete overlays – Test methods and theoretical modelling. Doctoral thesis, Luleå University of Technology, Luleå, Sweden
 67. Blanksvärd T, Täljsten B, Carolin A (2009) Shear strengthening of concrete structures with the use of mineral based composites (MBC). *J Compos Constr*, 13(25):25-34
 68. Mangat PS, O’Flaherty FJ (2000) Influence of elastic modulus on stress redistribution and cracking in repair materials. *Cem Concr Res* 30:125-136
 69. Hassan KE, Brooks JJ, Al-Alawi L (2001) Compatibility of repair mortars with concrete in hot-dry environment. *Cem Concr Compos* 23:93-101
 70. ACI Committee 224 (1992) Report ACI 224.2R-92, Cracking of Concrete Members in Direct Tension. American Concrete Institute, USA
 71. Fischer G, Li VC (2007) Effect of fibre reinforcement on the response of structural members. *Eng Frac Mech* 74(2007):258-272
 72. Li VC (1992) Performance Driven Design of Fibre Reinforced Cementitious Composites. In: Swamy RN (ed) Proceedings of 4th RILEM International Symposium on Fibre Reinforced Concrete, Chapman and Hall, pp 12 - 30
 73. Kabele P, Takeuchi S, Inaba K, Horii H (1999) Performance of Engineered Cementitious Composites in Repair and Retrofit: Analytical Estimates. In: Proceedings of HPRCC 3 - The Third International RILEM Workshop, Cachan, France, RILEM Publications, pp 617-627
 74. Hegger J, Voss S (2004) Textile reinforced concrete under biaxial loading. In: Proceedings of the 6th Rilem Symposium on Fibre Reinforced Concrete (FRC), BEFIB 2004, Varenna, Italy, pp 1463-1472
 75. Hartig J, Häußler-Combe U, Schicktanz K (2008) Influence of bond properties on the tensile behaviour of Textile Reinforced Concrete. *Cem Concr Compos* 30(10):898-906
 76. Brameshuber W (2006) Textile Reinforced Concrete: State-of-the-art report of RILEM technical committee 201-TRC. RILEM Publications
 77. Yang EH (2008) Designing added functions in Engineered Cementitious Composites. Doctoral thesis, University of Michigan, USA
 78. JCI-DFRCC Committee (2003) DFRCC Terminology and Application Concepts. *J Adv Concr Tech* 1(3):335-340
 79. Li VC (1993) From Micromechanics to Structural Engineering - the Design of Cementitious Composites for Civil Engineering Applications. *JSCE J Struc Mech Earth Eng* 10(2):37-48, 1993
 80. Li VC (1997) Post-crack scaling relations for fibre reinforced cementitious composites. *ASCE J Mat Civ Eng* 4(1):41-57
 81. Linsbauer HN, Tschegg EK (1986) Fracture energy determination of concrete with cube-shaped specimens. *Zement und Beton* 31:38-40

-
82. Brühwiler E, Whittmann FH (1990) The wedge splitting test: a method of performing stable fracture mechanics tests. *Eng Frac Mech* 35:117-125
 83. Blanksvärd T, Täljsten B (2008) Strengthening of concrete structures with cement based bonded composites. *J Nord Concr Res* 38:133-153
 84. Täljsten B, Blanksvärd T (2007) Mineral-Based Bonding of Carbon FRP to Strengthen Concrete Structures. *J Compos Constr* 11(2):120-128
 85. Kim YY, Kong HJ, Li VC (2003) Design of Engineered Cementitious Composite (ECC) Suitable for Wet-mix Shotcreting. *ACI Mat J* 100(6):511-518

PAPER V

“Shear design for concrete structures
strengthened with mineral-based
composites”

BY

Thomas Blanksvärd, Björn Täljsten and Lennart Elfgren

Submitted to

ACI Structural Journal in March 2009

Shear design for concrete structures strengthened with mineral-based composites

Thomas Blanksvärd, Björn Täljsten and Lennart Elfgren

Biography:

ACI member **Thomas Blanksvärd** is a PhD student at the Division of Structural Engineering, Luleå University of Technology in Sweden. He received his MSc in Civil Engineering in 2004 and his Lic Sc (Licentiate of Science) in 2007 both from LTU. His main research interest includes assessment of concrete structures together with concrete strengthening and rehabilitation using FRPs and Mineral Based Composites (MBC).

Björn Täljsten is a full Professor at Denmark Technical University in the area of structural engineering. He has been active in the area of advanced composites for use in civil engineering and in particular for strengthening of structures since the beginning of the 1990s. His research is today focused on rehabilitation, structural health monitoring, and the use of reliability theory for rehabilitation purposes.

ACI fellow **Lennart Elfgren** is a full Professor at Luleå University of Technology in Sweden. His research interests include assessment and strengthening of structures, fracture mechanics and cements with low environmental impact. He is an associate member of ACI Committees 355 “Anchorage to Concrete”, 445 “Shear and Torsion”, and 446 “Fracture Mechanics”.

Abstract The use of externally bonded FRPs (Fibre Reinforced Polymers) to strengthen concrete structures is a well known method to restore or increase the load bearing capacity. In this paper a novel strengthening system is presented that substitutes the epoxy for a mineral-based bonding agent. The system is termed mineral-based composites (MBC) and uses polymer modified mortars together with a carbon FRP grid. The focus within this paper is placed on shear design models to estimate the shear resistance of concrete beams strengthened with the MBC system. Three different shear design approaches are presented based on (1) “addition” approach using a 45° truss, (2) variable angle truss (VAT) and (3) modified compression field theory (MCFT). The proposed models are confirmed by an experimental program on strengthened and non-strengthened reinforced concrete beams with rectangular cross section. The results show that the proposed shear design models provide relatively good estimations of the shear resistance.

Keywords: Concrete; Shear; Compression Field Theory; Strengthening; Mineral Based Composites; MBC; FRP; Carbon Fiber

1 Introduction

Strengthening concrete structures in shear with the use of external fiber reinforced polymers (FRP) has been the topic of researchers since the end of the 1980s¹. The most common external concrete strengthening systems involve using glass- and/or carbon fibers (dry fibers or in a matrix) bonded to the concrete surface using an epoxy bonding agent. The results from using epoxy-based strengthening have shown excellent results when it comes to increasing the shear resistance of the strengthened structure^{2,3,4,5}. However, the use of epoxy bonding agents has several drawbacks. Thermosetting epoxies are considered toxic and can cause irritation and eczema when in contact with skin. This leads to restrictions in the working environment. Additionally, epoxies create diffusion tight surfaces which may lead to moisture and freeze and thaw problems, in particular for concrete structures. Curing of thermosetting adhesives is a chemical process and is dependent on the surrounding temperature and the recommended temperature at the time of application is often 10°C. Moreover, most epoxies cannot be applied on wet or damp surfaces. It is therefore of interest to substitute the epoxy bonding agent with a bonding agent that is more compatible with concrete. In addition to the above, epoxies are organic compounds with very different mechanical properties to concrete. Using a mineral-based binder, e.g. polymer modified mortars, is one way of counteracting the above-mentioned drawbacks of epoxy, but still using the benefits of the CFRP. The strengthening system evaluated in this paper is based on a polymer modified mortar as a bonding agent reinforced with a two dimensional, orthogonal, carbon FRP (CFRP) grid. This system is termed mineral-based composites (MBC)⁶.

This paper presents different approaches for designing the shear resistance of reinforced concrete beams strengthened with mineral-based composites. A comparison is made between theory and experimental investigations.

2 Research significance

To convince the end user that new strengthening methods are advantageous compared to existing methods not only laboratory test and demonstration projects are needed but also models for design. Designing the shear resistance for concrete structures is complicated and existing models give scattered results, even for non-strengthened structures. When concrete structures are strengthened in shear the design becomes even more complex taking the additional strengthening system into consideration. To be able to accurately design for shear strengthening, consistent models must be developed, based on mechanical and material level. This paper presents further development on existing shear models adopted for the previously mentioned MBC strengthening system.

3 Mineral-Based Composites (MBC)

The strengthening system described in the following is using a mineral-based binder, e.g. fine grained polymer modified mortar, and a CFRP grid with the tows placed orthogonal to each other. The strengthening system in the current research is applied in five subsequent steps. Firstly, the surface of the base concrete has to be roughened by removing damaged or poor concrete. This is done either by sandblasting, grinding or water-jetting. One advantage with this system is that the base concrete surface does not have to be smooth prior to application, as with many epoxy-based systems. Secondly, the prepared surface needs to be primed to prevent moisture transport from the wet mortar to the dry base concrete. Thirdly, a first layer of mortar is applied wet in wet with the primer. Fourthly, the CFRP grid is applied on the first layer of mortar and finally covered with the second layer of mortar. Figure 1 shows the different layers of mortars and a CFRP grid for shear application on a RC beam. There exist several publications on the MBC strengthening performed by the authors, flexural strengthening⁶, a full experimental investigation in shear⁷ and comparison of the MBC system to other existing mineral-based strengthening system⁸.

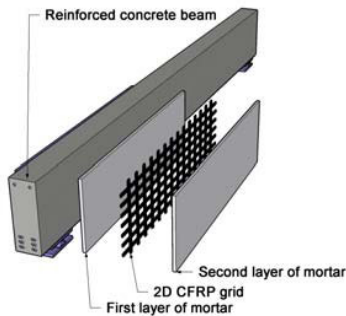


Fig. 1–Schematic overview of a system for shear strengthening using Mineral-Based Composites (MBC).

4 Shear Design

4.1 Background

When designing reinforced concrete with diagonal cracking, truss models are considered a rational and consistent basis and are implemented in most shear design codes such as the American ACI⁹, European Eurocode¹⁰, Swedish BBK¹¹ just to mention a few.

The shear resistance might be analyzed by a 45° truss analogy where the shear reinforcement performs as tensile ties. This truss analogy was foremostly derived by Morsch¹², see figure 2. However, the shear resistance based on the Morsch truss analogy is generally underestimated compared to experimental results. An improved agreement is obtained if the nominal total shear resistance of the concrete member, V_u , is understood as the sum of the shear resistance, V_c , at flexure-shear failure *without*

shear reinforcement and the shear resistance, V_s , obtained by the truss analogy at the yield strength of the shear reinforcement.

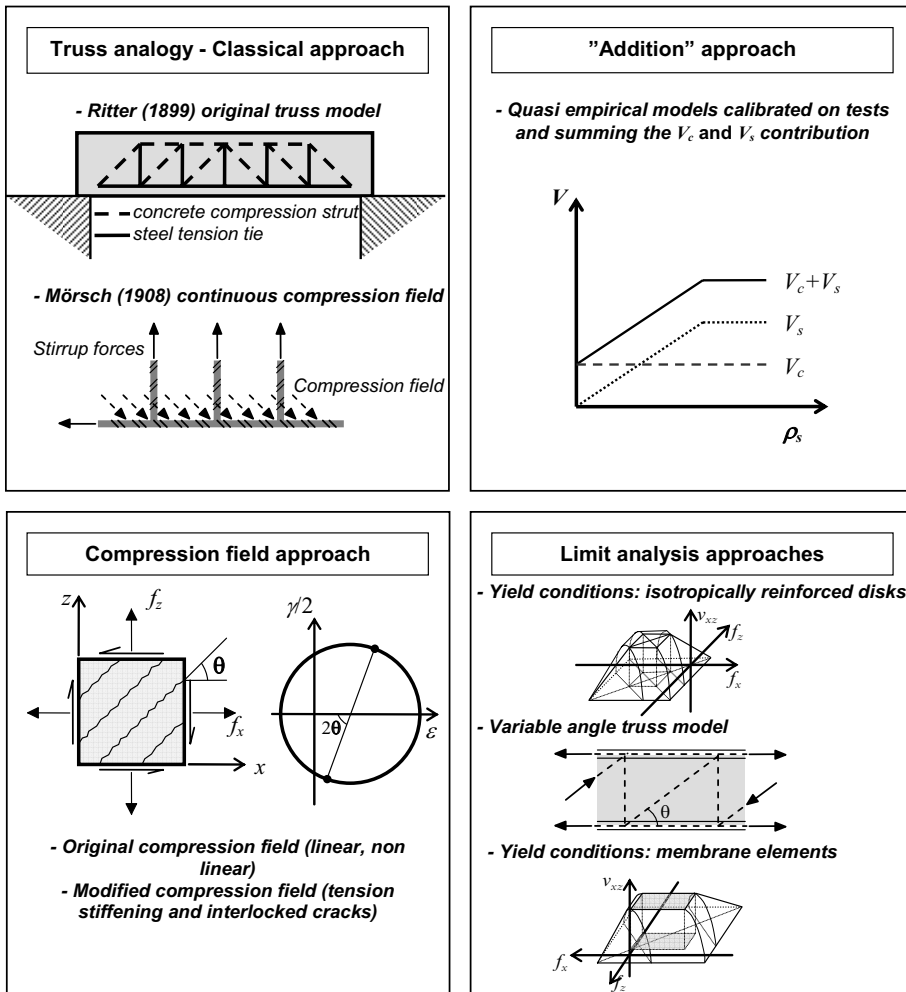


Fig. 2–Different methods for designing reinforced concrete structures for shear.

$$V_u = V_c + V_s \quad 1$$

The methodology described above is often referred to as the “additional principle” but is hereafter named “addition” approach and is based on regression on empirical data^{13,14,15}. This “addition” approach is implemented in the design codes ACI⁹ and BBK¹¹.

However, instead of compensating the conservative Morsch 45° truss analogy by adding a concrete contribution in the “addition” approach, the inclination of the diagonal concrete compressive strut could be assumed to be lower than 45°. This

approach is known as variable angle truss models (VAT), where the inclination of the diagonal compressive strut θ is set as an additional unknown.

During recent years new and more theoretically advanced shear models has been derived¹⁶. These are based on more profound theoretical foundations. One of these methods is the compression field approach which takes the compression softening of concrete due to successive cracking into consideration¹⁷ and the tensile resistance of concrete^{18,19}. Other methods are based on the theory of limit analysis and concrete plasticity²⁰. Here, the hypothesis is based on the fact that the web is fully plasticized in the ultimate limit state. Thus, the shear reinforcement yields simultaneously as the concrete in the web are deformed ideal plastic due to the diagonal compressive forces. Further development using concrete plasticity for members subjected to shear has also been made by the Cracked Membrane Model²¹.

A schematic overview and partitioning of the different fundamental shear design approaches is presented in figure 2. The shear designs are divided into the (a) Classical approach of truss analogy, (b) “Addition” approach, (c) Compression field approach and (d) Limit analysis approach. Note that the variable angle truss model is subcategorized in the limit analysis approach because it was put on a sound physical basis through the lower bound theorem and limit analysis²² by means of finding the additional unknown inclination, θ , of the compression strut. The variable angle truss model based on limit analysis is implemented in the Eurocode¹⁰ shear design.

4.2 Quasi-empirical “addition” approach

Early studies on the experimental shear behavior (stirrup strains) and the shear behavior predicted by the 45° Mörsh truss model is shown in figure 3. The conservatism in the 45° Mörsh truss model originates in neglecting the tensile stresses in the concrete and the assumption of the 45° inclination of the compressive strut. Thus, the model predicts that a beam with no shear reinforcement would have zero shear resistance. This is clearly not the case because concrete beams without shear reinforcement will fail after the formation of diagonal cracks. In the 1950s it was still recommended by researchers to use 45° Mörsh truss model for shear design²³. This approach will render in members having some reserve shear resistance when failing in flexure.

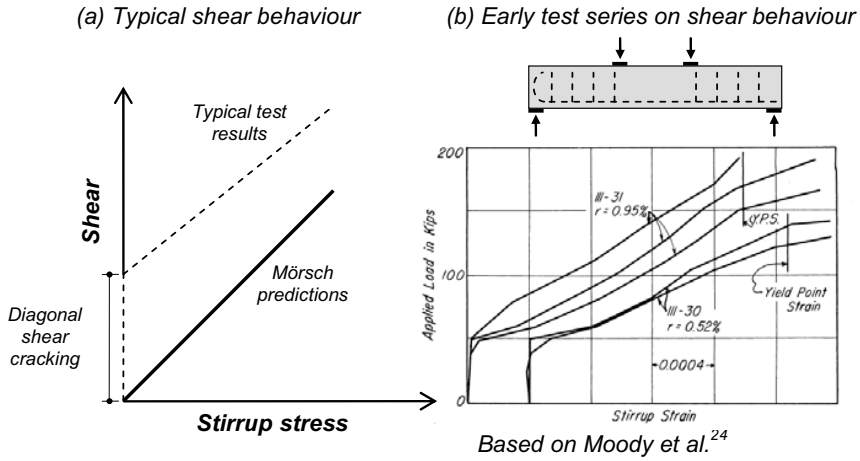


Fig. 3–Different methods for designing reinforced concrete structures for shear.

As mentioned above, the ACI⁹ and BBK¹¹ shear design models use the classical 45° Mörsch truss approach together with regression analysis based on experimental data. The ACI design is based on a systematic study of 440 specimens with no shear reinforcement and the identified influencing factors were longitudinal reinforcement ratio, moment to shear ratio and the concrete quality expressed in compressive strength¹³. As a simplification, for very high bending moments, the ACI shear contribution from the concrete is proposed as equation (2a and b) for flexure-shear cracking. In this simplification no consideration is taken to the dowel action or the size effect, although it is stated in ACI⁹ that the shear strength decreases as the depth increases. This size effect and dowel action is considered in the BBK¹¹ design and instead of using the influence of the concrete quality as a function of the square root of the compressive strength the tensile strength of the concrete is considered by a 70% reduction. The BBK¹¹ is based on the regression analysis by Hedman and Losberg¹⁵. For calculating the shear capacity contribution of the steel reinforcement, V_s , a straight forward 45° Mörsch truss approach is used.

$$V_c = 0.17\sqrt{f'_c} b_w d \text{ [SI units]} \quad 2a$$

$$V_c = 2\sqrt{f'_c} b_w d \text{ [US Customary]} \quad 2b$$

4.3 Limit analysis and concrete plasticity

The history of plasticity dates back to the 1860s, by Tresca²⁵. But it was not until the 1950s that it was put on a sound physical basis through researchers such as Daniel Drucker and William Prager. This section summarizes the basic concepts of limit analysis based on concrete plasticity for perfectly plastic material behavior. For simplicity a rigid perfectly plastic material behavior is assumed. By doing so, complicated formulations including elastic strains are avoided. A rigid-plastic material behavior is not a realistic estimation but can be used when the plastic strains are much

larger than the elastic strains, the different material behaviors are shown in figure 4. In plasticity theory the limit analysis is based on lower bound theorems (considering statically admissible state of stresses at or below yielding) and upper bound theorems (considering kinematically admissible state of deformation at or above yielding).

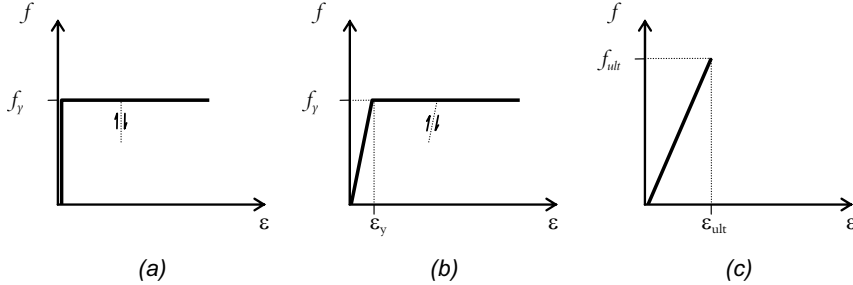


Fig. 4–Different material behavior, (a) rigid perfectly plastic, (b) elastic perfectly plastic and (c) linear elastic.

Nielsen²⁰ suggested a shear design approach for reinforced concrete using plasticity models based on the lower bound solution since this renders safe shear resistance. Shear design in Eurocode¹⁰ is based on the plasticity theory for the concrete contribution and the variable angle truss model. Note, the concrete contribution is only used for concrete members without shear reinforcement and should not be used in the case where steel shear reinforcement exists, as in the “addition” approach. For members with shear reinforcement the limitations of the inclination of the compressive strut are limited to $21.8^\circ \leq \theta \leq 45^\circ$ ($2.5 \leq \cot \theta \leq 1$). Thus, the concrete contribution to the shear strength is neglected but the conservatism in the 45° Mörsh truss approach is met by reducing the inclination of the compression strut. However, this inclination is not calculated but has to be assumed by the designer but within the above-mentioned limits.

A recent development by Kaufmann²⁶, based on limit analysis and concrete plasticity, uses a different approach by assuming a bi-linear material behavior of the steel reinforcement and introducing concrete compression softening and tension stiffening effects due to bond between reinforcement and concrete. This generates a quite intricate shear model known as the cracked membrane model (CMM). Solving the shear resistance according to a full cracked membrane model involves considerable numerical modeling. An approximate solution exists but then some vast simplifications are made such as assuming linear elastic behavior. However, this model is not included in the investigations of this paper.

4.4 Compression field theory

Compression field approaches assume fictitious rotating cracks that are stress free and parallel to the principal (diagonal) compressive direction. A uniform uniaxial compressive stress field is considered and thus neglects local variations of the stresses in the concrete and reinforcement due to tension stiffening. In a diagonally cracked

web the concrete is subjected to substantial tensile strains and the compressive strain may also need to be transmitted through previously formed cracks. In order to manage this discrepancy, Vecchio and Collins¹⁸ proposed the modified compression field theory (MCFT) taking the concrete tensile resistance into consideration.

However, there are some inconsistencies in the MCFT. The first is the assumption that the principal stress direction and the principal strain direction coincide with the crack direction, which is not necessarily true when comparing experimental tests to theory due to the complexity of concrete shear cracking. However Vecchio and Collins¹⁸ showed that the deviation between the directions of the principal stress and strain was not that significant and that the above-mentioned assumption was reasonable.

The MCFT often overestimates the shear resistance and to counter this problem a crack check based on the shear stresses acting on the crack surface (aggregate interlocking) was introduced^{18,27}. This is not in accordance with the assumption of the Mohr's circle of the principal stress plane not having any shear stresses, which is the foundation of MCFT. Nevertheless, reinforced concrete is a composite having scattering results when it comes to experimental tests and the MCFT gives reasonable estimations of the shear resistance during the load history. The software "Response" is based on the MCFT theory and developed by Evan Bentz in his doctoral thesis²⁸. Here a comparison of predictions of the MCFT to the experimental results of 534 beams showed very good agreement, independently of concrete compressive strength, shear span to depth ratio, beam depth, influence of longitudinal or transverse reinforcement etc. Of a total 534 of beams the ratio between experimental and predicted shear resistance was 1.05 with a COV of 12% which should be compared to the ACI⁹ average ratio of 1.2 and a wide scatter having a COV of 32%.

Using a full MCFT analysis for design requires that the 15 basic equations in MCFT have to be solved simultaneously by an iterative process²⁷. This process is not suitable for practical design and a simplified MCFT approach is given in²⁹ and also implemented in the Canadian design code³⁰. One of the main simplifying assumptions is that the shear strength of members with no stirrups is controlled by aggregate interlocking together with a conservative assumption that the failure occurs just before yielding of the transverse reinforcement. Further simplifications are also made by limiting the strains, such as for yielding of the stirrups ($\varepsilon_z \geq 0.002$), crushing of concrete ($\varepsilon_2 \approx 0.002$) and limiting the longitudinal strain at failure (ε_x) to 0.002. The calculation procedure of the shear resistance according to the simplified MCFT involves a few steps more than the shear design given by, e.g. ACI⁹. As a first step, the longitudinal strain ε_x has to be assumed and then this assumption has to be checked for convergence by control of the longitudinal equilibrium (x-direction) and assuming that the longitudinal reinforcement is not yielding. The upper limit of the maximum shear stress is assumed to be $0.25f'_c$ and the last check is to see if the longitudinal reinforcement can transmit the shear stress along the crack without exceeding its yield stress. In the simplified MCFT²⁹, the average ratio between experimental to predicted shear resistance for 102 concrete elements was 1.11 with a COV of 13%.

The simplified MCFT is basically a linear relationship when considering the longitudinal strain, ε_s , and gives reasonable results for strains given in the limited area of strain levels up to 0.002. Note, for the use of longitudinal reinforcement with higher strain capacity such as FRPs (strains ranging from approximately 0.01-0.03), a second order approximation based on MCFT and simplified MCFT can be found in³¹.

4.5 Estimation of shear resistance

All of the different proposed shear design methods mentioned in the previous sections give different estimations of the shear bearing capacity, especially for concrete beams with no shear reinforcement. For the shear design of the contribution from the stirrups to the shear resistance ACI⁹ and the BBK¹¹ give similar results since it is only the internal lever arm, d , that is varied. In the ACI⁹, d is used and in the BBK¹¹, $0.9d$ is used. In Eurocode¹⁰ the inclination of the diagonal compressive strut has to be chosen based on the given interval $21.8^\circ \leq \theta \leq 45^\circ$, where low inclination gives less conservative values and a high inclination gives more conservative values on the shear resistance of the steel shear reinforcement. In the MCFT approach this inclination rotates during the analysis. Since the contribution of the steel shear reinforcement in the shear design models^{9,11,10} is more or less straightforward this section will compare the shear resistance estimations of the different models for concrete containing no shear reinforcement. The estimations are compared to experimentally obtained shear resistances taken for the beam specimens C35s0, C40s0 and C55s0, see Table 2.

The results obtained from different ratios between calculated and experimentally obtained shear resistance for the three different concrete qualities are shown in figure 5. The concrete quality is taken as the ratio between the concrete compressive and tensile strength. All of the model predictions were conservative except for the BBK¹¹ which overestimated the resistance for lower concrete qualities. The model with the best predictions was the MCFT approach and the model with the most conservative predictions was the one in Eurocode¹⁰.

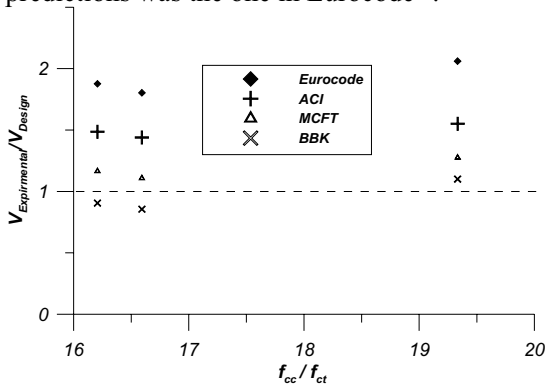


Fig. 5–Ratio between experimental and predicted shear resistance for beams C35s0, C40s0 and C55s0 made of concrete with different ratios between compressive and tensile strength.

4.6 Shear design for strengthened concrete structures

There exists a set of guidelines for strengthening concrete structures in shear, using externally bonded FRP to the concrete, for example^{32,33,34,35}. A comparison of different analytical approaches based on the most common shear design proposals is given in³⁶. In this comparison a database of over 200 beams strengthened in shear by FRP were surveyed and the results indicate a wide scatter of the experimental versus predicted shear resistance. Most of the guidelines practice the “addition” approach by adding the shear resistance contribution of the FRP to the steel and concrete shear resistance according to

$$V_u = V_c + V_s + V_f \quad 3$$

Using this approach makes it even more important that the proposed design is based on the same foundational shear approach, for example using the sum of V_c based on regression and V_s based on the 45° Mörsh truss approach^{9,11}. However, it can be argued that the V_f contribution is independent of the base concrete structure. But when carrying out shear design, the V_s and V_f contribution should be based on the same truss analogy (VAT or 45°). Thus, in this paper, the total shear capacity of a strengthened beam is considered to be modeled based on the same foundational theory, e.g. using a 45° truss for both V_c and V_f as in ACI Committee 440³². Using the design based on the variable angle truss model as in Eurocode¹⁰ based on concrete plasticity could involve some difficulties regarding the basic assumptions on the limits of the inclination of the compressive strut, θ , considering the elastic brittle behavior of the FRP versus the yielding behavior of steel shear reinforcement. However, since the concrete contribution is neglected for members with shear steel reinforcement there is some inherent safety in the design. This is further discussed below.

5 Experimental investigation

5.1 Materials

The materials used in the experimental study were concrete, reinforcement, a commercially available polymer modified mortar (StoCrete GM1) and three different CFRP grids (orthogonal tows). Tested mechanical properties for the different CFRP grids in both longitudinal and transversal direction are shown in Table 1 together with the geometrical properties provided by the manufacturer. The tensile testing procedure is given in⁷. The manufacturer provided mortar properties are; compressive strength 45 MPa (6.53 ksi) and modulus of elasticity 26.5 GPa ($3.84 \cdot 10^3$ ksi). The concrete compressive and tensile strength were tested on 150 mm (5.9 in) cubes and the compressive and tensile strengths for each beam specimen are shown in Table 2. The tensile behavior of the steel reinforcement was tested; the flexural reinforcement had a yield strength of 555 MPa (80 ksi) and a yield strain of 2.79%, and the shear reinforcement had a yield strength of 601 MPa (87 ksi) and a yield strain of 2.84%.

In addition, four of the beam specimens were also strengthened with two epoxy-bonded near surface mounted (NSM) CFRP bars to increase their bending capacity.

They had a rectangular cross section of 100 mm² (0.16 si.) and were bonded into sawed grooves in the concrete cover on the tensile side of the beams using a two component epoxy adhesive. The tensile properties are, as provided by the manufacturer; modulus of elasticity 260 GPa (37.7·10³ ksi) and ultimate strain 0.8%. The properties of the adhesive (as provided by the manufacturer) are tensile strength 31 MPa (4.5 ksi) and modulus of elasticity 7 GPa (1.0·10³ ksi).

Table 1-Manufacturer provided geometrical specifications and tested mechanical properties for the CFRP grids, S=small, M=medium and L=large.

| Grid | Grid spacing, mm (in.) | | Elastic modulus, GPa (10 ³ ksi) | | Ultimate strength, MPa (ksi) | | Tow area, mm ² (10 ⁻³ si) | | Fiber amount, g/mm ² (oz/si) |
|------|------------------------|--------------|--|-------------|------------------------------|---------------|---|------------------|---|
| | Long | Trans | Long | Trans | Long | Trans | Long | Trans | |
| S | 24 (0.98) | 25 (0.98) | 278 (40) | 366 (53) | 3546 (514) | 5214 (756) | 0.3570 (0.55) | 0.2395 (0.37) | 66 (2.90) |
| M | 42 (1.65) | 43 (1.69) | 404 (59) | 389 (56) | 4219 (611) | 4620 (670) | 0.9184 (1.42) | 0.9184 (1.42) | 159 (6.98) |
| L | 70 (2.76) | 72 (2.83) | 320 (46) | 423 (61) | 3877 (562) | 3772 (547) | 1.2684 (1.97) | 1.0710 (1.66) | 98 (4.30) |

5.2 Experimental set up

The concrete beam specimens had a rectangular cross section and were heavily reinforced in flexure using 12 Ø 16 mm (0.63 in.) in the bottom and two Ø 16 mm (0.63 in.) in the top. In total, 18 beams were tested. The varied parameters were; different concrete qualities¹⁰ (C35 (5.1 ksi), C40 (5.8 ksi) and C55 (8.0 ksi), based on cylindrical compressive strength), internal shear steel reinforcement ratios of 0, 3.59 and 5.03% and in total using three CFRP grids with different mechanical and geometrical properties, see Table 1.

All of the concrete beam specimens had similar geometries and were subjected to four-point loading, shown in figure 6. The specimens were reinforced in such a way that shear failure was directed to one half of the beam span, i.e. one shear span was over reinforced. Thus, only one shear span was strengthened and in this span the shear reinforcement and strengthening was varied. The different internal shear reinforcement ratios, stated above, correspond to no stirrups and stirrup distances of s=350 mm (13.8 in.) and s=250 mm (9.8 in.) respectively. The first category with no shear reinforcement gives the concrete contribution to the shear strength. The other two categories are mainly considering the interaction between concrete and internal shear reinforcement and the interaction between internal shear reinforcement and MBC strengthening. In this way, both the concrete contribution and the reinforced concrete contribution to shear resistance are evaluated together with the influence of MBC strengthening. All of the specimens were loaded using a controlled deformation rate of 0.01 mm/sec (3.9·10³ in./sec) except specimens marked with an asterisk in Table 2. These beams were load controlled at 10 kN/min (2.2 kips/min).

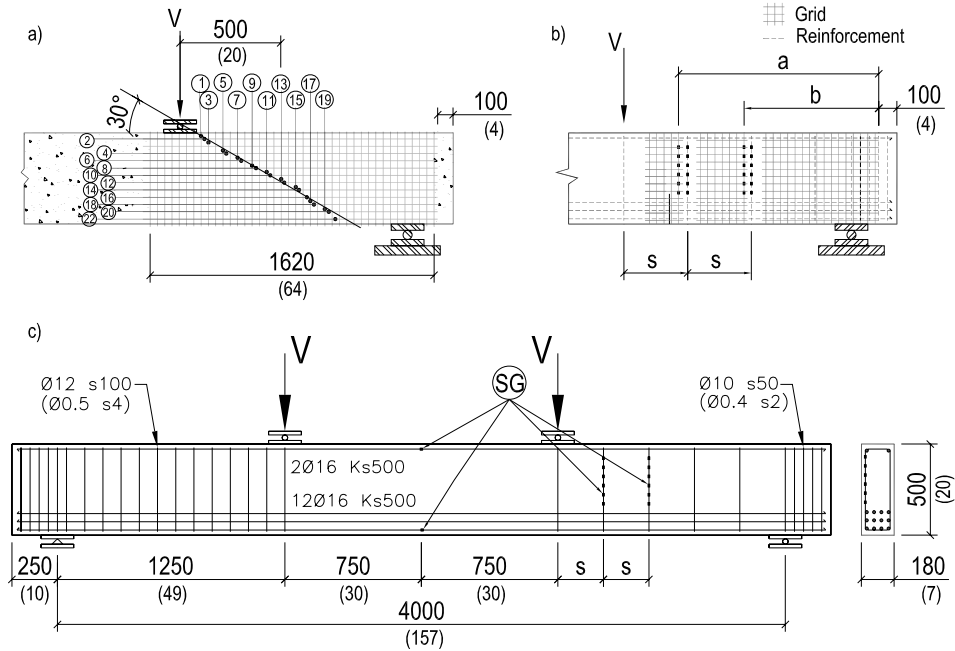


Fig. 6—(a) Strain gauges (SGs) aligned at a 30° angle (specimen C40s0-M_b), (b) SGs on transverse CFRP tows and (c) Experimental set-up and SGs on stirrups. The longitudinal reinforcement consist of 16 mm (0.64 in.) bars.

5.3 Strain gauge monitoring

A quite extensive monitoring program was established to record the strain development in the reinforcement and in the CFRP grid using electrical foil strain gauges (SG). Two different types of SGs, of different size, were used. To measure the strain in the steel reinforcement a gauge length of 5 mm (0.2 in.) was used (KFW-5-120-C1-11L3M2R) and to measure the strain in the CFRP grid a gauge length of 2 mm (0.08 in.) was used (KFWS-2N-120-C1-11L3M3R).

All of the beam specimens had strain gauges mounted on the compressive and tensile reinforcement located at the midsection of the beam. Six SGs were mounted on the two stirrups closest to the load in the weaker shear span. A similar SG set up was also used on the transverse CFRP tows. All of these SGs were mounted at 170 mm (7.7 in.) from the bottom of the beam and then with a distance of 50 mm (2 in.). In addition, SGs were also mounted at a presumed shear crack alignment of 30° for one of the beams with no internal shear reinforcement but strengthened with the MBC system (specimen C40s0-M_b). These SGs were mounted in pairs on both transverse and longitudinal CFRP tows. All SG set-ups are shown in figure 6. A more detailed elaboration of the experimental program, is given in^{7,37}.

Table 2-Beam specimens, concrete compressive and tensile strengths, failure loads and failure modes.

| Beam ^a | CFRP | Stirrup distance, mm, (in.) | Compressive strength, MPa (ksi) | Tensile strength, MPa, (ksi) | Failure load, kN (kips) | Failure mode ^b |
|----------------------|--------|-----------------------------|---------------------------------|------------------------------|-------------------------|---------------------------|
| C40s0 | - | - | 44.8 (6.5) | 3.6 (0.5) | 123.5 (27.7) | S |
| C40s0 ^l | - | - | 36.3 (5.3) | 3.1 (0.4) | 126.7 (28.5) | S |
| C40s0-M _a | Grid M | - | 53.6 (7.8) | 3.5 (0.5) | 244.9 (55.1) | S+R |
| C40s0-M _b | Grid M | - | 53.6 (7.8) | 3.5 (0.5) | 241.9 (54.4) | S+R |
| C40s0-S ^l | Grid S | - | 32.5 (4.7) | 3.4 (0.5) | 208.1 (46.8) | S+R |
| C40s0-M ^l | Grid M | - | 35.1 (5.1) | 3.8 (0.6) | 251.9 (56.6) | S+R |
| C40s0-L ^l | Grid L | - | 44.8 (6.5) | 3.1 (0.4) | 206.4 (46.4) | S+R |
| C35s0 | - | - | 47.0 (6.8) | 3.3 (0.5) | 130.6 (29.3) | S |
| C35s3 | - | 350 (13.8) | 47.6 (6.9) | 3.9 (0.6) | 346.0 (88.8) | C+S |
| C35s3-M | Grid M | 350 (13.8) | 52.4 (7.6) | 3.7 (0.5) | 336.9 (75.7) | C |
| C35s2-M ^r | Grid M | 250 (9.8) | 51.4 (7.5) | 3.5 (0.5) | 370.5 (83.3) | C |
| C55s0 | - | - | 63.8 (9.3) | 4.2 (0.6) | 158.8 (35.7) | S |
| C55s3 | - | 350 (13.8) | 73.3 (10.6) | 4.6 (0.7) | 318.9 (71.7) | S |
| C55s2 | - | 250 (9.8) | 83.5 (12.1) | 4.2 (0.6) | 361.4 (81.2) | C |
| C55s2 ^r | - | 250 (9.8) | 78.3 (11.4) | 4.1 (0.6) | 399.5 (89.8) | S |
| C55s3-M ^r | Grid M | 350 (13.8) | 77.3 (11.2) | 4.7 (0.7) | 369.5 (83.1) | C |
| C55s2-M ^r | Grid M | 250 (9.8) | 64.6 (9.3) | 3.9 (0.6) | 403.6 (90.7) | C |

a – the beam designation gives the concrete quality, stirrup spacing and CFRP grid size

b – S=shear, R=rupture of CFRP and C=concrete compression

l – the deformation rate during loading was not controlled, load controlled at 10 kN/min

r – these specimens were strengthened with NSM bars.

6 Analytical procedure

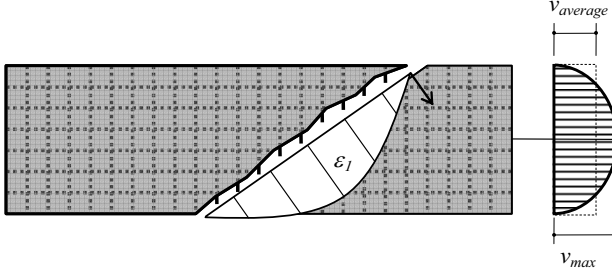
This section describes three shear design approaches for reinforced concrete beams with rectangular cross section strengthened with the MBC system. The internal shear steel reinforcement is vertical and only the transverse CFRP tows are considered whereas the longitudinal tows give such a small contribution that they can be neglected.

6.1 Effective strain in linear elastic material

The tensile behavior of CFRP is linear elastic up to the ultimate failure its behaviour can be modelled in a simple way by an effective strain. Further, a strain reduction factor, η , is introduced based on the ratio between the maximum shear stresses and the average shear stresses for a rectangular cross section³⁸, see equation(4), (5) and figure 7. For further discussion of effective strains for cracked cross sections, the reader is referred to⁴.

$$\varepsilon_{f_z,ef} = \eta \varepsilon_{fuz} \quad 4$$

$$\eta = \frac{v_{average}}{v_{max}} = \frac{V/A}{3V/(2A)} = \frac{2}{3} \quad 5$$



(a) Principal tensile strain

(b) Shear stress distribution

Fig. 7–(a) Principal tensile strain distribution along a diagonal crack, (b) shear stress distribution over a rectangular cross section.

6.2 “Addition” approach

The “addition” approach based on the 45° Mörsh truss gives the following expression for the steel contribution, see figure 8 setting the inclination of θ to 45°.

$$V_s = \frac{A_{sz} f_{sz}}{s} z \quad 6$$

For the transverse CFRP tows on both sides of the beam we obtain.

$$V_f = 2 \frac{A_{fz} f_{fz}}{s_{fz}} z \quad 7$$

6.3 Variable angle truss model approach

In the variable angle truss approach the inclination of the compressive strut is set as an additional unknown. The diagonal stress f_2 can be expressed by the shear force in the diagonal equilibrium in figure 8 b. Realizing from figure 8 c, that the diagonal compressive force from f_2 must be counteracted by the shear reinforcement and the transverse CFRP grid tows gives

$$V = V_s + V_f = \left(\frac{A_{sz} f_{sz}}{s} + 2 \frac{A_{fz} f_{fz}}{s_{fz}} \right) z \cot \theta \quad 8$$

Note, both the “addition”- and variable angle approach need to have upper limits of the ultimate load concerning the web compressive failure. These upper limits can be used as given in ACI⁹, BBK¹¹ and Eurocode¹⁰.

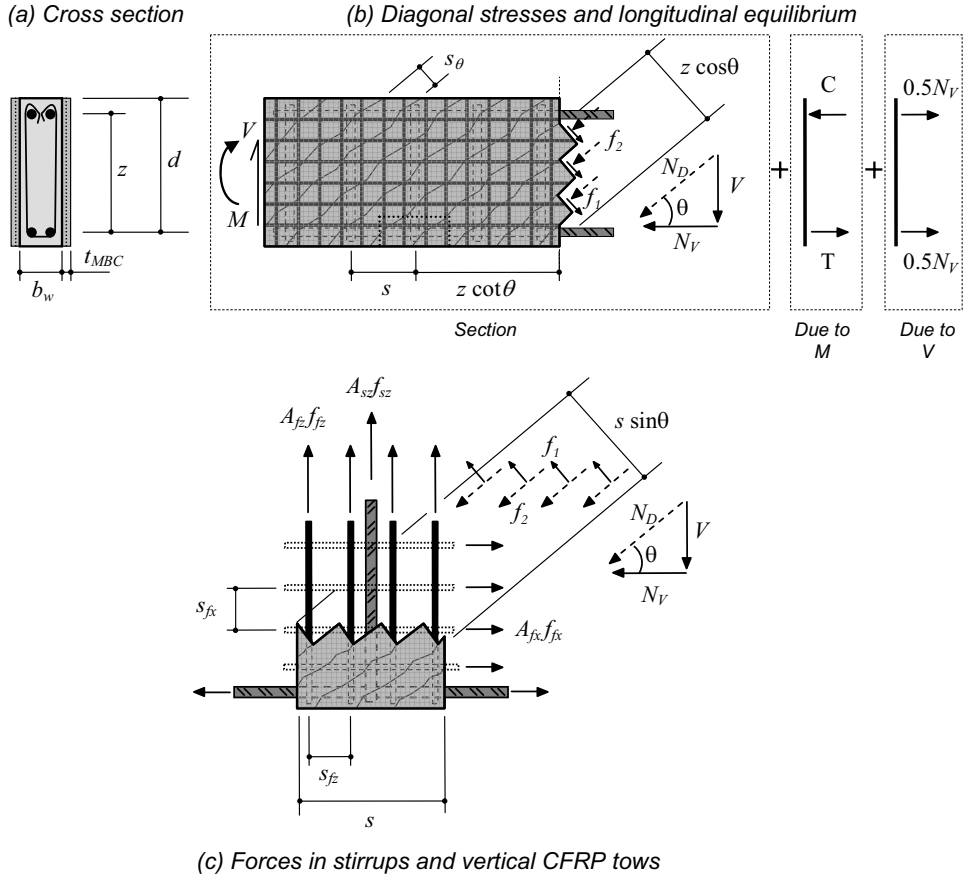


Fig. 8—Geometry and equilibrium for the MCFT approach developed for the MBC system.

6.4 MCFT approach

A summary of the equations used in the MCFT²⁷ adopted for a section strengthened with the MBC system is given in figure 9.

The following steps are used for solving the member response.

1. Choose a value for the principal strain, ϵ_l .
2. Estimate the inclination of principal compressive stress, θ .

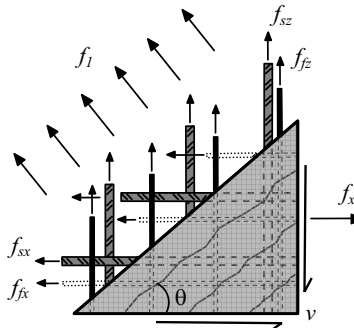
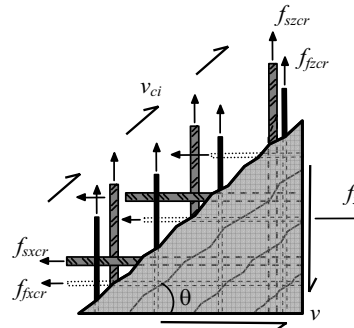
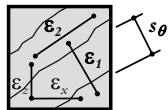
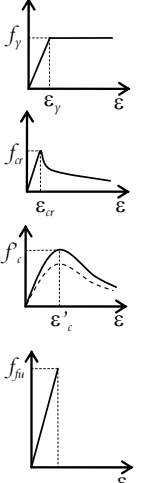
| | | |
|--------------------|---|--|
| EQUILIBRIUM |  <p><u>Average stresses</u></p> <ol style="list-style-type: none"> $f_x = \rho_x f_{sx} + \rho_{f_x} f_{f_x} + f_1 - v \cot \theta$ $f_z = \rho_z f_{sz} + \rho_{f_z} f_{f_z} + f_1 - v \tan \theta$ $v = (f_1 + f_2) / (\tan \theta + \cot \theta)$ |  <p><u>Stresses on crack</u></p> <ol style="list-style-type: none"> $f_{sxc} = \frac{(f_x - \rho_{f_x} f_{f_xcr} + v \cot \theta + v_{ci} \cot \theta)}{\rho_x}$ $f_{szc} = \frac{(f_z - \rho_{f_z} f_{f_zcr} + v \tan \theta + v_{ci} \tan \theta)}{\rho_z}$ |
| GEOMETRY |  | <p><u>Average strains</u></p> <ol style="list-style-type: none"> $\tan^2 \theta = (\epsilon_x + \epsilon_2) / (\epsilon_z + \epsilon_2)$ $\epsilon_1 = \epsilon_x + \epsilon_z + \epsilon_2$ $\gamma_{xz} = 2(\epsilon_x + \epsilon_2) \cot \theta$ <p><u>Crack widths</u></p> <ol style="list-style-type: none"> $w = s_\theta \epsilon_1$ $s_\theta = 1 / \left(\frac{\sin \theta}{s_{mx}} + \frac{\cos \theta}{s_{mz}} \right)$ |
| MATERIAL |  | <p><u>Stress – strain</u></p> <p>Steel:</p> <ol style="list-style-type: none"> $f_{sx} = E_s \epsilon_x \leq f_{yx}$ $f_{sz} = E_s \epsilon_z \leq f_{yz}$ <p>Concrete:</p> <ol style="list-style-type: none"> $f_1 = f_{cr} / (1 + \sqrt{500 \epsilon_1})$ $f_2 = \frac{f'_c}{0.8 + 170 \epsilon_1} \left[2 \frac{\epsilon_2}{\epsilon'_c} - \left(\frac{\epsilon_2}{\epsilon'_c} \right)^2 \right]$ <p>CFRP:</p> <ol style="list-style-type: none"> $f_{fx} = E_f \epsilon_x \leq f_{fux}$ $f_{fz} = E_f \epsilon_z \leq f_{fuz}$ |

Fig. 9–Summary of modified compression field theory used for MBC shear design, based on²⁹.

3. Calculate the diagonal crack width, w , using equation (9) and (10) in figure 9. The longitudinal and transverse average crack spacing, s_{mx} and s_{mz} , are calculated with

equation (9) and (10) based on the CEB-FIP code³⁹ when using deformed reinforcing bars.

$$s_{mx} = 2 \left(c_x + \frac{s_x}{10} \right) + \frac{d_{bx}}{10\rho_x} \quad 9$$

$$s_{mz} = 2 \left(c_z + \frac{s}{10} \right) + \frac{d_{bz}}{10\rho_z} \quad 10$$

Here c_x and c_z are the maximum clear cover distance in the longitudinal and the transverse direction respectively, s is the stirrup distance and s_x is the internal distance between the longitudinal reinforcement bars. For small distances between the longitudinal reinforcement bars, this contribution can be ignored. d_{bx} and d_{bz} is the diameter of the reinforcing bars, while ρ_x and ρ_z is the reinforcement ratio, in longitudinal and transverse direction respectively.

4. Estimate a level of the transverse strain, ε_z , and control that the stress level in the stirrups, f_{sz} , and in the transverse CFRP tows, f_{fz} , does not exceed the limiting stresses according to

$$f_{sz} = E_s \varepsilon_z \leq f_{sy} \quad 11$$

$$f_{fz} = E_{fz} \varepsilon_z \leq f_{fz,ef} \quad 12$$

5. Calculate the principal tensile stress according to equation (13) in figure 9. When assuming a principal tensile strain $\varepsilon_1 \leq \varepsilon_{cr}$, a linear relationship of f_1 is assumed according to Hooke's law, see also figure 9. Note that the two sets of stresses in figure 9, average stresses and stresses on the crack, must be statically equivalent. This limitation is also known as the "crack check"²⁸ and for these two sets of stresses to produce the same vertical component the requirement in equation (13) needs to be fulfilled. Here the stresses across the crack are substituted against the ultimate stresses, f_{sy} for the stirrups and $f_{fz,ef}$ for the transverse CFRP tows.

$$f_1 = v_{ci} \tan \theta + \frac{A_{sz}}{s b_w} (f_{sy} - f_{sz}) + 2 \frac{A_{fz}}{s_{fz} b_w} (f_{fz,ef} - f_{fz}) \quad 13$$

Here, v_{ci} is the shear stress across the crack due to aggregate interlocking shown in equation (15) in figure 9, note that a_g is the maximum aggregate size.

6. The total shear resistance, V , can be calculated using the equilibrium in figure 8 b and c and is given as.

$$V = \underbrace{f_1 b_w z \cot \theta}_{\text{concrete}} + \underbrace{\frac{A_{sz} z}{s} f_{sz} \cot \theta}_{\text{stirrups}} + 2 \underbrace{\frac{A_{fz} z}{s_{fz}} f_{fz} \cot \theta}_{\text{vertical CFRP tows}} \quad 14$$

7. The principal compressive stress, f_2 , is calculated using Mohr's circle of stress and the shear stress is assumed to be constant over the cross section. The principal compressive stress and the shear stress are then obtained as

$$f_2 = (\tan \theta + \cot \theta) v - f_1 \quad 15$$

$$v = V / (b_w z) \quad 16$$

8. Calculate the strength of the diagonal compression stress field, f_{2max} , by using equation (14) in figure 9.

9. Control that the calculated principal compressive stress is lower or equal to the strength of the diagonal compression field, $f_2 \leq f_{2max}$. If this requirement is not fulfilled, then go back to step 1 and choose a smaller ε_1 .

10. Calculate the transverse and longitudinal strains, ε_x and ε_z , along with the principal compressive strain, ε_2 , by elaborating equations (6), (7) and (14) in figure 9. The strains are then obtained as

$$\varepsilon_2 = \varepsilon'_c \left(1 + \sqrt{1 + f_2 / f_{2max}} \right) \quad 17$$

$$\varepsilon_x = \frac{\varepsilon_1 \tan^2 \theta + \varepsilon_2}{1 + \tan^2 \theta} \quad 18$$

$$\varepsilon_z = \frac{\varepsilon_1 + \varepsilon_2 \tan^2 \theta}{1 + \tan^2 \theta} \quad 19$$

11. Calculate the stresses corresponding to the strains obtained in step 10, f_{sz} and f_{fz} respectively. Then control that the estimation of the strain ε_z and the corresponding stresses, f_{sz} and f_{fz} , in step 4 is valid. If not, revise step 4 and proceed until the estimation corresponds to the calculated values.

12. Use a plane section analysis (see following section) and find the strain distribution corresponding to the moment due to the shear load obtained in step 6. Then check that the longitudinal strain obtained in step 10 is converging. If these two strains do not converge then revise the assumed inclination in step 3 until convergence is obtained. Note that the longitudinal strain obtained in step 10 is assumed to be located at $z/2$ (mid-depth of beam), for beams containing internal shear reinforcement. For beams with no internal shear reinforcement it is assumed to be located at the same level as the tensile reinforcement.

6.5 Influence of MBC thickness

The thickness of the MBC system gives an increase in the cross section which might also give a contribution to the shear resistance, depending on the thickness of the layer of the bonding agent. An engineering way of dealing with this is to assume that the increase in the width of the member is proportional to the elastic modulus by a factor η_{MBA} , shown in equation (20). By multiplying this factor to the thickness of the MBC, t_{MBC} , and adding this to the original width, b_w , of the base concrete member will render a new increased effective width of the strengthened member, b'_w , showed in equation (21).

$$\eta_{MBA} = \frac{E_{MBA}}{E_c} \quad 20$$

$$b'_w = b_w + 2\eta_{MBA} t_{MBC} \quad 21$$

Here E_{MBA} is the modulus of the mineral-based binder and E_c is the modulus of the base concrete. However, the thickness of the MBC system is often quite small in most MBC applications. This, together with the fact that most of the commercially

available binders have similar moduli as the base concrete, will allow the contribution of the binder to the shear resistance to be small or negligible. Nevertheless, neglecting the contribution of the binder in the MBC is a conservative approach for design.

6.6 Plane section analysis

Considering that “plane sections remain plane”, the stresses and strains can be calculated for a given concrete cross section. Concrete beams subjected to flexural loading commonly undergo several stages during loading. First, the concrete cross section is considered to be non-cracked, stage I. When the concrete tensile strength is exceeded cracks are formed and when the entire tension zone is cracked, the cross section has reached stage II. Finally, when the concrete compressive strength is attained the concrete beam has reached the ultimate limit stage, stage III. These three stages are shown in figure 10 b, for a concrete beam with a rectangular cross section.

However, the distinction between stage I and II can in some cases be hard to determine. A typical example of a moment-deflection diagram is given in figure 10a based on⁴⁰. This comparison with experiments is based on the ratio between cracked and non-cracked moment (M) and deflection (Δ). Note, that the chosen concrete tensile strength for going from non-cracked section to a cracked section significantly influences the analysis using the MCFT. A typical value for the cracking criteria is $1.5 f_{ct}$ (concrete tensile strength)⁴¹. In a solution procedure using the MCFT, the longitudinal strain, ϵ_x , is studied in the mid-depth of the cross section for beams with shear reinforcement. For a member having no shear reinforcement this strain is assumed to be at the same level as the highest longitudinal strain in the web²⁷. The reason for this is that as ϵ_x increases, the shear capacity decreases and members having shear reinforcement have considerable capacity for redistributing shear stresses from highly strained portions of the cross section to portions having less strain. While for members having no shear reinforcement and less capacity for redistribution, the higher strain level is chosen.

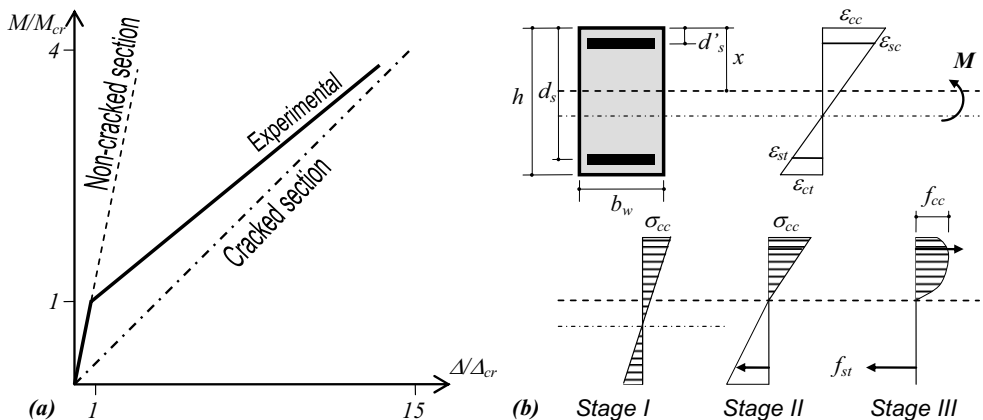


Fig. 10—(a) Typical moment-deflection for concrete members subjected to flexural loads, based on⁴⁰. (b) Different stages of a concrete beam with rectangular cross section subjected to flexural loading.

7 Comparison of predictions and experimental results

All of the experimentally obtained failure loads and failure modes together with compression and tensile strengths are shown in Table 2. The different failure modes are shear failure (S), rupture of the transverse CFRP tows (R) and concrete failure by crushing of the compression zone (C). All of the strengthened specimens, having internal shear reinforcement, failed by yielding of the tensile reinforcement and subsequently the crushing failure mode. It should be mentioned that the estimated shear resistance using the BBK¹¹ design rendered in lower estimations than experimentally obtained shear resistance.

Predictions of shear resistance were made for all of the beam specimens with no internal shear reinforcement using the experimentally obtained mechanical properties in the three different design proposals described above. These results were then compared to the experimentally obtained ultimate failure loads which are shown in the section of ultimate shear resistance, below. For the beams that failed by the crushing failure mode, the shear load and vertical strain development from both experiments and the ones predicted by the analytical solution based on the MCFT are shown in the section of shear load and vertical strain development.

7.1 Ultimate shear resistance

The ultimate shear resistance is calculated using the “addition” approach, the VAT approach and the MCFT approach for reference beams (beam specimens with no shear strengthening, e.g. C40s0, C40s0*) and for strengthened beams with different carbon fiber amounts, e.g. C40s0-M_a, C40s0M_b, C40s0-S*, C40s0-M* and C40s0-L*. The ratio between experimental and predicted failure loads are plotted against the ratio between transverse CFRP and concrete compressive strength ($\rho_{fz} f_{fuz} / f'_c$) in figure 11. Note, for the models requiring the cylinder concrete compressive strength, the cube strength in the design is taken as 83% for compressive strengths smaller than 45 MPa (6.5 ksi) and 75% for higher than 45 MPa (6.5 ksi)⁴². In the MCFT, ε'_c is taken as 0.002, the tensile cracking strain, ε_{cr} , as 0.00011 and the maximum aggregate size is 25 mm for all specimens. The tensile stress used in the MCFT is based on cylindrical tensile strength. Therefore, the tensile strength of the cube specimens is recalculated to cylindrical tensile strength according to⁴² as

$$f_{ct} = f_{cr} = 0.21 f_{c,cube}^{2/3} \quad 22$$

A comparison of experimental and predicted shear resistance ratio for the development of the “addition” approach for the MBC system is shown in figure 11. In this study, the beams have no internal shear reinforcement but different carbon fiber amounts (C35s0, C35s0-grid S,M,L).

Comparing the predictions of the different models in figure 11 it is clear that using the VAT approach as in the Eurocode will give extremely low accuracy for the MBC strengthened beams, although the least conservative inclination was chosen ($\theta=21.8^\circ$). But as the fiber amount is increased the predictions come closer to the experimentally obtained failure load. However, the predictions are still extremely low

compared to experiments. For the “addition” approach where the concrete contribution is considered, models based on ACI and BBK, give considerably improved predictions. The design proposal based on BBK results in the closest predictions although it overestimates the shear resistance of one of the reference beams, while the design based on ACI gives more conservative predictions. Finally, using the design based on MCFT gives excellent estimations.

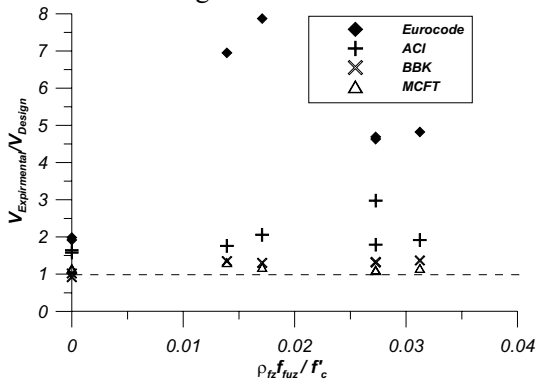


Fig. 11– Ratio of experimental vs. predicted values for the shear resistance of strengthened beams with *no* internal shear reinforcement as a function of the ratio between CFRP strengthening and concrete compressive strength.

The average ratio between experimental to predicted shear resistance for these 7 beams were; 1.96 with a COV of 24% for the design based on ACI, 1.22 with a COV of 15% for the design based on BBK, 4.70 with a COV of 48% for the design based on the VAT model and 1.16 with a COV of 6% for the design based on MCFT.

7.2 Shear load and transverse strain development

Predicted and experimentally found transverse strain development is presented in this section. The transverse strain development, for beam specimen C40s0-M_b (no stirrups) based on the predictions of the MCFT approach, is shown in figure 12 and with the strain readings from SG 13, located in the mid-depth of the beam, in figure 6a. Predicted strain development is calculated for both a non-cracked section and a cracked section. In addition, the same transverse strain development is compared to the different model predictions based on the “addition” approach and VAT, in figure 12. The results indicate that using MCFT with a cracked section analysis will give the best prediction of the transverse strain at ultimate limit state. The model based on BBK results in quite good agreement regarding the strain development but all predicted strains are conservative.

The transverse strain development for beams having internal shear reinforcement is shown in figure 13, for specimens C55s2-M^f and C35s3-M. Here, the predictions are based on cracked sections and are calculated at the point of the highest moment and shear (*point load*). In addition, the transverse strain is also calculated at a distance, *s* in figure 6b, of 250 mm (9.8 in.) and 350 mm (13.8 in.) from the load point

which corresponds to the line of the measured strains in the stirrups. The strains in figure 13 are taken from the SG on the stirrup closest to the load point and in mid-depth of the beam, see figure 6b. Note, the strains in the CFRP grid have only a moderate increase until a diagonal crack starts to develop, also typically shown in figure 3.

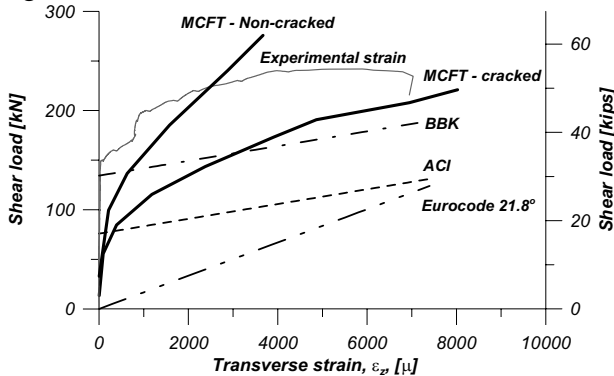


Fig. 12–Shear load and transverse strain development for specimen C40s0-M_b, (V_c+V_f)

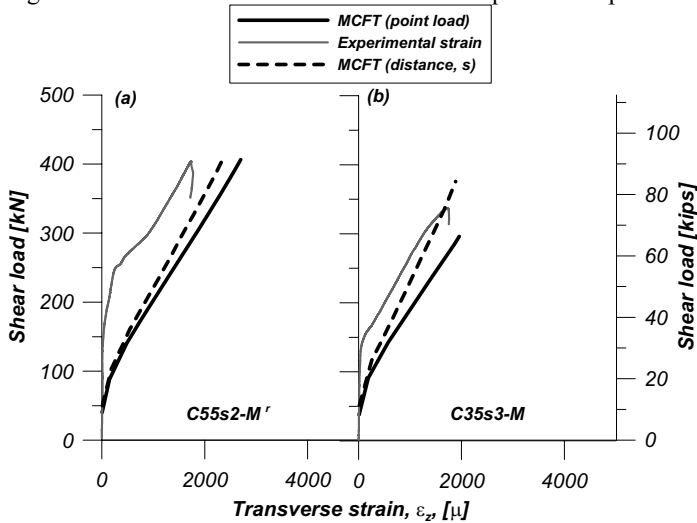


Fig. 13– Shear load as a function of transverse strain (a) specimen C55s2-M^r and (b) specimen C35s3-M.

All of the predicted strains in figure 13, for both specimens, are higher than the strains measured by the SGs for the same load step. However, the strain development of the predicted strains calculated at the point of maximum shear force and moment (point load) show a similar development as the measured strains. The predicted strains calculated at the same location as the measured strains (in the stirrup) show a steeper increase of strains for the C35s3-M specimen compared to the ones calculated at the point load, while for the C55s2-M^r specimens this difference is not as pronounced.

Note, for the NSM strengthened specimen C55s2-M^f, there is a larger variance between measured strains and predictions compared to the C35s3-M specimen.

8 Discussion of results

8.1 Material properties

One of the most important inputs in evaluating predictions based on proposed models is the assumed mechanical properties of the studied materials. In this paper, only a few tests were performed to obtain representative values. However, for comparison in between the models, the stated mechanical properties are assumed to be representative for the evaluated specimens.

8.2 Ultimate shear resistance

Comparing the predicted results to experimentally obtained failure loads, performed on specimens with *no* internal shear reinforcement and only strengthened with the MBC system, clearly shows that MCFT is the model that gives the best predictions. Second best were models based on the “addition” approach (especially the one based on BBK¹¹ which in turn gives much better estimations of the shear resistance than the VAT approach (based on Eurocode¹⁰). The latter gives highly conservative predictions for the shear resistance by excluding the concrete contribution to the shear resistance. Furthermore, assuming a 45° inclination of the compressive strut renders unrealistically low predictions when using the VAT approach. However, using the model based on the MCFT includes some iterative steps which can be time consuming. Thus, the models based on the “addition” approach are more straightforward and give conservative estimations.

The beam specimens containing internal shear reinforcement failed by yielding of the tensile reinforcement and subsequently crushing of the concrete, therefore no comparison of the ultimate shear resistance was possible. These specimens are evaluated in the section below.

8.3 Shear load and transverse strain relationship

Generally, all of the predicted transverse strains are higher for the same load step compared with the experimentally obtained results. For the “addition” approach and the VAT approach the predictions only vary linearly with the strain increase.

For the MCFT approach the horizontal equilibrium is considered and then the vertical strains will be dependent on the assumed stiffness of the concrete member. The stiffness of a concrete member is complicated to calculate exactly, which is also shown in figure 10. In this paper only an estimation of the stiffness has been done. A cracked section is assumed which then will render conservative predictions. In addition, the beam specimens in this paper were heavily reinforced in flexure and some of the beams were even additionally strengthened with bonded NSM. These large amounts of tensile reinforcement, considering the given beam geometry, will

probably imply that the stiffness response of these beams is even harder to predict. Nevertheless, the MCFT approach can be used for conservatively predicting the transverse strains. Further, as the amount of internal shear reinforcement is increased the difference of predicted strains between the point of maximum moment/shear and strains predicted in the shear span will decrease. This is due to the fact that a member having high amounts of shear reinforcement will have a better ability to redistribute stresses.

8.4 Limitations

The limiting value of the ultimate strain in the CFRP based on the proposed “effective strain” is based on a non cracked section. However, based on the results in this study this limiting factor of 0.67 is presumed to be a reasonable estimate.

In this paper, no consideration has been taken to pre-cracked or severely cracked beams. In such a case a conservative estimate of the shear resistance can be made using the VAT approach based on the Eurocode¹⁰.

Further research

In this study different fiber amounts have been investigated and results are promising. However, it should be pointed out that no consideration has been taken to the bond interaction between the mineral-based binder and the CFRP grid. The bond between the CFRP grid and the binder are mostly dependent on mechanical anchoring. Therefore, it is not known to what extent the upper limit of the carbon fiber amount affects the bond. Although, theoretically no upper limit exists on the amount of carbon fibers that can be included in the grid geometry, there is an upper limit of carbon fiber that can be used in the manufacturing process. Therefore further tests on the influence of CFRP grids with higher amounts of carbon fibers are recommended. Also, the transverse alignment of the fiber tow direction is not optimal for strengthening for diagonal shear cracking. Further enhancement of the grid geometry can be made by having a tri-axial geometry of the grid, having transverse and inclined $\pm 45^\circ$ tows. Then the design approach in this paper has to be revised taking the new geometry into consideration. In addition, further research should be done to investigate how both the MBC and the predicted models behave for pre-cracked beams.

Conclusions

Based on the ratio between predictions and experiments for the three proposed shear design approaches (“addition”/45° Mörsch, VAT and MCFT) it can be concluded that the MCFT approach gives the best predictions. However, this model includes iterative steps which can be time consuming. The predictions made by the “addition” approach give conservative results with less effort. The highly conservative approach by the VAT model excluding the concrete contribution to shear resistance can to some extent be used for severely cracked sections or a member that requires very conservative estimations.

It is also concluded that the transverse strain development predicted by the MCFT depends on the flexural stiffness of the beam (cracked or non-cracked section). Since it is not within the scope of this paper to evaluate the bending stiffness it is proposed to use a cracked section analysis when predicting the strain using the MCFT.

Overall, the MBC strengthening system performs well when applied as shear strengthening of concrete beams and the predictions of the shear resistance are also within reason.

Acknowledgements The research presented in this paper has been funded by several organizations. Here the Swedish National Road Administration, The Development Fund of the Swedish Construction Industry, Skanska AB and Sto Scandinavia are acknowledged.

Notations:

| | | | |
|---------------|--|-----------------------|---|
| a_g | Maximum aggregate size | ε_1 | Principal tensile strain |
| A_{fx} | Area in longitudinal CFRP tow | ε_2 | Principal compressive strain |
| A_{fz} | Area in Transverse CFRP tow | ε'_c | Concrete tensile strain at maximum tensile strength |
| A_{sx} | Longitudinal steel reinforcement area | ε_{cc} | Concrete compressive strain |
| A_{sz} | Transverse steel reinforcement area | ε_{cr} | Concrete compressive strain at maximum compressive strength |
| b_w | Width of concrete beam | ε_{ct} | Concrete tensile strain |
| b'_w | Effective width of concrete beam | ε_{fuz} | Ultimate strain in transverse CFRP tow |
| C | Compressive force | $\varepsilon_{fz,ef}$ | Effective strain in transverse CFRP tow |
| c_x | Maximum clear cover to the longitudinal reinforcement | ε_{st} | Strain in longitudinal steel reinforcement |
| c_z | Maximum clear cover to the transverse reinforcement | ε_{ult} | Ultimate strain in CFRP |
| d_{bx} | Diameter of longitudinal steel reinforcement | ε_x | Longitudinal strain |
| d_{bz} | Diameter of transverse steel reinforcement | ε_y | Yield strain in steel reinforcement |
| Δ | Deflection | ε_z | Longitudinal strain |
| Δ_{cr} | Deflection at flexural cracking | ε_z | Transverse strain |
| d'_s | Distance to centre of gravity for longitudinal compressive steel reinforcement | f_1 | Principal tensile stress |
| d_s | Distance to centre of gravity for longitudinal tensile steel reinforcement | f_2 | Principal compressive stress |
| E_c | Modulus of elasticity for concrete | f'_c | Concrete strength based on cylindrical specimens |
| E_{MBA} | Modulus of elasticity for mineral-based binder | f_{cc} | Concrete compressive stress |
| E_s | Modulus of elasticity for steel reinforcement | f_{cr} | Concrete tensile strength |

| | | | |
|---------------|--|---------------|---|
| f_{ct} | Concrete tensile stress | ρ_{fx} | Ratio for longitudinal CFRP |
| f_{fx} | Stress in longitudinal CFRP tows | ρ_{fz} | Ratio for transverse CFRP |
| f_{fz} | Stress in transverse CFRP tows | ρ_x | Ratio for longitudinal reinforcement |
| $f_{fz,ef}$ | Effective stress in transverse CFRP tows | ρ_z | Ratio for transverse reinforcement |
| f_{sx} | Stress in longitudinal steel reinforcement | s | Stirrup distance |
| f_{syx} | Yield stress in transverse steel reinforcement | σ_{cc} | Compressive stress in concrete |
| f_{sz} | Stress in transverse steel reinforcement | s_x | Distance between longitudinal reinforcement |
| f_{ult} | Ultimate strength in CFRP | T | Tensile force |
| f_x | Longitudinal stress | v | shear stress |
| f_y | Yield stress | v_{ci} | shear stress across crack |
| f_z | Transverse stress | V_c | Concrete shear resistance |
| γ_{xz} | Shear strain | V_f | Shear resistance for CFRP |
| h | Total depth of beam | V_s | Shear resistance for transverse reinforcement |
| η | Reduction factor for CFRP | V_u | Ultimate shear resistance |
| η_{MBA} | Modulus of elasticity ratio | w | Crack width |
| M | Applied moment | z | Internal lever arm |
| N_v | Longitudinal force due to shear | | |

References

1. Meier, U., "Bridge repair with high performance composite materials". *Material und Technik*, V. 4, 1987, pp. 125-128.
2. Triantafillou, T. C., "Shear strengthening of Reinforced Concrete Beams Using Epoxy-Bonded FRP Composites", *ACI Structural Journal*, V. 28, No. 2, 1998, pp. 5-15.
3. Carolin, A., "Carbon Fibre Reinforced Polymers for Strengthening of Structural Elements", Doctoral thesis 2003:18, Luleå University of Technology, Department of civil and environmental engineering, Sweden, ISBN: 91-89580-04-4, 178 pp.
4. Carolin, A., and Täljsten, B., "Theoretical Study of Strengthening for Increased Shear Bearing Capacity". *Journal of Composites for Construction*, V. 9, No 6, 2005, pp. 497-506.
5. Chen, J. F., and Teng, J. G., "Shear Capacity of Fiber-Reinforced Polymer-Strengthened Reinforced Concrete Beams: FRP Debonding", *Journal of Structural Engineering*, V. 129, No. 5, pp. 615-625.
6. Täljsten, B., and Blanksvärd, T., "Mineral-Based Bonding of Carbon FRP to Strengthen Concrete Structures", *Journal of Composites for Construction*, V. 11, No. 2, 2007, pp. 120-128.
7. Blanksvärd, T., "Strengthening of concrete structures by the use of mineral based composites". Licentiate thesis 2007:15, Luleå University of Technology, department of civil and environmental engineering, Sweden, ISBN: 91-86585-07-3, 300 pp.
8. Blanksvärd, T., and Täljsten, B., "Strengthening of concrete structures with cement based bonded composites", *Journal of Nordic Concrete Research*, V. 38, 2008, pp. 133-153.
9. ACI Committee 318., "Building code requirements for structural concrete (318M-08)", American Concrete Institute, Farmington Hills (MI, USA), 2008.

-
10. EC 2., “BS EN 1992, Eurocode 2: Design of concrete structures – Part 1-1: Common rules for building and civil engineering structures”. EN 1992-1-1, CEN (Comité Européen de Normalisation), European Committee for Standardisation, Brussels. December 2004
 11. BBK 04., “Boverkets handbok about concrete structures” [in Swedish], 2004, ISBN: 91-7147-816-7.
 12. Mörsch, E., “Der eisenbetonbau – seine theorie und anwendung“, 3. Auflage, Verlag Konrad Wittwer, Stuttgart, 1908, pp. 376.
 13. ACI-ASCE Committee 326., “Shear Diagonal Tension”, *ACI Journal*, V. 59, No. 3, 1962, pp. 277-333.
 14. Morrow, J. and Viest, I. M., “Shear Strength of Reinforced Concrete Frame Members Without Web Reinforcement”, *ACI Journal*, V. 53, No. 9, 1957, pp. 833-869.
 15. Hedman, O., and Losberg, A., “Designing concrete structures with respect to shear force” [in Swedish]. *Nordisk Betong*, V. 5, 1975, pp. 19-29.
 16. ASCE-ACI 445., “Recent Approaches to Shear Design of Concrete Structures”. *Journal of Structural Engineering*, V. 124, No. 12, 1998, pp. 1375-1417.
 17. Collins, M. P., “Towards a Rational Theory for RC Members in Shear”, *Proceedings ASCE*, V. 107, 1978, pp.649-666.
 18. Vecchio, F.J., and Collins, M.P., “The modified compression field theory for reinforced concrete elements subjected to shear”. *ACI Journal*, V. 29, No 2, 1986, pp. 219-252.
 19. Hsu, T. T. C., “Softened truss model theory for shear and torsion”. *ACI structural journal*, V. 85, No. 6, 1988, pp. 624-635.
 20. Nielsen, M. P., “Limit analysis and concrete plasticity”. Second edition. Boca Raton, Florida, CRC Press LLC, 1999, ISBN: 0-8493-9126-1.
 21. Kaufmann, W., and Marti, P., “Structural concrete: Cracked Membrane Model”. *Structural Engineering*, V. 124, No. 12, 1998, pp. 1467-1475.
 22. Kupfer, H., “Erweiterung der Mörschen fachwerkanalogie mit hilfe des prinzipls vom formänderungarbeit“. *CEB Bulletin d'information*, 40, 1964, pp. 44-57.
 23. Hognestad, E. “Fundamental concepts in ultimate load design of reinforced concrete members”. *ACI Journal Proceedings*, V. 48, No. 6, 1952, pp. 809-830.
 24. Moody, K. G., Viest, I. M., Elstner, R. C. and Hognestad, E. “Shear strength of reinforced concrete beams part 1 – Tests of simple beams”. *ACI Journal Proceedings*, V. 51, No. 12, 1954, pp. 317-332.
 25. Tresca, H., “Mémoire sur l'écoulement des corps solides soumis de fortes pressions”, C.R. Acad. Sci., Paris, 59, 1864, pp. 754.
 26. Kaufmann, W., “Strength and deformations of structural concrete subjected to In-plane shear and normal forces”. Doctoral thesis, Institut für Baustatik und Konstruktion, ETH, Zürich, 1998, pp. 147
 27. Collins, M. P., and Mitchell, P., “Prestressed concrete structures”. New Jersey: Prentice-Hall, inc. ISBN: 0-13-691635-X, 1991, 776 pp.
 28. Bentz, E. C., "Sectional Analysis of Reinforced Concrete Members," PhD Thesis, Department of Civil Engineering, University of Toronto, 2000, 310 pp.
 29. Bentz, E.C., Vecchio, F.J., and Collins, M.P., “The simplified MCFT for calculating the shear strength of reinforced concrete elements”, *ACI Structural Journal*, V. 103, No. 4, 2006m pp. 614-624.
 30. CSA Committee A23.3, “Design of concrete structures (CSA A23.3-4)”, Canadian Standards Association. Mississauga, 2004, 214 pp.

-
31. Hoult, N. A., Sherwood, E. G., Bentz, E. C., and Collins, M. P., "Does the Use of FRP Reinforcement Change the One-Way Shear Behavior of Reinforced Concrete Slabs?", *Journal of Composites for Construction*, V. 12, No. 2, 2008, pp. 125-133.
 32. ACI Committee 440. "Guide for the design and construction of externally bonded FRP systems for strengthening concrete structures", *ACI 440.2R-08*, Detroit, 2008, 76 pp.
 33. Fib bulletin 14. "Design and use of externally bonded fibre reinforced polymer reinforcement (FRP EBR) for reinforced concrete structures" Technical report, TG 9.3, July 2001, ISBN 2-88394-054-1, 138 pp.
 34. CAN/CSA-S806-02, "Design and Construction of Building Components with Fibre-Reinforced Polymers", Canadian Standards Association, Toronto, Canada, 2002, 187 pp.
 35. Täljsten, B., "FRP Strengthening of Existing Concrete Structures: Design Guidelines", Technical report, Luleå University of Technology, Luleå, Sweden, ISBN: 91-89580-03-6, 228 pp.
 36. Sas, G., "FRP strengthening of RC beams and walls", Licentiate thesis 2008:39, Luleå University of Technology, Department of civil, mining and environmental engineering, Sweden, 107 +57 pp.
 37. Blanksvärd T., Täljsten B., and Carolin A, "Shear strengthening of concrete structures with the use of mineral based composites (MBC)". *Journal of Composites for Construction*, V. 13, No. 1, 2009, pp. 25-34
 38. Popov, E. P., "Engineering Mechanics of Solids". New Jersey: Prentice-Hall, inc. ISBN: 0-13-081534-9, 1999, 863 pp.
 39. CEB-FIP model code, "Model code for concrete structures: CEB-FIP International recommendations", 3rd edition, Comité Euro-International du béton, Paris, 1972, pp. 348.
 40. Branson, D. E., "Deformation of concrete structures", McGraw-Hill, Inc., U.S., ISBN: 0-07-007240-X, 1977, 546 pp.
 41. Betonghandbok - konstruktion "Concrete handbook – Construction" (In Swedish). Second edition. Solna: AB Svensk byggtjänst, ISBN: 91-7332-533-7, 1990, 791 pp.
 42. Betonghandbok - material "Concrete handbook – Material" (In Swedish). Second edition. Solna: AB Svensk byggtjänst, ISBN: 91-7333-266-6, 1994, 791 pp.

PAPER VI

“Shear crack propagation in MBC
strengthened concrete beams”

BY

Thomas Blanksvärd, Anders Carolin and Björn Täljsten

Published in

*Proceedings of the Fourth International Conference on FRP Composites in Civil
Engineering (CICE2008), 22-24 July 2008, Zurich, Switzerland*

Shear crack propagation in MBC strengthened concrete beams

T. Blanksvärd & A. Carolin

Luleå University of Technology, Division of Structural Engineering, Luleå, Sweden

B. Täljsten

Technical University of Denmark, Department of Civil Engineering, Lyngby, Denmark

ABSTRACT: Repair and upgrading existing concrete structures using FRPs and an epoxy adhesive as the bonding agent has some disadvantages when it comes to compatibility to the base concrete. Epoxies are often restricted by regulations of use, have low permeability which may create freeze/thaw problems, poor thermal compatibility to the base concrete and are often sensitive to the nature of the surface of the base concrete and surrounding temperature. By using mineral based composites (MBC) some of these challenges can be overcome. MBC refers here to a cementitious bonding agent and a carbon FRP grid. This paper is a part of an ongoing study of MBC systems. Emphasis is placed on the cracking behavior of the MBC system used for shear strengthening of RC beams. Traditional foil strain gauges and photometric measurements have been used for monitoring of the cracking behavior. In this study it is shown that the use of mineral based shear strengthening postpones the formation of macro-cracks and that a considerably strengthening effect could be achieved.

1 INTRODUCTION

Repair and upgrading of existing concrete structures are becoming more and more common due to degradation processes, changes in structural use, code adoptions and economical considerations. Previously, traditional repair and upgrading techniques was limited to enlargement of cross sections with installation of extra steel reinforcement, external prestressing systems or change of loading path. Today also the use of FRP (fiber reinforced polymers) or dry fibers adhesively bonded to the concrete is a common strengthening method for concrete structures. The most commonly utilized FRPs and fibers are made of carbon (C) or glass (G). These can be designed as laminates, sheets or bars mounted on the surface or as near surface mounted bars in the concrete cover (Oehlers et al. 2007; Nordin & Täljsten 2006). Although strengthening systems using epoxy as the bonding agent has shown good results in form of bonding and application, there exist some drawbacks.

(a) There are regulations on how to handle the epoxy bonding agents, based on the risk for eczema and toxicity of the components. (b) It has low permeability and is diffusion-tight which for example can provoke freeze/thaw problems. (c) Poor thermal compatibility to the base concrete, which may cause unfavourable constraints. (d) The surface of the base concrete has to be free from water and the recommended temperature at time for application and hardening should not be below 10 °C at. (e) Depending on the amount of FRP coverage, it may also be difficult to assess the structure.

Upgrading of civil structures with mineral based composites gives a high compatible repair and strengthening system with the base concrete. Mineral based composites (MBC) are in this paper used synonymously for upgrading with FRP materials together with a polymer modified or polymer reinforced cement. Consequently, the use of these mortars should prevent some of the disadvantages with the organic resins such as epoxy. The fibers utilized in combination with cementitious bonding agent can be designed in different ways. Up-to-date, some of the com-

monly used designs of fiber are unidirectional dry fibers, Wiberg (2003), textiles in form of meshes made from woven, knitted or unwoven rovings of fibers in different directions, (Triantafillou & Papanicolaou 2006; Brückner et al. 2006) or FRPs where the fibers are assigned as a grid with two orthogonal directions, Blanksvärd (2007). The formability of the dry fibers and the textile meshes are in favor of FRP grid where the fibers are embedded into a matrix. On the other hand studies on the impregnation of dry fibers with polymers, e.g. epoxy, implicates on much higher bond strength to the cementitious bonding agent compared to the use of impregnated fibers. This is due to the low ability of the cementitious bonding agent to penetrate the dry fiber rovings, (Raupach et al. 2006; Shilang & He 2007). Considering the bond, it is therefore advantageous to use impregnated fibers (FRPs) than using dry fibers.

There are however some uncertainties regarding the use of mortars as the bonding agent. These are primarily; (i) the bond in the transition zone between the base concrete and the FRP and especially the bond between the base concrete and the mortar which can be influenced by drying shrinkage, (ii) Durability regarding fatigue. (iii) Influence on the structural performance regarding both micro and macro cracking of the structural system.

It is of great interest to be able to monitor the composite action between the MBC systems and the concrete structure. One way of evaluating the composite action is to monitor the crack formations that progress in a shear strengthened structure during loading. However, monitoring the formation of cracks in concrete requires special monitoring tools. Firstly, the formation of cracks needs to be established. The formation of cracks does not start immediately but can be considered as an accumulation of micro-cracks while the load is increasing. When these micro cracks have created a certain level of damage, a macro-crack will form.

It is suggested in Hegger et al. (2004), based on experimental and theoretical investigations, that a non linear process is preceding the formation of macro-cracks. In viz., it is shown that the use of laser-interferometry and strain gauges on the stirrups can give an indication of the redistribution of forces before the appearance of macro cracks, by means of monitoring the linearity during the initial loading. Also for the post cracking behavior, it is shown that methods of photometric measurement make it possible to investigate the strain distributions prior to the formation of visible shear cracks (Lee & Al-Mahaidi 2008; Sonnenberg & Al-Mahaidi 2007). This paper will show the potential of postponing the formations of macro-cracks by the use of mineral based strengthening.

2 MINERAL BASED STRENGTHENING

Previous studies show that the use of MBC for shear strengthening reaches similar strengthening effects as the use of epoxy bonded carbon fiber sheets, Blanksvärd (2007). The MBC system used in this research contains of a cementitious binder, a CFRP grid and a concrete surface primer. Generally, the surface of the base concrete needs to be roughened to remove the cement laitance to achieve a good bond between the base concrete and the mortar. Examples of roughening techniques are sandblasting or water jetting. In laboratory environments, or on smaller defined surfaces, a hand lay-up method can be used to apply the MBC. Prior to mounting the MBC system the base concrete surface has to be primed using to prevent moisture transport from the wet mortar to the base concrete. The hand lay-up technique used in this study basically consists of the following; first a layer of mortar is immediately applied to the primed surface, next, the CFRP grid is placed on the first layer of mortar followed by an additional layer of mortar applied on the grid. A graphical representation of the hand lay-up MBC method, after sandblasting, is shown in Figure 1. The system can also be applied by spraying. However, different application techniques are not further discussed in this study.

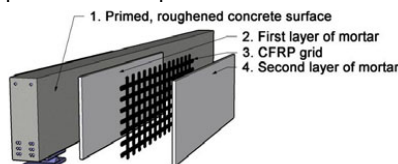


Figure 1. Graphical overview of the MBC strengthening system.

3 EXPERIMENTAL SET-UP

In total, 11 reinforced concrete beams with a rectangular cross section have been tested. The chosen loading scheme for all specimens were 4-point loading. Experimental set-up, geometries and reinforcement scheme are recorded in Figure 2. The concrete beams were reinforced in such a way that shear failure was directed to one of the shear spans. This design is motivated by the fact that the beams then only needed to be strengthened and monitored in one span. Common to all of the concrete beams is that they are reinforced with 12 Ø16 mm steel bars at the bottom and two Ø16 mm at the top of the beam as flexural and compression reinforcement. The shear reinforcement constitutes of Ø10 mm stirrups with a distance 50 mm at the supports and Ø12 mm stirrups with the distance 100 mm in the heavily reinforced shear span. The densification of the shear reinforcement over the supports is designed to secure the anchorage of the longitudinal reinforcement. Further, the strengthened shear span of the beam specimens has three different designs of the shear reinforcement, which can be categorized as *no* shear reinforcement, stirrups with a distance $s = 350 \text{ mm}$ and stirrups with a distance $s = 250 \text{ mm}$. The first category mainly distinguishes the behavior of the beam with no shear reinforcement and without the MBC system. The other two mainly assess the influence of the interaction between steel shear reinforcement and the MBC strengthening system. The steel shear reinforcement had a yield strength of 601 MPa and a yield strain of 2.84 ‰. Also the concrete strength varied, two different concrete qualities were used corresponding to C35 and C55 according to EC 2-1 (2004). Average values for the mechanical properties of the concrete qualities and mortar are recorded in table 1, tested according to DIN EN 196-1 (2005). Values for the properties of the fibers in the CFRP grid, as provided by the manufacturer, are also recorded in table 1.

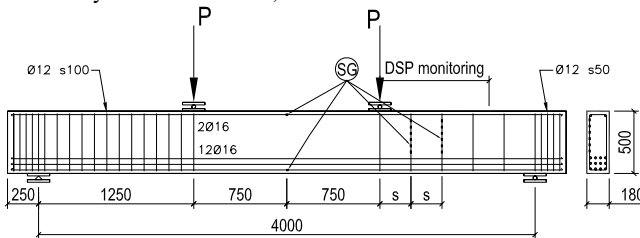


Figure 2. Test set-up, geometry, reinforcement scheme, DSP monitored surface and SG set-up.

Table 1. Mechanical properties for utilized materials.

| | Tensile strength [MPa] | Compression strength [MPa] | Modulus of elas- ticity [GPa] | Fracture energy [N/m] |
|------------------------|---------------------------|-------------------------------|----------------------------------|--------------------------|
| Concrete quality C35 | 48.9 | 2.8 | 31.4 | 155 |
| Concrete quality C55 | 73.5 | 3.4 | 24.9 | 135 |
| Mortar | 65.6 | 3.0 (2.4) | 22.3 | - |
| CFRP – vertical tows | 3800 | - | 284 | - |
| CFRP – horizontal tows | 3800 | - | 253 | - |

4 MONITORING

A quite extensive measuring program was used to record the behavior of the tested beams. This includes monitoring the load with a load cell, Linear Variable Differential Transducers (LVDT) for measuring deflections and settlements, electrical foil strain gauges (SG) for local strain measurements and photometric strain measurement for global strain measurements. The loading was deformation controlled and the deformation rate was set to 0.01 mm/s, measured at the midpoint of the beam specimens. For a more detailed description of the experimental program the reader is referred to Blanksvård (2007).

4.1 Strain gauge set-up

Two different types of SGs were used to measure strains on the CFRP grid and steel reinforcement. A gauge length of 5 mm was used (KFW-5-120-C1-11L3M2R) to measure strains on the steel reinforcement. In the case of measuring the strains on the CFRP grid the tows are quite narrow and a gauge length of 2 mm had to be used (KFWS-2N-120-C1-11L3M3R).

All beam specimens had SGs on the compressed and tensile longitudinal steel reinforcement at half span of the beam, see figure 2. Twelve SGs were applied on the two stirrups closest to the load for beam specimens with shear steel reinforcement in the weakened or strengthened shear span. Set-up for the SG assessment is recorded in Figure 2.

To compare the CFRP strain to the strain in the steel stirrups a similar assessment as for the SGs mounted on the stirrups was affiliated to the CFRP grid. By placing SGs on the steel stirrups, CFRP and using photometric strain measurement (see below) it was possible to compare strains in the steel stirrups (internal concrete) to strains in vertical CFRP tows (internal MBC) as well as strain fields obtained by the photometric strain measurements.

However, due to the design of the CFRP grid it was not possible to mount the SGs at exactly the same position as the steel reinforcement SGs. After casting the concrete beam specimens, the steel stirrups was located using a metal detector and the SGs were mounted onto the nearest vertical CFRP tow corresponding to the stirrup with SGs applied, leading to a maximum horizontal dislocation of 20 mm. The first SG on the stirrup and on the vertical CFRP tow was applied 170 mm from the bottom of the beam, just above the tensile reinforcement. The internal distance between the following SGs were then 50 mm, see also Figure 2.

4.2 Photometric measurement

Traditional strain measurements using strain gauges only measure local strains, while photometric strain measurements can indicate the global strain behavior of a specific surface. Photometric monitoring is a non-contact measurement by taking photos of the area studied. The photos were taken prior to loading (reference) and at certain load steps using a digital resolution camera (Canon EOS 5D). Photos were taken at load steps every 5 kN.

The pictures were processed into a raw format (grey scale) and trimmed so that only the investigated area remains. All photos was then analyzed by a computer software based on speckle pattern correlation (DSP), developed at Luleå University of Technology (Carolin et al. 2004; Svanbro 2004). The photos are divided into different sub-pictures and their point of gravity is calculated, see figure 4. The centre of gravity is then calculated for all individual sub-pictures. The accuracy becomes higher if the sub-pictures are chosen to be large. A large number of pixels within the sub-picture will also increase the accuracy of the positioning. Speckle pattern correlation analysis will find the same sub-picture in the second loading condition even if the pattern has deformed or moved. The size and the distance of the sub-pictures can be chosen as desired.

The strains are calculated by correlating the sub-pictures during loading to the unloaded reference. For the software to work properly and give adequate results the photographed area needs to be given pattern or divergent colors. In this case the strengthened area was given a random pattern by using an epoxy adhesive to adhere a mix of white and black sand.

Results from the speckle pattern correlation analysis can be plotted as shear strains, principal strains or strains in any arbitrary direction. In this study the accuracy of the strain measurements was 300 μ strain. The monitored surface was set to 880 x 500 mm, see figure 2 and figure 6.

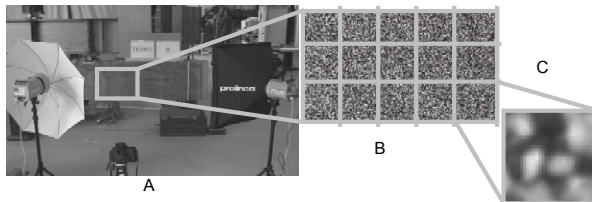


Figure 3. Set-up of the digital speckle correlation, A) Test set-up using cameras and flashes, B) Part of the monitored surface, C) Sub-picture.

5 RESULTS AND DISCUSSION

The pre-cracking behavior of the strengthened and non strengthened specimens was observed by the monitored strains with a SG in the midpoint of the stirrups. Figure 4 A and B shows the strain development in the stirrup 700 mm from the load for a beam specimen with concrete quality C35 with and without MBC. The first visual shear crack was formed at a shear force of 186 kN (without MBC) and 285 kN (with MBC). Figure 4 B shows the initial part of the strains for a more detailed overview of the linear behavior. Here the strains behave linear up to a shear force of 57 kN (without MBC) and 79 kN (with MBC). Thereby the formation of macro-cracks initiates long before the appearance of the first visual shear crack. Comparing a beam with and without MBC, it is clear that the strengthening reduces strain levels in the stirrup for low shear forces and continues to do so for higher load levels.

The linearity at low load levels becomes harder to detect when the shear reinforcement is increased due to low strain levels in the stirrups in the initial load levels. This is shown in figure 4 C for a beam specimen with higher concrete quality (C55) and shear reinforcement ratio ($s=250$ mm). Still, the strain in the stirrup for the MBC strengthened specimen has lower strains for the same shear load level compared to a non strengthened one. This behavior was noticed for all specimens with and without strengthening for different concrete qualities and different steel reinforcement ratios.

Shear strengthening of a beam with MBC will reduce the strains in the stirrups compared to a non strengthened one. Thus, the vertical CFRP tows will attain and redistribute some of the above mentioned strains. Figure 5 shows the shear cracks and strains in the vertical CFRP tow at different shear loads. Here it is possible to see that there are strain concentrations in the vicinity of the formation of shear cracks.

The post cracking behavior and global strain distribution is monitored by the photometric measurement. Figure 6 shows the monitored principal strains at different load steps. The monitored area are shown in figure 6 for beam specimens with a stirrup distance of 350 mm and concrete quality C35 both with and without the MBC strengthening system. The load steps were taken at shear loads of 200 and 260 kN. By comparing the specimens with and without the MBC strengthening system, it is clear that the MBC system reduces the strains even for a load of 200 kN. When the load is increased the MBC system still reduces the principal strains at the load 260 kN compared to a non strengthened specimen. Further, the photometric strain measurement indicated on shear crack formations long before first visual appearance.

All of the recorded principal strains in figure 6 have the same scale. Only the direction and relative size are given, for values on the principal strain the reader is referred to Blanksvärd (2007).

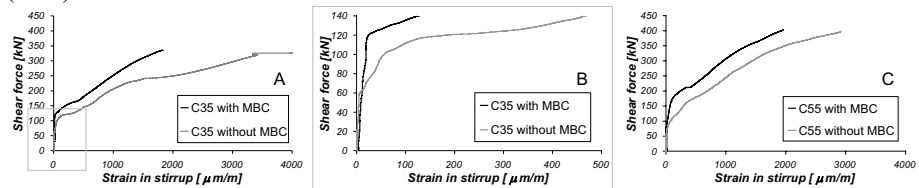


Figure 4. Strains in measured in stirrup with and without MBC for specimens with A) Concrete C35 $s=350$ mm, B) Part of the initial strains in C35 $s=350$ mm, C) Concrete C55 $s=250$ mm.

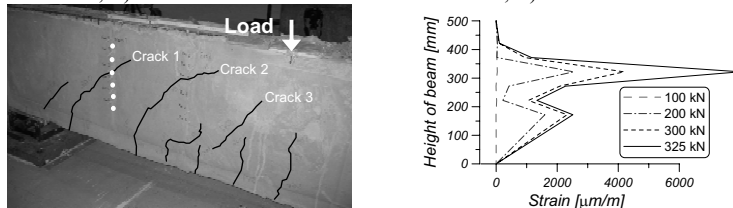


Figure 5. To the left, shear crack propagation, white dots locates SGs on the CFRP grid. To the right, strains monitored in the vertical CFRP tow located at 680 mm from the load.

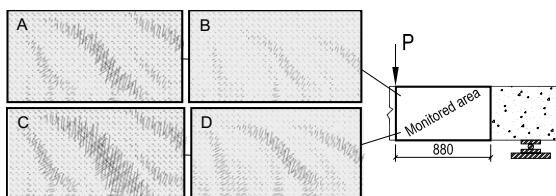


Figure 6. Photometric measurement of the principal strains for concrete quality C35 and $s=350$ mm. A) Without MBC at 200 kN, B) With MBC at 200kN, C) Without MBC at 260kN, D) With MBC at 260 kN.

6 CONCLUSIONS

In the pre-cracking stage, macro-cracks preceded the formation of visual shear cracks. The formation of macro cracks appear at 31 % of the first visual shear crack load for non strengthened specimens and 28 % for strengthened specimens, when studying strains in the stirrups. MBC strengthening increase the macro-crack formation by 38 % for specimens with concrete quality C35 and $s=350$ mm and 35-67 % for all C55 specimens. MBC has a better reduction of macro-cracking for specimens with low shear reinforcement ratios. High reinforcement ratios are transferring tensile stresses in a more continuous manner during the macro-cracking. This is explained by low strain levels in the stirrups in the initial load levels which make the transition between micro- and macro cracking less distinguished. Strain concentrations in vertical CFRP tows in the vicinity of shear cracks indicates on a good bond between the CFRP and the mortar. This bond-slip behavior will be the outcome of future research. The post cracking behavior was monitored by using photometric strain measurement. It was noted that strengthening with MBC reduces the principal strains for all load steps in comparison to a non strengthened specimen. It was also possible to detect shear crack formations before the visual inspection.

7 REFERENCES

- Brückner, A., Ortlepp, R., and Curbach, M. 2006. Textile reinforced concrete for strengthening in bending and shear. *Materials and Structures*, 39, 741-748.
- Blanksvärd, T. 2007. *Strengthening of concrete structures by the use of mineral based composites*. Licentiate thesis 2007:15, Luleå University of Technology, Division of Structural Engineering.
- Carolin, A., Olofsson, T. Täljsten, B. 2004. Photographic Strain Monitoring for Civil Engineering. *Proc. in FRP Composites in Civil Engineering, CICE 2004, Adelaide, Australia*, 593-600.
- DIN EN 196-1. 2005. Methods of testing cement - Part 1: Determination of strength.
- Hegger, J., Sherif, A., and Görtz, S. 2004. Investigation of pre- and postcracking shear behavior of prestressed concrete beams using innovative measuring techniques. *ACI Structural Journal*, 101(2), 183-192.
- Lee, T.K., and Al-Mahaidi, R. 2008. An Experimental investigation on shear behaviour of RC T-beams strengthened with CFRP using photogrammetry. *Composite Structures*, 82, 185-193.
- Nordin, H., and Täljsten, B. 2006. Concrete beams strengthened with prestressed near surface mounted CFRP. *Composites for Construction*, 10(1), 60-68.
- Oehlers, D.J., Rashid, R., and Seracino, R. 2007. IC debonding resistance of groups of FRP NSM strips in reinforced concrete beams. *Journal of composites for construction*, 11(4), 401-409.
- Raupach, M., Orlowsky, J., Büttner, T., Dilthey, and U., Schleser, M. 2006. Epoxy impregnated textiles in concrete – Load bearing capacity and durability. *Proc., the 1st international RILEM symposium: Textile reinforced concrete*, RILEM, Aachen, Germany, 55-66.
- Shilang, X.U., and He, L.I. 2007. Bond properties and experimental methods of textile reinforced concrete. *Journal of Wuhan University – Materials Science Edition*, 22(3). 529-532.
- Sonnenberg, A.M.C., and Al-Mahaidi, R. 2007. Investigation of dowel shear in RC beams using photogrammetry. *Magazine of Concrete Research*, 59(9), 621-626.
- Svanbro, A. 2004. *Speckle interferometry and correlation applied to large-displacement fields*. Doctoral thesis 2004:05, Luleå University of Technology, Division of Experimental Mechanics.
- Triantafyllou, T.C., and Papanicolaou, C.G. 2006. Shear strengthening of reinforced concrete members with textile reinforced mortar (TRM) jackets. *Materials and Structures*, 39, 85-93.
- Wiberg, A. 2003. *Strengthening of concrete beams using cementitious carbon fibre composites*. Doctoral Thesis, Royal Institute of Technology, Structural Engineering, 100 44 Stockholm, Sweden, p 140. ISSN 1103-4270.

